The U.S. Department of Energy Experimental Program to Stimulate Competitive Research

DOE EPSCOR

State/National Laboratory Program Review

July 22-24, 2008

Oak Ridge, TN

Hosted by Oak Ridge National Laboratory

This document was produced under contract number DE-AC05-06OR23100 between the U.S. Department of Energy and Oak Ridge Associated Universities.

Forward

The annual review of the U.S. Department of Energy's Experimental Program to Stimulate Competitive Research (DOE EPSCoR) program is scheduled for July 22-24, 2008 in Oak Ridge, Tennessee. The host is the Oak Ridge National Laboratory (ORNL) and it is significant to note the registration of over 110 faculty, students, research scientists, and research administrators from 29 states and Puerto Rico. Nine DOE National Laboratories are registered to participate in the review and will discuss opportunities to stimulate networking and partnership to make the most of their unique scientific capabilities. The program is designed to achieve three major objectives: 1) Review projects currently funded by the DOE EPSCoR program; 2) Identify and stimulate interactions between the EPSCoR university community and the DOE National Laboratories; and 3) Provide a forum for exchange of information and ideas regarding the opportunities for energy-related research to contribute to the world's future energy needs.

DOE EPSCoR Program Review – A poster session is scheduled for the evening of Wednesday, July 23rd, where approximately 35 posters representing DOE-funded EPSCoR projects are anticipated. Poster topics range from thermochemical conversion of woody biomass, to chemicals, to materials for solid state power conversion, to genomics underlying and supporting land reclamation. More poster topics include cutting-edge topics on photovoltiacs, plasma turbulence modeling, transport in soil systems and climate system modeling, all of which were funded by DOE EPSCoR. In addition, DOE national laboratories are presenting some of their user facilities in poster or booth form. The posters are supplemented by a few oral presentations of DOE EPSCoR supported work during the daytime sessions.

University/DOE Laboratory Interactions – A major goal of the EPSCoR meeting is to stimulate interactions between the University community and the DOE national laboratories. The schedule features presentations highlighting the scientific and collaborative opportunities, not only at Oak Ridge National Laboratory, but also across the DOE system in areas of Synchrotron-Based Research, Neutron Scattering, Bioenergy Research and Nanoscience/Nanotechnology. This is capped by panel discussion on Thursday chaired by Greg Snow, of the University of Nebraska, on details regarding partnering with the national laboratories. The panel includes presentations by each national laboratory represented at the meeting. Later in the afternoon, the DOE national laboratory representatives will be available in break-out rooms for informal discussions regarding specific opportunities for collaboration and to answer detailed questions.

Exchange of Information and Ideas Regarding Opportunities for Energy-Related Research – The keynote address by Isiah Warner, Vice Chancellor, Office of Strategic Initiatives, and Boyd and West Professor of Analytical Chemistry at Louisiana State University, will, among other topics, note the breadth of our human resource potential and provide some pointers on how to maximize that potential. Teri Odom, Associate Professor of Chemistry and, by courtesy Materials Science and Engineering, at Northwestern University, will discuss Scientific Grant challenges. William Gern, Vice President, Office of Research and Economic Development, University of Wyoming, will

discuss the Potential Contributions of the EPSCoR community to Energy Research. Andrew Schwartz, Program Manager for the Experimental Condensed Matter Physics, Division of Materials Sciences and Engineering, Office of Basic Energy Sciences, Office of Science, will provide an overview of funding opportunities in the Office of Basic Energy Sciences as well as other opportunities in the Department of Energy. Technological and Scientific capabilities and research opportunities at ORNL will be presented by Ken Tobin, Director of the Measurement Science and Systems Engineering Division, at ORNL and by Jim Roberto, Deputy Director for Science and Technology, ORNL. Cross-cutting research opportunities in Materials under Extreme Environments will be presented by Pete Tortorelli, Manager, of the Basic Energy Sciences Program in the Materials Science and Technology Division at ORNL and the specific opportunities afforded by Advanced Nuclear Energy Systems will be presented by David Hill, Deputy Director, Science and Technology at the Idaho National Laboratory.

It is my hope that this meeting will be productive as a review, as a stimulant for research interactions and collaborations, and as an inspiration to further research addressing our energy-related problems and opportunities. It is hoped that the laboratory tours Wednesday afternoon will further stimulate your interest in collaborations and in becoming a facility user. I encourage you to raise questions and to engage in discussions throughout the meeting. I welcome and appreciate your suggestions for improvements to the meeting/review for future years. An evaluation form will be sent to you electronically for your comments.

In closing, I wish to thank the ORNL and its staff for their support in hosting this meeting. I wish to especially thank Judy Trimble, Linda Horton, Al Ekkebus, and Jim Roberto; Angela Beach and her colleagues; and everyone who with their presentations, their logistical assistance, or suggestions have helped to make this meeting possible. It is a pleasure to thank all the speakers for preparing their presentations, the session chairs for moderating during Q/A time and keeping us on schedule, and to thank the national laboratories representatives who have travelled here to engage with the EPSCoR community. DOE EPSCoR would also like to thank Sophia Kitts, Tammy Click, Barbara Cohen, Deborah Garland, Donna Thomas and their colleagues from the Oak Ridge Institute for Science and Education for their continued commitment to excellence in support of the DOE EPSCoR office.

Tim Fitzsimmons

Table of Contents

Table of Contents i

Agenda viii

Poster List xiv

Speaker Abstracts

California

Stanford Linear Accelerator Center

New Opportunities in Ultrafast X-ray Science
A. M. Lindenberg 1

Idaho

Idaho State University, University of Idaho, Boise State University

Incorporation of Novel Nanostructured Materials into Solar Cells and Nanoelectronic Devices
Rene Rodriguez 2

Illinois

Northwestern University

Directing Matter and Energy: Five Challenges for Science And the Imagination
Teri W. Odom 6

Maine

University of Maine

Making of a Forest Biorefinery – The Maine Difference
Hemant Pendse 7

West Virginia

West Virginia University

Adventures in Neutron Magnetometry of Magnetic Multilayers
David Lederman 8

Submitted Abstracts

Alabama

Auburn University

Effect of SOFC Interconnect-Coating Interactions on Coating Properties and Performance
Jeffrey W. Fergus 9

University of Alabama

DOE-EPSCoR: Exchange Interactions in Epitaxial Intermetallic Layered Systems
P. LeClair 13

University of Alabama, Huntsville

Theoretical Investigation of Plasma Jets Driven Magnetoinertial Fusion using Smooth Particle Hydrodynamics
Jason Cassibry 17

Alaska

University of Alaska, Fairbanks

Influence of Sea Ice on Arctic Marine Sulfur Biogeochemistry in the Community Climate System Model
Clara J. Deal 18

Delaware

University of Delaware, Newark

Key Physical Mechanisms in Nanostructured Solar Cells
Valeria Gabriela Stoleru 22

University of Delaware and Brown University

Center for Spintronics and Biodetection (CSB)
John Q. Xiao 26

Kansas

Kansas State University

Excitation Energy Transfer in Natural Photosynthetic Complexes and Chlorophyll Trefoils: Hole-Burning and Single Complex/Trefoil Spectroscopic Studies
Ryszard Jankowiak..... 30

Kentucky

University of Louisville

α-Fe2O3 Nanowire Array Based Electrodes for Self-Driven Photoelectrochemical Cells
Boris Chernomordik..... 34

Field Enhanced, Thermionic Emission using Conical Carbon Nanopipette Arrays
S. Dumpala..... 35

Nanowire Based Anodes for Lithium Ion Batteries
Praveen Meduri 36

Synthesis of 3-Dimensional "Tree" Like Nanowire Architectures for Solar Energy Conversion
Chandrashekhar Pendyala..... 37

Band-Edge Engineered Hybrid Nanowire Structures for Dye Sensitized Solar Cells
M. K. Sunkara 38

Post Synthesis Modification of Metal Oxide Nanowires for Photoelectrochemical Hydrogen Production
Jyothish Thangala..... 39

Louisiana

Louisiana State University

Inhomogeneous Disordered Dirac Fermions: From Heavy Fermion Superconductors to Graphene
Ilya Vekhter 41

Tulane University

Novel Quantum Phenomena in Layered Ruthenates
Zhiqiang Mao 44

Maine

University of Maine

Implementation Phase I: Thermochemical Conversion of Woody Biomass to Fuels and Chemicals
Hemant P. Pendse 48

Montana

Montana State University

Linear Thermal Expansion Measurements with Sub-Atomic Resolution for the Study of Phase Transitions in Novel Condensed Matter Systems
John J. Neumeier 52

Nebraska

University of Nebraska, Lincoln

Rational Design of Molecular Ferroelectric Materials and Nanostructures
Stephen Ducharme 56

The Luminosity Measurement for the DZERO Experiment at Fermilab
Gregory R. Snow 60

Nevada

Desert Research Institute

Hydraulic Properties of Layered Soils and Its Impact on Water Flow – Anisotropy and Numerical Simulations
Jianting Zhu 64

University of Nevada, Las Vegas

Investigations on the Fundamental Surface Reactions Involved in the Sorption and Desorption of Radionuclides
Sherry Faye 68

New Hampshire

University of New Hampshire and Dartmouth College

Center for Integrated Computation and Analysis of Reconnection and Turbulence (CICART)
A. Bhattacharjee 71

North Dakota

University of North Dakota and North Dakota State University

North Dakota's DOE EPSCoR Infrastructure Improvement Program, "Advances in the Fundamental Understanding of Coal Combustion Emission Mechanisms"
Wayne S. Seames 75

Oklahoma

Oklahoma State University

Optoelectronic Properties of Carbon Nanostructures
John W. Mintmire 76

University of Oklahoma

Ro-vibrational Relaxation Dynamics of PbF Molecules
Neil Shafer-Ray 80

EPSCoR Program at OCHEP
Mike Strauss 84

South Carolina

Clemson University

Surface Anchoring of Nematic Phase on Carbon Nanotubes: Nanostructure of Ultra-High Temperature Materials
Amod A. Ogale 88

Phase II: The Next Generation Thermoelectric Materials for Solid State Cooling & Power Generation Applications
Terry M. Tritt 92

University of South Carolina

Analysis and Development of A Robust Fuel for Gas-Cooled Fast Reactors
Travis W. Knight 96

South Dakota

South Dakota School of Mines & Technology

Lattice-Mismatched III-V Epilayers for High-Efficiency Photovoltaics
S. P. Ahrenkiel 100

University of South Dakota

Liquid Argon-Based Direct Dark Matter Searches at Homestake
Dongming Mei 103

Tennessee

University of Tennessee

Resonant Ultrasound Studies of Spin Glasses and Geometrically Frustrated Magnets
Veerle Keppens 107

High Throughput Analysis of the Low Dose Radiation Transcriptome
Michael A. Langston 111

West Virginia

West Virginia University

Direct Utilization of Coal Syngas in High Temperature Fuel Cells
Ismail Celik 115

Land Reclamation for Bioenergy: Genomics of Adaptation of Populus to Marginal Sites
Stephen P. DiFazio 123

Hydrogen Absorption in Pd-based Nanostructures
David Lederman 124

Wyoming

University of Wyoming

New Catalysts for Ionic Hydrogenations
Dean M. Roddick 127

Author Index 130

Participant List 131

DOE EPSCoR ANNUAL PROGRAM REVIEW AND WORKSHOP 2008
U.S. Department of Energy
Experimental Program to Stimulate Competitive Research (DOE-EPSCoR)

Hosted by Oak Ridge National Laboratory

Oak Ridge, Tennessee
July 22-24, 2008

AGENDA

Tuesday, July 22, 2008

American Museum of Science and Energy

5:00 – 6:00 p.m.	Early Registration (Bus will pick up at hotels at 5:00 p.m.)
6:00 – 8:00 p.m.	*Opening Session* Introductions, Announcements, and Keynote Address Light food and cash bar (6:00 – 7:00 p.m.)
7:00 – 8:00 p.m.	*Keynote Speaker* – **Isiah M. Warner**, Vice Chancellor, Office of Strategic Initiatives and Boyd Professor and Philip W. West Professor of Analytical and Environmental Chemistry, Louisiana State University, Baton Rouge, Louisiana
8:00 p.m.	Buses depart for hotels

Wednesday, July 23, 2008

7:15 a.m.	Bus transportation from hotels to Tennessee Conference Center, ORNL

Oak Ridge National Laboratory

7:30 - 8:30 a.m.	Registration, Continental Breakfast, and Poster Set Up
Session I	**Energy Challenges and Opportunities** **Co-Chairs: Jim Roberto, ORNL and Tim Fitzsimmons, DOE**
8:30 – 8:50 a.m.	*Welcome and Introductory Remarks* – **Jim Roberto**, Deputy Director for Science and Technology, Oak Ridge National Laboratory (ORNL); **Tim Fitzsimmons**, Program Manager, U.S. Department of Energy EPSCoR Office

Wednesday, July 23, 2008 (continued)

8:50 – 9:15 a.m.	*Directing Matter and Energy: Five Challenges for Science and the Imagination* – **Teri W. Odom**, Associate Professor, Department of Chemistry, Northwestern University, Evanston, Illinois
9:15 – 9:40 a.m.	*EPSCoR Community Potential Contributions to Energy Research* – **William Gern**, Vice President, Office of Research & Economic Development, University of Wyoming, Laramie, Wyoming
9:40 – 10:05 a.m.	*Energy Frontiers Research Centers (EFRCs) & Single Investigator and Small Group Research (SISGR) Opportunities* – **Andrew Schwartz**, Program Manager, Experimental Condensed Matter Physics Research Activity, Materials Sciences and Engineering Division, Office of Basic Energy Sciences, U.S. Department of Energy, Washington, DC
10:05 – 10:15 a.m.	Discussion – Q & A
10:15 – 10:30 a.m.	Break
10:30 – 10:55 a.m.	*DOE Technology Programs at ORNL* – **Ken Tobin**, Director, Measurement Science and Systems Engineering Division, Oak Ridge National Laboratory, Oak Ridge, Tennessee
10:55 – 11:20 a.m.	*ORNL Science Programs* – **Jim Roberto**, ORNL
11:20 – 11:45 a.m.	Lunch (Boxed)
11:45 – 12:15 p.m.	*Luncheon Speaker I*: *Research Opportunities in Extreme Environments* – **Peter Tortorelli**, Acting Manager, Basic Energy Sciences Program, Materials Science and Technology Division, Oak Ridge National Laboratory, Oak Ridge, Tennessee
12:15 – 12:45 pm	*Luncheon Speaker II: Advanced Nuclear Energy Systems* – **David Hill**, Deputy Laboratory Director – Science and Technology, Idaho National Laboratory, Idaho Falls, Idaho
12:45 – 1:10 p.m.	Break
Session II	**Synchrotron Based Research** **Chair: Zhiqiang Mao**, Associate Professor, Department of Physics, Tulane University, New Orleans, Louisiana
1:10 – 1:35 p.m.	*New Opportunities in Ultrafast X-ray Science* – **Aaron M. Lindenberg**, Assistant Professor, Materials Science and Engineering, Stanford University and Photon Science, Stanford Linear Accelerator Center, Stanford, California

Wednesday, July 23, 2008 (continued)

1:35 – 2:00 p.m.	*Detailed Investigations of Interactions Between Ionizing Radiation and Neutral Gases* – **Allen Landers**, Assistant Professor, Department of Physics, Auburn University, Auburn, Alabama
2:00 – 2:15 p.m.	Break
Session III	**Neutron Scattering Research** **Chair: Takeshi Egami**, Professor, University of Tennessee, Knoxville, Tennessee
2:15 – 2:40 p.m.	*Neutron Scattering, Comic Strips, and Video Games* – **Roger Pynn**, Professor, Department of Physics, Indiana University, Bloomington, Indiana
2:40 – 3:05 p.m.	*Neutrons – A Tool for Scientific Research* – **Dean Myles**, Director, Neutron Scattering Science Division, Oak Ridge National Laboratory, Oak Ridge, Tennessee
3:05 – 3:30 p.m.	*Adventures in Neutron Magnetometry of Magnetic Multilayers* – **David Lederman**, Professor, Department of Physics, West Virginia University, Morgantown, West Virginia
3:30 – 3:45 p.m.	Break
Session IV	**ORNL Facility Tours**
3:45 – 5:30 p.m.	Concurrent Tours A. Center for Nanophase Materials Sciences and Spallation Neutron Source B. National Center for Computational Sciences C. High Temperature Materials Laboratory and Shared Research Equipment User Facility D. High Flux Isotope Reactor E. BioEnergy Science Center
Session V	**Posters and Networking**
5:30 – 7:30 p.m.	Poster Session, Tennessee Conference Center Lobby, Working dinner
7:30 p.m.	Buses depart for hotels

Thursday, July 24, 2008

7:15 a.m.	Buses from hotels to the ORNL Tennessee Conference Center

Oak Ridge National Laboratory

7:30 – 8:30 a.m.	*Registration* Continental Breakfast, Tennessee Conference Center Lobby Poster Session, Tennessee Conference Center Lobby
Session VI	**Bioenergy Research** **Chair: Jonathan Mielenz,** Manager, Oak Ridge National Laboratory Biomass Program, Biosciences Division, Oak Ridge National Laboratory
8:30 – 8:40 a.m.	Welcoming remarks for Day II and for Session VI – A Brief Introduction to the DOE Biomass Program. **Tim Fitzsimmons** and **Jonathan Mielenz**
8:40 – 9:05 a.m.	*Biofuels R&D: Process Options, Economics, Sustainability, and Pressing Issues* – **Mike Cleary,** Director, National Bioenergy Center, National Renewable Energy Laboratory, Golden, Colorado
9:05 – 9:30 a.m.	*The Bioenergy Centers* – **Reinhold Mann**, Associate Laboratory Director, Biological and Environmental Sciences, Oak Ridge National Laboratory, Oak Ridge, Tennessee
9:30 – 9:55 a.m.	*The Next Generation of Biofuels* – **Wayne Seames**, Associate Professor, Chemical Engineering Department, University of North Dakota, Grand Forks, North Dakota
9:55 – 10:20 a.m.	*Making of a Forest Biorefinery - The Maine Difference* –**Hemant P. Pendse**, Professor, Chemical and Biological Engineering Department, University of Maine, Orono, Maine
10:20 – 10:30 a.m.	Break
Session VII	**Nanoscience and Nanotechnology** **Chair: Mike Simpson,** Group Leader, Center for Nanophase Materials Science, Oak Ridge National Laboratory, Oak Ridge, Tennessee
10:30 – 11:00 a.m.	*DOE's Nanoscience Centers* – **Kathleen Carrado Gregar**, Manager, User and Outreach Programs, Center for Nanoscale Materials, Argonne National Laboratory, Argonne, Illinois
11:00 – 11:25 a.m.	*Incorporation of Novel Nanostructured Materials into Solar Cells and Nanoelectronic Devices* – **Rene Rodriguez**, Professor, Department of Chemistry, Idaho State University, Pocatello, Idaho

Thursday, July 24, 2008 (continued)

11:25 – 11:50 p.m.	*Materials and Architectures for Energy Conversion* – **Eric A. Grulke**, Professor, Department of Chemical and Materials Engineering and Associate Dean for Research and Graduate Studies, University of Kentucky, Lexington, Kentucky
11:50 – 12:20 p.m.	Lunch (Boxed)
Session VIII	**Opportunities for Collaboration** **Chair: Greg Snow**, Associate Professor, University of Nebraska, Lincoln
12:20 – 1:50 p.m.	Introductory Remarks, "Working with the National Laboratories," Panel – National Laboratory Presentations **Cynthia Jenks**, Ames Laboratory **Gretchen Cisco**, Brookhaven National Laboratory **Kathleen Carrado Gregar and Harold Myron**, Argonne National Laboratory **Mike Cleary**, National Renewable Energy Laboratory **Kelly Sullivan**, Pacific Northwest National Laboratory **Marie Garcia**, Sandia National Laboratory **David Hill**, Idaho National Laboratory **Jim Roberto**, Oak Ridge National Laboratory
1:50 – 2:20 p.m.	Questions and Discussion
2:20 – 2:30 p.m.	Break
2:30 – 3:30 p.m.	Break Out Sessions for Collaboration Discussions with National Laboratory and User Facility and Center Representatives **Cynthia Jenks**, Ames Laboratory **Gretchen Cisco**, Brookhaven National Laboratory (via speakerphone) **Kathleen Carrado Gregar** and **Harold Myron**, Argonne National Laboratory **Mike Cleary**, National Renewable Energy Laboratory **Kelly Sullivan**, Pacific Northwest National Laboratory **Marie Garcia**, Sandia National Laboratory **Jim Roberto**, Oak Ridge National Laboratory
3:30 – 4:00 p.m.	Summary and Closing Remarks, **Jim Roberto**, Oak Ridge National Laboratory, and **Tim Fitzsimmons**, U.S. Department of Energy
4:00 p.m.	Buses depart for hotels

DOE EPSCoR Program Directors Working Group
Satellite Meeting
Thursday, July 24, 2008

Doubletree Hotel

5:00 p.m.	DOE EPSCoR Program Directors Working Group Meeting
~1hr	Working Dinner, Doubletree Hotel
1 hr	*Tentative* -- New Implementation Award Presentations, **Principal Investigators of the pending new awards or their designees**
½ hr	DOE EPSCoR News and Updates, **Tim Fitzsimmons**, DOE EPSCoR Program Manager
<1 hr	Program Director Discussion/Questions and Answers
~8:30 p.m.	Adjourn

Poster List

Alabama

Auburn University

Energy Conservation for Real-Time Wireless Networks
Xiao Qin, Kiranmai Bellam, Adam Manzanares, and Xiaojun Ruan

Auburn University and Pacific Northwest National Laboratory

Effect of SOFC Interconnect-Coating Interactions on Coating Properties and Performance
Jeffrey W. Fergus

University of Alabama

Catalytic and Electrochemical Applications of Doped Carbon Supports: Interactions with Metal Nanoparticles
Wei An, Chethan Acharya, and C. Heath Turner

Exchange interactions in Epitaxial Intermetallic Layered Systems
Z. Lu, M. Walock, G.J. Mankey, Patrick. LeClair

University of Alabama, Huntsville

Guiding Light with Metal: Ultra-Long Range Surface Plasmon-Polaritons along Metal Strips
Junpeng Guo and Ronen Adato

Alaska

University of Alaska, Fairbanks and Los Alamos National Laboratory

Influence of Sea Ice on Arctic Marine Sulfur Biogeochemistry in the Community Climate System Model
Clara Deal (UAF), Meibing Jin (UAF), Scott Elliott (LANL), Elizabeth Hunke (LANL), Mathew Maltrud (LANL)

Colorado

National Renewable Energy Laboratory

NREL's Areas of Expertise
Michael Cleary

Iowa

Ames Laboratory

Poster #1: Partnership Opportunities with Ames Laboratory – Materials Research Poster
Poster #2: Partnership Opportunities with Ames Laboratory – Equipment/Facilities
Cynthia Jenks

Kansas

Kansas State University, Concordia University (Montreal, Quebec, Canada), and National Renewable Energy Laboratory

Low-Energy Chlorophyll States in the CP43 Antenna Protein Complex-Spectral Hole Burning and Simulations
Nhan Dang, Mike Reppert, Valter Zazubovich, Michael Seibert, Rafael Picorel, Ryszard Jankowiak

Kentucky

University of Louisville

Post Synthesis Modification of Metal Oxide Nanowires for Photoelectrochemical Hydrogen Production
Jyothish Thangala, Vidya Chakrapani, Suhail Malhotra and Mahendra K. Sunkara

Field Enhanced, Thermionic Emission using Conical Carbon Nanopipette Arrays
S. Dumpala, D. Mudd, A. Safir, R. W. Cohn, M.K. Sunkara and G.U. Sumanasekera

Synthesis of 3-Dimensional "Tree" Like Nanowire Architectures for Solar Energy Conversion
Chandrashekhar Pendyala and Mahendra K Sunkara

Band-Edge Entineered Hybrid Nanowire Structures for Dye Sensitized Solar Cells
S. Gubbala, V. Chakrapani, V. Kumar, and M.K. Sunkara

University of Louisville and Jozef Stefan Institute, Slovenia

α-Fe2O3 Nanowire Array Based Electrodes for Self-Driven Photoelectrochemical Cells
Boris Chernomordik, Uros Cvelbar, Vidhya Chakrapani, Miran Mozetic, Mahendra K. Sunkara

University of Kentucky

Evaporation-Driven Assembly and Tuning of Titania Thin Films with Orthogonally Aligned Hexagonal Channels
Stephen E. Rankin, Qingliu Wu, and Venkat R. Koganti

Louisiana

University of Louisiana, Lafayette

Resource and Energy-Aware Distributed Block-Based LU Decomposition on Wireless Sensor Networks
Sherine Abdelhak, Soumik Ghosh, Jared Tessier, Magdy Bayoumi

Object Detection, Extraction and Image Fusion using Hybrid Techniques in Video Sensor Networks
Mayssa Al-Najjar, Milad Ghantous, Soumik Ghosh, Magdy Bayoumi

Tulane University and Los Alamos National Laboratory

Novel Quantum Phenomena in Layered Ruthenates
Zhiqiang Mao, David Fobes, Zhe Qu, Jin Peng, Leonard Spinu, and Wei Bao

University of Louisiana at Lafayette, Louisiana State University, and Southern University at Baton Rouge

Ubiquitous Computing and Monitoring System (UCoMS) for Discovery and Management of Energy Resources
Michael Khonsari, Nian-Feng Tzeng, Magdy Bayoumi, Hongyi Wu, Christopher D. White, Dmitri Perkins, Boyun Guo, Mohammad Madani, Soumik Ghosh, Gabrielle Allen, Zhou Lei, Mayank Tyagi, Tevfik Kosar, Juan Lorenzo, Doug Moreman, Mathieu Kourouma

Maine

University of Maine

Implementation Phase I: Thermochemical Conversion of Woody Biomass to Fuels and Chemicals
Hemant P. Pendse, M. Clayton Wheeler, William J. DeSisto, Brian G. Frederick, and Adriaan van Heiningen

Montana

Montana State University

Linear Thermal Expansion Measurements with Sub-Atomic Resolution for the Study of Phase Transitions in Novel Condensed Matter Systems
John J. Neumeier, Mario S. da Luz, Richard Bollinger, David Cebulla, and Brandon McGuire

Nebraska

University of Nebraska

Rational Design of Molecular Ferroelectric Materials and Nanostructures
Stephen Ducharme, James M. Takacs, Zhonjin Ge, Rafal Korlacki, Jihee Kim, Jeremy Johnston, Yong Wang, Serge M. Nakhmanson

University of Nebraska and the Fermi National Accelerator Laboratory (Fermilab)

The Luminosity Measurement for the DZERO Experiment at Fermilab
Gregory R. Snow

Nevada

Desert Research Institute, Pacific Northwest National Laboratory, and Florida State University

Hydraulic Parameter Uncertainties in Heterogeneous Soils and Implications in Flow and Transport
Jianting Zhu, Ming Ye, Philip D. Meyer, Ahmed E. Hassan, Feng Pan, Yanxia Zhao, Shankar Neelakrishnan

University of Nevada, Las Vegas, Desert Research Institute, and University of Nevada, Reno

Investigations on the Fundamental Surface Reactions Involved in the Sorption and Desorption of Radionuclides
Sherry A. Faye, Richard Gostic, Julie Gostic, Craig Bias, Jen Fisher, Jim Bruckner, Duane Moser and Ken Czerwinski

New Hampshire

University of New Hampshire

Center for Integrated Computation and Analysis of Reconnection and Turbulence (CICART)
Kai Germaschewski and Amitava Bhattacharjee

New Mexico

Sandia National Laboratories

Sandia National Laboratories World-Class User Facilities
Marie L. Garcia

Oklahoma

Oklahoma Center for High Energy Physics

Oklahoma Center for High Energy Physics
Mike Strauss

Oklahoma State University and Oak Ridge National Laboratory

Electronic Properties of Quasi-One-Dimensional Nanostructures
John W. Mintmire, Thushari Jayasekera, Junwen Li, Pavan Pillalamarri, Vasantha Jogireddy, and Vincent Meunier

South Carolina

Clemson University

The Next Generation Solid State Power Conversion Materials
Terry M. Tritt, J. He, F. Drymiotis, T. S. Little, J. W. Kolis, M.S. Daw and A. Rao

South Dakota

South Dakota School of Mines and Technology

Poster 1: Crystallization of Titania Thin Films, Nanoparticles, and Nanofibers
S. P. Ahrenkiel, J. C. Johnson, S. Mishra, R. Chandrasekar, L. Zhang, H. Fong

South Dakota School of Mines and Technology and the National Renewable Energy Laboratory

Poster 2: Lattice-Mismatched III-V Epilayers for High-Efficiency Photovoltaics
S. P. Ahrenkiel , R. J. Nesheim, M. W. Wanlass, J. J. Carapella

University of South Dakota

Thermal Diffusion and Depleted Argon
Jason Spaans and Dongming Mei

Tennessee

ORNL/Partnerships

ORNL User Facilities
Jennifer Palmer

University of Tennessee and Oak Ridge National Laboratory

Resonant Ultrasound Study of the Vanadate Spinel MnV_2O_4
Y. Luan, V. Keppens, O. Garlea, R. Jin, and D. Mandrus

West Virginia

West Virginia University and Oak Ridge National Laboratory

Land Reclamation for Bioenergy: Genomics of Adaptation of Populus to Marginal Sites
Stephen P. DiFazio, Danielle Ellis, Gancho T. Slavov, Jonathan Cumming, and Timothy J. Tschaplinski

New Opportunities in Ultrafast X-ray Science

A.M. Lindenberg

PULSE Institute, Stanford Linear Accelerator Center, Menlo Park, CA, 94025

Department of Materials Science and Engineering, Stanford University, Stanford, CA, 94305

Email:aaronl@stanford.edu

The use of femtosecond x-ray pulses to probe materials opens up new windows into atomic-scale structural and electronic dynamics, through both x-ray scattering and x-ray absorption techniques. The advent of new sources of femtosecond x-rays at synchrotrons and free electron lasers (FELs) dramatically increases the range of accessible time-scales and length-scales that can be probed, and provides new methods for elucidating how atoms move in materials in real time [1-5]. In this talk, an overview of the state of the art experiments in the field of ultrafast x-ray science and an outlook on new experimental opportunities will be provided.

References

[1] A.M. Lindenberg, J. Larsson, K. Sokolowski-Tinten et al., "Atomic-scale visualization of inertial dynamics", Science **308**, 325 (2005).

[2] K.J. Gaffney, A.M. Lindenberg, J. Larsson et al., "Observation of structural anisotropy and the onset of liquid-like motion during the non-thermal melting of InSb", Phys. Rev. Lett., **95**, 125701 (2005).

[3] D.A. Reis and A.M. Lindenberg, "Ultrafast x-ray scattering in solids". In *Light Scattering in Solids IX*, Edited by M. Cardona and R. Merlin (2007).

[4] P.B. Hillyard, K. J. Gaffney, A.M. Lindenberg et al., "Carrier-density-dependent lattice stability in InSb", Phys. Rev. Lett., **98**, 125501 (2007).

[5] A.M. Lindenberg, S. Engemann, K.J. Gaffney et al., "X-ray diffuse scattering measurements of nucleation dynamics at femtosecond resolution", Phys. Rev. Lett., **100**, 135502 (2008).

Incorporation of Novel Nanostructured Materials into Solar Cells and Nanoelectronic Devices

Rene Rodriguez (PI),[1] Joshua Pak,[1] Alan Hunt,[2] Alex Punnoose,[3] Dmitri Tenne,[3] Leah Bergman,[4] Chris Berven,[4] You Qiang,[4] Pamela Shapiro,[5] Chien Wai [5]

[1] Dept. of Chemistry, Idaho State Univ., Pocatello, ID 83209
[2] Dept. of Physics, Idaho State Univ., Pocatello, ID
[3] Dept. of Physics, Boise State Univ., Boise, ID
[4] Dept. of Physics, Univ. of Idaho, Moscow, ID
[5] Dept. of Chemistry, Univ. of Idaho, Moscow, ID

I) Program Scope

This project interweaves the scientific studies of 10 research groups from the three universities in Idaho. These research efforts are focused in two main areas: 1) the magnetic and optical properties of bulk and nanoparticle semiconductors with possible applications to detectors and memory: and 2) studies of nanoparticle formation and the role of size, packing, and doping on optical, magnetic, and electronic properties of films of these materials. As part of these efforts, a primary aim of the program is to train both graduate and undergraduate students on a variety of experimental techniques at all three campuses, increasing their scientific aptitude while helping to knit the research efforts together.

II) Recent Progress

Magnetic and Optical Properties of Bulk and Nanoparticle Semiconductors

Several of the researchers are working on cooperative projects in this area. The research groups of Profs. Punnoose, Qiang, Bergman, Berven, and Tenne are working on the ferromagnetic and optical properties of doped ZnO and ZnO/MgO alloys. Profs. Pak, Rodriguez, and Shapiro have been looking at the synthesis and optical properties of ternary chalcogenide semiconductors, ($Cu(In,Ga)(S,Se)_2$), and Prof. Wai has been preparing metal sulfide nanoparticles.

Prof. Qiang's group has recently produced and investigated ferromagnetic doped ZnO nanoclusters. The optical and ferromagnetic properties of the clusters have been studied as a function of size and concentration. Studies are being done on ZnO nanoclusters doped with various percentages of Co ranging from 0.2% to 30%. PL, magnetic and magneto-resistance measurements were conducted on these doped nanoclusters and the optical and magnetic properties of the doped clusters were found to be dependent on the concentration of the dopants. A giant magnetoresistance effect was discovered in doped ZnO cluster films. Additionally core-shell ZnO-Zn nanoclusters have been synthesized and characterized.

The research group of Prof. Punnoose has measured the bandgap of ZnO nanoparticles in the 4 nm to 20 nm range produced under a controlled synthesis. ZnO nanoparticles encapsulated with a fluorescent dye have been synthesized for the first time as part of this project. Interactions between the dye and ZnO nanoparticles are being investigated with the aid of Dr. Tenne's group.

Prof. Bergman's group has concentrated on the $Mg_xZn_{1-x}O$ nanoalloy system. ZnO has bandgap ~ 3.4 eV while MgO has a bandgap ~ 7.5 eV; thus the $Mg_xZn_{1-x}O$ alloy system may give a new optically tunable family of wide-bandgap materials. $Mg_xZn_{1-x}O$ nanocrystals of average size ~ 30 nm and of the wurtzite structure were synthesized in Dr. Bergman's lab.[1] This family of materials has deep excitonic levels and as such exhibits superb luminescence efficiency at and above room-temperature. $Mg_xZn_{1-x}O$ is environmentally friendly and is a cost effective synthetic material for stable UV-optical applications. Measurements on the conductivity of the $Mg_xZn_{1-x}O$ nanoparticles by Prof. Berven's group indicate an anti-doping effect that results in a lowering of the electrical conductivity in MgZnO nanoparticles when exposed to H_2 gas. This is opposite what would be expected since H_2 is known to act as a dopant.

The synthesis of ternary chalcogenide nanoparticles has been accomplished using the single source precursor molecule, SSP like $(PPh_3)_2CuIn(SEt)_4$. The first synthesis of nanoparticles using these types of materials was performed at high temperatures (>180°C) by Dr. Hepp's group at NASA-Glenn in dioctyl phthalate solvent.[2] Prof. Pak's group has been able to control the size more effectively using a microwave synthesis, and with the inclusion of ethanedithiol, using hexane or pentane as a solvent, nanoparticles ranging from 2 to 15 nm have been synthesized at temperatures between 120 and 160°C.

More recently, $CuInS_2$, nanoparticles were synthesized in supercritical CO_2 by the research groups of Profs. Pak and Rodriguez. Nanoparticles ranging from 2nm to 6 nm were synthesized from 60-90°C. The average reaction time was roughly 20 minutes and good size control was obtained. Prof. Shapiro's group has also been able to synthesize ternary nanoparticles of $CuInS_2$, at room temperature, by exposing the SSP in dioctyl phthalate solvent to ultraviolet light.[3] The reaction time was much longer.

Dr. Wai's group has also been involved in producing nanoparticles using a water-in-supercritical CO_2 microemulsion process. Metal or metal sulfide nanoparticles of different sizes have been synthesized in supercritical CO_2 by adjusting the size of the water domain, the water to surfactant molar ratio (the W value) of the microemulsion.[4] Also, at a fixed W value, the density of the supercritical fluid affects the size of the nanoparticles synthesized by this method. By controlling both the W value and the density of the supercritical fluid phase, semiconductor nanoparticles (CdS and ZnS) of any size in the approximate range 1-10 nm can be synthesized.

Studies of Nanoparticle Formation and the role of Size, Packing and Dopant on Device Properties

The role of nanoparticle size and their packing are important fundamental considerations that, when fully addressed, will likely lead to better devices. Conduction and separation of the electrons and holes through nanoparticle semiconductors is essential to the use of nanoparticles in these types of devices. Studies to date have examined titanium dioxide and copper indium disulfide. To study the size and packing effects on conduction and electron-hole separation, a standard testing device may be constructed in addition to measuring the spectroscopic and electronic properties of the individual components.

Prof. Hunt's research group has focused on constructing a reproducible standard photovoltaic device for testing the effects of size, packing, and doping. The standard device chosen to study the effect of size and packing of the semiconductor TiO_2 is a dye sensitized solar cell, DSSC. Initially, the DSSC devices constructed varied by more than 100%, using the same dye and construction methods. Light source variation, construction methodology, and source meter connection were all examined and modified, and the cell-to-cell variation has been reduced to ~10%.

Prof. Qiang's group has the capability to prepare nanoparticles of tunable sizes from 3-100nm of titanium dioxide and titanium oxide black nanoparticles with their magnetron sputter gun. Some DSSCs made with these materials have been constructed and tested. DSSCs constructed with TiO black had low efficiencies. Prof. Rodriguez' group has prepared silver doped TiO_2 by mixing TiO_2 with silver nitrate followed by photoreduction upon exposure to UV light. Mixtures containing 0.25 and 1.0 % silver in TiO_2 were prepared. The silver-doped TiO_2 was used to construct DSSCs in three ways. In two of the preparations, only one layer of the two TiO_2 coatings contained silver. In the last prep, both coats utilized the silver doped TiO_2. The two coats of 0.25% silver-doped TiO_2 provided a more efficient solar cell than the control cell, which did not contain any silver.

Studies related to the mechanism nanoparticle formation of $CuInS_2$ from the SSP compounds were conducted by Prof. Shapiro's research group. Using the light activated decomposition and the SSP nanoparticle formation method mentioned previously, molecular clusters were isolated and a crystal structures were determined providing information towards drawing more of a conclusion regarding the formation of $CuInS_2$ from the SSP.

III) Future Plans

Magnetic and Optical Properties of Bulk and Nanoparticle Semiconductors

For the studies where ZnO has been encapsulated by at dye, investigation of the changes in the optical properties of oxide semiconductor nanoparticles when attaching different organic molecules on their surface will continue in collaboration with Dr. Tenne's group. Attempts will be made to tailor the carrier type and concentration in semiconductor oxide nanoparticles, using ferromagnetic semiconductor films to investigate how their magnetic, electrical and optical properties vary as a function of film thickness, substrate type, preparation temperature, and oxygen partial pressure.

Studies on the oxidation states of the doped cluster oxides are necessary as the oxygen plays a major role in the characteristics of the samples. For characterization of the samples, SQUID equipment as well as the facilities at EMSL like XRD, XPS, AFM, TEM, and PL measurements will be utilized. To improve the understanding and control of molecular level structural, optical, and transport properties of nanoclusters, further studies on the interfacial phenomena of surface and atomic composition for doped nanoclusters will be pursued.

For the $Mg_xZn_{1-x}O$ alloy system, goals are set on making high quality nanoalloys over the entire composition range. The optical and phonon dynamics of these nanoalloys will be examined including studies under extreme environments of temperature and pressure. Copper-doped MgZnO will also be synthesized for optomagnetic applications.

Supercritical carbon dioxide formation of both the ternary chalcogenides from SSPs and binary semiconductors from microemulsions will continue. Inclusion of Ga, Al, and Ag in these systems will be pursued in addition to Se. The possibility of the formation of alloys of these materials will be studied.

Studies of Nanoparticle Formation and the role of Size, Packing and Doping on Device Properties

Different sizes of TiO_2 and perhaps ZnO nanoparticles will be deposited in a thin film on conductive glass by You Qiang's group using the magnetron sputtering gun. The conductivity and morphology of the deposited films will be examined. The films will also be used to make DSSCs using N3 dye. The efficiencies of the solar cells will be compared to help quantify the effect of size and packing on the films. Films with several sizes of nanoparticles will also be synthesized to systematically alter the packing in the films

Novel dyes will also be synthesized to study the effect of changing the molecular structure on the DSSC characteristics. More metals will be examined for their potential as a dopant in the TiO_2 to enhance the electron conduction and production in DSSCs. Besides varying the work function of the metal, the effect of surface plasmons on the efficiency will also be taken into account.

Further attempts to characterize the kinetics and mechanism of photochemical decomposition of various single source precursors will continue. Additional studies of the SSP decomposition using Ga and/or Se containing SSPs performed by XRD and TEM will be used to characterize products from the photolysis of different precursors supplied by the Pak group containing Ag, Al, and a new bidentate chelating phosphine ligand.

IV) References

1. "Ultraviolet photoluminescence and Raman properties of MgZnO nanopowders", Leah Bergman, John L. Morrison, Xiang-Bai Chen, Jesse Huso, and Heather Hoeck, Appl. Phys. Lett. 88, 023103 (2006).

2. Nanocrystalline Chalcopyrite Materials (CuInS2 andCuInSe2) via Low-Temperature Pyrolysis of Molecular Single-Source Precursors Castro, S. L.; Bailey, S. G.; Raffaelle, R. P.; Banger, K. K.; Hepp, A. F. Chem. Mater. 15(16); 3142-3147 (2003).

3. Preparation of Ultrafine Chalcopyrite Nanoparticles via the Photochemical Decomposition of Molecular Single-Source Precursors Nairn, J. J.; Shapiro, P. J.; Twamley, B.; Pounds, T.; von

Wandruszka, R.; Fletcher, T. R.; Williams, M.; Wang, C.; Norton, M. G. NanoLett 2006, 6, 1218-1225.

4. "Continuous Tuning of CdS and ZnS Nanoparticle Size in a Water-in-Supercritical Carbon Dioxide Microemulsion", C. Fernandez and C. M. Wai, Europ. J. Chem. 2007, 13, 5838-5844.

V) <u>DOE Sponsored Publications</u>

1. Gardner, Joseph S.; Shurdha, Endrit; Lau, Lisa D.; Wang, Chongmin: Rodriguez, Rene G.; Pak, Joshua J., "Rapid and Size Control Synthesis of $CuInS_2$ Nanoparticles via Microwave Irradiation." J. Nanoparticle Research, 10, 633-641, (2008).
2. R. Rodriguez, D. Pulsipher, L. Lau, E. Shurdha, J. Pak, M. Jin, K. Banger, and A. Hepp "Pulsed-Spray Radiofrequency PECVD of $CuInS_2$ Thin Films", Plasma Chem. Plasma Proc. 26(2), 137. (2006)
3. Jiji Antony, You Qiang, Faheem Muhammad, Daniel Meyer, David E. McCready, and Mark H. Engelhard "Ferromagnetic semiconductor nanoclusters: Co-doped Cu_2O", Appl. Phys. Letters, 90, 013106 (2007)
4. Jiji Antony, You Qiang, "Cathodoluminescence from a device of carbon nanotube-field emission display with ZnO nanocluster phosphor", Nanotechnology 18 295703, (2007)
5. C. M. Wang, D. R. Baer, J. E. Amonette, M. H. Engelhard, Y. Qiang, and J. Antony, "Morphology and Oxide Shell Structure of Iron Nanoparticles Grown by Sputter-Gas-Aggregation", Nanotechnology, 18 255603 (2007)
6. C. M. Wang, D. R. Baer, J. E. Amonette, M. H. Engelhard, M. J. Antony, Y. Qiang, and J. Cazaux, "Electron Beam Induced Thickening of the Protective Oxide Layer around Fe Nanoparticles", Ultramicroscopy, 108 43-51(2007)
7. Y.F. Tian, J. Antony, R. Souza, Y. Qiang, S.S. Yan and L.M. Mei, "Giant positive magnetoresistance in Co-doped ZnO nanocluster films", Appl. Phys. Lett., in press, 2008
8. C. M. Wang, L. V. Saraf, and Y. Qiang, "Microstructures of ZnO films deposited on (0001) and r-cut α-Al_2O_3 using MOCVD", Thin Solid films, in press. 2008.
9. H. Wang, D. Wingett, M. H. Engelhard, K. M. Reddy, J. Layne, P. Turner, K. Feris, D. Tenne, C. Wang and A. Punnoose, "FITC Encapsulated Fluorescent ZnO Particles with Cell-specific Toxicity for Cancer Treatment and Biomedical Applications" Journal of Materials Science: Materials in Medicine, submitted, 2007
10. A. Thurber, K. M. Reddy, V. Shutthanandan, M. H. Engelhard, C. Wang, J. Hays* and A. Punnoose, "Ferromagnetism in chemically synthesized CeO_2 nanoparticles by Ni doping" Physical Review B, 76, 165206 (2007).
11. C. Van Komen, A. Thurber, K. M. Reddy, J. Hays and <u>A. Punnoose,</u> "Structure – magnetic property relationship in transition metal doped tin dioxide nanoparticles", Journal of Applied Physics (Accepted 2007)
12. Xiang-Bai Chen, Jesse Huso, John L. Morrison, and Leah Bergman, "The properties of ZnO photoluminescence at and above room temperature" J. Appl. Phys. 102, 116105 (2007).
13. Leah Bergman, Jesse Huso, and John Morrison, "Bandgap Engineered MgZnO Nanocrystals for Photoluminescence Applications Electrochemical Society, 212th Meeting Abstract book, 702, 1328 (2007).
14. Jesse Huso, John L. Morrison, Heather Hoeck, Erin Casey, Leah Bergman, T. D. Pounds, and M. G. Norton, "Low temperature LO-phonon dynamics of MgZnO nanoalloys" Appl. Phys. Lett. 91, 111906 (2007)
15. W. M. Hlaing Oo, M. D. McCluskey, J. Huso, and L. Bergman, "Infrared and Raman Spectros. of ZnO Nanoparticles Annealed in H_2," J. Appl. Phys., 102, 043529 (2007).
16. Carlos Fernandez and Chien M. Wai, "Continuous Tuning of CdS and ZnS Nanoparticle Size in a Water-in-Supercritical Carbon Dioxide Microemulsion", Europ. J. Chem., 13, 5838-5844 (2007).

Directing Matter and Energy: Five Challenges for Science and the Imagination

Teri W. Odom
Northwestern University, 2145 Sheridan Road, Evanston, IL 60208
todom@northwestern.edu

This talk will describe the five most important scientific questions and technical challenges identified by the Basic Energy Sciences Advisory Committee (BESAC) Grand Challenges report. This report was written in response to a request from the Office of Science and includes the input from numerous BESAC and Grand Challenges subcommittee meetings. These questions include: (1) How do we control material processes at the level of electrons? (2) How do we design and perfect atom- and energy-efficient synthesis of revolutionary new forms of matter with tailored properties? (3) How do remarkable properties of matter emerge from complex correlations of the atomic or electronic constituents and how can we control these properties? (4) How can we master energy and information on the nanoscale to create new technologies with capabilities rivaling those of living things? (5) How do we characterize and control matter away—especially very far away—from equilibrium?

Title: Making of a Forest Biorefinery - The Maine Difference

Dr. Hemant Pendse
Professor and Chair, Chemical and Biological Engineering Dept.,
Managing Director, Forest Bioproducts Research Initiative (FBRI)
University of Maine, Orono, ME 04469 USA
E-mail: pendse@maine.edu

Abstract

Biomass wastes derived from forestry, pulp and paper production and forest stewardship activities provide an abundant supply of feedstock to support biorefineries. UMaine's Forest Bioproducts Research Initiative (FBRI) has been established to *advance understanding about the scientific underpinnings, system behavior, and policy implications for the production of forest-based bioproducts that meet societal needs for materials, chemicals and fuels in an economically and ecologically sustainable manner.* The primary focus of the FBRI, funded by the National Science Foundation EPSCoR grant for Research Infrastructure Improvement is to develop and modify industrial processes, for co-production of fuels, chemicals and wood-fiber based products. Integrated biorefinery processing wood chips with hemicellulose extraction, prior to pulping, where xylan-rich aqueous extract can be used to produce fuels, chemicals, and bioplastics, while the partially treated woodchips are converted into market pulp is a promising platform. This is made possible with the use of the patent pending technology for controlled and selective pre-extraction of hemicelluloses from wood and while preserving the fiber to make the same amount of pulp of the same quality. A partnership involving University of Maine (UMaine), RSE Pulp & Chemical (RSE) and American Process Incorporated (API) has been selected for a grant of up to $30 million from the US Department of Energy to design, build and operate a small scale commercial biorefinery in Old Town, Maine. The proposed biorefinery facility will be installed in an existing pulp mill in Old Town, Maine, and will produce fuel ethanol and other chemicals from wood extract.

Adventures in Neutron Magnetometry of Magnetic Multilayers

David Lederman
Department of Physics, West Virginia University, Morgantown, WV 26506-6315
David.Lederman@mail.wvu.edu

Abstract

Neutron scattering is an invaluable tool for characterizing magnetic materials as a result of the relatively strong interaction between the neutron's spin and the magnetic moments in the material of interest. In particular, neutron scattering can be used to measure the depth profile of the magnetization in magnetic thin films and multilayers by measuring grazing angle reflectivity. In other cases, neutron diffraction can be used to determine the lateral size of antiferromagnetic domains. Over the past ten years, my group at West Virginia University has used neutron scattering to help solve various problems related to magnetic multilayers, including the importance of interface vs. bulk spin-dependent scattering in giant magnetoresistance (GMR),[1,2] the relation between exchange bias blocking temperature and the Néel temperature in ferromagnetic/antiferromagnetic bilayers,[3] and the measurement of antiferromagnetic domains in exchange-biased ferromagnetic/antiferromagnetic bilayers,[4] among others. These experiments have yielded knowledge about the behaviour of materials relevant to magnetic storage technology (i.e., hard disks and non-volatile magnetic memory) that could someday be used to fabricate novel magnetoelectronic devices.

References

[1] T. Charlton, D. Lederman, and G. Felcher, "Temperature Dependence of the Magnetoresistance of Co/Re Superlattices", in *Applications of Ferromagnetic and Optical Materials, Storage and Magnetoelectronics*, Vol. 674 of *Materials Symposium Proceedings*, edited by B. J. H. Stadler, K. Bussmann, W. Egglehoff, and E. S. Murdock, (Materials Research Society, Pittsburgh, 2001), p. T1.4.1.

[2] T. Charlton, D. Lederman, S. M. Yusuf, and G. P. Felcher, "Anisotropy of the sublattice magnetization and magnetoresistance in Co/Re Multilayers on $Al_2O_3(11\underline{2}0)$", *J. Appl. Phys.* **85**, 4436 (1999).

[3] H. Shi, D. Lederman, K. V. O'Donovan, and J. A. Borchers, "Exchange Bias and Enhancement of Néel Temperature in Thin NiF_2 Films", *Phys. Rev. B* **69**, 214416 (2004).

[4] M. R. Fitzsimmons, D. Lederman, M. Cheon, H. Shi, J. Olamit, I. V. Roshchin, and I. K. Schuller, "Antiferromagnetic domain size and exchange bias", *Phys. Rev. B* **77**, 224406 (2008).

Effect of SOFC Interconnect-Coating Interactions on Coating Properties and Performance

Jeffrey W. Fergus
Auburn University
Materials Research and Education Center
275 Wilmore Laboratories, Auburn, AL 36849
jwfergus@eng.auburn.edu

I. Program Scope

Solid oxide fuel cells (SOFCs) are a promising technology for high-efficiency, low-emission energy conversion. The high operating temperature of SOFCs improves the tolerance to fuel type and purity, so that SOFCs can be used with a wide variety of fuels, including those derived from biological sources, such as swithgrass and poultry litter, which are widely available in the state of Alabama. The higher temperature, however, also accelerates unwanted reactions, which places stringent requirements on the materials used. This project addresses one of these high temperature materials challenges – specifically, protective ceramic coatings for metallic interconnects.

The project is a collaborative effort between Auburn University and Pacific Northwest National Laboratory (PNNL), where protective coatings for metallic SOFC interconnects have been successfully developed. However, the reasons for the good performance are not completely understood. Improved understanding of the transport properties and stability of successful coatings can guide further improvements in coating performance. Auburn University's role is to perform fundamental thermodynamic and kinetic studies on the successful coating systems with the objective of providing a basic understanding of the protection provided by the coatings and use this understanding to identify approaches for the development of improved coatings for SOFC interconnects.

II. Recent Progress

Project has not yet started.

III. Future Plans

The protective coating provides three major functions, which are illustrated in Figure 1. One function is to reduce the growth rate of the scale on the interconnect alloy by limiting the supply of oxygen, which requires low oxygen-ion conductivity. The coating is also in electrical series with the electrochemical cell, so it must have good electrical conductivity to minimize electrical resistance and the associated ohmic overpotential. In addition, coatings are used to reduce chromium volatility, so the coating must have a low chromium solubility and/or diffusivity to provide a barrier to outward transport of chromium. Simultaneously satisfying all these requirements is a challenge, since the objective is to both increase (high electrical conductivity) and decrease (low oxygen-ion conductivity and low chromium permeability) transport rates.

The project addresses three aspects of coating properties and performance: i) thermodynamics, ii) transport properties and iii) physical properties. The thermodynamic aspects include phase equilibria, crystal structure stability and chemical activity. The transport properties to be evaluated include conductivity (electronic and ionic) and diffusion rates. The physical properties

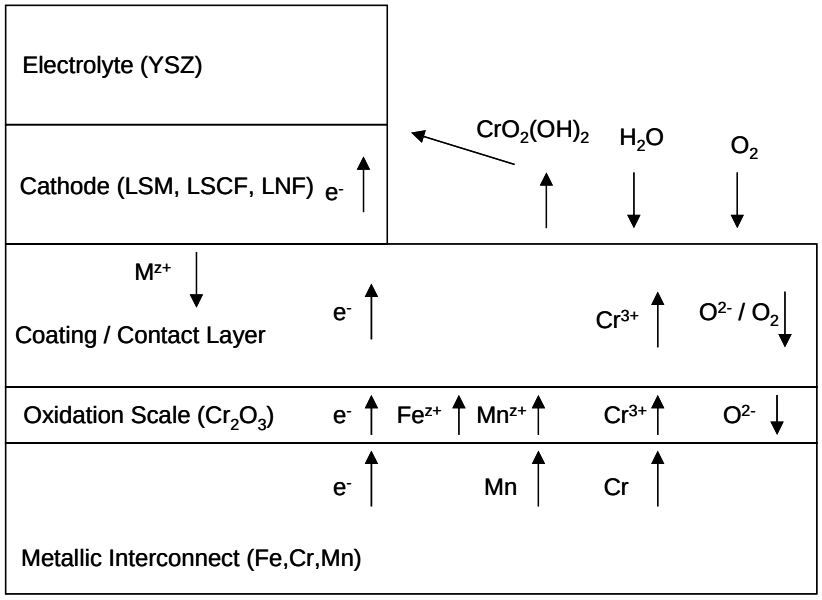

Figure 1. Schematic of transport in coating.

are those that are important for coating performance, such as the coefficient of thermal expansion (CTE) and fracture toughness. These aspects will be evaluated first for the original coating composition and then the effects of interaction of the coating with other fuel cell components will be evaluated. In addition to evaluating the degree of interaction, the impact of the interaction on coating performance will be determined by preparing bulk analogues of the compositions expected after the interaction occurs. Characterization of these bulk analogues will provide valuable information for evaluating any changes in the performance after interaction with other components. Finally, the results will be used to identify compositions with potentially improved performance and these promising compositions will be similarly evaluated. This knowledge and understanding will allow coatings to be designed so that the expected compositional changes during operation increase the conductivity in an amount that offsets the increase in resistance due to growth the chromia scale. In this case, the coating electrical resistance, and thus the associated overpotential, will be constant with time, so fuel cell performance will not degrade during operation.

The initial focus of the project will be on the spinel $(Mn,Co)_3O_4$, which is the most promising coating material identified by PNNL. One important issue for SOFC interconnect coating materials is the solubility and diffusivity of chromium in the coating. The Mn-Co-O phase diagram in Figure 2 shows that the spinel phase (S) can exist for all compositions of $(Mn,Co)_3O_4$, but not for all temperatures [1]. For the composition that has shown the best performance as a coating, $Mn_{1.5}Co_{1.5}O_4$, the cubic spinel is stable between 700ºC and 1200ºC. At higher temperatures, the cations are reduced to lower oxidation states and the rocksalt structure forms, while at lower temperatures a tetragonal form of the spinel structure (Hausmannite) forms. Cooling $Mn_{1.5}Co_{1.5}O_4$ slowly from above 700ºC results in a two-phase (cubic + tetragonal) mixture, but with rapid quenching a single-phase tetragonal structure can form [2,3]. Transmission electron microscopy shows the formation of twins in the tetragonal phase indicating a martensitic transformation that could possibly result in improved toughness [4]. The phase stability also depends on oxygen partial pressure and the spinel structure is stable to lower oxygen partial pressure as the manganese content increases [5].

The primary interaction of concern for the coating material is with chromium. The manganese-chromium spinel ($MnCr_2O_4$) is stable in typical SOFC operating temperatures and has a range of stoichiometry [6,7]. Cobalt can replace manganese in this structure to form a $(Mn,Co)Cr_2O_4$ solid solution, which is in equilibrium with Cr_2O_3 at 1300ºC [8]. The interconnect coating will likely be in contact with the spinel formed on the alloy surface, so the most relevant equilibrium is between the $(Mn,Co)_3O_4$ and $(Mn,Co)Cr_2O_4$ solid solutions. A phase diagram with this equilibrium is not available, but this region in the Mn-Co-Cr-O system is shown schematically in Figure 3. All corners of this region have the spinel structure, so interaction is possible. However, chromium is not observed in a $Mn_{1.5}Co_{1.5}O_4$ coating [9,10], which suggests that the solubility of chromium is low. Phase separation can occur in spinel systems, such as in the Mn-Co-Fe-O system [11], so the two solid solutions may not mix. However, it also may be possible that chromium does dissolve in the $(Mn,Co)_3O_4$, but then diffuses at a sufficiently low rate such that the steady-state between diffusion through the coating and volatilization from the surface maintains the chromium content below the solubility limit. Characterization of the phase equilibria in this system will be performed to determine

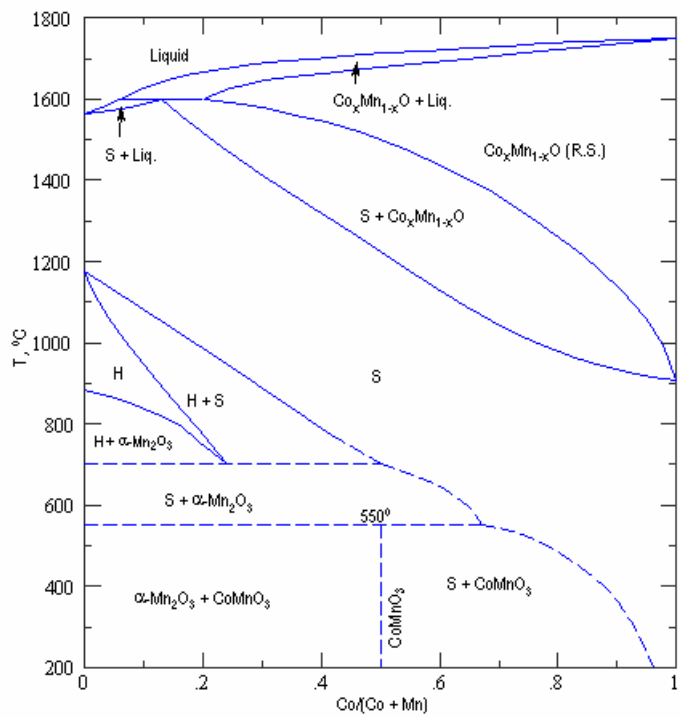

Figure 2. Co-Mn-O equilibrium phase diagram [1].

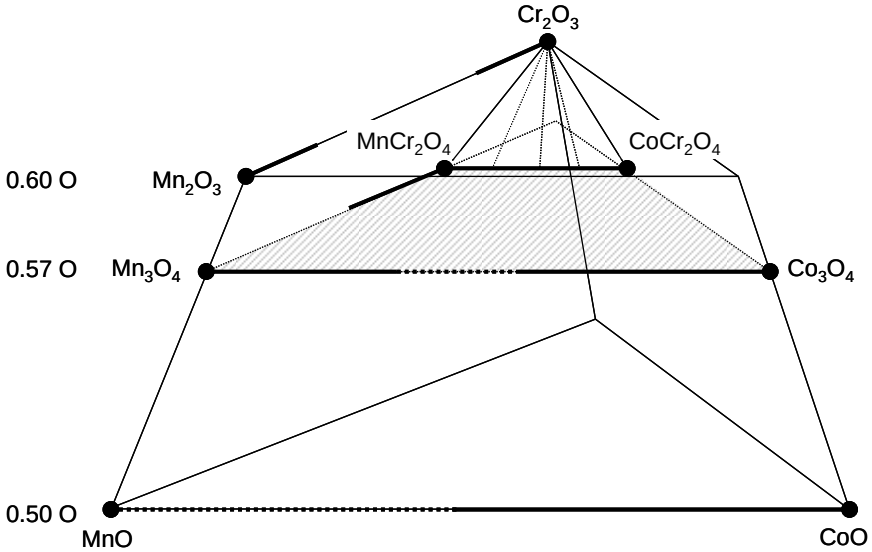

Figure 3. Mn-Co-Cr-O simplified schematic phase diagram.

whether it is the solubility limit or the diffusivity or both that provides the good coating performance.

In an SOFC, the interconnect coating is part of the electrical circuit so electrical conductivity is important. The conductivity of $MnCo_2O_4$ is higher than that of $MnCr_2O_4$ [10,12] and the highest conductivity for $(Mn,Co)_3O_4$ spinels is for the composition with a 1:1 cation ratio (*i.e*. $Mn_{1.5}Co_{1.5}O_4$) [4]. The reason for the maximum in conductivity is not known, but it corresponds to the minimum in the free energy of mixing [13]. One of the factors in the conductivity is the cation valence, which will determine the electron charge carriers. In the case of $(Mn,Co)_3O_4$, although manganese tends to have the higher valence, both cations can have +2 or +3 valence, so mixing of valences (Co^{+2}/Co^{+3} and Mn^{+2}/Mn^{+3}) occurs [13,14]. The proportion of Co^{3+} increases with increasing manganese content [15,16] and for a 1:1 ratio of the two cations, as in $Mn_{1.5}Co_{1.5}O_4$, the average valence must be +2.67. This is apparently beneficial for either the number or mobility of charge carriers, since the 1:1 ratio has the highest conductivity. The addition of chromium in the $(Mn,Co)_3O_4$ spinel could affect the conductivity, but this has not been reported, so conductivity behavior of $(Mn,Co)_3O_4$ doped with chromium, and other potential contaminants, will be characterized in this project.

References

1. Figure 09570: $CoO-MnO-Mn_2O_3$, ACerS-NIST Phase Equilibria Diagrams (American Ceramic Society, Westerville, OH and the U.S. Secretary of Commerce Washington DC, 2005).
2. E. Vila, R.M. Rojas, J.L. Martín de Vidales and O. García-Martínez, *Chem. Mater.* **8** (1996) 1078-1083.
3. J.L. Martín de Vidales E. Vila, R.M. Rojas and O. García-Martínez, *Chem. Mater.* **7** (1995) 1716-1721.
4. Z. Yang, G.-G. Xia, X. Sun, M. Chou, X.S. Li, G.D. Maupin, Z. Nie, S.P. Simner, J.W. Stevenson and P. Singh, 5th International Fuel Cell Science, Engineering & Technology, New York, NY, June 18-20, 2007.
5. Figure 10341: $CoO-MnO-Mn_2O_3$, ACerS-NIST Phase Equilibria Diagrams (American Ceramic Society, Westerville, OH and the U.S. Secretary of Commerce Washington DC, 2005)
6. I.-H. Jung, *Solid State Ionics* **177** (2007) 765-777.
7. Figure 10655: $MnO-Cr_2O_3-Mn_2O_3$, ACerS-NIST Phase Equilibria Diagrams (American Ceramic Society, Westerville, OH and the U.S. Secretary of Commerce Washington DC, 2005)
8. N. Koc and M. Timucin, *J. Am. Ceram. Soc.* **88**[9] (2005) 2578-2585.
9. Z. Yang, G. Xia and J.W. Stevenson, *Electrochem. Solid-State Lett.* **8**[3] (2005) A168-A170.
10. Z. Yang, G.-G. Xia, H.-H. Li and J.W. Stevenson, *Int. J. Hydrogen Energy* **32**[16] (2007) 3648-3654.
11. Figure 10211: $CoO-Co_2O_3-Fe_2O_3-Mn_2O_3$, ACerS-NIST Phase Equilibria Diagrams (American Ceramic Society, Westerville, OH and the U.S. Secretary of Commerce Washington DC, 2005)
12. X. Chen, P.Y. Hou, C.P. Jacobson, S.J. Visco and L.C. De Jonghe, *Solid State Ionics* **176**[5-6] (2005) 425-433.
13. A. Navrotsky, *J. Inorg. Nucl. Chem.* **31** (1969) 59-72.
14. H.S.C. O'Neill and A. Navrotsky, *Am. Minerol.* **69** (1984) 733-753.
15. E. Rios, P. Chartier J.-L. Gautier, *Solid State Sci.* **1**[5] (1999) 267-277.
16. J.L. Gautier, E. Ríos, M. Gracia, J.F. Marco and J.R. Gancedo, *Thin Solid Films* **311** (1997) 51-57.

IV. DOE Sponsored Publications

Project has not yet started.

DOE-EPSCoR: Exchange Interactions in Epitaxial Intermetallic Layered Systems

P. LeClair* (PI) and G.J. Mankey (co-PI)
Department of Physics and MINT Center
Box 870324
University of Alabama
* pleclair@ua.edu

The goal of this research is to develop a fundamental understanding of the exchange interactions in epitaxial intermetallic alloy thin films and multilayers, including films and multilayers of Fe-Pt, Co-Pt and Fe-P-Rh alloys deposited on MgO and Al_2O_3 substrates. Our initial results have revealed that these materials have a rich variety of ferromagnetic, paramagnetic and antiferromagnetic phases which are sensitive functions of composition, substrate symmetry and layer thickness. Epitaxial antiferromagnetic films of FePt alloys exhibit a different phase diagram than bulk alloys. The antiferromagnetism of these materials has both spin ordering transitions and spin orienting transitions.

The objectives include the study of exchange-inversion materials and the interface of these materials with ferromagnets. Our aim is to formulate a complete understanding of the magnetic ordering in these materials, as well as developing an understanding of how the spin structure is modified through contact with a ferromagnetic material at the interface. The ultimate goal is to develop the ability to tune the phase diagram of the materials to produce layered structures with tunable magnetic properties. The alloy systems that we will study have a degree of complexity and richness of magnetic phases that requires the use of the advanced tools offered by the DOE-operated national laboratory facilities, such as neutron and x-ray scattering to measure spin ordering, spin orientations, and element-specific magnetic moments. We plan to contribute to DOE's mission of producing "Materials by Design" with properties determined by alloy composition and crystal structure. We have developed the methods for fabricating and have performed neutron diffraction experiments on some of the most interesting phases, and our work will serve to answer questions raised about the element-specific magnetizations using the magnetic x-ray dichroism techniques and interface magnetism in layered structures using polarized neutron reflectometry.

Through application of these techniques to understand the materials fabricated in our laboratory, we will employ a tight feedback loop to tailor the magnetic properties on demand. Developing the ability to control magnetic anisotropy is essential for creating the next generation of magnetic storage media (for hard disks, for example), where individual bit sizes have already become smaller than 100nm in the largest dimension. Still smaller bits and higher storage density will require the ability to exquisitely tailor magnetic media properties at the atomic level, the ultimate goal of our study.

THE $FePt_3$ SYSTEM

Fe_xPt_{100-x} alloys have been the subject of various theoretical and experimental investigations because of their rich spin structure, which is strongly dependent on composition, ordering, and temperature[1,2,3,4,5,6,7,8,9]. For example, the chemically disordered $Fe_{25}Pt_{75}$ phase is ferromagnetic, whereas the chemically ordered $FePt_3$ phase is antiferromagnetic. The ordered $FePt_3$ structure is similar to $AuCu_3$,[29] the $L1_0$ structure, whereas that of the disordered alloy is face-centered cubic. Disordered $FePt_3$ has each lattice site occupied by, on average, 1/4 Fe and 3/4 Pt atoms, where the fractions represent probabilities (atomic fractions).

The antiferromagnetic properties of Fe_xPt_{100-x} ($23 \leq x \leq 29$) alloys in bulk form were studied extensively for the first time with neutron diffraction by Bacon.[10] Fe moments in stoichiometric $FePt_3$ order as alternating ferromagnetic sheets in the (110) planes as shown in Fig. 1 and exhibited a very high moment ($3.3\mu_B$ / Fe atom). Bulk $FePt_3$ exhibits an antiferromagnetic spin structure with a wave vector $Q_1 = 2\pi/a$ (1/2 1/2 0) below T_{N1}~160 K. In Fe-rich alloys ($x > 26$) a spin structure transition to a second antiferromagnetic phase, $Q_2 = 2\pi/a$ (1/2 0 0) occurs below T_{N2}~100 K. The Q_1 phase is completely suppressed when x reaches 30.[11,12]

We were the first to show that thin films exhibit different antiferromagnetic ordering than bulk samples.[45] This neutron diffraction study of the antiferromagnetism in epitaxial Fe_xPt_{100-x} thin films (x = 27 and 30) grown on MgO(110) and *a*-axis sapphire substrates showed that for $FePt_3$ (111) grown on *a*-axis sapphire, the spin structure is the same as the bulk with x = 27 film exhibiting transitions at T_{N1} and

T_{N2}[45]. The film with x = 30 exhibited similar behavior with respect to the appearance of a Q_2 phase with increasing Fe content but with a T_{N2}~140 K. In sharp contrast, $FePt_3$(110) grown on MgO(110) exhibited only the Q_1 phase for both compositions x = 27 and x = 30 with the onset of the Q_2 phase suppressed. The differences in behavior of the $FePt_3$ films grown on MgO(110), compared to those grown on *a*-axis sapphire and bulk $FePt_3$, are attributed to higher strain and defect densities in the former. Also, the (110) surface in $FePt_3$ has an uncompensated surface at $T_{N2} < T < T_{N1}$ (1/2 1/2 0 ordering), whereas it is compensated for $T < T_{N2,}$ where the spins have a (1/2 0 0) ordering.[45,46] The ability to make a spin compensated or uncompensated surface in the same antiferromagnet by varying the temperature or substrate is a compelling reason and a useful starting point to study the complicated problem of exchange bias. Additionally, the low Néel temperature of $FePt_3$ (160 K) makes it possible to perform field-cooling experiments where the sample is cooled through the Néel temperature under the application of a field while avoiding temperatures where structural changes may occur at the interface.

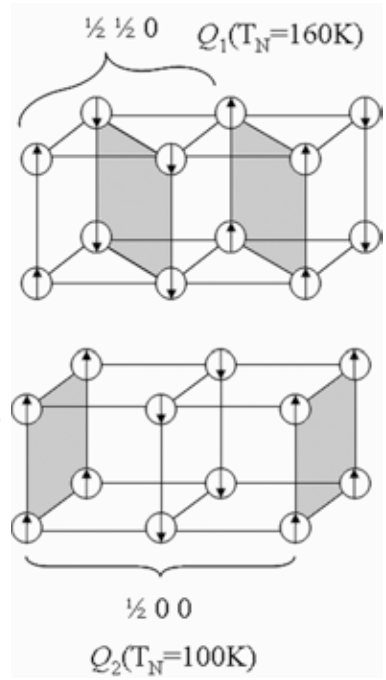

FIG. 1: Two types of antiferromagnetic ordering in $FePt_3$. The arrows represent the direction of Fe moments. The Pt atoms that reside on the face centers are omitted.

THE FE-PT-RH SYSTEM

Early measurements of FeRh alloys showed an abrupt increase in the magnetization as the temperature increased through a critical value.[13] The critical temperature increased with increasing Rh content, and a temperature hysteresis associated with the magnetization change was observed. X-ray diffraction studies showed that the crystal structure was a CsCl type above the transition temperature, whereas at a lower temperatures it partially transformed to an fcc structure. Later work revealed that the CsCl structure was retained below the transition temperature and through the transition temperature, but the volume of the unit cell expanded rapidly by 1%.[14] Neutron diffraction showed that the first-order phase transition corresponded to an antiferromagnetic to ferromagnetic transformation in the ordered phase.[15] Bulk FeRh shows an (1/2 1/2 1/2) antiferromagnetic spin ordering.[16] The (1/2 1/2 1/2) antiferromagnetic ordering has been confirmed in the case of thin films as well and is responsible for exchange coupling in bilayer films.[17]

The magnetic structure of bulk alloys of bcc and fcc of FeRh and FePt are well studied, in addition to the centered tetragonal, ct, structures of Fe-Pt-Rh. The substitution of Rh by Pt in the FeRh system was found to be effective in stabilizing the ct phase over a wide range of Pt concentrations [24 mani]. $Fe_{50}Pt_{50-x}Rh_x$ alloys provide a model system that can be used to study the effects of lattice distortion on the magnetic properties. An interesting property of the $Fe_{50}Pt_{50-x}Rh_x$ ct alloys is the first-order phase transition from the low-temperature AF state to the high-temperature paramagnetic or ferromagnetic state. $Fe_{50}Pt_{50-x}Rh_x$ (x~10) exhibits a temperature dependent antiferromagnetic-ferromagnetic-paramagnetic triple point near 400 K as shown in Fig. 2.2.1.[18]

We have determined the temperature and composition dependent spin structure of $Fe_{50}Pt_{50-x}Rh_x$ films grown on MgO(100). In particular, we have used a combination of neutron diffraction and SQUID magnetometry in alloy thin films, to determine that thin film exhibit similar phase transition behavior. We have clearly demonstrated that both antiferromagnetic and ferromagnetic phases are accessible and we have produced a sample which transforms from antiferromagnetic to ferromagnetic phases simply by varying the temperature.

NEUTRON DIFFRACTION OF FEPTRH

A rather fortuitous fact in our favor is the key difference between neutron and x-ray diffraction in the Fe-Pt-Rh system. The difference between x-ray and neutron diffraction patterns Fe-Pt-Rh alloys is remarkable. For Cu K-alpha radiation. the x-ray structure factors[19] for Fe, Rh, and Pt are 25, 45 and 74 e atom^{-1} and for thermal neutrons, the coherent scattering cross sections[26] are 9.45, 5.87 and 9.6 fm,

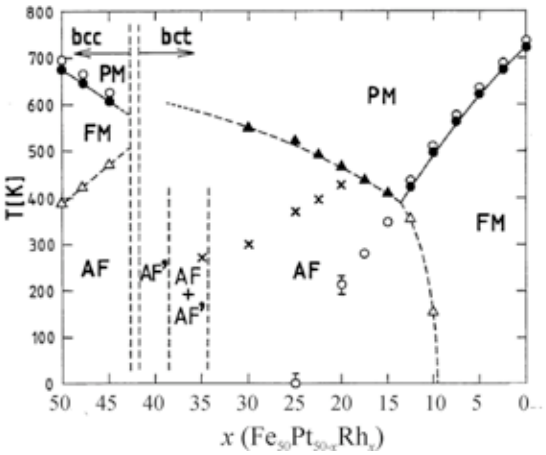

Fig. 2: Phase diagram of bulk $Fe_{50}Pt_{50-x}Rh_x$ alloys. The crosses represent the temperatures at which the antiferromagnetic susceptibility shows an anomaly.[52]

respectively. The intensities for superlattice peaks due to chemical ordering are determined by the chemical contrast,[29] which for x-rays is the difference in chemical structure factors and for neutrons is the difference in coherent scatting cross sections. The intensities of the structural peaks are determined from the averages of these quantities. Thus for an equi-atomic alloy of FePt, the superlattice x-ray diffraction peaks have nearly equal intensity as the structural peaks. For neutrons, the superlattice peaks have only 1% of the intensity of the structural peaks. However, coherent neutron scattering also includes magnetic scattering which for Fe, approximately 1/3 of the chemical scattering cross section given above. Since the magnetic scattering is a gauge of the magnetization component perpendicular to the scattering plane of the neutrons, significant diffraction intensity of the (100) type is a direct measure of the ferromagnetic ordering perpendicular to the scattering plane of the neutron diffraction experiment.

The preliminary neutron diffraction experiments show that the antiferromagnetic phases with x in the range of 10 - 30 exhibit a variety of spin ordering phases with (1/2 1/2 1/2), (1/2 1/2 3/2), and (1/2 0 0). Of particular importance for this proposal is the fact that we have produced a film which exhibits both ferromagnetic and antiferromagnetic phases simply by varying the temperature. This corresponds to drawing a vertical line through the phase diagram in Fig. 2 at a value of x = 10. Applying a high magnetic field can also significantly reduce the transition temperature. For example, with no magnetic field applied the sample exhibited a transition temperature of 350 K, and the application of a 12 T magnetic field resulted in a reduction in the transition temperature to 225 K as shown in Fig. 3. For these experiments we have exploited the fact that the intensity of the (100) diffraction peak is a probe of the ferromagnetic ordering, so we have also confirmed the increase of ferromagnetic ordering as the antiferromagnetic order decreases.

OPEN QUESTIONS AND FUTURE PLANS

We have recently produced epitaxial FePtRh films on MgO substrates that exhibit a variety of antiferromagnetic phases as a function of temperature as determined by neutron diffraction experiments (Sect. 2.2). In addition, we have shown that films produced by magnetron sputtering have sufficient compositional control and crystallinity to afford the ability to tune the temperature of the phase transition. Experiments on these samples performed in collaboration with Dr. J. Lee Robertson at the High Flux Isotope Reactor and Dr. Dieter Lott at the ILL neutron facility as a function of applied magnetic field indicate that the transition can also be driven with magnetic field. However, some fundamental questions regarding the spin structure and phase transition behavior remain to be investigated. These questions include:

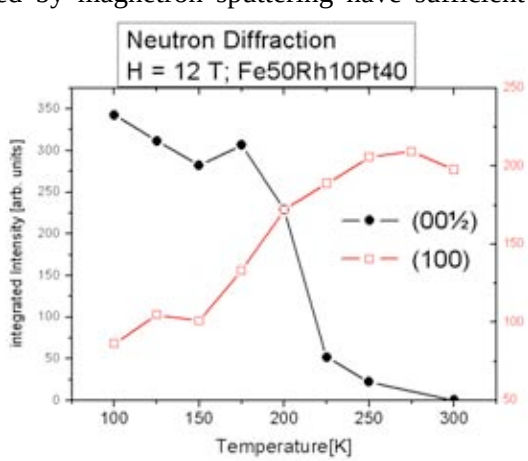

Fig. 2.3: Integrated intensity of the AF (001/2) and AF (100) reflections vs. temperature at H=12 Tesla.

What is the effect of grain size on the phase transition behavior?

When approaching a magnetic phase transition, the correlation length tends to infinity, and long-range fluctuations become increasingly important.[20] More importantly, the key role of long-range fluctuations means that close to a phase transition, sample inhomogeneity such as grain boundaries can dominate the observed behavior. The

presence of grain boundaries provides an upper wavelength finite size cutoff for fluctuations, which in turn can broaden the temperature profile of the phase transition.

What are the effects of compositional gradients on the spin ordering behavior? Composition gradients can be produced both laterally across the substrate surface and vertically through the film thickness. A further complication arises when considering one species may preferentially migrate to the grain boundaries. Given the strong compositional dependence of magnetic ordering in FePtRh, one could envision that spatial variation of composition could lead to, *e.g.*, ferromagnetic grain boundaries in an otherwise antiferromagnetic film, which could have profound effects on both spin ordering *and* the phase transition behavior.

What is the arrangement of the sublattice magnetizations? While our previous experiments using neutron probes have given a wealth of information about the spin ordering and magnetic phase transitions in FePtRh, neutrons alone cannot easily give information about *unique* non-collinear spin arrangements, nor can they uniquely determine the moments on each atom (Fe, Pt, and Rh). This is the raison d'être for the proposed x-ray dichroism experiments, which will allow us to extra the magnitude of the spin and orbital moments on each atomic site. Combined with neutron data, we can uniquely reconstruct the complete atomic magnetic structure.

Can we determine the spin wave dispersion in ferro- *and* antiferro- magnetic FePtRh? One ultimate goal is to perform *inelastic* neutron measurements on antiferromagnetic thin films to determine spin dynamics. This will answer a fundamental question - can spin dynamics be controlled with defects, as exchange biasing appears to be?

To date, spin wave dispersion in an antiferromagnetic *thin film* has yet to be measured. Among the main reasons for this are insufficient neutron flux and analyzer sensitivity (leading to prohibitively long acquisition times), and a lack of longer wavelength neutrons to more effectively probe the larger magnetic unit cell. Recent upgrades at HFIR to include a cold neutron source have led to dramatic improvements in flux *and* longer wavelength neutrons. When sufficiently high quality samples are realized, a primary goal will be to measure the spin wave dispersions in both the FM and AFM phases of FePtRh.

---

[1] N. I. Kulikov, J. Phys. F **15**, 1139 (1985).
[2] N. I. Kulikov, E. T. Kulatov, and S. I. Yakhimovich, J. Phys. F **15**, 1127 (1985).
[3] K. Sumiyama, and G. M. Graham, Solid State Commun. **19**, 241 (1976).
[4] S. Takahashi, and K. Ikeda, Phys. Rev. B **28**, 5225 (1983).
[5] S. Takahashi, and A. Y. Takahashi, J. Phys. **4**, L339 (1992).
[6] S. Maat, Master's Thesis, The University of Alabama, 2000.
[7] S. Maat et al., J. Magn. Magn. Mater. **265**, 1 (2003).
[8] M. Kohgi, and Y. Ishikawa, J. Phys. Soc. Jpn. **49**, 985 (1980).
[9] Y. Tsunoda, D. Tsuchiya, and Y. Higashiyama, J. Phys. Soc. Jpn. **72**, 713 (2003)
[10] G. E. Bacon, and J. Crangle, Proc. R. Soc. London A **272**, 387 (1963).
[11] S. Maat et al., Phys. Rev. B **63**, 134426 (2001)
[12] V.V. Krishnamurthy, I. Zoto, G.J. Mankey, J.L. Robertson, S. Maat, E.E. Fullerton, I. Nwagwu, and J.K. Akujieze, Phys. Rev. B. **70**, 024424 (2004)
[13] M. Fallot, Ann. Phys. (Paris) **10**, 291 (1938)
[14] F. d. Bergevin, and L. Muldawer, Compt. rend. **252**, 1347 (1961).
[15] F. d. Bergevin, and L. Muldawer, Bull. Am. Phys. Soc. **159**, 6 (1961).
[16] G. Shirane, R. Nathans, and C. W. Chen, Phys. Rev. **134**, A1547 (1964).
[17] J. U. Thiele, S. Maat, J. L. Robertson, and E. E. Fullerton, IEEE Trans. Magn. **40**, 2537 (2004).
[18] S. Yuasa, H. Miyajima, and Y. Otani, J. Phys. Soc. Jpn. **63**, 3129 (1994); S. Yuasa et al., J. Phys. Soc. Jpn. **63**, 855 (1994).
[19] Chantler, C.T., J. Phys. Chem. Ref. Data 29(4), 597-1048 (2000); and Chantler, C.T., J. Phys. Chem. Ref. Data 24, 71-643 (1995).
[20] Landau, L.D. and Lifshitz, E.M., Statistical Physics Part 1, vol. 5 of Course of Theoretical Physics, Pergamon, 3rd Ed. (1994).

THEORETICAL INVESTIGATION OF PLASMA JETS DRIVEN MAGNETO-INERTIAL FUSION USING SMOOTH PARTICLE HYDRODYNAMICS

Jason Cassibry, Seth Thompson, and Nilesh Dhote[1]

Propulsion Research Center, University of AL-Huntsville, Huntsville, AL 35899, USA

Abstract

Our 3 year program is a research effort to assess the effectiveness of using smoothed particle hydrodynamics (SPH) to theoretically investigate plasma jets driven magnetoinertial fusion (PJMIF) research. We have performed ignition studies using Lindl-Widner diagrams, and liner implosion in cylindrically and spherically symmetric geometries are underway. These diagrams have been recently applied to exergy and energy rate balances for plasma-driven magnetoinertial fusion (PLMIF). The motivation for this study is to identify possible PLMIF ignition regions, and to guide the implosion studies conducted with the 1D, 2D, and 3D tools. To conduct this study, we developed a new alpha deposition model from Monte Carlo simulations for spherical magnetized targets and a finite difference thermal conduction model for heat transfer from the target to the liner. We identified conditions in which the thermal conduction from the target is sufficient to burn a narrow layer of the plasma liner, which significantly contributes to the fusion output power. Because of perceived interest in our alpha deposition model, we are now extending this work to more realistic magnetic field topologies and providing results to the community. Implosion dynamics are currently being studied with a 3D hydro code based on Smooth Particle Hydrodynamics (SPH). We have made comparisons of the SPH model with another MHD code and with analytical test cases. Studies in merging of jets in 3D geometries are now underway. The physics at the interface play an important role in the peak pressure which can be reached during implosion. Specifically, the downshift in Mach number causes a reduction in pressure, but the effect improves as the number of jets is increased. Scaling laws will be shown for peak pressure and confinement time vs. the number of jets.

Keywords: magnetoinertial fusion, smooth particle hydrodynamics, plasma physics

Sponsors: Propulsion Research Center and DOE.

[1] **Contact author:** Nilesh Dhote, UAHuntsville, OB432, Huntsville, AL 35899, USA, nileshdhote27@gmail.com, (256) 603-3866

"Influence of Sea Ice on Arctic Marine Sulfur Biogeochemistry in the Community Climate System Model"

Clara J. Deal (PI), Meibing Jin (co-PI),
Scott Elliott*, Elizabeth Hunke*, and Mathew Maltrud*
International Arctic Research Center, University of Alaska Fairbanks
PO Box 757340, 930 Koyukuk Drive, Syun-Ichi Akasofu Bldg. 408
Fairbanks, Alaska 99775-7340
*Los Alamos National Laboratory, Los Alamos, New Mexico
deal@iarc.uaf.edu

I.) Program Scope:

To reduce the uncertainty in predictions from global climate models (GCMs), important model components of the climate system, such as feedbacks between arctic marine biogeochemistry and climate need to be reasonably and realistically modeled. Biological activities in high latitude seas are an important source of dimethylsulfide (DMS) to the atmosphere [1]. Warming temperatures and diminishing sea ice could dramatically alter oceanic emissions of DMS in the arctic [2]. Because a large change in the release of DMS to the atmosphere has the potential to affect the climate system through changes in cloud properties, it is important to improve our understanding of and our ability to predict the dynamics of volatile sulfur at high latitudes. Prediction of oceanic DMS emissions in this region requires (1) understanding/diagnosing the marine processes that control the variability of seawater reduced-sulfur concentrations, and (2) incorporating the results into prognostic, process-based modeling approaches capable of projecting the dynamics of DMS into the next few decades.

The climate-relevance of DMS results from its oxidation in the atmosphere to various sulfur constituents (i.e. sulfuric acid, sulfur dioxide, and methane sulfonic acid or MSA) that play important roles in atmospheric chemistry, the production and evolution of aerosols, and consequently the radiative balance of the atmosphere and climate. Shaw [3] was the first to suggest a role for sulfur in climate regulation, hypothesizing that sulfate aerosols derived from DMS cool the Earth by reflecting incoming solar radiation. Charlson et al. [4] further postulated a feedback loop between phytoplankton, DMS, cloud albedo, and climate, whereby temperature impacts DMS emissions (Figure 1).

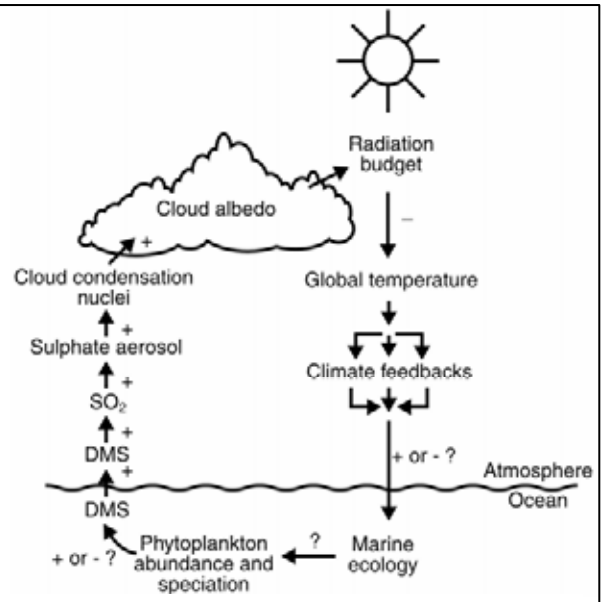

Figure 1. Mechanism by which marine algae may influence cloud albedo through production of DMS (Figure from Surface Ocean Lower Atmosphere Study Science Plan).

The hypothesized DMS-cloud albedo-climate feedback is especially germane to the arctic because clouds influence the physical processes most important for the warming of the Arctic and the melting of sea ice. Also, ice algae are among the major producers of the DMS precursor, dimethylsufoniopropionate, or DMSP. Utilizing observations of DMS(P) in and near sea ice, we will include DMS production by sea ice algae and DMS biogeochemistry in an ice-ocean ecosystem model.

This research first involves model development to improve the representation of marine sulfur biogeochemistry in the arctic, where a disproportionate warming is expected (ACIA 2004). Initial phases are followed by global-scale simulations to understand/diagnose the control of sea-ice-related processes on the variability of DMS dynamics. This study will help build GCM predictions that quantify the relative current and possible future influences of arctic marine ecosystems on the global climate system. An ice-ocean model embedded in a GCM will also provide a tool to help integrate, synthesize and ultimately improve understanding of arctic marine ecosystems under the growing risk of environmental degradation due to increased marine transport and access to arctic resources.

Our overall research objective is to improve the treatment of arctic marine biogeochemistry in the Community Climate System Model (CCSM). Our focus is on capturing the observed DMS distributions using mechanistic models (and not attempting to fully capture all the feedbacks at this point).

Our specific research objectives are:

1) Develop a state-of-the-art ice-ocean DMS model for application in climate models, using observations to help constrain the most crucial parameters.

2) Improve the global marine sulfur model used in CCSM by including DMS biogeochemistry in the Arctic.

3) Assess how sea ice influences DMS dynamics in the arctic marine environment and predict how it will do so in the future.

II. Recent Progress:

Funding of this DOE EPSCoR project will begin in July 2008.

III.) Future Plans:

Working closely with the Climate Ocean Sea Ice Model (COSIM) team at Los Alamos National Laboratory, our goal is to add sea-ice algae and arctic DMS production and related biogeochemistry to the global Parallel Ocean Program (POP) coupled to the

LANL sea ice model (CICE). Focus is on development of an ice-ocean ecosystem DMS biogeochemistry module for the POP-CICE component of CCSM. Since proximity to sea ice can also influence water column DMS biogeochemistry, the existing CCSM ocean DMS module will need to be modified for the Arctic; e.g. addition of sea ice means new habitats in the model, i.e. SIZ, MIZ, and open leads.

In this project, temporal and spatial modeling scales will range from as short as days for the prognostic 1-D modeling, up to interannual cycles over decades on the global scale. Rather than reconfigure domains and boundary conditions, we will focus our analysis of the global-scale output on the Arctic Region. Initial model development will be conducted on the local scale corresponding to the DMS and DMSP observations and biophysical mooring data (e.g. fixed location, cruise transect), and thus will provide a link between the observations and process studies, and larger temporal and spatial scales. For model development extending basin-wide and beyond, satellite data will allow model calibration (e.g. chlorophyll a concentration) over wider areas and longer time periods (e.g. monthly). Working across a range of scales will allow us to effectively bridge small-scale processes and the GCM.

The foundation for our biogeochemical modeling will be the union of three ocean ecosystem models: the CCSM standard Doney-Moore-Lindasy (DML) as currently augmented with a global reduced sulfur cycle (Moore et al. 2004; Chu and Elliott 2007), the 1-D ice ecosystem–water column ecosystem model of Jin et al. (2006b; 2007), and the 1-D water column DMS model of Jodwalis (Deal) et al. (2000). The latter two were designed for northern high latitudes.

We plan to modify the DML coding to include features from the PIs' 1D ice-ocean ecosystem model such as ice-related functional types and interactions of biogeochemical variables between sea ice and the underlying marine environment. Thereby the different ecosystem models will be merged/joined in the way of new coding. The plan for connecting the models for different media is as follows. First, ice algal biogeochemistry routines will be developed in CICE, driven by prescribed nutrient fields. Second, the enhanced open water ecology will be developed. *Phaeocystis* and other Arctic specific organisms will be added to the DML in POP. They will be represented initially in the way that DML treats the coccolithophores in the global ocean, through implicit segregation from the broad category "small phytoplankton" bin. Once Arctic ecosystem structures are complete in both CICE and POP an intermediate step is to merge the two. The computational coupling for this is already in place. CICE will import ice bottom nutrient concentrations from POP and POP will receive organisms and detritus from the ice above. Los Alamos is working on this set of linkages right now. They should be in place before the project begins.

During the last year of the project we plan to transfer routines developed for the representation of high-latitude biogeochemistry in POP-CICE into the full CCSM. At a minimum, multi-year demonstration runs are planned as a prelude to later work. We will attempt to run the coupled CCSM several decades into the future in order to document the effects of reducing sea-ice extent on the general biogeochemistry as well as the sulfur

cycle. An alternative that we may consider would be to draw upon IPCC-like forcing scenarios from offline.

IV.) References:

1. A. Kettle and M.O. Andreae, J. Geophys. Res., **105**, 26,793 (2000).
2. A.J. Gabric, B. Qu, P. Matrai and A.C. Hirst, Tellus, **57B**, 391 (2005).
3. G.E. Shaw, Climatic Change, **5**, 297 (1983).
4. R.J. Charlson, J.E. Lovelock, M.O. Andreae and S.G. Warren, Nature, **326**, 655 (1987).
5. Surface Ocean-Layer Science Plan http://www.uea.ac.uk/env/solas/
6. ACIA, Impacts of a Warming Arctic: Arctic Climate Impact Assessment. Cambridge University press (2004).
7. J.K. Moore, S.C. Doney, and K. Lindsay, Global Biogeochem. Cycles, **18**, GB4028 (2004).
8. S. Chu and S. Elliott, In: *Environmental Sciences and Environmental Computing* Volume **3**, P. Zannetti, D.Rouson and S. Elliott (Editors), FiatLux Publications and The EnviroComp Institute (2007).
9. M. Jin, C.J. Deal, J. Wang, N. Tanaka, and M. Ikeda, J. Geophys. Res. **111**, C03002, doi:10.1029/2005JC002994, (2006b)
10. M. Jin, C. Deal, J. Wang, V. Alexander, R. Gradinger, S. Saitoh, T. Iida, Z. Wan, and P. Stabeno, Geophys. Res. Lett., **34**, L06612, doi:10.1029/2006GL028849, 2007.
11. C.M. Jodwalis (Deal), R.L. Benner and D.L. Eslinger, J. Geophys. Res., **105**, 14,387 (2000).

Key Physical Mechanisms in Nanostructured Solar Cells

Principal Investigator: Valeria Gabriela Stoleru, Materials Science and Engineering, University of Delaware, Newark, DE; gstoleru@udel.edu

Co-Principal Investigator: Christiana B. Honsberg, Electrical and Computer Engineering, University of Delaware, Newark, DE; honsberg@udel.edu

Collaborator: Andrew G. Norman, National Renewable Energy Laboratory, Golden, CO; andrew_norman@nrel.gov

A. Pancholi and Y. C. Zhang, S. B. Bremner, University of Delaware, Newark, DE

Program Scope

Nanostructured solar cells (which include quantum dot-, quantum well-, and quantum wire-based solar cells) have attracted significant interest in the last years since they offer the promise of both high efficiency and low cost, offering a way to reach thermodynamic efficiency limits as well as cost targets. High efficiency is achievable because nanostructured materials are required in order to implement several advanced-concept solar cell designs which can exceed the one-junction Shockley-Queisser efficiency limit, such as solar cells utilizing the two-photon absorption and impact ionization processes, and the quantum well or the intermediate band solar cells, which incorporate multiple-energy levels. Further, through processes such as up/down conversion, they allow improvement of existing solar cell efficiencies through the addition of coatings containing nanostructures. In addition to their efficiency potential, nanostructured solar cells offer the promise of low cost since substantial research efforts are focused on developing low-cost self-assembly approaches to fabricate nanostructures.

While generalized efficiency-limit calculations have predicted high efficiencies for nanostructured solar cells, substantial fundamental theoretical and practical challenges still exist in their implementation. A central factor hindering their development are the theoretical and experimental unknowns regarding the excitation, recombination, and transport properties of solar cells. The goal of the proposed research is to theoretically and experimentally investigate the excitation, recombination, and transport properties on which advanced concept solar cells rely. More specifically, the goal of the project is to study physical and loss mechanisms in nanostructured solar cells and determine properties of nanostructures required for high efficiency solar cells, develop optimum solar cell designs based on experimental findings, and determine the most important properties of the nanostructured solar cells. The proposed work primarily focuses on nanostructure based intermediate band solar cells using multiple absorption and multiple energy level approaches.

Recent Progress

Study of Electronic Coupling in Vertically-Stacked (In,Ga)As QD Structures

In order for the mini-bands or intermediate bands to form, the QD wave functions **must** overlap, and thus the dots have to be positioned close enough to allow tunneling. The two structures analyzed consist of multilayer (In,Ga)As QDs. Sample A was grown by molecular beam epitaxy (MBE) on (001) GaAs substrate. The structure contains 50 periods of QDs formed by the deposition of 2.7 monolayers (MLs) of InAs, separated by ~ 45 nm GaAs barriers and capped by a 250 nm GaAs layer. Sample B was grown by metal-organic chemical vapor deposition

(MOCVD) on (311)B GaAs. This structure consists of 50 periods of QDs formed by the deposition of 6.1 ML of $In_{0.47}Ga_{0.53}As$, separated by 10 nm GaAs barriers and capped by a 300 nm GaAs layer. Although the two structures were grown by different techniques, the question we are trying to address here, which is "*how the QD layer separation affects the electronic coupling between the dots*" should have little dependence on the epitaxial growth technique.

Figure 1 shows the excitation density dependent PL spectra at 4.4 K. For sample A, the PL peak energy remains almost constant with increasing excitation density. The PL intensity increases

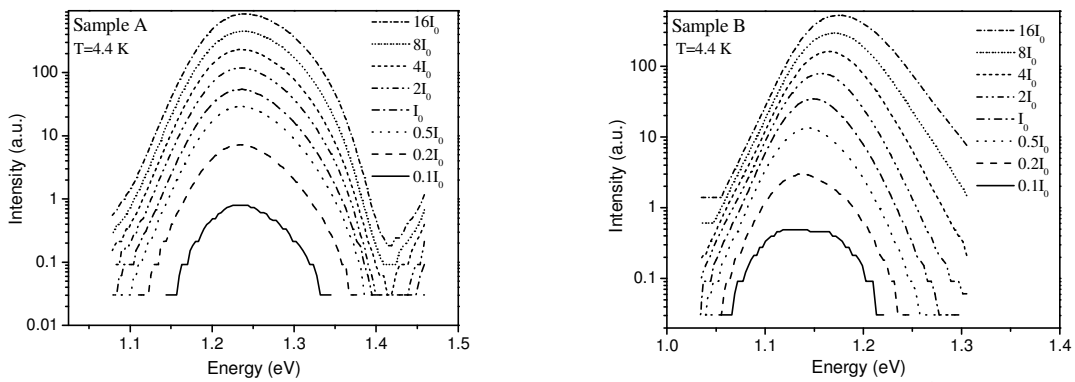

Figure 1: Excitation density dependent PL spectra taken at 4.4 K (I_0=13.2 W/cm^2).

linearly across most of the detection energy range, except at very low excitation density, where the defect effects are more pronounced. This indicates that the carriers are randomly captured and localized in QDs with different sizes. For sample B, the PL peak shows a blueshift of ~ 39 meV when the excitation density is increased from 1.3 to 211 W/cm^2; also, the PL intensity shows state filling-like behavior at lower energies. This can be attributed to the vertical electronic coupling of the dots in sample B, which allows for the incoherent tunneling of the carriers from a small to a large dot through the thin GaAs barrier. The tunneling process in sample B is favored due to the lower barrier thickness and the large volume of InGaAs QDs compared to that of the InAs QDs in sample A. The lateral tunneling is negligible due the large (> 50 nm) lateral spacing between the dots.

Effects of Strain-Compensated Ga(As,P) Barriers on Physical and Optical Properties of (In,Ga)As QDs

We studied the effect of strain compensation barrier on the structural quality, the electronic coupling between the dots, and the radiative lifetime in multilayer InGaAs QD structures grown on GaAs (311) B substrates by MOCVD. The intrinsic region of the samples consists of 50 periods of QDs formed by the deposition of 6.1 ML of $In_{0.47}Ga_{0.53}As$, separated by 10 nm Ga(As,P) barriers. The surface was capped by a 300 nm GaAs layer. The samples are different in the P composition of the barrier layer, which is nominally 0.8% (M1), 1.5% (M2), 14% (M3) and 18% (M4). The compressive strain in the InGaAs QDs is compensated by tensile strain in the Ga(As,P) barriers, and the P composition required to minimize the average strain is about 16%. Uncapped multilayer QD samples were also grown for atomic force

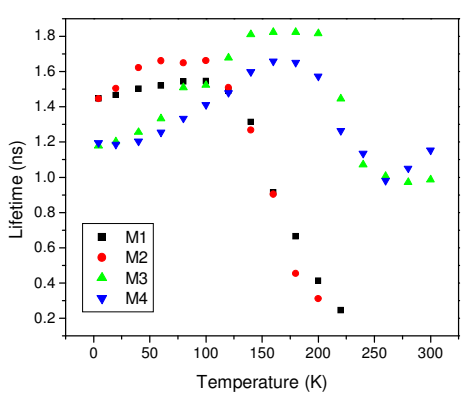

Figure 2: Temperature-dependent radiative lifetimes for samples M1, M2, M3, and M4.

microscopy (AFM) studies. We observed that the strain compensation effect induced by adding P into the barriers plays a significant role in improving the quality of the structures. The cross-sectional transmission electron microscopy (TEM) analysis (not shown here) shows high density of harmful dislocations being present in sample M1, due to the lattice mismatch between the QD material and the substrate. By contrast, negligible misfit or threading dislocations are present when the P composition in barrier was increased to 14% (M3). This observation was also verified by the high-temperature PL spectra, which showed an increase in the PL intensity for high P content samples by one order of magnitude. The low-temperature PL analysis revealed that the high P content samples have a higher PL peak energy, which can be explained by a smaller dot average size and a higher quantum confinement presented by the increased barrier height, and a narrower PL linewidth, which can be attributed to the strain balancing presence in these structures, which can improve the size distribution of the dots, as indicated by AFM analyses. The effects of structural quality and electronic coupling between the dots on the carrier dynamics were studied via TRPL. Figure 2 shows temperature-dependent TRPL spectra with constant excitation power of 56.25 W/cm^2. An increased radiative lifetime was found at room temperature in samples with higher P content in the barrier, which may be due to lower dislocation density as a result of strain compensation and/or strong carrier confinement in the QDs provided by the barrier.

Effects of Strain-Reducing Ga(As,Sb) Barriers on the Radiative Lifetime of InAs QDs

We proposed and analyzed a novel structure, in which the QDs are embedded in type-I/type-II barrier/matrix structures with long radiative recombination lifetimes both in the dots and in the barriers. The structures were grown by MBE on (001) GaAs and consist of 2 ML of InAs QDs sandwiched between GaAsSb strain-reducing layers (SRLs), and capped by a 50 nm GaAs layer. Samples Sb1 and Sb2 have symmetric bottom and top barriers with thicknesses of 20 nm, and 10 nm, respectively, while in sample Sb3 the barriers are asymmetric (30 nm on the bottom and 10 nm on the top of the dots).

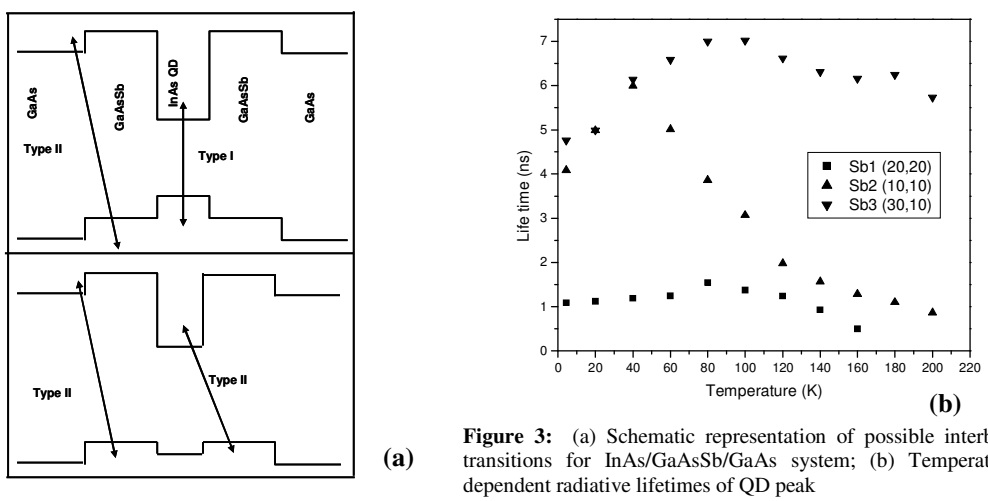

Figure 3: (a) Schematic representation of possible interband transitions for InAs/GaAsSb/GaAs system; (b) Temperature-dependent radiative lifetimes of QD peak

The Sb content in the barriers is about 12% in all samples, as measured by X-ray diffraction. According to our bandstructure calculations, this choice for the Sb content in the barriers should insure a negligible valence band offset between GaAsSb and InAs in bulk. We analyzed the effects of strain on the band alignment, which ultimately causes the QDs to act like either type-I or type-II, and the effects of the type-II SRLs on the dot carrier dynamics.

Temperature-dependent TRPL (Fig. 3b) reveals an initial increase in the carrier lifetime in the low temperature range for all samples, which is due to thermal recycling of the carriers to higher energy states and subsequent recombination into the ground state. The radiative lifetimes for barrier-related PL peaks in Sb2 and Sb3 were determined to be ~ 4-5 ns at 4 K. These decay times are larger than those observed in conventional type-I heterostructures, such as InGaAsP/GaAsP QWs, and are consistent with observed lifetimes in literature for type-II heterojunctions (i.e., spatially-separated electrons in the conduction band of the GaAs matrix combine with low energy GaAsSb valence band holes, leading to type-II transitions). Although a type-I interface is calculated for the bulk unstrained GaAs/GaAsSb (12% Sb) system, we believe that it is the complex strain in dots, barriers, and matrix, which ultimately allows for the transition from the bulk type-I into a type-II interface in the structures analyzed. This argument is further strengthened by the lifetime measurements. Sb1 shows relatively short lifetime (~ 1-2 ns) and we believe that the band alignment in Sb1, in which the GaAsSb barriers are thick and the dots are relatively large, is a type-I. Similar lifetimes on the order of 1-2 ns have been observed for type-I transitions in other InAs QD structures. The possible band alignments for these samples are schematically illustrated in Fig. 3(a).

Future Plans

The goal of the proposed project is to demonstrate physical mechanisms which have not been previously observed in high efficiency nanostructured photovoltaic solar cells, to experimentally characterize the structures and the devices in order to determine the impact and the causes of non-idealities, to develop models which include non-idealities and can be used to determine device design rules and optimum solar cell structures based on the new physical mechanisms, and finally, to experimentally implement optimized device structures. The research plan is divided into several components:

(1) Growth and characterization of quantum well and quantum dot nanostructures;

(2) Theoretical studies, growth and characterization of quantum well- and quantum dot-based devices, in order to facilitate the demonstration of radiative coupling between multiple quasi-Fermi levels in nanostructured multiple energy level solar cells;

(3) Theoretical studies, growth and characterization of devices in order to support the demonstration of: (a) transport of carriers in solar cells in which the nanostructures (quantum wells, quantum wires, or quantum dots) are spaced such that their wave-functions do not overlap, and (b) transport of carriers in closely-spaced quantum dot nanostructures;

(4) Modeling, growth, fabrication, and characterization of quantum dot- and quantum well-based solar cell devices.

Recent Publication

1. **A. Pancholi**, Y. C. Zhang, V. G. Stoleru, M. Hanna, and A. G. Norman, (In,Ga)As/Ga(As,P) quantum dot structures for solar cell applications – submitted to *Applied Physics Letters*.
2. **A. Pancholi**, J. Boyle, V. G. Stoleru, S. Bremner, and C. B. Honsberg, Effect of strain reducing Ga(As,Sb) barrier layer thickness on radiative lifetime of InAs quantum dots – submitted to *Applied Physics Letters*.
3. Y. C. Zhang, **A. Pancholi**, V. G. Stoleru, M. Hanna, and A. G. Norman, Optical anisotropy of InGaAs/Ga(As,P) quantum dots grown on GaAs (311)B substrates, *Applied Physics Letters* - **91**, 223109, (2007).
4. Y.C. Zhang, **A. Pancholi,** and V.G. Stoleru, Size-dependent radiative lifetime in vertically stacked (In,Ga)As quantum dot structures, *Applied Physics Letters*, **90**, 183104, (2007).

Center for Spintronics and Biodetection (CSB)

DOE Award: DE-FG02-07ER46374

John Q. Xiao (PI), Edmund Nowak, Yi Ji, Branislav Nikolić, James Kolodzey*, Shouheng Sun**

Department of Physics and Astronomy, University of Delaware, Newark, DE,
*Department of Electrical and Computer Engineering, University of Delaware, **
Department of Chemistry, Brown University, Providence, RI

I. Program Scope

The objectives of the Center for Spintronics and Biodetection (CSB) are: (1) Revealing fundamental physics of generation, manipulation, and detection of low dissipation spin current, (2) identifying and controlling fluctuations and noise in magnetic nanostructures to attain pico-Tesla magnetic field detectivity at low frequencies, (3) advancing magnetic nanotechnology for sensitive biodetection including synthesizing of stable monodisperse magnetic nanoparticles (NPs) with high moments for improved signal/noise ratio, and understanding of the interactions between functionalized NPs and the magnetic sensor's surface and biological molecules, and (4) education and mentoring of students and supporting State's science and technology developments

II. Recent Progress:

The fundamental physics behind spintronics consists of generation, manipulation, and detection of low dissipation spin current, which is one of important objectives in current program. Two experimental schemes have been used to investigate the fundamental physics: one is based on lateral non-local spin valves (NLSV) where the spin current is generated by passing current through non-local effect, the other is a vertical structures when spin current is generated by spin pumping with precessing ferromagnetic moment.

Non-local Spin Valves: An electron beam evaporator has been set up for the angle deposition technique which is an important step in the fabrication of non-local spin valves (NLSV). In addition, a variable temperature magneto-transport measurement system is in operation with an 8 Tesla magnetic field available. This system will be used for the measurement of non-local spin valve structures. A number of non-local spin valve devices have already been successfully fabricated (see Figure 1). Measurements are underway to characterize these devices.

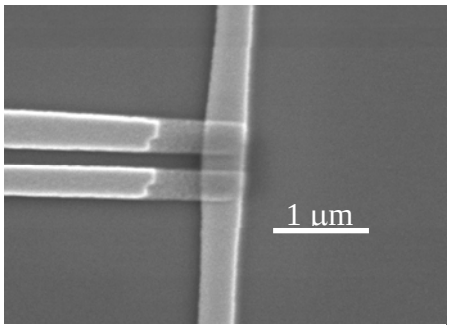

Figure 1. SEM picture of a non-local spin valve (NLSV) fabricated.

Microwave Assisted Magnetization Switching: With vertical structure, we are able to investigate the critical role of magnetization dynamics in spintronics. We have incorporated microwave into spin polarized transport measurements to study microwave assisted magnetization switching and understood the nonlinear FMR in magnetic thin films[6,8].

Gilbert Damping Enhancement: Gilbert damping enhance is an indirect way to probe the spin current pumped from a precession ferromagnet (FM) into neighboring nonmagnetic layer (NM). We have determined Gilbert damping constant in magnetic thin films by developing flip-chip FMR measurements with refined extraction procedure to eliminate the contributions from imperfection of the coplanar waveguide (CPW). With these instrument developments, we are able to observe Gilbert damping enhancement in spin valves (SVs) and magnetic tunnel junctions (MTJs). We found that the Gilbert damping constant is larger in the antiparallel configuration than in the parallel configuration in both SVs and MTJs. The observation cannot be explained with existing theories. The results have been submitted to APL [4].

Direct Electrical Detection of Spin Pumping Singal: We have also performed direct electric measurements on spin current by observing dc voltage from precessing magnetization in tunnel structures. We observed about μV dc voltage from the precessing magnetization of FeNi in Cu/FeNi/AlO_x/Al and Cu/FeNi/AlO_x/FeCo tunnel structures. Our results have reviewed new physics relating nonlocal magnetization dynamics in tunnel structures that cannot be explained by the existing theory. The results on the Cu/FeNi/AlO_x/Al structures have been published in Physical Review Letters [1].

Theoretical Development: Ref. [1] reported the observation of the voltage signal from a precessing ferromagnet we have provided theoretical support to show that conventional spin pumping theory [Rev. Mod. Phys. **77**, 1375 (2005)] cannot be directly applied to the experimental systems containing tunnel barriers. Our conclusion is based on the evaluation of the so-called spin mixing conductance G^{mix} for a tunnel barrier. This quantity allows to describe spin transport of the transverse components of spin (where magnetization of the FM layer defines longitudinal direction) and plays important role in both spin transfer torque and (its inverse) spin pumping by rotating. We used two-terminal set-up to calculate the reflection matrices entering the definition of G^{mix}. When the barrier is thick, we indeed find $\mathrm{Re}\left(G^{mix}\right)/G = 0.5$, while larger values are possible in very thin barriers. In addition, we also find sizable imaginary part of $\mathrm{Im}\left(G^{mix}\right)$, which is typically neglected in transparent FM/NM contacts but can plays important role in explaining recent experimental observation of sizable out of plane component of the spin transfer torque. However, these values cannot be reconciled with the fits of experimental data in Ref. [1] which require $\mathrm{Re}\left(G^{mix}\right)/G > 1$. For both spin pumping and spin torque in MTJs it would be important to investigate further properties of G^{mix} when the barrier has non-trivial spin-dependent interactions, such as magnetic impurities or spin-orbit coupling, and phases of reflection coefficients become non-trivial so that larger values could be expected.

MTJs with MgO barrier: It is critical to develop MTJs with high TMR value in order to achieve to pico-Tesla magnetic field detectivity. We have investigated the effects of crystal orientation, growth temperature, post-annealing, interface roughness and impurity states in MgO base MTJs. Room temperature tunneling magnetoresistance (TMR) value larger than 310% has been achieved. We have studied real-time evolution of TMR in CoFeB/MgO/CoFeB junctions during annealing. The TMR quickly developed at the early stage of the annealing, followed by a slow approach. The evolution of TMR was

correlated with the structural changes of the CoFeB electrodes and MgO barriers during the annealing [9].

Sensor Noise: We have extended electronic noise spectroscopy capabilities to 6 MHz. This is essential for characterizing both the shot noise and thermal magnetic noise in devices. We have derived a theoretical model for the noise performance of magnetic tunnel junction sensors. The model uses the empirical parameters for electronic and magnetic $1/f$ noise contributions that were obtained from our experiments. Our noise modeling has been incorporated in an Excel™ spreadsheet to enable rapid evaluation of the effect of changing the various sensor parameters. The evaluation enables rapid optimization of sensor performance. One of the most valuable aspects of the evaluation process is that it allows the user to avoid over-design in achieving some of the more difficult sensor goals. For example, it was found that the level of magnetic $1/f$ noise meant that TMR values in excess of 100% were so far into the regime of diminishing return as to be pointless. The outstanding scientific issues center on to what extent are magnetic fluctuations due to hysteresis. Preliminary data and analysis indicate that the fluctuations are in equilibrium and can be described reasonably well by a fluctuation dissipation theorem for the magnetization. Understanding the source of magnetic instabilities in the sensor is crucial for ultra-sensitivity.

Magnetic Tag: Our objective is to selectively immobilize magnetic nanoparticles onto the pre-printed Au dots on MTJ sensor surface. We passivated the silica surface by trimethoxy(octadecyl) silane, while leaving the Au part intact. A single strand DNA (ss-DNA) which is thiolated on one end and biotinylated on the other end, was incubated with the wafer to selectively immobilize ss-DNA onto the gold surface. Fe3O4 NPs were PEGylated and conjugated with Neutravidin and incubated with the ss-DNA functionalized Au dots to selectively immobilize these particles onto the gold surface via avidin-biotin interaction. Initial tests did not yield selective binding due likely to the hydrophobic interactions between hydrocarbon from silane and nertravidin.

Management, Outreach, and Collaboration: We had first internal review meeting with our External Advisory Board (EAB) in February, 2008. CSB webpage (http://www.physics.udel.edu/~csb/) has also been established where our research activities and other activities in spintronics from many research groups in the world. Work with Delaware State EPSCoR office, CSB has collaborated with newly established Center for Critical Zone Research (CCZR) (http://cczr.dbi.udel.edu/). We have collaborated with the NanoCenter at University of Maryland to access the e-beam facilities. User proposal to the Center for Nanoscale Materials at Argonne National Laboratory has been recently approved. We have collaborated with scientists at NIST (Dr. William Egelhoff, Gaithersburg), Army Research Laboratory (Dr. Alan Edelstein), Nonvolatile Electronics (Dr. Cathy Nordman), and Seagate (Drs. Sunita Gangopadhyay, Dimitrove Dimitar, Eric Singlton) related to understanding magnetization dynamics and improving noise performance in sensors. A distinct benefit for the Center has been the availability of state-of-the-art devices (read-head sensors) for noise studies.

III. **Future Plans**:

We will continue to (1) understand the spin current generated from NLSV and spin pumping effects, (2) develop Nonequilibrium Green Function-based code combined with

density functional theory input to treat spin pumping and shot noise in MgO-based MTJs, (3) understand the time dependence of TMR during annealing, (4) carry out a systematic study on the annealing time dependence of noise (shot noise,1/f noise, magnetic noise) in MgO based MTJs, (5) further characterize low frequency magnetic and electrical noise properties of MgO-based MTJs that will be used to refine the model for signal to noise performance of the magnetic sensors. In parallel, micron-sized sensors will be fabricated and their surfaces functionalized for the immbolization of magnetic nanoparticles, (6) develop magnetic nanoparticles with suitable surface function and immobilize NPs onto sensor surface.

IV Publications

1. T. Moriyama, R. Cao, X. Fan, G. Xuan, B. K. Nikolić, Y. Tserkovnyak, J. Kolodzey, and J. Q. Xiao, "Tunnel barrier enhanced voltage signal generated by magnetization precession of a single ferromagnetic layer", Physical Review Letters **100**, 067602 (2008).
2. Y. Tserkovnyak, T. Moriyama, and John Q. Xiao, "Tunnel-barrier enhanced voltage induced by magnetization dynamics", submitted to Physical Review B.
3. T. Moriyama, R. Cao, J. Q. Xiao, J. Lu, X. R. Wang, Q. Wen, and H. W. Zhang, "Magnetization reversed by microwave in magnetic tunnel junctions", Journal of Applied Physics **103**, 07A906 (2008).
4. T. Moriyama, X. Fan, R. Cao, B. Nikolic, J. Q. Xiao, Y. Q. Wen, and H. W. Zhang, "Gilbert damping enhancement in magnetic tunnel junctions", submitted to Applied Physics Letters.
5. W. G. Wang, K. J. Yeeb, D. H. Kimc, X. R. Wang, C. Ni, T. Moriyama, A. Mathew, R. Opilae, T. Zhu, and J. Q. Xiao, "Properties Of (Zn,Cr)Te Films Fabricated By Magnetron Sputtering", Physical Review B (in press).
6. T. Moriyama, X. Fan, Y. Q. Wen, H. W. Zhang, and J. Q. Xiao, "FMR spectroscopy with very large precession cone angle in magnetic tunnel junctions", submitted to IEEE Transactions on Magnetics.
7. Y. Z. Liu, W. G. Wang, T. Moriyama, J. Q. Xiao, and Z. Zhang, "Direct measurement of barrier asymmetry in AlOx/ZrOy magnetic tunnel junctions using off-axis electron holography", Physical Review B **75**, 134420 (2007).
8. T. Moriyama, R. Cao, J. Q. Xiao, J. Lu, X. R. Wang, Q. Wen, and H. W. Zhang, "Microwave-assisted magnetization switching of Ni80Fe20 in magnetic tunnel junctions", Applied Physics Letters **90**, 152503 (2007).
9. W.G. Wang, C. Ni, A. Rumaiz, Y. S. Wang, X. Fan. T. Moriyama, R. Cao and J. Q. Xiao, *"Real-time Evolution of Tunneling Magnetoresistance During Annealing in CoFeB/MgO/CoFeB Junctions"* Appl. Phys. Lett., In-press.
10. R. L. Dragomirova, L. P. Zârbo, and B. K. Nikolić, *Spin and charge shot noise in mesoscopic spin Hall systems*, preprint arXiv:0804.2076 (2008), submitted to Phys. Rev. Lett.
11. J. Xie, K. Chen, H.-Y. Lee, C. Xu, A. R. Hsu, S. Peng, X. Chen, S. Sun, "Ultra-Small c(RGDyK)-Coated Fe3O4 Nanoparticles and Their Specific Targeting to Integrin αvβ3-rich Tumor Cells", J. Am. Chem. Soc. submitted.

Excitation energy transfer in natural photosynthetic complexes and chlorophyll trefoils: hole-burning and single complex/trefoil spectroscopic studies.

Ryszard Jankowiak (PI), Kansas State University, Department of Chemistry, 111 Willard Hall, Manhattan KS, 66502; Phone: (785) 532-6785; E-mail: <ryszard@ksu.edu>

I. Program Scope:

The research in this program is related to energy-relevant sciences including studies on photosynthetic energy capture by bacteria and artificial arrays, and is in line with the current interests of the Department of Energy. It is anticipated that our research will shed more light on the performance of solar conversion systems including natural as well as artificial systems. Spectral hole-burning (SHB) and single photosynthetic complex/trefoil spectroscopy will be used to study the excitonic structure and excitation energy transfer (EET) processes as they occur in *Chlamydomonas reinhardtii* (*Chlamy*) PSI and PSI-LHCI, CP47 from spinach Photosystem II (PSII), and different chlorophyll (Chl) trefoils. To accomplish this goal we will use more sensitive readout techniques in SHB to study bulk/single photosynthetic complexes and Chl trefoils embedded in solid matrices at low temperature. Experimentally determined parameters will allow for better modeling of excitonic structure, low-energy states, and EET dynamics at a quantitative level. Chl trefoils are of great interest, as they cover a wide range of the solar spectrum, show rapid transfer of energy and form self-assembling aggregates.

Our long-range goal is to improve understanding of the electronic properties of the cofactors and the EET processes in both CP47 and *Chlamy* PSI. The key objectives are: i) identify chlorophylls (Chls) that contribute to the "low-energy traps" in CP47 and PSI; ii) examine their function and the origin of their large spectral shifts, and improve modeling of PSI and CP47 absorption and hole-burned (HB) spectra. We will demonstrate that non-photochemical hole growth kinetics (HGK) determined with a suitably wide range of burn intensities can resolve excited Q_y states with overlapping absorption bands in CP47 and PSI complexes. Findings will be compared with data obtained by zero-phonon-line action spectroscopy and hole widths. A model will be tested that the different kinetics of holes burned in the region of several overlapping low-energy bands can provide information on EET between directly excited Chls and their neighbours in *Chlamy* PSI and PSI-LHCI. Finally, excitonic modeling studies will be performed for various antenna complexes (e.g. CP47 complex) and Chl trefoils. The Chl trefoils are of great interest, since they represent linked donor-bridge-acceptor molecular systems in which efficient, nearly distance-independent, photoinduced charge separation occurs. We will compare SHB and single trefoil spectroscopy (STS) data with time domain results. It is of great interest to use the experimental data generated by SHB/STS along with excitonic calculations to provide more insight into the electronic structure of these Chl trefoils, where the bridge is a conjugated organic molecule analogous to natural carotenes that transfer charge over long distances. Our rationale is that a better understanding of the structure-function relationship of natural systems will facilitate the development of artificial photovoltaic devices.

To accomplish the goals of this program a partnership and collaboration has been established between the National Renewable Energy Laboratory (NREL) in Denver and the Department of Chemistry at Kansas State University (KSU). Collaboration has also been established with Prof. M. Wasielewski (*Northwestern University*) to study the electronic structure of various Chl trefoil arrays and with Prof. P. Fromme (Arizona State University) to study PSI.

II. Recent Progress:

Very recently, we have completed studies related to electronic structure and excitation transfer dynamics of one of the antenna complexes of Photosystem II (PSII), i.e. the CP43 complex (see abstracts below). Similar studies are under way for the second antenna complex, i.e. the CP47 complex and other photosynthetic complexes described in the Program Scope. The papers on CP43 have been submitted for publication in *Journal of Physical Chemistry B* (2008). Our recent data on CP43 and preliminary data on CP47 are forcing us to rethink PSII entirely. We anticipate that these studies will help us to resolve a number of critical aspects of PSII which remain controversial.

The CP43 Proximal Antenna Complex of Higher Plant Photosystem II Revisited: Modeling and Hole Burning Study (I)

Nhan C. Dang[1], Valter Zazubovich[2], Mike Reppert[1], Bhanu Neupane[1], Rafael Picorel[3,#], Mike Seibert[3], and Ryszard Jankowiak (PI)[1,]*

[1]Department of Chemistry, Kansas State University, Manhattan, KS 66506, USA;
[2]Department of Physics, Concordia University, Montreal H4B1R6 Quebec, Canada;
[3]National Renewable Energy Laboratory, Golden, CO 80401, USA

Abstract

The CP43 core antenna complex of Photosystem II is known to possess two quasi-degenerate "red"-trap states [R. Jankowiak et al. J. Phys. Chem. B 2000, 104, 11805]. It has been suggested recently [V. Zazubovich and R. Jankowiak, J. Lum. 2007, 127, 245] that the site distribution functions (SDFs) of the red states (A and B) are uncorrelated and that narrow holes are burned in the subpopulations of chlorophylls (Chls) from states A and B that are the lowest-energy Chl in their complex and previously thought not to transfer energy. This model of uncorrelated excitation energy transfer (EET) between the quasi-degenerate bands is expanded by taking into account both electron-phonon and vibrational coupling. The model is applied to fit simultaneously absorption, emission, zero-phonon action, and transient hole burned (HB) spectra obtained for the CP43 complex with minimized contribution from aggregation. It is demonstrated that the above listed spectra can be well fitted using the uncorrelated EET model, providing strong evidence for the existence of efficient energy transfer between the two lowest energy states A and B (either from A to B <u>or</u> from B to A) in CP43. Possible candidate Chls for the low-energy A and B states are discussed, providing a link between CP43 structure and spectroscopy. Finally, we propose that persistent holes originate from regular NPHB accompanied by the redistribution of oscillator strength due to excitonic interactions, rather than photoconversion involving Chl-protein hydrogen bonding as suggested before [J.L. Hughes et al., Biochemistry 45, 12345, 2006]. In the accompanying paper (II) it is demonstrated that the model discussed in this manuscript is consistent with excitonic calculations, which also provide very good fits to both transient and persistent HB spectra obtained under non-line narrowing conditions.

Low-Energy Chlorophyll States in the CP43 Antenna Protein Complex: Simulation of Various Optical Spectra (II)

Mike Reppert[1], Valter Zazubovich[2], Nhan C. Dang[1], Mike Seibert[3], and Ryszard Jankowiak(PI)[1,]*

[1]Department of Chemistry, Kansas State University, Manhattan, Kansas 66506, USA
[2]*Department of Physics, Concordia University, Montreal, Quebec H4B 1R6, Canada*
[3]National Renewable Energy Laboratory, Golden, CO 80401, USA

Abstract

The CP43 protein complex of the core antenna of higher plant Photosystem II (PSII) has two quasi-degenerate "red" absorption states. It has been shown in the accompanying paper **I** (Dang N.C. et al, *J. Phys. Chem*. **xx**, xx, 2008) that the site distribution functions (SDFs) of red-states *A* and *B* are uncorrelated and the narrow holes are burned in *subpopulations* of chlorophylls (Chls) from states *A* and *B* that are the lowest-energy pigments in their particular CP43 complexes and cannot further transfer energy downhill. In this work, we present the results of a series of Monte Carlo simulations using the 3Å-structure of the PSII core complex from cyanobacteria [Loll, B. et al., *Nature* 2005, **303**, 1040] to model absorption, emission, persistent, and transient hole burned (HB) spectra. At the current structural resolution, we found calculated site energies (obtained from INDO/S calculations) to be only suggestive as their values are different for the two monomers of CP43 in the PS II dimer. As a result, to probe the excitonic structure, a simple fitting procedure was employed to optimize Chl site energies from various starting values corresponding to different *A/B* pigment combinations in order to provide simultaneously good fits to several types of optical spectra. It is demonstrated that the shape of the calculated absorption, emission, and transient/persistent hole-burned (HB) spectra is consistent with experimental data and our model for excitation energy transfer (EET) between two quasi-degenerate lowest-E states (*A* and *B*) with uncorrelated SDFs discussed in paper **I**. Calculations revealed that absorption changes observed near 670 nm in the non-line narrowed persistent HB spectra (assigned by Hughes et al. [*Biochemistry*, 2006, **45**, 12345] to photoconversion involving Chl-protein hydrogen-bonding), are most likely the result of non-photochemical hole burning (NPHB) accompanied by the redistribution of oscillator strength due to modified excitonic interactions. We argue that a unique redistribution of oscillator strength during the NPHB process helps to assign Chls contributing to the low-energy states. It is demonstrated that the 4.2 K asymmetric triplet-bottleneck (transient) hole is mostly contributed to by both *A* and *B* states, with the hole profile described by a sub-ensemble of pigments, which are the lowest-energy pigments (B_s- and A_s-type) in their complexes. The same lowest-energy Chls contribute to the observed fluorescence spectra. Based on our excitonic calculations the best Chl candidates that contribute to the low-energy *A* and *B* states are Chl 44 and Chl 37, respectively.

III. Future Plans:

The long term goal is to reach a better understanding of the excitonic structure and EET processes in *Chlamy* PSI, CP47 from spinach PSII, and various Chl trefoils that could have application in future photovoltaic devices. Our future plans are:

1. Perform SHB and SPCS (including pressure type experiments) to study isolated CP47 from spinach PSII. Compare and correlate results obtained for CP47 with those recently obtained for CP43 (manuscript in preparation; see also [1,2]). Measure fluorescence excitation and emission spectra of single CP47 complexes to avoid ensemble averaging and correlate the data with those obtained by SHB for macroscopic samples in glasses. Explore whether absorption and

transient/persistent HB spectra obtained for CP47, which seems to possess three low energy states at 684, 687, and 690 nm [3], can be accounted for by considering fast EET between some of these quasi-degenerate bands. This need is driven by our recent HB data and modeling studies on CP43 ([2], unpublished data] and PSI-CP43′ [4]. One of the hypotheses to be tested is that 687/690 nm bands are excitonically coupled and contributed to by Chls 12 and 13, while the 684 nm band is mostly localized either on Chl 23 or Chl 25 (vide infra).

2. Demonstrate that nonphotochemical hole growth kinetics (HGK) determined with a suitably wide range of burn intensities (when combined with zero-phonon hole width measurements) can resolve excited Q_y states with overlapping absorption bands in CP47 complexes with overlapping low energy states. Compare findings with data obtained by ZPL action spectroscopy and hole widths. Develop a model for HGK that includes a distribution of possible EET rates between different states. The hypothesis to be tested is that the different kinetics of holes burned in various regions of several overlapping quasi-degenerate low-energy states will allow us to extract the distribution of EET rates between these states.

3. Measure fluorescence excitation and emission spectra of single *Chlamy* PSI-LHCI and PSI complexes to avoid ensemble averaging. Then correlate the data from single complex experiments with those obtained by SHB for macroscopic samples of PSI and PSI-LHCI in glasses. Test to what degree the disruption of specific interactions of the PSI core and LHCI is responsible for the observed changes in the red edge of the PSI Q_y absorption band. Test whether the hole burning wavelength dependence of the nonphotochemical HGK could provide information on EET between directly excited Chls and their neighbours in *Chlamy* PSI and PSI-LHCI. Test the hypothesis that this approach can provide new information on the Chl-pools located in the interface between LHCI and the PSI core.

4. Perform high-resolution spectroscopic and excitonic modeling studies of Chl trefoil arrays. These arrays are of great interest, since they represent linked donor-bridge-acceptor molecular systems in which efficient, nearly distance-independent, photoinduced charge separation occurs. The bridge, in this case, is a conjugated organic molecule analogous to the carotenes which transfer charge over long distances in natural PC. Compare SHB and single trefoil spectroscopy (STS) data with time domain data obtained in Prof. Wasielewski's group. Perform SHB on both well dispersed and aggregated Chl trefoils/trefoil arrays in glasses and polymers to shed more light on EET and charge transfer rate(s) in solid matrices.

References

[1] R. Jankowiak, V. Zazubovich, M. Rätsep, S. Matsuzaki, M. Alfonso, R. Picorel, M. Seibert, G. J. Small *J. Phys. Chem. B* **104** (2000) 11805.

[2] V. Zazubovich, R. Jankowiak, *J. Lum.* ***127*** (2007) 245.

[3] H.-C. Chang, R. Jankowiak, C. F. Yocum, R. Picorel, M. Alfonso, M. Seibert, G. J. Small, *J. Phys. Chem. B* **98** (1994) 7717.

[4] K. J. Riley, V. Zazubovich, R. Jankowiak, *J. Phys. Chem B* **110** (2006) 22436.

V. DOE sponsored Publications. Two papers have been submitted for publication to *J. Phys. Chem. B* (see section II) and two papers on CP47 complex are in preparation.

α-Fe_2O_3 NANOWIRE ARRAY BASED ELECTRODES FOR SELF-DRIVEN PHOTOELECTROCHEMICAL CELLS

Boris Chernomordik[1], Uros Cvelbar[2], Vidhya Chakrapani[1], Miran Mozetic[2] and Mahendra K. Sunkara*[1]

[1]Department of Chemical Engineering, University of Louisville, 106 Ernst Hall, Department of Chemical Engineering, University of Louisville, Louisville, KY 40292. [2]Plasma Laboratory F4, Jožef Stefan Institute, Jamova 39, Ljubljana SI-1000, Slovenia,

*Corresponding Author: mahendra@louisville.edu

Iron oxide, Fe_2O_3, is a promising material for water splitting reaction using solar energy due to its stability and optimal bandgap of 2 eV.[1,2] Even the recent efforts, however, using Fe_2O_3 thin film materials reported low efficiencies due to poor carrier transport within these films.[3,4]

Recently, we developed a novel method to synthesize arrays of α-Fe_2O_3 nanowires, which are single crystal and have highly ordered oxygen vacancy planes (see Fig. 1 and 2).[5,6] As one-dimensional nanostructures, these nanowires offer many other benefits to PEC electrolysis, such as high surface area, reduced charge carrier diffusion distance, and a preferential direction for charge diffusion. Furthermore, due to the ordered-oxygen vacancy planes in these nanowires, the resistivity that has plagued this material may become a non-issue.[7]

In preliminary investigation of as-synthesized a-Fe_2O_3 nanowires, photoluminescence and optical absorbance measurements confirmed a bandgap energy of 2.1 ± 0.05 eV (see Fig. 3 and 4).

In this poster, we will discuss both synthesis and photoelectrochemical properties of a-Fe_2O_3 nanowire arrays grown on Fe foils.

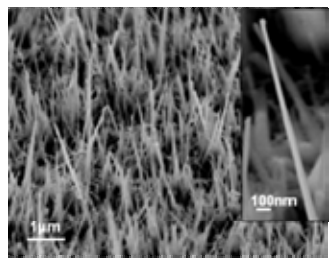

Fig. 1

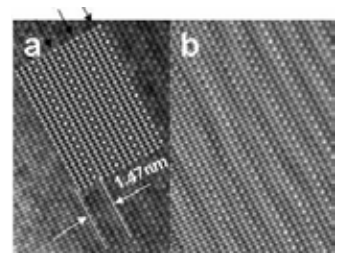

Fig. 2

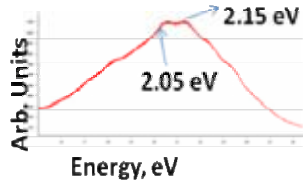

Fig. 3

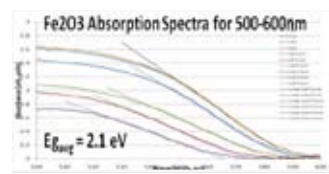

Fig. 4

The authors gratefully acknowledge the financial support from the DOE-EPSCoR Program (DE-FG02-07ER46375) and Kentucky Space Grant Consortium (KSGC) for fellowship.

References

(1) Hardee, K. L.; Bard, A. J. *J. of the Electrochem. Soc.*, **1976**, *123*, 1024-1026.
(2) Kennedy, J. H.; Anderman, M. *J. of the Electrochem. Soc.*, **1983**, *130*, 848-852.
(3) Lindgren, T.; Wang, H. L.; Beermann, N.; Vayssieres, L.; Hagfeldt, A.; Lindquist, S. E. *Solar Energy Mater. and Solar Cells* **2002**, *71*, 231-243.
(4) Ingler, W. B.; Khan, S. U. M. *Electrochem. and Solid State Lett.*, **2006**, *9*, G144-G146.
(5) Cvelbar, U.; Chen, Z.; Sunkara, M. K.; Mozetic, M. *Small* **2008**, *In press.*
(6) Chen, Z.; Cvelbar, U.; Mozetic, M.; He, J.; Sunkara, M. K. *Chem. of Mater.*, **2008**, 20, 3224-3228.
(7) Kennedy, J. H.; Frese, K. W. *J. of the Electrochem. Soc.*, **1978**, *125*, 723-726.

Field Enhanced, Thermionic Emission using Conical Carbon Nanopipette Arrays

S. Dumpala, D. Mudd, A. Safir, R. W. Cohn, M.K. Sunkara and G. U. Sumanasekera*
University of Louisville, Louisville, KY 40241

Correspondence: gusuma01@louisville.edu

ABSTRACT

Multi walled Carbon nanotubes are known to be efficient cathodes for field emission devices. Here, we report a recent experimental study of high emission current densities exceeding 200 mA/cm^2 and breakdown electric field lower than 2 Volts/μm from novel cold cathodes consisting of conical shaped carbon nanopipettes (CNP). CNP were grown by CVD on Pt wire and have apex as sharp as 10 nm with micron scale bases and lengths ranging from 3-10 μm. The field emission experiments were conducted under high vacuum ($< 10^{-7}$ Torr) in a dedicated chamber for bulk samples. In a comparative study, field emission properties of ultra long multiwalled carbon nanotubes grown by chemical vapor deposition using Fe catalysts on silicon substrates were studied. The experimental value for the field enhancement factor, β, defined as $E_{eff} = \beta E_{appl}$ where, E_{appl} is the applied electric field and E_{eff} is the effective field at the emission point, exceeds 7500 for CNPs. This value is more than twice the best value obtained from aligned multiwall carbon nanotubes (MWCNT) and reported in the literature. CNP's conical bases and low density seem to contribute significantly to the reduction of the screening effect and to the field emission enhancement. The β value measured for varying separations between the cathode and anode is found to be independent for smaller separations but linearly dependent for larger separations. Results of field emission for individual CNPs and MWNTs inside a scanning electron microscope equipped with a nano manipulator (ZYVEX Inc.) will be presented and compared. Finally results from theoretical modeling to understand the field emission properties such as proximity of neighboring nanopipettes, ratio between the inter-CNP distance vs. pipette lengths will be presented.

NANOWIRE BASED ANODES FOR LITHIUM ION BATTERIES

Praveen Meduri (1), Chandrashekhar Pendyala (1), Vivekanand Kumar (1), Gamini U. Sumanasekera (2) and Mahendra K. Sunkara (1,*)

(1) Dept. of Chemical Engineering
(2) Department of Physics

University of Louisville
Louisville, KY 40292

*Corresponding author:
Phone – 502-852-1558, Fax – 502-853-6355,
email – mahendra@louisville.edu

ABSTRACT

One-dimensional, nanowire based materials are promising candidates for Lithium-ion battery electrodes due to their faster charge transport, better conducting pathways and good strain relaxation.[1] In this poster, we illustrate the use of metal oxide nanowire material systems as anodes for Li-ion batteries.

The theoretical specific capacities of the metal oxides (650~950 $mAhg^{-1}$) are much higher than that of carbonaceous materials and they are semi conducting in nature. Of the various metal and metal oxide materials systems, both tin (Sn) and tin oxide (SnO_2) have a high capacity (Sn: 994 $mAhg^{-1}$; SnO_2:781 $mAhg^{-1}$)[2] compared to that of graphite (372 $mAhg^{-1}$). However, significant capacity fading with cycling is a problem due to enormous volume changes during Li alloying and de-alloying leading to crystallographic deformation, which in the case of Sn is as high as 259%.

The battery cell used for testing has a three electrode configuration with auxiliary, working and reference electrodes. The auxiliary and the reference electrodes are both lithium metal foils. Chronopotentiometry studies were performed to study the change in specific capacity with cycling.

The SEM images of the as synthesized pure phase SnO_2 nanowires is shown in Figure 1a. Fig 1b is an image of the post-lithiated SnO_2 sample. Figure 2 shows the specific capacity with cycles using the SnO_2 nanowire electrode. The first discharge cycle capacity is 2500 $mAhg^{-1}$ which is higher than the theoretical value. But the capacity quickly fades to <200 $mAhg^{-1}$ in a few cycles. The irreversibility in the first few cycles may be due to the formation of a surface electrolyte interface (SEI).

In this poster, we also illustrate new architectures based on metal oxide nanowire systems that show excellent stability and mechanical integrity with cycling for up to 100 cycles. The concept can be extended to other material systems including Si, Ge and other alloys.

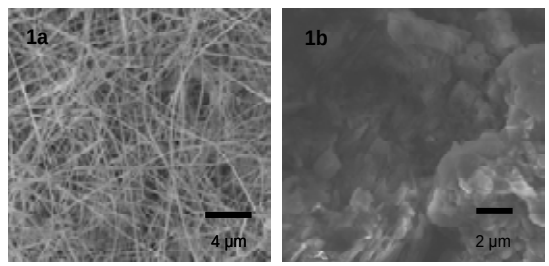

Figure 1: SEM images of (a) As synthesized pure phase SnO_2 nanowires. (b) Post-lithiated sample of SnO_2 nanowires.

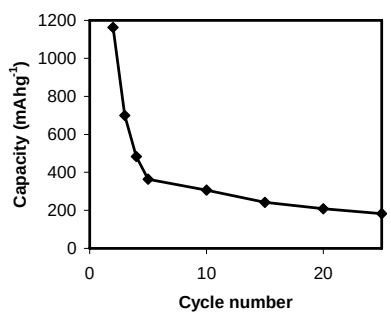

Figure 2: Specific capacity (from the 2nd cycle) of pure phase SnO_2 nanowires with cycles.

References

[1] A. S. Aricó, P. Bruce, B. Scrosati, J. –M. Tarascon, W. V. Schalkwijk, *Nat. Mater.* **2005**, *4*, 366.
[2] G. Derrien, J. Hassoun, S. Panero, B. Scrosati, *Adv. Mater.* **2007**, *19*, 2336.

Acknowledgements

Authors acknowledge financial support from the US Department of Energy (DE-FG02-05ER64071) and DOE-EPSCoR Program (DE-FG02-07ER46375).

Synthesis of 3-dimensional "tree" like nanowire architectures for solar energy conversion

Chandrashekhar Pendyala and Mahendra K. Sunkara

Department of Chemical Engineering, University of Louisville, Louisville, KY 40292

ABSTRACT

Synthesis of 3-dimensional tree like nanostructures of ternary III-Sb-N ($Ga_{1-x}In_xN$ and $Ga_{1-x}Sb_xN$) compounds is of tremendous importance in photoelectrochemical and other solar energy applications. Our earlier studies show that such tree-like architectures for Group III-nitride and Group III-antimonide can be grown without the use of any foreign catalysts. The results showed that the Group III metal mediated one-dimensional growth [1, 2].

Recently, our experiments with Group III-antimonides show that antimony (group V species) droplets can also mediate tip-led growth. Fundamentally, these results have high significance specifically with our rationalization of self-catalysis schemes for nanowire growth and nanoscale, tree-like structures.

Several experiments are conducted to investigate the underlying factors that control tip-led growth of Group III-nitride and Group III-antimonide nanowires. In order to conduct controlled experiments, our CVD reactor is equipped with a home-built, MOCVD precursor delivery system shown in Figure 2 for Group III metal and antimonide species.

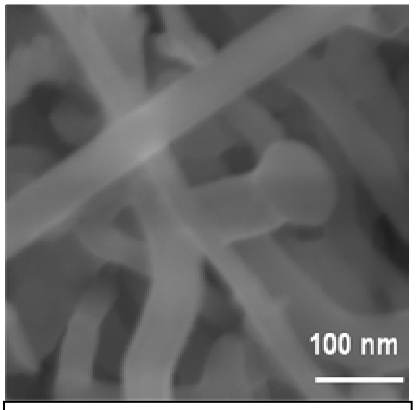

Figure 1: GaSb nanowires grown using a self-catalysis scheme.

Figure 2: Photograph showing our home-built, **MOCVD precursor delivery system.**

Acknowledgements: Authors acknowledge financial support from US Department of Energy (DE-FG02-05ER64071 and DE-FG02-07ER46375) and University of Louisville.

References:

[1] S. Vaddiraju, et.al. Nano Letters 5(8), 1625-1631(2005)

[2] H. Li, et.al. Advanced Materials, 18(2), 216 (2006)

BAND-EDGE ENGINEERED HYBRID NANOWIRE STRUCTURES FOR DYE SENSITIZED SOLAR CELLS.

S. Gubbala, V. Chakrapani, V. Kumar, and M.K. Sunkara
Department of Chemical Engineering, University of Louisville, University of Louisville, Louisville, KY 40292

Dye sensitized solar cells based on one dimensional materials are gaining increased importance as an alternative to the nanoparticle based DSSCs due to their better charge collection efficiencies compared to nanoparticle based cells.

The SnO_2 nanowire based DSSCs cells exhibit a 200 mV higher V_{oc} than that using SnO_2 nanoparticle based cells [1]. This is attributed to the more negative flat band potential of nanowires compared to the nanoparticles. These nanowires were further modified using titania nanoparticles. The rationale for such modification with titania nanoparticles is based on the relative locations of band edge positions as illustrated in Figure 1. The conduction band edge of SnO_2 is more positive than TiO_2. Thus, the electrons injected from the dye into the TiO_2 will be efficiently injected into the SnO_2 nanowires. The more negative conduction band edge of TiO_2 acts as a barrier for electron recombination from SnO_2 to the electrolyte. The excellent transport properties of the interconnected nanowires allow for fast transport of electrons into the back contact. These nanowires showed an open circuit voltage of 720 mV and an efficiency of 4.1% compared to 2.5% obtained with pure SnO_2 nanowire matrix. The corresponding IV curves are shown in Figure 2. The electron transport time constants for SnO_2 nanowire matrix were an order of magnitude lower and the recombination time constants are about 100 times higher than that of TiO_2 nanoparticles.

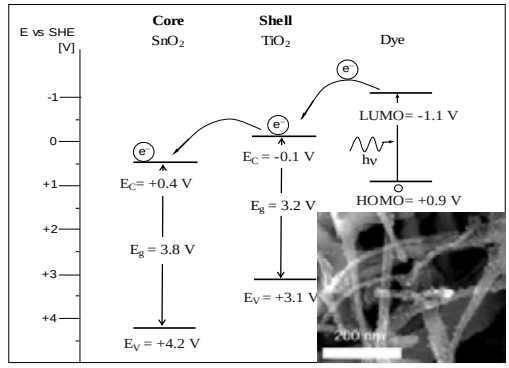

Figure 1: Band edge engineering of SnO_2 nanowires.

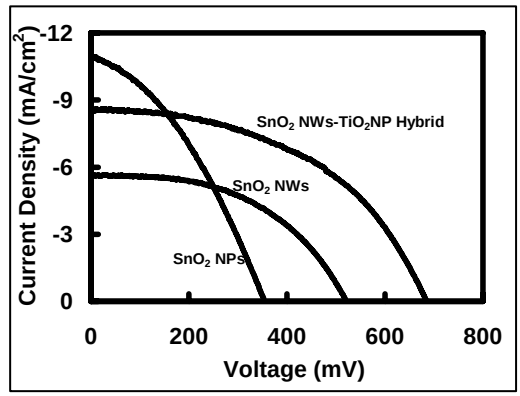

Figure 2: IV characterstics of SnO_2 NP's, NW's and hybrid structures.

In this study, nanowires were synthesized by reactive vapor transport of tin on quartz substrates [2]. These devices can be easily scaled up by producing nanowires in bulk quantities where they can be synthesized in substrate free, gas phase environments [3].

The authors gratefully acknowledge the financial support from the U.S. Department of Energy (DE-FG02-05ER64071) and DOE-EPSCoR Program (DE-FG02-07ER46375).

References:

1. S. Gubbala, V. Chakrapani, V. Kumar and M.K. Sunkara, Adv. Func. Mater., in press (2008)
2. R. Rao, H. Chandrasekaran, S. Gubbala, M. K. Sunkara, C. Doraio, S. Jin, A. M. Rao, J. of Electron. Mater. 2006, 35, 941-946.
3. V. Kumar, J. Kim and M.K. Sunkara, to be submitted (2008).

Post Synthesis Modification of Metal Oxide Nanowires for Photoelectrochemical Hydrogen Production

Jyothish Thangala, V. Chakrapani, S. Malhotra and Mahendra K. Sunkara*

*Corresponding Address:mahendra@louisville.edu
Department of Chemical Engineering, University of Louisville, Louisville, KY 40292

Highly crystalline one dimensional metal oxide nanowire arrays are of great interest due to their high surface area and fast charge transport characteristics. Such nanowire arrays are of significant interest for applications like electrochromic devices, solar cells, photo-electrochemical water splitting and field emission devices. Hence there is an intense search for newer materials with improved chemical stability and optical properties. In this work, we performed post synthesis nitridation of oxide nanowire arrays and powders to form new phases of materials for higher visible light absorption.

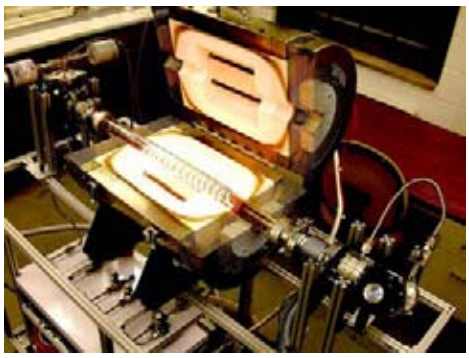

Fig 1. Scaled up Hot-Filament CVD Reactor

A novel and versatile method for the large-scale synthesis of metal oxide nanowire arrays and mat-like thin films on different substrates such as amorphous quartz, fluorinated tin oxide (FTO), tungsten and titanium will be presented. The synthesis concept involves chemical vapor transport of metal oxide vapor phase species using air or oxygen flow over hot filaments onto substrates kept at a distance.[1,2] Figure 1 shows the photograph of a scaled up hot filament CVD reactor designed and built at UofL. Figure 2 shows the SEM image of WO_3 array on FTO substrates. The post process modification of metal oxide nanowire arrays with exposure to different gases resulted in complete transformation to the respective nitride and metal NW arrays.[3] The crystallinity and the morphology of the nanowires is maintained after the transformation process. These results with post-process modification suggest that one can use the hot-wire assisted process to make oxide NW arrays and easily transform them to their metal and metal nitrides. Post process modification of other metal oxide nanowires like zinc oxide and tin oxide also showed some interesting results.

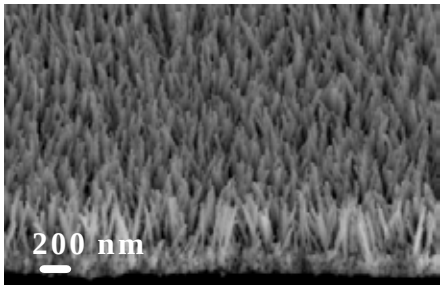

Fig 2. SEM image of WO_3 nanowire array. Post synthesis nitridation showed no change in the morphology

Figure 3 shows the Tauc plot obtained from UV-Vis spectroscopy. Oxidized WO_3 has a band gap of 3 eV. On the other hand nitridation leads to a reduction in the band gap from 3 eV to 2.5 eV. The photoelectrochemical

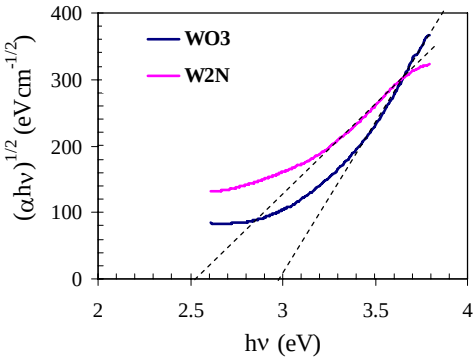

Fig 3. UV Vis data showing a reduction in the band gap from 3.0 eV to 2.5 eV upon nitridation

measurements were done in a three electrode configuration and the results will be presented.

References:

[1]S. Vaddiraju, H. Chandrasekaran and M.K. Sunkara, *J. Am. Chem. Soc.*, 125 (36), 10792 (2003)
[2]J. Thangala, S. Vaddiraju, R. Bogale, R. Thurman, T. Powers and M. K. Sunkara, *Small*, 3, 890 (2007)
[3]J. Thangala, Z. Q. Chen, A. H. Chin, C. Z. Ning and M. K. Sunkara, *Manuscript submitted*

DOE EPSCOR program

Inhomogeneous disordered Dirac fermions: from heavy fermion superconductors to graphene

PI: Ilya Vekhter
Department of Physics and Astronomy
Louisiana State University
Baton Rouge, LA 70803-4001
email: vekhter@lsu.edu

Program scope. This is a newly funded partnership effort in support of energy needs between Louisiana State University and Los Alamos National Laboratory to conduct fundamental research focusing on developing a better understanding of materials with new functionalities to develop the means to control and adjust their properties. We initially selected two distinct and very promising classes of new materials, which would serve as a testing ground for many of the novel phenomena in condensed matter physics. The first is the heavy fermion 115 series, where the interplay of strong interactions between the electrons leads to a rich variety of competing phases and anomalous properties. Our objective is to determine the origin and to establish a functional effective theory description of these phases and transitions between them. There are currently two conceptually different theoretical approaches reflecting diverging viewpoints on the origin of the correlated behavior. By use of methods of many body theory with both analytical and numerical implementation, we will compute experimentally measured properties under doping, applied pressure and magnetic field, compare them with experiment, and establish the framework for future studies of correlated matter. The outcome of this work is likely to strongly favor one of the competing descriptions of heavy fermion compounds, will clarify the nature of interactions, and will impact our thinking about many interacting systems.

The second emphasis of the proposal is the study of the properties of graphene and graphene-based structures. This choice is grounded in the potential of pure two-dimensional graphene as a new material for post-silicon electronics. We will focus on the properties of superconducting structures involving graphene, and consider the effect of the bound states near the boundaries and impurities using a combination of first-principles calculations with many-body techniques. These states are essential for, and often control the properties of low-dimensional systems, and their understanding is a major step towards applications of graphene. In further effort to consider the real-world potential of graphene we focus on the influence of intrinsically generated ripples and the associated inhomogeneities on the electronic, transport, and superconducting properties, especially in bilayer systems with tunable carrier density. Our success, which will be measured by reaching detailed agreement with experiment and guiding future studies, will help define the potential application of graphene and other two-dimensional molecular solids in modern technology and at the frontier of science.

Recent progress. Since this is newly funded program, recent progress has not been supported by DOE, but was conducted with the (now expired) help of the Louisiana Board of Regent. This support enabled the PI to stay at the forefront of the research and laid the foundation for the DOE-supported activities. Among recent achievements:

Understanding of the incomplete Kondo screening in antiferromagnetic metals. With V. Aji and C. M. Varma (UC Riverside) we studied the fate of a spin-1/2 impurity in the itinerant antiferromagnetic metallic phase via a renormalization group analysis and a variational calculation [1]. We

found that the local moment-conduction electron interaction hamiltonian in an antiferromagnetic metal is spin non-conserving. We showed that for a general location of the impurity the ground state has a partially unscreened moment. We calculated the magnitude of this residual moment and the variation of the spin polarization with energy for a substitutional impurity as a function of the staggered magnetization. Our results imply that the usual Kondo effect only occurs if the impurity is placed at points where the magnetization is zero. This is the first step in understanding the ordered phase of Lattice Kondo model and its approach to criticality.

Analysis of the surface bound states and prediction of ground state surface spin currents in non-centrosymmetric superconductors. With M. Eschrig (Universität Karlsruhe, Germany) and A. B. Vorontsov (LSU and University of Wisconsin, Madison) we investigated the influence of spin-orbit coupling in a non-centrosymmetric superconductor on its ground state properties near a surface [2]. We determined the spectrum of Andreev bound states due to surface-induced mixing of bands with opposite spin helicities for a Rashba-type spin-orbit coupling. We found a qualitative change of the Andreev spectrum when we accounted for the suppression of the order parameter near the surface, leading to clear signatures in the surface density of states. We also computed the spin current at the surface, which has spin polarization normal to that of the bulk current. The magnitude of the current at the surface is enhanced in the normal state compared to the bulk, and even further enlarged in the superconducting phase. This work has consequences for the development of spin electronics.

Determination of the order parameter in $CeIrIn_5$. Following a controversial claim, based on the results of the thermal conductivity measurements [3], that the shapes of the superconducting gap in $CeCoIn_5$ and $CeIrIn_5$ are very different, I and A. B. Vorontsov [4] analyzed the behavior of the thermal conductivity in quasi-two-dimensional superconductors with line nodes (zeroes of the energy gap in momentum space). We showed that a simple model of the open Fermi surface with vertical line nodes is insufficient to describe the data. We proposed two possible extensions of the model taking into account additional modulation of the gap along the axial direction of the open Fermi surface and dependence of the interplane tunneling on the direction of the in-plane momentum, and suggested further experiments aimed at clarifying the shape of the superconducting gap in $CeIrIn_5$.

These experiments now have been done by the group of Y. Matsuda in Japan, and analysed with participation of the PI [5]. They led to conclusion that the gap shape in $CeIrIn_5$ and $CeCoIn_5$ is the same, supporting theories that aim to investigate both materials within the same framework.

Future plans. The work described above serves as a preparation for initiation of the detailed project described in the original proposal for DOE. In particular, the establishment of the gap shape using the thermal conductivity results is very important. The experimental group of J. D. Thompson at Los Alamos recently acquired a vector magnet which will be used to carry out the measurements of the specific heat in the 115 heavy fermion series under rotated magnetic field, and under pressure [6]. The theory of these effects has been developed by the PI, and this will be a fertile ground for ongoing collaborations [7].

We also started research on the superconductivity in graphene between LSU and Los Alamos, that is expected to be brought to fruition with the help of the grant. The research on the surface bound states in non-centrosymmetric superconductors helped develop the formalism that will be used in determining the spectrum of Andreev bound states, a specified first year target of the proposal.

Our other main emphasis during the first year of the grant will be making experimentally verifiable predictions on the coexistence of the magnetism and superconductivity in heavy fermion

systems. This task has now become even more urgent in light of recent discovery of superconductivity in pnictide FeAs-based materials, where the two ordering phenomena coexist. At Los Alamos, the detailed study of the Ce-115 materials remains high on the agenda, and the PI will continue collaborating with experimentalists on this subject.

References

[1] V. Aji, C. M. Varma, and I. Vekhter, "Kondo effect in an antiferromagnetic metal: Renormalization group analysis and a variational calculation", Phys. Rev. B **77**, 224426 (2008).

[2] A. B. Vorontsov, I. Vekhter, and M. Eschrig, "Surface bound states and spin currents in noncentrosymmetric superconductors", arXiv:0804.2464 (unpublished); *Physica B* **403**, 1095 (2008).

[3] H. Shakeripour, M. A. Tanatar, S. Y. Li, C. Petrovic, and L. Taillefer, "Hybrid Gap Structure of the Heavy-Fermion Superconductor $CeIrIn_5$", Phys. Rev. Lett. **99**, 187004 (2007).

[4] I. Vekhter and A. B. Vorontsov, "Interplane and intraplane heat transport in quasi-two-dimensional nodal superconductors", Phys. Rev. B **75**, 094512 (2007).

[5] Y. Kasahara, T. Iwasawa, Y. Shimizu, H. Shishido, T. Shibauchi, I. Vekhter, and Y. Matsuda, "Thermal Conductivity Evidence for a $d_{x^2-y^2}$ Pairing Symmetry in the Heavy-Fermion $CeIrIn_5$ Superconductor", Phys. Rev. Lett. **100**, 207003 (2008).

[6] T. Park, E. D. Bauer, and J. D. Thompson, "Probing the nodal gap in the pressure-induced heavy fermion superconductor $CeRhIn_5$", arXiv:0806.3308 (unpublished).

[7] A. Vorontsov and I. Vekhter, "Nodal structure of quasi-2D superconductors probed by a magnetic field", *Phys. Rev. Lett.* **96**, 237001 (2006); "Unconventional superconductors under rotating magnetic field I: density of states and specific heat", Phys. Rev. B **75**, 224501 (2007).

"Novel Quantum Phenomena in Layered Ruthenates"

Zhiqiang Mao
zmao@tulane.edu
Physics Department, Tulane University, New Orleans, LA 70118

I.) Program Scope:

Strongly correlated oxides have been the subject of intense study for the last two decades. Many of these materials exhibit exciting new properties and enhanced functionality: examples include high temperature superconductivity in cuprates and colossal magnetoresistance in manganites. Recently, perovskite-related ruthenates have become a new focus within this field. They exhibit a rich variety of fascinating ordered ground states, unprecedented for a transition metal oxide series. Spin-triplet superconductivity, metamagnetic quantum criticality, itinerant ferromagnetism, antiferromagnetic Mott insulating, and half-metallic behavior were all found in close proximity to one another. These diverse ground states originate from the strong interplay of charge, spin, lattice, and orbital degrees of freedom. They offer a unique opportunity to tune the system and study the physics of novel quantum phases. Since small perturbations in the active lattice and orbital degrees of freedom can lead to giant responses, the ground state properties of the ruthenates are extremely sensitive to impurities. Controlled studies of new phases require samples of exceptionally high quality. This project aims at searching for novel quantum phenomena in ruthenate materials using high purity single crystals, grown by the floating-zone technique, and investigating the underlying physics.

II.) Recent Progress:

We have made a remarkable progress in this project during this grant period, as summarized in following:

(1) Origin of the metamagnetic transition of $Sr_4Ru_3O_{10}$

$Sr_4Ru_3O_{10}$ shows a ferromagnetic transition at $T_c \approx 100$ K; followed by a second transition at $T^* \approx 50$ K [1]. Below T^*, a first order metamagnetic transition is induced by an in-plane magnetic field. Our early experiments revealed that this metamagnetic transition occurs via a phase separation process with magnetic domain formation [2,3]. This phase separation process results in very unusual transport properties: the magnetoresistivity shows switching behaviors and it involves structure distortion [4]. In this grant period, we performed systematic magnetoresistivity, thermoelectric property, and Hall effect measurements on $Sr_4Ru_3O_{10}$. These experiments have enabled us to make a remarkable progress in understanding this unusual itinerant metamagnetism. Our results show that this metamagnetism originates from a multiple-band effect, i.e., both ferromagnetic and metamagnetic bands coexist. The metamagnetic bands are derived from the Ru $4d_{xz,yz}$ orbitals and they are polarized only when the in-plane field is above the metamagnetic transition field. We also find that such an orbital-dependent metamagnetic transition gives rise to an anomaly in Hall effect.

We have measured the in-plane angular dependence of in-plane and c-axis magnetoresistivity, i.e., $\rho_{ab}(\Phi,B)$ and $\rho_c(\Phi,B)$ under various magnetic fields as shown in Fig. 1. $\rho_{ab}(\Phi,B)$ shows typical characteristics of an Ising ferromagnetic state. For the fields below the

metamagnetic transition B_c, it exhibits a two-fold symmetry $\sin^2\phi$-like oscillations; this feature originates from spin-orbital coupling which results in the presence of magnetic easy axis. For the fields above the metamagnetic transition, $\rho_{ab}(\Phi,B)$ shows a four-fold symmetry oscillation with the minimums occurring along [100] and [010] directions, consistent with the fact that the spin-orbital coupling effect has less impact on magnetotransport properties for a fully polarized FM state. $\rho_c(\Phi,B)$, however, exhibits distinctly different features from $\rho_{ab}(\Phi,B)$; it shows no oscillation for $B < B_c$, and a four-fold symmetry oscillation for $B > B_c$ with the minimums occurring along [110] and [1-10] directions (see Fig. 1). Since ρ_{ab} and ρ_c probes transport properties from different orbitals, our observation on the difference between $\rho_{ab}(\Phi,B)$ and $\rho_c(\Phi,B)$ provides a strong evidence for our early argument that the magnetism in $Sr_4Ru_3O_{10}$ is orbital dependent, i.e. FM bands from Ru $4d_{xy}$ orbital coexist with metamagnetic bands from Ru $4d_{xz,yz}$ orbitals. The Ru $4d_{xz,yz}$ orbitals are polarized only when the in-plane field is larger than B_c. We have completed most related work for this subproject and are in process of writing a paper.

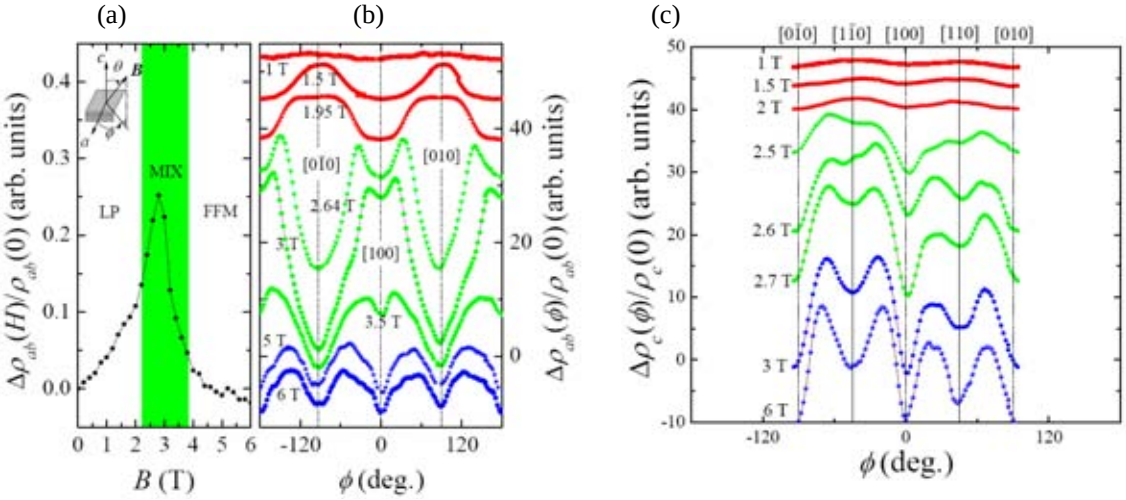

Figure 1: a) In-plane resistivity vs. magnetic field at 2 K. The peak near 3T corresponds to a metamagnetic transition. LP, lowly polarized phase; FFM, forced ferromagnetic phase; MIX, the mixed phase of LP and FFM. The inset show the definition of polar angle θ and azimuthal angle ϕ. (b) Azimutal angle dependence of the normalized in-plane magnetoresistance at various magnetic fields. (c) Azimutal angle dependence of the normalized *c*-axis resistivity.

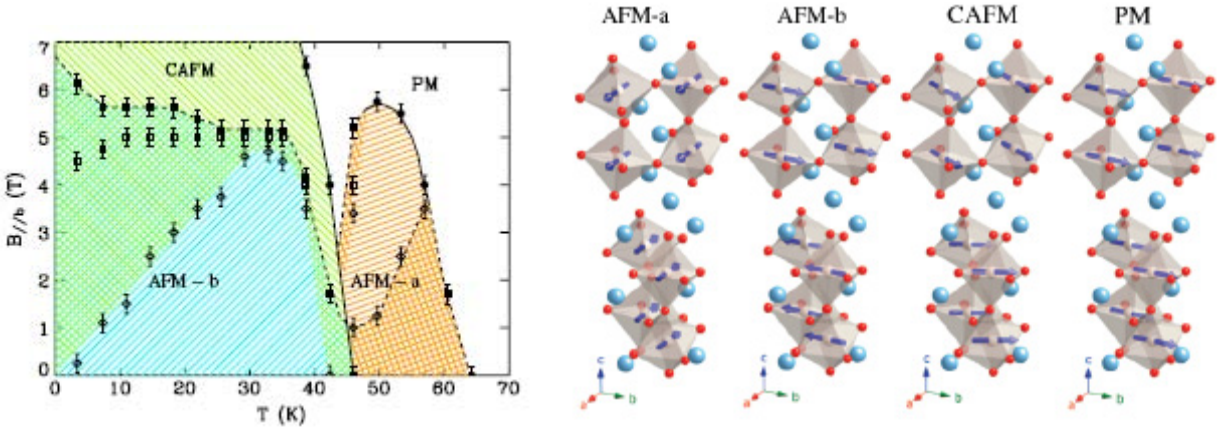

Figure 2. Left panel: Phase diagram of $Ca_3Ru_2O_7$ in a magnetic field applied along the *b*-axis. The solid lines denote continuous phase-transitions, and dashed lines first-order ones. The hysteresis regions are marked by cross-lines. Magnetic structures of these four phases are shown in the right panel. AF-a: antiferromagnetic phase with the easy

axis along the *a*-axis. AF-b: antiferromagnetic phase with the easy axis along the *b*-axis. CAF: canted antiferromagnetic phase. PM: paramagnetic phase.

(2) Bulk spin valve and giant magnetoresistivity in $Ca_3Ru_2O_7$

We have further extended our study to calcium ruthenate $Ca_3Ru_2O_7$. This compounds orders antiferromagnetically at 56K [5]; it has attracted a great deal of interest since it shows a giant magnetoresistive (GMR) effect. The spin-valve mechanism for the GMR effect has been proposed [6]. However, the spin-valve explanation runs into severe difficulty with the astounding recent experimental conclusion that the fully spin-polarized phase is the least favorable for electronic conduction. We have recently solved this problem through systematic neutron scattering measurements on large single crystals of $Ca_3Ru_2O_7$ in collaboration with Wei Bao at Los Alamos national lab. We have successfully determined the phase-diagram and magnetic structures of this material (see Fig. 2). The determination of these magnetic structures provides a solid evidence for the bulk spin-valve mechanism for the magnetoresistivity effect of this material. This work has been published in *Phys. Rev. Lett.* ***100****, 247203 (2008).*

(3) 2D ferromagnetic instability $(Sr_{1-x}Ca_x)_3Ru_2O_7$

We have performed systematic magnetization, Hall effect, and specific heat measurements on $(Sr_{1-x}Ca_x)_3Ru_2O_7$ using high-quality single crystals. We find that this system approaches an unusual limiting magnetic state with heavy mass quasiparticles for $0.08 < x < 0.4$: while FM correlations are extremely strong, the system is not ordered and forms a cluster spin glass phase at low temperatures; non-FL behavior occurs as the cluster spin glass phase is suppressed [7]. These behaviors suggest that this state is in close proximity to a 2D ferromagnet instability. Therefore this material may provide a new arena for exploring novel physics of 2D ferromagnetism. This work has been submitted to *Phys. Rev. Lett*.

The progress we achieved during this grant period not only advances our understanding of unusual magnetism of double and trilayered ruthenates, but also is expected to generate further interests in ruthenate physics.

III.) <u>Future plans:</u>

- Our preliminary neutron scattering measurements on $Sr_4Ru_3O_{10}$ shows that its metamagnetic transition involves structure distortion. Our next goal is to make larger single crystals and carry out further neutron scattering measurements on this material to systematically investigate the characteristics of the structure distortion and identify its magnetic structure. This work will be done in collaboration with Dr. Bao.
- It has been suggested that the structure distortion near the metamagnetic transition of $Sr_4Ru_3O_{10}$ may result in the presence of orbital ordering or polarization. We will investigate this issue using a resonant x-ray scattering technique in collaboration with Dr. Islam at Argonne National Lab.
- We have observed preliminary evidence for an anomalous Hall effect near the metamagnteic transition of $Sr_4Ru_3O_{10}$. We will conduct systematic measurements to clarify its origin.
- We will grow single crystals of the $(Sr_{1-x}Ca_x)_4Ru_3O_{10}$ solid solution series and characterize their properties. Fascinating properties have been observed in both single-layered and double-layered solid solution series, $Ca_{2-x}Sr_xRuO_4$ and $(Sr_{1-x}Ca_x)_3Ru_2O_7$. Interesting properties is expected as well for $(Sr_{1-x}Cax)_4Ru_3O_{10}$.

- $(Sr_{1-x}Ca_x)_3Ru_2O_7$ shows rich physics, as summarized above. We will continue to explore novel orbital-related physics in this system. We will perform systematic directional magnetoresistivity measurements to extract orbital information to study the role of the orbital degree of freedom in driving magnetic phase transitions. We will also conduct neutron scattering measurements for the sample with x =0.2 to study the nature of the unusual 2D nearly ferromagnetic state.
- Our previous study has revealed unusual oscillations in tunneling magnetoresistance of $Sr_3Ru_2O_7$; these oscillations likely result from unusual surface electronic states, which couple with applied magnetic field. We will perform the following studies to clarify its underlying physics: a) Carry out systematic tunneling measurements on junctions prepared on differently oriented crystallographic surfaces. Tunneling measurements on precisely oriented crystals will allow us to systematically study the anisotropic properties of this oscillation behavior. b) Measure the dependence of the oscillations on field orientations using a rotating sample stage.
- Use orbital-resolved soft x-ray absorption (SXAS) and soft x-ray emission spectroscopy (SXES) to study the electronic band properties of Sr_2RuO_4, $Sr_3Ru_2O_7$, and $Sr_4Ru_3O_{10}$ through collaboration with Drs. Ederer and Islam.

IV.) <u>References:</u>

(1) M.K. Crawford, R.L. Harlow, W. Marshall, Z. Li, G. Cao, R.L. Lindstrom, Q. Huang, and J.W. Lynn, Phys. Rev. B **65**, 214412 (2002).
(2) Z.Q. Mao, M. Zhou, J. Hooper, V. Golub, and C.J. O'Connor, Phys. Rev. Lett. **96**, 077205 (2006).
(3) D. Fobes, M.H. Yu, M. Zhou, J. Hooper, C.J. O'Connor, M. Rosario, and Z.Q. Mao, Phys. Rev. B **75**, 094429 (2007).
(4) R. Gupta, M. Kim, H. Barath, S.L. Cooper, and G. Cao, Phys. Rev. Lett **96**, 067004 (2006).
(5) G. Cao, L. Balicas, Y. Xin, E. Dagotto, J.E. Crow, C.S. Nelson, and D.F. Agterberg, Phys. Rev. B **67**, 060406 (2003).
(6) D.J. Singh and S. Auluck, Phys. Rev. Lett. **96**, 097203 (2006).
(7) Z. Qu, L. Spinu, H. Q. Yuan, V. Dobrosavljeviμc, W. Bao, J. W. Lynn, M. Nicklas, J. Peng, T. J. Liu, D. Fobes, E. Flesch, and Z. Q. Mao, submitted to *Phys. Rev. Lett*.

V.) <u>DOE sponsored Publications in 2007-2008</u>:

Spin-valve effect and magnetoresistivity in single crystalline $Ca_3Ru_2O_7$,
Wei Bao, Z.Q. Mao, Z. Qu, J.W. Lynn, Phys. Rev. Lett. **100**, 247203 (2008).

Magnetic field-induced electronic phase transition in $Sr_4Ru_3O_{10}$ at low temperatures,
Z.A. Xu, X.F. Xu, R.S. Freitas, Z.Y. Long, M. Zhou, D. Fobes, M.H. Fang, P. Schiffer, Z.Q. Mao, and Y. Liu, Phys. Rev. B **76**, 094405 (2007).

"Implementation Phase I: Thermochemical Conversion of Woody Biomass to Fuels and Chemicals"

Hemant P. Pendse,[1] M. Clayton Wheeler,[1] William J. DeSisto,[1,3] Brian G. Frederick,[2,3] and Adriaan van Heiningen[1]

The University of Maine
Chemical and Biological Engineering,[1] Chemistry,[2] and Laboratory for Surface Science and Technology,[3] Orono, ME 04469-5737
http://www.forestbioproducts.umaine.edu/DOE_Project.php

I) Program Scope

UMaine's DOE EPSCoR research cluster is implementing new catalyst R&D infrastructure and addressing fundamental science and engineering pathways for *thermochemical conversion* of woody biomass to fuels and chemicals, an area of increasing importance to Maine's forest products industry. A major technical focus is on upgrading of biomass pyrolysis oils. Major roadblocks in thermally upgrading pyrolysis oil, a complex highly-oxygenated liquid, include improving the heating value through catalytic oxygen removal, identifying favorable reaction pathways, and developing production methods for optimum upgrading. Oxygen removal is accomplished by reacting the pyrolysis oil with hydrogen over an appropriate catalytic metal/support combination. This process is often referred to as hydrodeoxygenation. Pyrolysis oils are being characterized, and catalysts are being developed to improve the chemical compositions of the biomass pyrolysis products.

This research will enable wood product industries to diversify their products to include biomass derived fuels and chemicals by helping to (1) understand the composition and properties of woody biomass derived pyrolysis oil (2) improve the heating value of pyrolysis oil and improve properties related to transportability through catalytic hydrodeoxygenation (3) overcome economic barriers to Fischer-Tropsch Liquids (FTL) synthesis by reducing stringent current syngas cleaning requirements, and (4) improve quality of FTL.

Scientific and Technical Merit highlights of this program include: (1) an innovative combinatorial screening micro-array platform integrated with vibrational spectroscopies, (2) synthesis and physical characterization of novel size-selective catalyst/supports using engineered mesoporous (1-10 nm diameter pores) materials, (3) advances in fundamental knowledge of novel support/multi-metal catalyst systems tailored for pyrolysis oil upgrading, (4) rapid ink-jet synthesis techniques for micro-support/catalyst library generation, and (5) characterization of woody biomass-derived pyrolysis oils.

Our *multi-disciplinary, multi-institutional* research cluster is part of a larger Forest Bioproducts Research Initiative at the University of Maine which is addressing one of the seven key areas of Maine's Science and Technology Action Plan. Additionally, new collaborations are being developed between The University of Maine and Colby, Bates, and Bowdoin Colleges. The project currently involves five graduate and five undergraduate students. It is important to note that individual student projects are highly integrated among the Investigators' areas of expertise. This model provides a significant level of collaboration among the students and faculty and a truly multidisciplinary educational experience. We will compare our recent progress and planned activities to Table 1 which lists the projected research milestones from the original proposal.

Table 1. Research Cluster Milestones and Target Dates from UMaine's DOE EPSCOR Proposal

Projects (see Table 4-2)	Fall 2007	Spring 2008	Summer 2008	Fall 2008	Spring 2009	Summer 2009	Fall 2009	Spring 2010	Summer 2010
1. Innovative Reaction Schemes and Technologies **van Heiningen Postdoctoral Student**	Task 1.1; Milestone 1A Determine the feasibility and conditions of pyrolysis oil upgrading utilizing CaO.		Task 1.2 and 1.3; Milestone 1B Commissioning of the CRCL including the pyrolysis reactor, AMI-200RHP and BenchCAT. Demonstrate production of the pyrolysis oil, synthesis of FT liquids from pure syngas, and initial pyrolysis oil upgrading experiments.		Task 1.4; Milestone 1C Scale up of hydrodeoxygenation catalysts and comparison with micro-support/catalyst screening results (with Project 3).		Tasks 3.5 and 4.6; Milestones 3E and 4F Novel Support/Catalyst Exploration		
2. Characterization and Upgrading of Maine Woody Biomass-derived Pyrolysis Oil **van Heiningen Ph.D student**	Tasks 2.1-2.3; Milestone 2A Build reactor system to make pyrolysis oil production of pyrolysis oils from native Maine woody biomass sources and analysis of physical and chemical characteristics.			Tasks 2.4 and 2.5; Milestone 2B Production of upgraded pyrolysis oils using hyrodeoxygenation catalysts. Chemical analysis of the main components of the product and selection of model compounds.		Tasks 2.6 and2.7; Milestone 2C Synthesis, characterization and evaluation of next generation hydrodeoxygenation support/catalysts.			
3. Hydrodeoxygenation of Model Woody Biomass-Derived Pyrolysis Oil **Frederick Ph.D. student**	Task 3.1; Milestone 3A Synthesis and physical characterization of bulk hydrodeoxygenation catalyst/support systems. Task 3.2 Develop ink jet printing (Zeomatrix)		Task 3.2; Milestone 3B Test ink jet printing of micro-Co/Mo mesoporous silica catalysts on substrate and characterize. Analyze data and plan experiments for scale-up in CRCL.		Task 3.3;Milestone 3C Hydrodeoxygenation of selected model compounds on bulk Co/Mo catalysts in CRCL.	Task 3.4;Milestone 3D Microhotplate array screening of Co/Mo catalysts w/ model compounds and comparison to bulk catalysts.	Task 3.5; Milestone 3E Novel Support/Catalyst Exploration		
4. Catalysts for Fischer-Tropsch Conversion of Biomass-Derived Syngas **DeSisto Ph.D. Student**	Task 4.1; Milestone 4A Synthesis and physical characterization of bulk FTL catalyst/support systems.		Task 4.2; Milestone 4B Commissioning of CRCL and evaluation of catalysts for FTL. .		Task 4.3; Milestone 4C First synthesis, characterization and evaluation of micro-catalysts on combinatorial platform	Tasks 4.4 and 4.5; Milestone 4D and 4E In-situ characterization and identification of novel catalysts at ORNL user facilities (ongoing)		Task 4.6; Milestone 4F Novel Support/Catalyst Exploration	
5. Combinatorial Platform and High Throughput Methods for Rapid Catalyst Screening **Wheeler Ph.D. Student**	Task 5.1 Model microhotplate thermal & fluid flow properties, & calorimetric response		Task 5.2 Milestone Fabricate mHP array	Task 5.3; Milestone 5A Characterize heat distribution & fluid flow characteristics	Task 5.4;Milestone 5B Define FTL catalyst library according to Design of Experiments. Integrate Raman & FTIR microscopy.	Tasks 5.5 and 5.6; Milestone 5C and 5D Screen FTL Library to predict optimal catalysts for testing on BenchCat. Determine critical input parameters. Develop data analysis techniques.		Task 5.7; Milestone 5E Predict optimum hydrodeoxygenation support/catalyst composition for characterization and comparison in Project 3	
6. Advisory Committee Meetings		X		X	X		X		X
7. AAAS Evaluations			X			X			X

The colored text in the table corresponds to milestones in the detailed project descriptions presented later in Section 4e and indicates interactions and overlap of Core Areas of Expertise within each project according to the following key:

Reaction Engineering and Innovative Processing Strategies (van Heiningen, Frederick, Stemmler, Shattuck Wheeler)

Synthesis and Physical Characterization of Novel Catalysts (DeSisto, Lad, Austin, Shattuck, Orono Spectral Solutions, Zeomatrix, Wheeler, Frederick, ORNL)

Combinatorial Catalyst Screening using Microarrays and In-Situ Spectroscopy (Wheeler, Collins, Zeomatrix, Orono Spectral Solutions)

Fundamental Reaction Mechanisms and Kinetics of Model Systems (Frederick, Austin, Shattuck, Wheeler)

II) Recent Progress

Project 1

Task 1.1 - We have one graduate student working on pyrolysis oil upgrading using CaO. She has installed and been trained on Karl Fisher titration for water content analysis. She is currently assembling her reactor apparatus and beginning CaO upgrading experiments using mixtures of model pyrolysis oil compounds. We expect to test our methods using real mixtures by end of summer 2008.

Task 1.2 - Commissioning of the AMI 200-RHP is already complete. The fluid bed pyrolysis reactor is currently being fabricated. The BenchCAT is now planned to be implemented as three individually-instrumented reactor systems. The first system will be purchased summer 2008.

Project 2

Task 2.1 - The pyrolysis reactor is being fabricated by our staff technicians and should be completed by end of summer 2008.

Project 3

Task 3.1 – See task 4.1 below.

Task 3.2 – A prototype ink jet deposition system has been fabricated and demonstrated for depositing droplets of silica sols in precise locations. Current work is focused on reducing the droplet size by using smaller-diameter piezoelectric jets.

Project 4

Task 4.1 – We have one graduate student synthesizing mesoporous catalyst materials, and two graduate and two undergraduate students working on reaction and physical characterization. Accomplishments include comparison of silica-supported iron and cobalt catalysts via co-condensation and incipient wetness impregnation techniques. They have been physically characterized after oxidation, reduction, and reaction using TEM to examine pore structure and XRD to determine metal particle size and oxidation state.

Task 4.2 – The mesoporous catalysts have been characterized for BET surface area, oxidation, reduction, and FT production using the AMI200RHP.

Project 5

Task 5.1 – We have one graduate student working on combinatorial platform design. The thermal response of the microhotplate has been calculated, and an adiabatic operation scheme has been chosen that will maximize the thermal sensitivity of the devices to the heat generated by a chemical reaction.

Task 5.2 – A four sensor array has been fabricated. A technique for depositing catalyst suspensions on the array has been tested. Tests to determine our ability to measure differences in heat generation by supported catalysts are currently being conducted.

Status of Facilities Infrastructure Improvements:

1. Altamira catalyst characterization system online
2. Pyrolysis reactor under fabrication
3. Micromiretics micropore BET delivered
4. Karl Fisher water titration apparatus online
5. Amsterdam Density Functional code implemented
6. Prototype inkjet deposition system demonstrated
7. Raman laser replaced

Collaborations and Activities Supported by this Grant:

1. DeSisto, Frederick, Pendse, Wheeler – July 2007 – Attended annual EPSCOR conference at NREL in Boulder, CO
2. Kick-off meeting: October 2007, Attendees: UMaine, Colby, Bates, Bowdoin, Altamira, Orono Spectral Solutions
3. DeSisto, Frederick, Wheeler, and van Heiningen, visited Esteban Chornet – Enerkem – Sherbrooke, QC, Canada – November 2007 – Enerkem will supply UMaine with cylinder of biomass-derived syngas for catalyst testing.
4. DeSisto and Frederick visited ORNL – November 2007 – submitted two user proposals.
5. Pendse visited University of Concepción, Chile – March 2008 – Reciprocal visit by Ljubisa Radovic (Penn State/UConcepsión) April 2008 – Planning joint proposal submission for catalytic pyrolysis oil upgrading utilizing biomass char supports.

III) Planned Activities for Next Year:

- We are on target with respect to the activities in Table 1, and we plan to increase our emphasis on pyrolysis oil upgrading.
- We have defined five new projects for collaborations with Colby, Bates and Bowdoin Colleges that will complement the originally-proposed research goals. The students and projects began in Summer 2008.
- We have recruited a graduate student that is interested in using neutron scattering to characterize catalysts. Therefore, collaborations with ORNL will be pursued in this area.

Linear Thermal Expansion Measurements with Sub-Atomic Resolution for the Study of Phase Transitions in Novel Condensed Matter Systems

John J. Neumeier (PI), Mario S. da Luz, Richard Bollinger, David Cebulla, and Brandon McGuire
Physics Department, Box 173840, Montana State University, Bozeman, MT 59717-3840
neumeier@physics.montana.edu

I. Program Scope

The thermal expansion is a fundamental property of solids that can provide information about phase transitions, lattice dynamics, electronic phenomena, and their interrelationship. It is essential to any complete thermodynamic analysis of a solid. This program involves the development of new tools for measuring the thermal expansion of solids. One of the best measurement methods is capacitance-based. That is, the sample's expansion causes the gap between two parallel metal plates to change. This gap is determined by measuring the capacitance. With this technique, length changes of 0.1 Å can be resolved. For a 1 mm long sample, the relative resolution is 1 part in 10^8. This is at least 1000 times better than high-resolution x-ray or neutron diffraction. As a result, capacitive dilatometry is a powerful tool that compliments diffraction techniques and other microscopic probes.

This project involves the development and advancement of a thermal expansion cell constructed entirely of fused quartz (also called fused silica). There are two distinct advantages of this cell over conventional cells made of copper. Fused quartz has among the smallest known thermal expansions between 30 K and 400 K. As a result, the correction for the thermal expansion of the material from which the cell is made is very small. Secondly, the cell is constructed entirely of fused quartz, which leads to small differential thermal expansion effects and a small addenda.

In addition to the core project of developing the fused-quartz cell, we have developed a cell for measuring the magnetostriction of solids. A prototype magnetostriction cell was completed and tested in 2007 and 2008. This cell uses a physical properties measurement system (PPMS) from Quantum Design as its cryogenic platform. This new cell design is innovative. It provides a test bed for a future project, a thermal expansion cell constructed of single-crystal sapphire.

This grant is provided through the DOE Program entitled, *Building EPSCoR-State National Laboratory Partnerships*. Substantial collaboration with Argonne, Oak Ridge and Los Alamos National Laboratories has been developed with the assistance of these funds. The PI has obtained samples from Drs. David Mandrus and Rongyin Jin at ORNL and Dr. John Mitchell at ANL. Another collaboration with scientists at the pulsed-field branch of the National High Magnetic Field Laboratory (NHMFL) plans to incorporate a fused-quartz magnetostriction cell into the user program. A graduate student supported by this grant, Richard Bollinger, recently visited LANL to conduct measurements of the bulk modulus of Niobium to compliment his thermal expansion investigations. A number of other visits between MSU and national laboratories have also occurred.

II. Recent Progress

We recently published a paper describing the construction, calibration, and performance of our fused quartz thermal expansion cell (or dilatometer cell) in Review of Scientific Instruments [1]. Thermometry issues that are critical to thermal expansion were explained in this publication; this is the first time this aspect has been discussed in the literature. A detailed comparison of our cell to typical thermal expansion cells constructed of copper is also included. It reveals the exceedingly large corrections for that must be made in typical measurements with a copper dilatometer cell. Our publication sets a new standard for the capacitive-based thermal expansion technique.

Fig. 1 shows a schematic of our cell. The cell is composed of 5 pieces. Two L-shaped pieces form the stationary and moveable capacitor plates. On the vertical faces of the L-shaped pieces, a 100 Å/1000 Å Cr/Au film is evaporated to form the metallic capacitor plates. The L-shaped pieces are joined with two fused quartz plates (12 mm x 14 mm x 0.14 mm); these act as springs. The springs are glued to the L-shaped pieces using a mixture of talcum powder and sodium silicate solution. The stationary L-shaped piece has a cutout on the top with a 3˚ angle, relative to the capacitor plate. The sample is placed on top of the moveable plate and a wedge, also with a 3˚ angle, is pushed parallel to the capacitor plates to wedge the sample between it and the moveable plate. This applies tension to the springs to establish the desired

capacitor gap at room temperature. Figure 2 shows an assembled dilatometer cell with a mounted sample. Wedges with a variety of widths are fabricated to accommodate samples of different lengths.

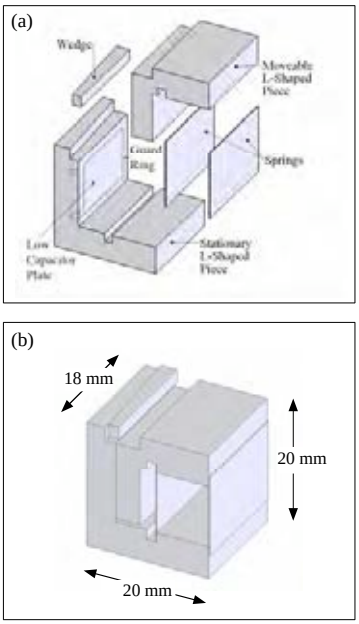

Fig. 1. (a) Exploded view of the fused quartz dilatometer cell. (b) Assembled view of the cell.

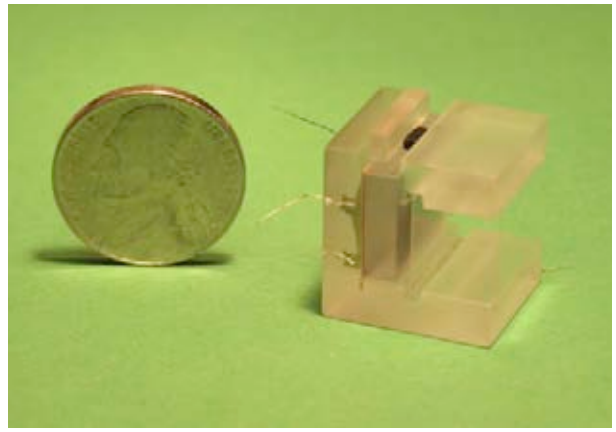

Fig. 2. (color) Dilatometer cell with a sample installed. A US nickel (21.2 mm diameter) helps to appreciate the size. The wires visible in the foreground are connected to the low capacitor plate and guard ring.

We have developed a fused-quartz cell for use in measuring the magnetostriction of solids. The design of this cell is shown in Fig. 3 and an actual cell is shown in Fig. 4. It capitalizes on many of the design aspects of the cell in Figs. 1 and 2, but is a tilt-plate design. A single spring at the top of the cell allows the movable plate to tilt relative to the stationary plate. At the bottom of the cell, the sample and a fused quartz wedge define the plate separation after installing the sample at room temperature. The capacitance plates have length b and width w. The observed capacitance C is related to the sample length $L = d+a$ through

$$C = \frac{\varepsilon w}{\arctan\left(a/b\right)} \ln\left(\frac{d+a}{d}\right). \tag{1}$$

In Eq. (1), d is the plate separation a distance b away from the sample and ε is the dielectric constant of

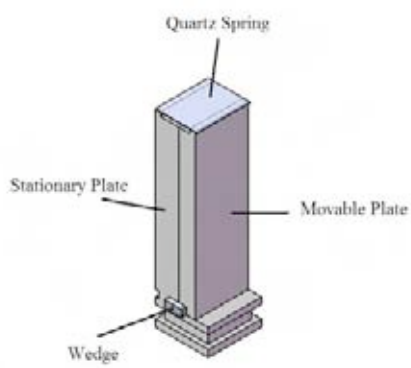

Fig. 3. Schematic of a fused-quartz cell for measuring the magnetostriction of solids. This is a tilt-plate design.

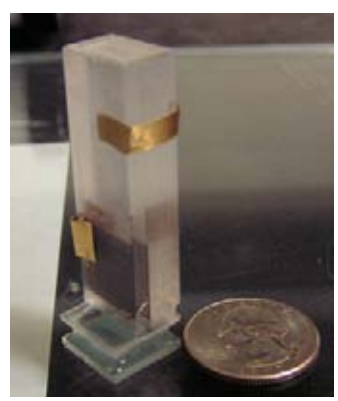

Fig. 4. (color) Fused-quartz magnetostriction cell. The metal springs are used to hold the cell together when gluing the fused-quartz spring in place.

the gas between the cell plates. In 2007 we worked together with Dr. Sonia Francoual of the NHMFL,with the goal of making a smaller cell to place in the 100 tesla pulsed-field magnet at Los Alamos. Dr. Francoual spent two weeks at Montana State University in 2007. During this time she fabricated two cells for testing in the 60 tesla pulsed-field magnet. She is currently working on this project with the hope of testing the cells later in 2008. The PI made two visits to the NHMFL in 2007 to discuss this project.

We briefly highlight some recent results. The magnetostriction cell was used to measure oscillations in the sample length associated with the de Haas-van Alphen effect in Aluminum [2]. These measurements, shown in Fig. 5, illustrate the excellent resolution of the cell. As part of our collaboration with ORNL, we measured the thermal expansion of antiferromagnetic Na_xCoO_2 [3]. This work illustrated the second-order (i.e. continuous) nature of the antiferromagnetic phase transition using fundamental thermodynamics [4] and analysis of the critical behavior. In our investigations of the quasi-one dimensional electrical conductor $Li_{0.9}Mo_6O_{17}$ we focused on the occurrence of superconductivity at 1.9 K, which is unexpected for a one-dimensional system. Our findings [5] indicate that a dimensional crossover occurs at 28 K. Below this temperature, the interchain separation facilitates a more three-dimensional behavior, which is responsible for superconductivity. This discovery aids in our understanding of the anomalous electrical transport in this system [6]. Graduate student Richard Bollinger has measured the thermal expansion coefficient of Niobium in the vicinity of the normal-superconducting phase transition at T_c = 9.3 K. These data are shown in Fig. 6. The distinct jump at T_c is expected from theoretical considerations for a second-order phase transition. It is important to realize that this feature is extremely small, generally requiring sub-angstrom resolution of length changes in order to observe it [7]. Although this jump has been measured once previously, the quality of our data are better and we are able to do a complete thermodynamic analysis using heat capacity and T_c as a function of hydrostatic pressure data, all measured on the same sample. Finally, we mention some fascinating results on the same single crystal of Niobium. We observe a large, broad feature in the thermal expansion coefficient μ between 210 K and 260 K where μ increases by over 80%. We have, through collaboration with Dr. Albert Migliori at LANL, also measured the bulk modulus where a feature occurs in the same temperature range. At present, we suspect this to be associated with some anomalous phonon modes.

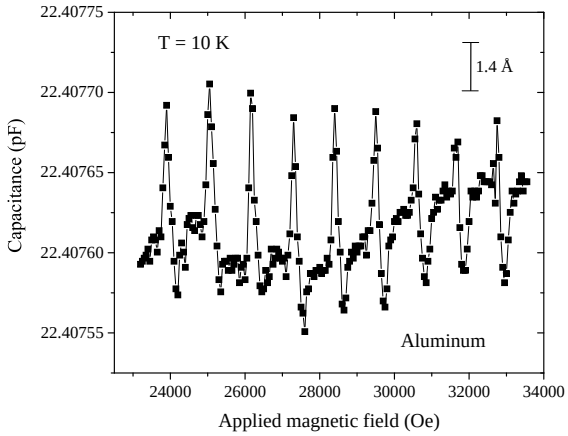

Fig. 5. Magnetostriction of Aluminum illustrating de Haas-van Alphen oscillations. 1.4 Å bar indicates the absolute length change for the 1 mm long sample.

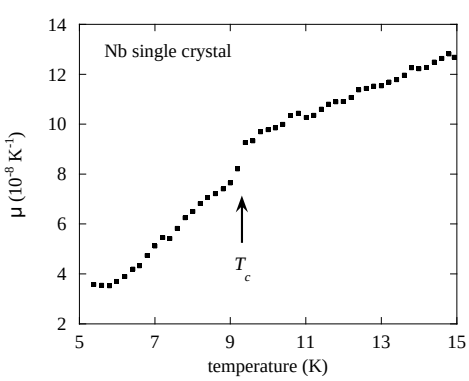

Fig. 6. Thermal expansion coefficient in the vicinity of the normal-superconducting phase transition for Niobium.

III. Future Plans

We will continue our investigations of the thermal expansion and magnetostriction of novel condensed matter systems using the tools we have developed. One of our major goals in the coming year is to develop a thermal expansion cell constructed of single-crystal sapphire. Sapphire has an excellent thermal conductivity and a relatively small thermal expansion coefficient below 30 K. Furthermore, its thermal expansion is very well-behaved. These properties will allow us to extend the range of our experiments from the current limit of 5.5 K to 0.3 K. We anticipate using a tilt-plate design similar to the magnetostriction cell in Figs. 3 and 4. Sapphire is particularly hard to fabricate. However, it is readily available as discs that have been crystallographically oriented. This is important since the thermal expansion of

sapphire is anisotropic. We will make this cell using two discs of sapphire that are connected via a single sapphire spring, similar to the single-spring design used in our magnetostriction cell of Figs. 3 and 4.

IV. References (numbers in boldface were supported by the DOE)

[1] J. J. Neumeier, R. K. Bollinger, G. E. Timmins, C. R. Lane, R. D. Krogstad, and J. Macaluso, *Capacitive-based dilatometer cell constructed of fused quartz for measuring the thermal expansion of solids*, Rev. Sci. Instrum. 79 (2008) 033903.

[2] B. A. Green, Jr. and B. S. Chandrasekar, *Observation of oscillatory magnetostriction in Bismuth at 4.2 K*, Phys. Rev. Lett. 11 (1963) 331.

[3] C. A. M. dos Santos, J. J. Neumeier, Y.-K. Yu, R. K. Bollinger, R. Jin, D. Mandrus, and B. C. Sales, *Thermodynamic nature of the antiferromagnetic transition in* Na_xCoO_2, Phys. Rev. B 74 (2006) 132404.

[4] J. A. Souza, Y.-K. Yu, J. J. Neumeier, H. Terashita, and R. F. Jardim, *Method for Analyzing Second-Order Phase Transitions: Application to the Ferromagnetic Transition of a Polaronic System*, Phys. Rev. Lett. 94 (2005) 207209.

[5] C. A. M. dos Santos, B. D. White, Y.-K. Yu, J. J. Neumeier, and J. A. Souza, *Dimensional Crossover in the Purple Bronze* $Li_{0.9}Mo_6O_{17}$, Phys. Rev. Lett. 98 (2007) 266405.

[6] C. A. M. dos Santos, M. S. da Luz, Y.-K. Yu, J. J. Neumeier, J. Moreno and B. D. White, *Electrical transport in single-crystalline* $Li_{0.9}Mo_6O_{17}$*: A two-band Luttinger liquid exhibiting Bose metal behavior*, Phys. Rev. B 77 (2008) 193106.

[7] J. J. Neumeier, T. Tomita, M. Debassai, J. S. Schilling, P. W. Barnes, D. G. Hinks, and J. D. Jorgensen, *Negative thermal expansion of* MgB_2 *in the superconducting state and anomalous behavior of the bulk Grüneisen function*, Phys. Rev. B 72 (2005) 220505(R).

Other publications associated with this DOE-EPSCoR grant

(i) J. A. Souza, J. J. Neumeier, and Y.-K. Yu, *Magnetic signatures of ferromagnetic polarons in* $La_{0.7}Ca_{0.3}MnO_3$*, Colossal magnetoresistance is not a Griffiths Singularity*, submitted to Phys. Rev. B.

(ii) J. A. Souza, J. J. Neumeier, B. D. White, H. Terashita, and Yi-Kuo Yu, *Scaling behavior of diverging and finite continuous phase transitions: Application to ferromagnetic and antiferromagnetic manganese oxides*, submitted to Phys. Rev. B.

(iii) B. D. White, C. A. M. dos Santos, J. A. Souza, K. J. McClellan, and J. J. Neumeier, *Crystal growth and characterization of Marokite* $CaMn_2O_{4+\delta}$, J. of Crystal Growth 310 (2008) 3325.

(iv) H. D. Zhou, E. S. Choi, J. A. Souza, J. Lu, Y. Xin, L. L. Lumata, B. S. Conner, L. Balicas, J. S. Brooks, J. J. Neumeier, and C. R. Wiebe, *Magnetic-polaron-driven magnetoresistance in the pyrochlore* $Lu_2V_2O_7$, Phys. Rev. B Rapid Commun. 77 (2008) 020411(R) (4 pages).

(v) M. S. da Luz, C. A. M. dos Santos, J. Moreno, B. D. White, and J. J. Neumeier, *Anisotropic electrical resistivity of quasi-one-dimensional* $Li_{0.9}Mo_6O_{17}$ *determined by the Montgomery Method*, Phys. Rev. B 76 (2007) 233105 (3 pages).

(vi) J. A. Souza, J. J. Neumeier, R. K. Bollinger, B. McGuire, C. A. M. dos Santos, and H. Terashita, *Magnetic susceptibility and electrical resistivity of* $LaMnO_3$*,* $CaMnO_3$*, and* $La_{1-x}Sr_xMnO_3$ $(0.13 \leq x \leq 0.45)$ *in the temperature range 300-900 K*, Phys. Rev. B 76 (2007) 24407 (6 pages).

DOE-DEPSCoR – National Laboratory Partnership Program
Award DE-FG02-08ER46498
Project Duration July 2008 to June 2011

Rational Design of Molecular Ferroelectric Materials and Nanostructures

PIs: **Stephen Ducharme,[1] James M. Takacs**
Post-Docs: **Zhonjin Ge,[2] Rafal Korlacki[1]**
Students: **Jihee Kim,[1] Jeremy Johnston,[1] Yong Wang[1]**
DOE Partner **Serge M. Nakhmanson[3]**

[1]*Department of Physics and Astronomy,* [2]*Department of Chemistry*
Nebraska Center for Materials and Nanoscience, University of Nebraska, Lincoln
[3]*Interfacial Materials Group, Materials Science Division,*
Argonne National Laboratory, Argonne, IL 60439-4838

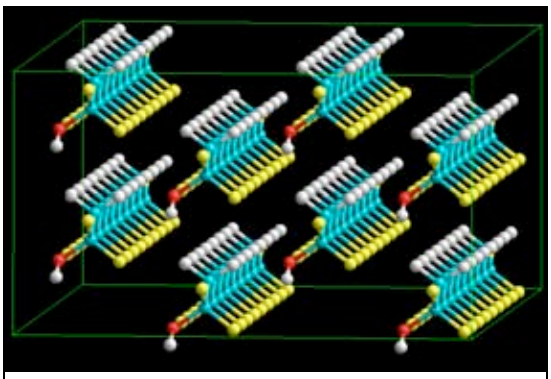

Fig. 1. Structure of a VDF oligomer.

An essential component of sustainable energy policy is the development of new materials for use in low-cost, energy-efficient transducer arrays and electronic devices. Among the most promising and versatile materials for these technologies are ferroelectric polymers based on vinylidene fluoride (VDF, CH_2CF_2). The VDF backbone and large built-in dipole moment is the fundamental structure of the prototypical ferroelectric polymer which, in bulk and thin film form, exhibits remarkable ferroelectric and electroactive properties.[1,2] The purpose of this project is to learn the fundamental relationships between the molecular structure and physical properties of two nanostructured analogs of PVDF, VDF oligomers like OH-$(CH_2$-$CF_2)_8$-CF_3 (**Fig. 1**). With the rapid advances in both synthetic manipulation and first-principles modeling, it is now possible to optimize material properties through manipulation of atomic and nanoscale structure.

The study of PVDF and its copolymers has spanned more than four decades, with particular attention to ferroelectricity and related physical properties, such as the piezoelectric and pyroelectric responses. As with many crystalline polymers the study of ferroelectric polymers is hampered by the fact that the method of crystallization from solution generally produces polymorphous samples with incomplete macroscopic alignment. Several recent innovations further advanced the field of ferroelectric polymers. The application of Langmuir-Blodgett (LB) deposition to the VDF copolymers,[3] enabling the first studies of two-dimensional ferroelectricity.[1] Another innovation was the recent demonstration of ferroelectricity in VDF oligomer crystals,[4,5] which consist of linear VDF, are functionally equivalent to PVDF, but are easier to handle and crystallize. These differ from PVDF only by the fact that they consist not of long polymers, but of finite lengths of VDF. Encouraged by this work, we have synthesized a series of VDF oligomers suitable for production of self-assembled nanoscale structures. Concurrent development in the 1990s of Modern Polarization Theory, the application of Berry-phase methods to the calculation of polarization in ferroelectrics, enabled the application of powerful first-principles computation to ferroelectrics,[6] in particular PVDF,[7,8] VDF copolymers,[9] and promising analogs.[7,10] The vinylidene fluoride oligomers are of interest because they exhibit ferroelectric polarization hys-

teresis like their polyvinylidene fluoride (PVDF) counterparts, yet can form molecular crystals and high-quality crystalline thin films. By proper choice of terminal group R, we can form highly crystalline thin films by Langmuir-Blodgett (LB) deposition. Unlike the LB films formed from PVDF copolymers,[11] the oligomer LB films have the chain axes (along the C-C backbone) perpendicular to the film, and the dipole moments are oriented in the film plane.

Vinylidene fluoride oligomers were prepared via the *tert*-butyl peroxy pivalate-initiated iodine transfer oligomerization of VDF with trifluoromethyl iodide.[12] This method produces very narrowly dispersed oligomer via fractional precipitation and contains very few defects (ca. 1%, as determined from proton NMR), a feature which is crucial for the studies described below. The films for the present study were prepared from oligomers $CF_3(CH_2CF_2)_nR$ with VDF count n = 14±1, and 15±1 and R = OH, and I, respectively, formed 20 monolayers thick samples by Langmuir-Blodgett deposition on silicone substrates and annealed at 135 °C for one hour. [11] The oligomers lend themselves to fabrication of high quality LB films with the chains oriented perpendicular to the film (Fig. 2), since they are good amphiphiles, and therefore we have made films of both OH and Iodine terminated oligomers with varying lengths. For example, *oligo*$(VDF)_n$-I with n = 14 VDF units exhibited a pressure-area compression isotherm (**Fig. 3**) indicating excellent Langmuir layer behavior.

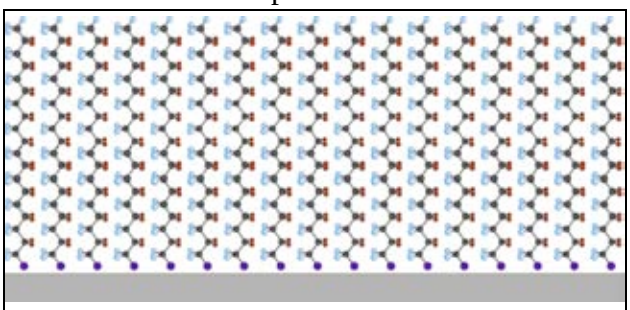

Fig. 2. VDF oligomer copolymer film structure.

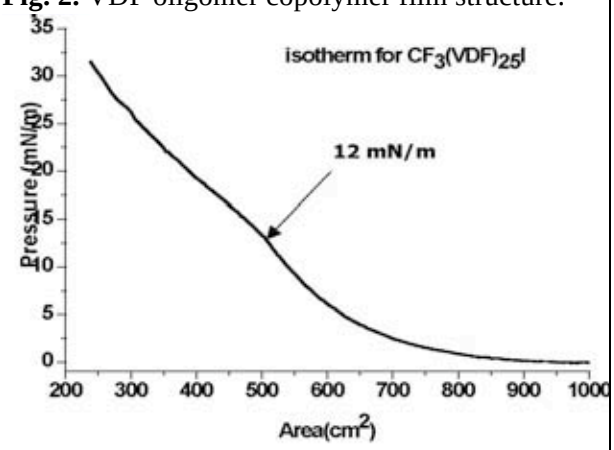

Fig. 3. Pressure-area isotherm of an oligomer Langmuir layer before deposition.

The crystal quality and molecular orientation were determined by theta-2theta x-ray diffraction using both out-of-plane and in-plane diffraction geometries. The x-ray diffraction results (**Fig. 4**) are consistent with a highly crystalline film having an orthorhombic unit cell indexed so that the oligomer chains are along the (001) direction and the net dipole moment along the (101) direction. The unit cell dimensions a = 8.6 Å, b = 4.8 Å and c = 2.6 Å are in excellent agreement with the unit cell of ferroelectric PVDF.[13] This also means that the VDF chains have all-trans conformation – gauche bonds would expand the

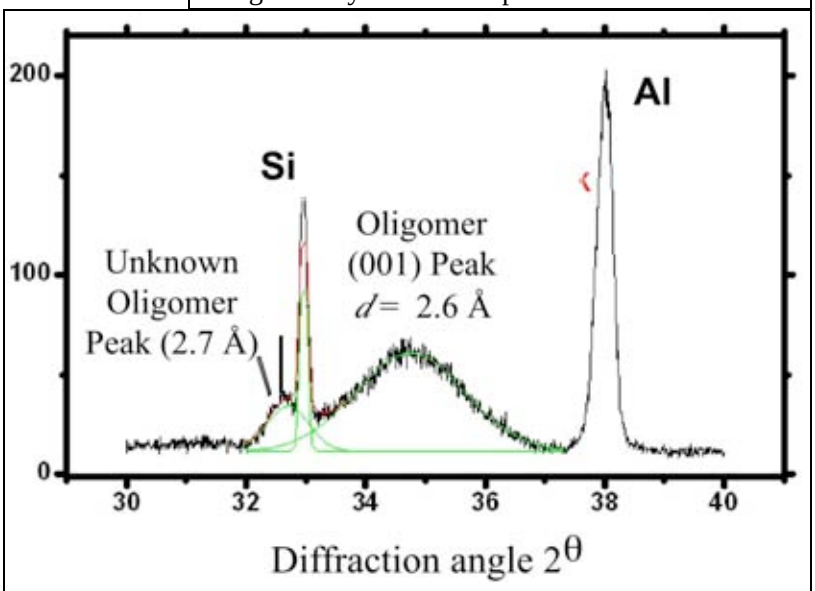

Fig. 4. Out-of-plane X-ray diffraction peaks from a 20-ML *oligo*VDF-I LB films made by LB deposition on Si.

a and *b* spacings by 10%.

The perpendicular orientation and all-trans conformation were confirmed by spectroscopic infrared ellipsometry (**Fig. 5**). Oligomers with n = 10 did not form crystalline films, nor did they orient so well normal to the substrate, indicating that such short oligomers are not crystalline at room temperature. This is similar to the transition from solid to waxy to liquid states with decreasing length in medium-length alkanes (paraffins).[14] Infrared spectra were recorded with infrared spectroscopic ellipsometer and WVASE32™ software from the J. A. Woollam Company. The experimental absorption bands were extracted from the ellipsometric spectra Ψ and Δ using the Lorentz oscillator analysis.[15] The theoretical vibrational modes were calculated using using PQS ver. 3.3 software from Parallel Quantum Solutions, which implements the density functional theory employing a hybrid potential (designated B3LYP) and split-valence basis set with polarization and diffuse functions on all heavy atoms (6-31+G*) for slightly shorter molecules with VDF count n=9. The ellipsometry data and the calculations agree well on the major absorption bands (**Fig. 5**). Furthermore, the polarization anisotropy clearly shows that the molecules are oriented with their long axes normal to the substrate, while in case of polyvinylidene fluoride Langmuir-Blodgett films the polymer chains are parallel to the substrates.[11] The molecular conformation of the oligomers is consistent with the all-trans conformation of the ferroelectric form of PVDF. The results of density functional theory calculations allow verification of empirical band assignments and force fields of vinylidene fluoride-based oligomers and polymers, widely present in the literature.

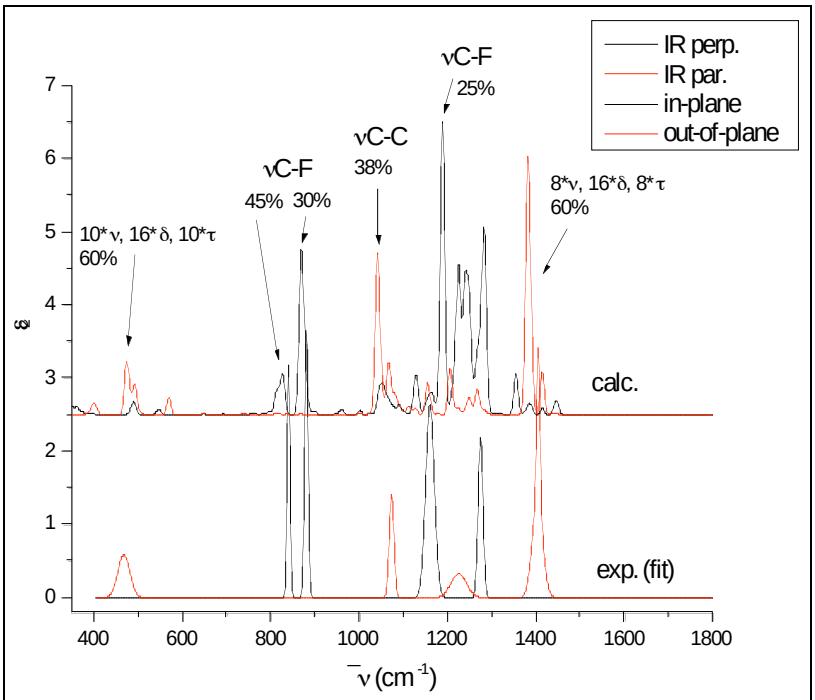

Fig. 5. Infrared vibrational modes from molecular modeling (top) and spectroscopic ellipsometry (bottom).[13] The mode assignments are consistent with the structure oriented as shown in Fig. 2.

The simulation and modeling of structural, electronic and dynamical properties of the oligomer systems will be carried out from first principles, utilizing the density functional theory approach. The recently developed "modern theory of polarization" formulated in terms maximally-localized Wannier functions will be used for calculating the polar properties of periodic oligomer crystals, such as dielectric constants, spontaneous polarization, pyroelectric response and piezoelectric response.[16] The power of this approach is illustrated in Fig. 6, which shows that the dipolar coupling increases the crystal polarization by 50% when compared to the isolated polymer chains.

We thank Dan Thompson for assistance with the ellipsometer operation. This work was supported by the Nebraska Research Initiative.

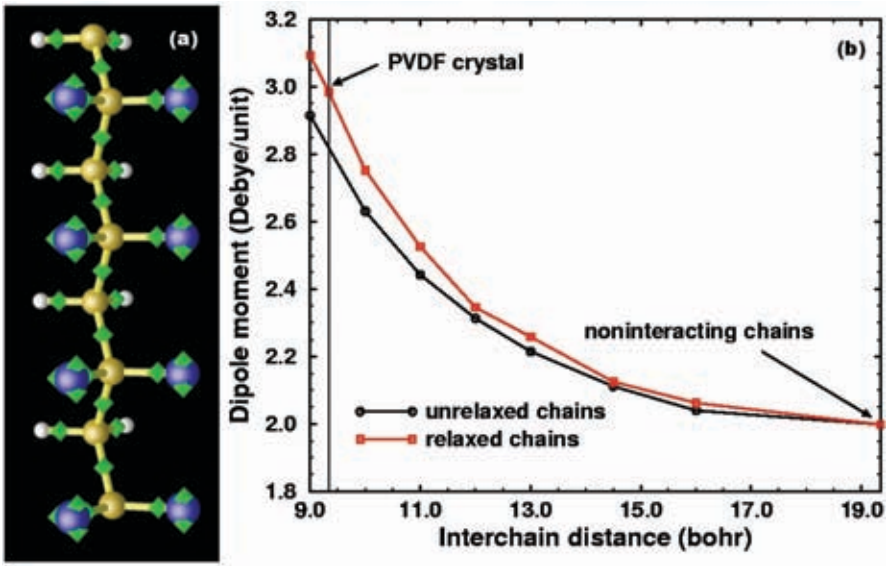

Fig. 6. Structure and charge distribution in ferroelectric PVDF. (a) Segment of a β-PVDF chain where carbon atoms are yellow and fluorines blue. The green diamonds mark the positions of the WF charge centers computed for an isolated infinite β-PVDF chain. (b) Average z component of the VDF unit dipole moment in an infinite β-PVDF chain as the chains are brought together to form a crystal. [9]

References

[1] Alexander V. Bune, Vladimir M. Fridkin, Stephen Ducharme, L. M. Blinov, S. P. Palto, A. V. Sorokin, S. G. Yudin, and A. Zlatkin, Nature (London) **391**, 874 (1998).

[2] Qiming Zhang, Vivek Bharti, and X. Zhao, Science **280** (26 June), 2101 (1998); A. Gerber, M. Fitsilis, H. Kohlstedt, R. Waser, T. J. Reece, S. Ducharme, and E. Rije, J. Appl. Phys. **100**, 5 (2006).

[3] S. Palto, L. Blinov, A. Bune, E. Dubovik, Vladimir Fridkin, N. Petukhova, K. Verkhovskaya, and S. Yudin, Ferro. Lett. **19** (3/4), 65 (1995).

[4] K. Noda, K. Ishida, T. Horiuchi, K. Matsushige, and A. Kubono, J. Appl. Phys. **86**, 3688 (1999).

[5] K. Noda, K. Ishida, A. Kubono, T. Horiuchi, H. Yamada, and K. Matsushige, Japanese Journal of Applied Physics, Part 1 (Regular Papers, Short Notes & Review Papers) **40**, 4361 (2001).

[6] J. Bernholc, S. M. Nakhmanson, and M. Buongiorno Nardelli, Computing in Science and Engineering (CISE) **6** (6), 12 (2004); D. A. Tenne, *et al.*, Science **313**, 1614 (2006).

[7] S. M. Nakhmanson, M. Buongiorno Nardelli, and J. Bernholc, Phys. Rev. Lett. **92** (11), 115504 (2004).

[8] N. J. Ramer and K. A. Stiso, Polymer **46** (23), 10431 (2005).

[9] S. M. Nakhmanson, M. Buongiorno Nardelli, and J. Bernholc, Phys. Rev. B **72**, 115210 (2005).

[10] Matt Poulsen, D. Sahadeva Reddy, S. M. Nakhmanson, Menjun Bai, Y. Wen, James M. Takacs, J. Bernholc, V.M. Fridkin, and Stephen Ducharme, in preparation (2007).

[11] Stephen Ducharme, S. P. Palto, and Vladimir M. Fridkin, in *Ferroelectric and Dielectric Thin Films*, edited by Hari Singh Nalwa (Academic Press, San Diego, 2002), Vol. 3, pp. 545.

[12] Bruno Ameduri, Catherine Ladaviere, Frederic Delolme, and Bernard Boutevin, Macromolecules **37** (20), 7602 (2004).

[13] E. Bellet-Amalric and J. F. Legrand, Eur. Phys. J. B **3** (2), 225 (1998).

[14] P. H. Geil, *Polymer Single Crystals*. (Interscience, New York City, 1963).

[15] Mengjun Bai, Matt Poulsen, A. V. Sorokin, Stephen Ducharme, C. M. Herzinger, and V. M. Fridkin, J. Appl. Phys. **94**, 195 (2003).

[16] R.D. King-Smith and D. Vanderbilt, Physical Review B (Condensed Matter) **47**, 1651 (1993); R. Resta, Reviews of Modern Physics **66** (3), 899 (1994).

The Luminosity Measurement for the DZERO Experiment at Fermilab

Principal Investigator: Gregory R. Snow
E-mail: gsnow@unlhep.unl.edu
Co-Principal Investigators: Kenneth Bloom, Daniel Claes, Aaron Dominguez
Department of Physics and Astronomy
116 Brace Hall
University of Nebraska-Lincoln
Lincoln, Nebraska 68588-0111

Introduction

This abstract is being submitted at the very beginning of a grant from the DOE/EPSCoR National Laboratory Partnership Program. Hence, this abstract will focus on the scope of the project and future plans. The grant supports a strong partnership between the experimental high energy physics group in the University of Nebraska-Lincoln (UNL) Department of Physics and Astronomy and the Fermi National Accelerator Laboratory (Fermilab) in Batavia, Illinois, to measure the proton-antiproton luminosity at the DZERO experiment. Our primary partner and contact person at Fermilab is Dr. Dmitri Denisov, co-spokesperson of the DZERO experiment and a senior physicist (Scientist II) employed by Fermilab.

Project scope and description

The luminosity measurement is crucial to the entire physics program of DZERO and Fermilab as a whole, and the UNL group has the leadership and expertise needed to make it a success. The DZERO experiment is one of two large experiments operating at Fermilab's Tevatron Collider, the world's highest energy particle accelerator. The experiment is a key element in the DOE High Energy Physics program's mission to discover the elementary constituents of matter and energy, explore the basic nature of space and time, and probe the interactions between them. The UNL high energy physics group has been a leading member of the DZERO collaboration for many years and has contributed in a number of important areas. This project will expand the group's present role in the luminosity measurement, an area suffering from a loss of critical human resources. UNL faculty member Gregory Snow serves as the Principal Investigator (PI) of the project and Co-Principal Investigators will be UNL faculty members Kenneth Bloom, Daniel Claes, and Aaron Dominguez. The project supports two junior University of Nebraska positions, one postdoctoral research associate and one graduate student, who will be supervised in their contributions to the luminosity measurement for the 3-year period of the project by the project's PIs. This 3-year period corresponds to the last 2 years of the DZERO experiment's Run II data taking and a subsequent year of data analysis to publish the experiment's final results.

Primary project objective: The addition of University of Nebraska human resources supported by the grant will help ensure that Fermilab's DZERO experiment has a reliable luminosity measurement through the end of Run II data taking and an easily-accessible

repository of luminosity information for all collaborators performing physics analyses through the publication of its final physics results.

The UNL Department of Physics and Astronomy Instrument Shop will also contribute to DZERO's luminosity measurement by preparing a set of scintillation counters that will be needed to replace the existing detectors in the experiment's Luminosity Monitor during a shutdown of the Tevatron accelerator, yet to be scheduled, in late 2008 or 2009. Working closely with the Scintillation Detector Development Center, one of Fermilab's Technical Centers in the Particle Physics Division, this experience will enhance the UNL Instrument Shop's technical base which will, in turn, heighten its readiness to contribute to future detector construction projects that involve scintillation counters.

Secondary project objective: The collaboration between the UNL Instrument Shop and Fermilab's Scintillation Detector Development Center will enhance the University of Nebraska's future role as a particle detector R&D and production facility for future high energy physics experiments.

Overall project objective: The targeted project supported by the grant will enhance the University of Nebraska's presence in both frontier high energy physics research in DZERO and particle detector development, and it will thereby serve the goals of the DOE Office of Science and the Experimental Program to Stimulate Competitive Research (EPSCoR) for the state of Nebraska.

The DZERO Luminosity Measurement: An essential ingredient in all cross section measurements made by the DZERO experiment is the luminosity used to normalize the data sample. The luminosity, L, is determined by measuring the counting rate of inelastic proton-antiproton collisions recorded by the DØ luminosity monitor system [1]:

$$L = \frac{1}{\sigma_{eff}} \frac{dN}{dt}, \qquad (1)$$

where σ_{eff} is the effective inelastic cross section seen by the LM. The effective cross section is derived from the total inelastic cross section, $\sigma_{inelastic}$(1.96 TeV) = 60.7 ± 2.4 mb [2], used by both the DØ and CDF collaborations for Run II luminosity determinations. The cross section σ_{eff} differs from $\sigma_{inelastic}$ by the LM system geometric acceptance and efficiency for registering inelastic events. Both the acceptance and efficiency are determined from Monte Carlo simulated inelastic events run through a detailed simulation of the LM detector and response. The LM consists of two arrays of 24 wedged-shaped plastic scintillators radiating outward from the beam pipe located at z = ±140 cm where the positive z direction is the proton beam direction. The arrays, shown in Fig. 1, cover the pseudo-rapidity region $2.7 < |\eta| < 4.4$.

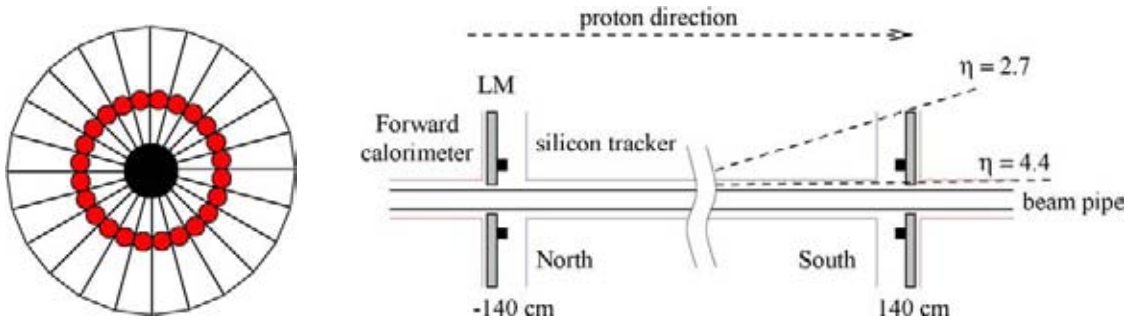

Figure 1. The Luminosity Monitor layout. The *r*-φ view is on the left. The *r*-*z* view of the two arrays is shown on the right.

In practice, the luminosity is calculated by inverting the expression

$$P(0) = e^{-\sigma_{eff} L/f} \times (2e^{(-\sigma_{SS}/2f)L} - e^{-\sigma_{SS} L/f}) \ , \qquad (2)$$

where $P(0)$ is the probability that a bunch crossing does not produce a coincidence of in-time hits recorded in each of the two LM arrays, σ_{SS} ($SS \equiv$ single-sided) is the effective cross section for only one of the arrays to fire, and f is the crossing frequency for a given beam bunch. This approach is referred to as the *counting zeros* technique. During data-taking, $P(0)$ is measured for each of the 36 separate bunch crossings. Each $P(0)$ is determined by counting events over a time period of about one minute, chosen long enough that the statistical uncertainty on $P(0)$ is much less than 1%, but short enough that the instantaneous luminosity changes negligibly. The luminosity-dependent term in parentheses on the right side of equation (2) is due to the presence of multiple interactions per bunch crossing. This term accounts for beam crossings that have no proton-antiproton interactions that produce hits in both luminosity arrays, but have two or more interactions that each fire a single array and jointly produce hits in both arrays.

Maintaining the LM detector system and making luminosity information available to collaborators for physics analysis has required a group of 8 people who comprise the experiment's Luminosity Working Group. The Working Group is responsible for the following distinct aspects of the luminosity measurement:

(i) Monitoring the performance of the LM detector system (both the scintillation counters and the associated readout electronics);

(ii) Monitoring the effects of radiation damage on the scintillators as they are exposed to the particle flux resulting from high-luminosity proton-antiproton collisions;

(iii) Replacing the scintillation counters when radiation damage decreases their light output and efficiency below an acceptable level;

(iv) Determining the calibration constants, σ_{eff} and σ_{SS}, that convert measured rates in the LM detectors to absolute luminosity;

(v) Producing and verifying daily/weekly/monthly reports of integrated luminosity to the experiment and the laboratory;

(vi) Filling and verifying the luminosity database which is the repository of luminosity information for the experiment;
(vii) Maintaining the tools collaborators employ to access luminosity information for physics analysis and responding to frequent user questions on the use;
(viii) Maintaining and updating the experiment's luminosity web page and other documentation;
(ix) Reporting the status of the luminosity measurement at meetings of the experiment's physics conveners and spokespersons and at weekly experiment operations meetings;
(x) Participating in Fermilab's Joint Luminosity Working Group that meets periodically to review the luminosity measurements of the DZERO and CDF experiments and the Accelerator Division.

The Principal Investigator of this proposal, Professor Gregory Snow, has served as co-convener of the Luminosity Working Group since January 2006. He will remain in this position through the end of the current data-taking period, Run IIb, providing key leadership for this measurement.

Future Plans

Near-term future plans include: (i) Recruit and hire postdoctoral research associate and enlist UNL graduate student as full-time research assistant, (ii) Assign and train new group members to ongoing Luminosity Working Group operations tasks enumerated above, (iii) Prepare scintillator wedges for the upcoming replacement of Luminosity Monitor detectors at UNL, (iv) Replace LM detectors during the next Tevatron shutdown and commission new detectors, (v) New group members become involved in physics analysis projects in consultation with faculty PI and co-PIs, and (vi) Maintain the luminosity measurement partnership with the DZERO management and Fermilab technical staff via exchange visits and videoconference discussions.

Bibliography and References Cited

[1] C-C. Miao, FERMILAB-Conf-98/395-E (1998); V.M. Abazov *et al.*, Nucl. Instr. and Methods **A565**, 463 (2006), FERMILAB-Pub-05/341-E (2005).
[2] S. Klimenko, J. Konigsberg, T.M. Liss, FERMILAB-FN-0741 (2003).

DOE sponsored publications

T. Andeen *et al.*, "The DØ Experiment's Integrated Luminosity for Tevatron Run IIa", FERMILAB-TM-2365 (2007), http://lss.fnal.gov/archive/test-tm/2000/fermilab-tm-2365.pdf. G. Snow is the primary author of this public Fermilab Technical Memo which is referenced in all DZERO publications that quote the assessed luminosity and its uncertainty used in Run II physics analyses.

A full list of DZERO Run II publications (published, accepted, and submitted) can be found at: http://www-d0.fnal.gov/www_buffer/pub/Run2_publications.html.

Hydraulic Properties of Layered Soils and Its Impact on Water Flow – Anisotropy and Numerical Simulations

Jianting Zhu (PI)[*], Ming Ye[§], Dongmin Sun[†], Philip Meyer[‡],
Yanxia Zhao[*], Ahmed Hassan[*], Feng Pan[*] and Rushikesh Veni [*]
[*]Desert Research Institute, Las Vegas, NV 89119, [§]School of Computational Science, Florida State University, Tallahassee, FL 32306, [†]University of Houston-Clear Lake, Houston, TX 77058, [‡]Pacific Northwest National Laboratory, Richland, WA 99352

I.) Program Scope:

Soil hydraulic properties are critical in modeling and predicting flow and transport in the unsaturated zone. Simulations of water flow and contaminant transport in heterogeneous soils are often hampered by lack of measurements of soil hydraulic parameters which are time-consuming and difficult, making it necessary to rely on other sources of information. Naturally layered soil formation makes it even more difficult to predict water movement and contaminant transport in the subsurface. We seek to address a number of issues related to the heterogeneous hydraulic property characterizations and applications in simulating a complex field injection experiment at Hanford site in southeastern Washington State. Specific objectives are to:

(1) Develop innovative ANN-based pedo-transfer functions (PTFs) to estimate soil hydraulic parameters using "soft" data (e.g., particle size distribution and soil texture and bulk density etc.). The PTFs will incorporate parameter distributions obtained from the extended Bayesian updating method and eliminate the artificial correlation of output hydraulic parameters.

(2) Establish equivalent anisotropic hydraulic conductivities for unsaturated soil formations, typical for Hanford site.

(3) Propose a new Bayesian geostatistical inference method to estimate spatial correlation scale of inputs to the developed neural network models. Heterogeneous input fields will be generated and fed to the neural network models to generate heterogeneous fields of soil hydraulic parameters that can be used for numerical simulation and uncertainty analyses.

The outcomes facilitate subsurface flow and contaminant transport modeling and improve the defensibility of model results. Systematic and quantitative consideration of the parametric heterogeneity and uncertainty can properly address and further reduce predictive uncertainty for contamination characterization and environmental restoration at DOE-managed sites such as the Hanford and other sites.

II.) Recent Progress:

We use the hydraulic property model of van Genuchten[1], which closely fits measured water-retention and conductivity data of many soil types[2],

$$\theta(h) = \theta_r + (\theta_s - \theta_r)\left[1 + (\alpha h)^n\right]^{-m} \tag{1}$$

$$K(h) = K_S \left\{1 - (\alpha h)^{mn}\left[1 + (\alpha h)^n\right]^{-m}\right\}^2 \left[1 + (\alpha h)^n\right]^{-m/2} \tag{2}$$

where h is the soil water suction head [L], θ is the soil water content [L^3L^{-3}], θ_r is the residual water content [L^3L^{-3}], θ_s is the saturated water content [L^3L^{-3}], K_S is the saturated hydraulic conductivity [L/T], α is the shape factor, approximately equal to the

inverse to the air entry value [L^{-1}], n is the pore size distribution index [-], and m is the empirical constant which can be related to n by $m = 1-1/n$.

II.1. Artificial Neural Network Based Pedo-transfer Functions (PTFs)

The traditional neural network based PTFs utilize the mean square error (MSE) objective function (denoted *Function* 1) (i.e., the sum of the squared errors of the neural network prediction of the soil hydraulic properties). We try to develop a suite of new neural network models to estimate soil hydraulic parameters. These neural networks have the same input and output variables, but different objective functions, which will incorporate sequentially the site soil hydraulic parameter measurements, parameter probability distributions, (denoted *Function* 2), and will incorporate the parameter correlations among different hydraulic parameters (denoted *Function* 3). Since non-conventional objective functions are used, new neural network algorithms are needed. In doing so, the computation of the derivatives of the objective function with respect to the neural network weights is a key step in implementation of neural network models. This can be accomplished in two steps, (1) the derivative of the objective function with respect to the output hydraulic parameters, and (2) the derivative of the output parameters with respect to the weights. Using a synthetic data set calculated based on the multiple regression models of Rawls and Brakensiek [3], we first test and investigate the ANN models with three different objective functions described above. Then 53-point hydraulic parameter set and the associated texture and bulk density data set collected from the Hanford site are the used to train the ANN models. Table 1 shows correlation coefficients between the original and the ANN model predicted hydraulic parameters for three different objective functions. We can see a better correlation trend when using objective *Function* 2 and *Function* 3.

Table 1: Correlation coefficient between the original and the ANN predicted hydraulic parameters

	Function 1	*Function* 2	*Function* 3
θ_r	0.2044	0.5252	0.5498
θ_s	0.5651	0.6056	0.6649
$\log(\alpha)$	0.5273	0.6093	0.6436
$\log(n)$	0.6732	0.7251	0.7161
$\log(K_S)$	0.8654	0.8980	0.9000

II.2. Parallel and Perpendicular Unsaturated Hydraulic Conductivities and Anisotropy

For saturated flows, it is well known that the equivalent parallel hydraulic conductivity is equal to the arithmetic mean of all individual hydraulic conductivities and the equivalent perpendicular hydraulic conductivity is equal to the harmonic mean of all individual hydraulic conductivities. Due to the non-linear relationship between the unsaturated hydraulic conductivity and the saturation, the validity of the same schemes for unsaturated flows needs to be examined. This study investigates equivalent hydraulic conductivities for unsaturated vertical flows under two distinct soil layering scenarios, layers parallel to flows (i.e., parallel vertical slabs/columns) and layers perpendicular to flows (i.e., horizontal layers). The two scenarios are referred to as horizontal heterogeneity scenario and vertical heterogeneity scenario respectively. Results demonstrate that the arithmetic mean for horizontal heterogeneity scenario and the

harmonic mean for vertical heterogeneity scenario, extended from the saturated flow situations, would introduce large relative errors in simulating the flux for coarser textured soils and for heterogeneous soils with large hydraulic parameter variances (see Figure 1).

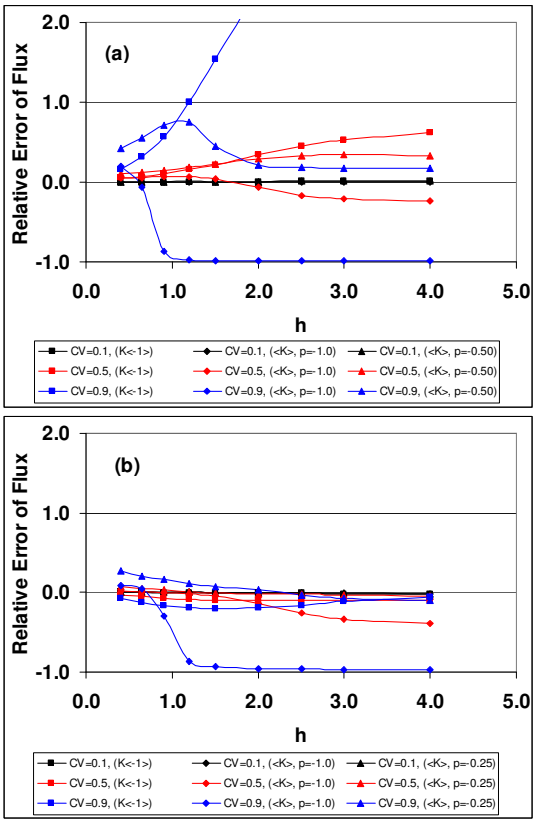

Figure 1: Relative error of flux as functions of *h* under various average hydraulic conductivity schemes

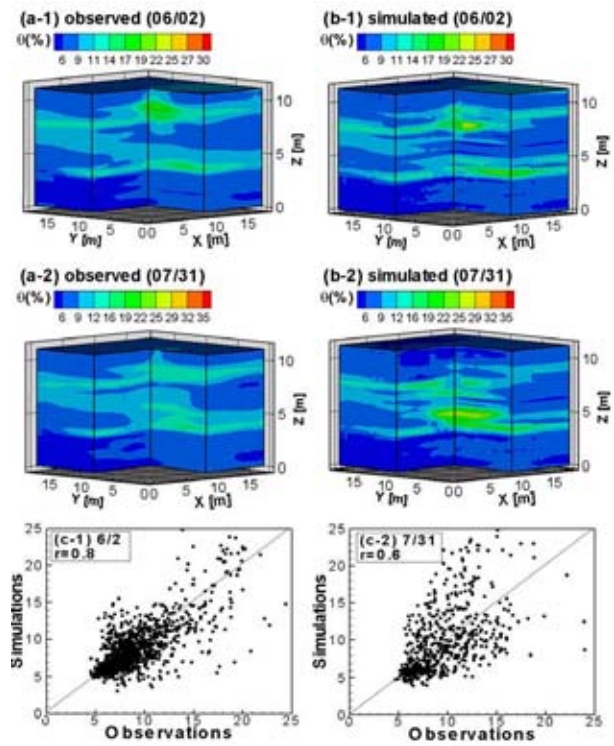

Figure 2: Comparison between field measured and simulated moisture contents

<u>II.3. Simulation of Field Injection Experiments in Heterogeneous Unsaturated Soils</u>

We develop a methodology to integrate data that can be easily obtained with data on soil hydraulic properties via cokriging and artificial neural network (ANN)-based pedotransfer functions. The method is applied to generate heterogeneous soil hydraulic parameters at a field injection experiment in southeastern Washington State. Stratigraphy at the site consists of imperfectly stratified layers with irregular layer boundaries. Cokriging is first used to generate three-dimensional heterogeneous fields of bulk density and soil texture using an extensive data set of field-measured soil moisture, which carry signature about site heterogeneity and stratigraphy. Soil texture and bulk density are subsequently input into an ANN-based site-specific pedotransfer function to generate three-dimensional heterogeneous soil hydraulic parameter fields. The parameter estimates are then used to simulate a field injection experiment at the site. A relatively good agreement is obtained between the simulated and observed moisture contents. The spatial distribution pattern of observed moisture contents as well as the moisture movement is captured well in the simulations. We are able to reproduce the observed splitting of the moisture plume in a coarse sand unit that is sandwiched between two fine-textured units (see Figure 2).

III.) Future Plans:

We seek to develop an approach by combining the neural network based PTF results with the thin layer concept to explore capillary pressure-dependent anisotropy for a wide range of soil texture and soil bulk density to improve basic understanding of capillary pressure-dependent anisotropy of unsaturated layered soils.

The probability distributions of hyper-parameters of the soil hydraulic parameters from the Hanford site will be evaluated. We will extend the Bayesian updating algorithm to update the hyper-parameters without the restriction that the hyper-parameters follow normal distributions and then apply the developed algorithm to the parameters gathered from the Hanford site. The estimation of posterior distributions of the parameter correlation scales will also be conducted.

We will continue to evaluate the ANN based PTF performance by incorporating various statistical features of the hydraulic parameters in the objective functions which can be better controlled for the synthetic cases before using and testing the successful PTFs to actual field hydraulic parameter data collected from the Hanford site. We will then use the parameter data sets from the available field measurements for extensive ANN training and validation to obtain improved ANN-based PTFs.

Using the estimated posterior distributions of hyper-parameters and the correlation scales, together with the developed PTFs, we can then generate spatially heterogeneous random hydraulic parameter fields that will be used for the numerical simulations of the vadose zone processes and compare the simulations with the observed field data at the Hanford site. Uncertainty analysis will also be conducted.

IV.) References:

1. van Genuchten, M.Th., **1980**. A closed-form equation for predicting the hydraulic conductivity of unsaturated soils. *Soil Sci. Soc. Am. J.,* 44, 892–898.

2. Leij, F. J., W. B. Russell, and S. M. Lesch, **1997.** Closed-form expressions for water retention and conductivity data, *Ground Water*, 35(5), 848-858.

3. Rawls, W. J., and D. L. Brankensiek, **1985**. Prediction of soil water properties for hydrologic modeling, in *Proceedings of Symposium on Watershed Management*, pp. 293-299, American Society of Civil Engineers, New York.

V.) DOE-EPSCoR Sponsored Articles (Selected Highlights): since 2007

Simulation of field injection experiments in heterogeneous unsaturated media using cokriging and artificial neural network, M. Ye, R. Khaleel, M. G. Schaap, and J. Zhu, Water Resour. Res., 43, W07413, doi:10.1029/2006WR005030, **2007**.

Equivalent parallel and perpendicular unsaturated hydraulic conductivities: Arithmetic mean or harmonic mean?, J. Zhu, Soil Sci. Soc. Am. J., in press, **2008**.

Effective Soil Hydraulic Parameters for Transient Flows in Heterogeneous Soils, Zhu, J., and Sun, D., Vadose Zone J., revised, **2008**.

Tension-Dependent Hydraulic Conductivities of Anisotropic Unsaturated Soils, J. Hydrol., Zhu, J., and Sun, D., submitted, **2008**.

Investigations on the fundamental surface reactions involved in the sorption and desorption of radionuclides

Sherry Faye[1], Richard Gostic[1], Julie Gostic[1], Craig Bias[1], Jen Fisher[2], Jim Bruckner[2], Duane Moser[2] and Ken Czerwinski[3,4]*
stocks2@unlv.nevada.edu
[1] Radiochemistry PhD Program, University of Nevada, Las Vegas
[2] Desert Research Institute, Las Vegas, NV
[3] Department of Chemistry, University of Nevada, Las Vegas
[4] Harry Reid Center for Environmental Studies, University of Nevada, Las Vegas

Faculty and Associated Institutions

Prof. Ken Czerwinski*, Department of Chemistry and Harry Reid Center, University of Nevada, Las Vegas
Prof. Clemens Heske, Department of Chemistry, University of Nevada, Las Vegas
Dr. Thomas Hartmann, Idaho National Laboratory
Dr. Duane Moser, Desert Research Institute, Las Vegas, NV
Prof. Manoranjan Misra, Prof. L. Glen McMillion, Ph.D., Metallurgical and Materials Science Engineering, University of Nevada, Reno

*4505 Maryland Parkway, Box 454003, Las Vegas, Nevada 89154-4003, Phone: 702-895-0501, Fax: 702-895-3094, E-mail: czerwin2@unlv.nevada.edu

Program Scope

Reactions that control the interactions of radionuclides with surfaces are varied and complex. Depending upon the surface, radionuclide oxidation state, and solution conditions, the reactions at the surface can be driven by ion exchange, sorption, precipitation, or complexation [i- iv]. These reactions will control both the removal of a radionuclide from the solution phase onto a surface (defined by the general term sorption) as well as the return of a radionuclide from the surface to a solution (defined as desorption). The fundamental interactions of radionuclides with surfaces have implications in a wide variety of areas of interest to the Department of Energy (DOE) such as environmental fate and transport, emergency response, site decontamination and remediation, separation and treatment of nuclear waste and repository site development.

Our efforts are directed at understanding the sorption and desorption behavior of radioactive contaminates from surfaces, with an emphasis on actinide elements and technetium. These studies will be performed to ascertain the fundamental mechanisms involved in radionuclide interactions with surfaces. The results will be described, based on chemical kinetics and thermodynamics, to permit data inclusion into several existing surface interaction models. The surfaces will include minerals, organics, and manmade materials. In addition, the impact of microbial modifications of these surfaces will be explored.

Characterization of the surfaces includes bulk analysis by surface area measurements, particle size distribution, X-ray diffraction, microprobe analysis, chemical extractions, and molecular and cultivation-based microbial community structure assessments. Studies on surface interactions will include XPS, XAFS, X-ray emission spectroscopy, TEM analysis, SEM characterization and AFM. Sorption and desorption of radionuclides will also be examined spectroscopically and radiochemically to determine kinetic and thermodynamic relationships.

Outside of the technical domain this program has two other objectives: the development of facilities at participating institutes to perform cutting edge research on radionuclide interactions with surfaces and providing a source of researchers for the DOE with expertise in radiochemistry and radiobiology.

Recent Progress

Evaluation of Surface and Bulk Imaging: Techniques for Environmental Samples

Soil samples obtained from the Boeing Michigan Aeronautical Research Center (BOMARC) accident site in New Jersey, containing discrete weapons grade plutonium particles have been analyzed utilizing several of the techniques previously discussed. Recently, focus has shifted to more advanced methods of imaging in order to more precisely locate the hot particles within the core. High Resolution Computed Tomography (HRCT) is a fast method for hot particle localization (<5.0 hrs/core) that maintains all of the spatial information in the core while allowing the analyst to pin-point the location of high Z, high density materials with great accuracy, instead of relying on the intrinsic decay properties of the materials of interest. By combining the high spatial resolution of HRCT with conventional radioanalytical techniques we have greatly improved our ability to locate and recover hot particles from soil cores.

8 Bit JPEG Image of a Single Core

Field of View = 65 x 65 mm
Pixel Size = 63.5 x 63.5 um
Slice Depth = 37mm
Slice Thickness = 74.3um

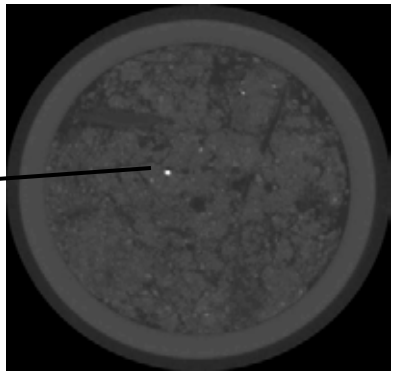

This bright spot matches the estimated location, in both depth and horizontal position of the primary source of activity in the core localized with a hand held detector.

Separation Techniques from Complex Matrices

Rapid, reliable and accurate separation methods are needed for analysis that can handle high throughput and non-standard environmental matrices. A vacuum box setup has been designed that allows Eichrom TEVA, TRU and DGA resins to be used simultaneously for separation of actinides from complex matrices. Using this setup, procedures have been developed for rapid multi-elemental analysis with high selectivity, high load capacity and minimized waste.

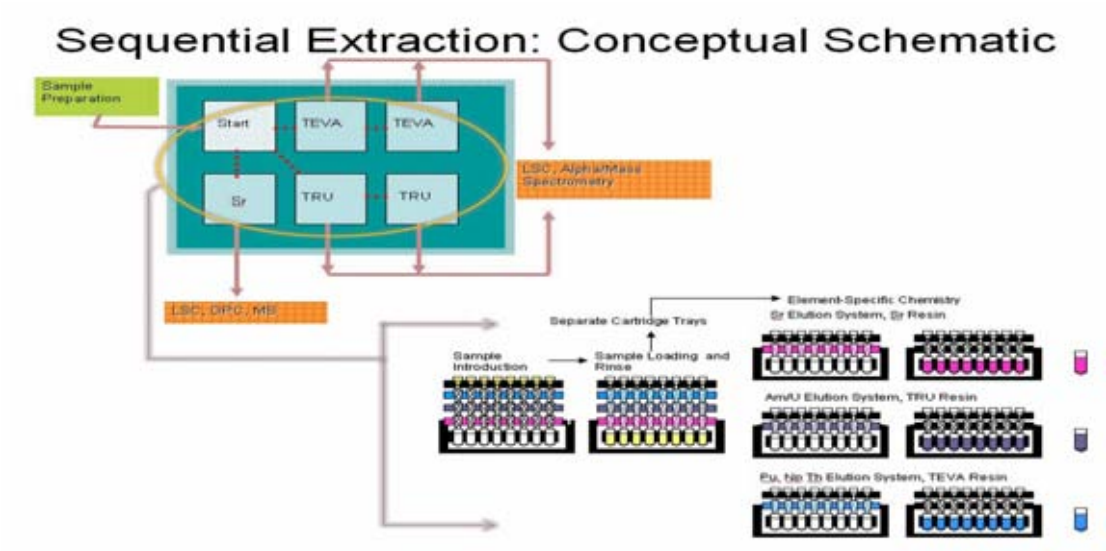

Future Work

Sorption and Desorption on Tuff in the Presence of Bacteria

Experiments will be conducted in order to determine the effect on sorption and desorption of radionuclides to tuff in both the presence and absence of bacteria. Tuff from the Nevada Test Site will be ground to sizes smaller than 500 µm, surface area will be measured and the mineral composition determined by X-ray diffraction. Sorption of single actinide, mixed actinide and Technetium systems (^{233}U, ^{237}Np, ^{239}Pu, ^{241}Am, and ^{99}Tc) to the NTS tuff will be measured in the presence and absence of *Shewanella oneidensis* (MR-1), a bacteria known to reduce Uranium and other metals. The kinetics and distribution coefficients will be determined using ICP-MS, liquid scintillation counting and chemical separation procedures as needed. SEM will also be used to monitor the changes in the morphology of the tuff due to bacterial action. This combined data set will allow for greater understanding and improved modeling of the effects of bacteria on the sorption of actinides and Technetium to NTS tuff.

Acknowledgements

The authors of this study would like to thank Dr. Richard Ketcham of the High-Resolution X-ray Computed Tomography Facility at The University of Texas at Austin (UTCT) for his assistance and Lt. Col. Craig A. Bias and Lt. Col. Steven E. Rademacher of the United States Air Force for their assistance in obtaining samples from the BOMARC site.

This work has been funded by DOE/EPSCoR Partnership Grant DE-FG02-06ER46295.

References

i. Kim, J.I.: Chemical Behavior of Transuranic Elements in Natural Aquatic Systems, Handbook on the Physics and Chemistry of the Actinides, A.J. Freeman and C. Keller Eds., Elsevier Publishers, 1986, 413-455.

ii. Von Gunten, H.R., and Benes, P.: Speciation of Radionuclides in the Environment. *Radiochim. Acta*, **69**, 1-29 (1995).

iii. Silva, R.J. and Nitsche, H.: Actinide Environmental Chemistry, *Radiochim. Acta*, **70/71**, 377-396 (1995).

iv. Moulin, V and Moulin, C.: Radionuclide Speciation in the Environment: A Review. *Radiochim. Acta*, **89(11-12)**, 773-778 (2001).

Center for Integrated Computation and Analysis of Reconnection and Turbulence (CICART)

A. Bhattacharjee (PI)[1*], B. Chandran[1], L.-J. Chen[1], K. Germaschewski[1], P. Isenberg[1], J. Klewicki[1], C.-S. Ng[1], B. Vasquez[1], B. Rogers[2]

[1] Space Science Center / Department of Physics
University of New Hampshire
39 College Rd
Durham, NH 03824
* amitava.bhattacharjee@unh.edu

[2] Department of Physics and Astronomy
Dartmouth College
6127 Wilder Laboratory
Hanover, NH 03755

1 Program Scope

The University of New Hampshire (UNH) and Dartmouth College established the Center for Integrated Computation and Analysis of Reconnection and Turbulence (CICART) under the auspices of the Department of Energys Experimental Program to Stimulate Competitive Research (DoE/EPSCoR). The principal participants of CICART constitute an interdisciplinary group, drawn from the communities of applied mathematics, astrophysics, computational physics, fluid dynamics, and fusion physics. It is a main premise of CICART that fundamental aspects of magnetic reconnection and turbulence in fusion devices, smaller-scale laboratory experiments, and astrophysical plasmas can be viewed from a common perspective, and that progress in understanding in any of these interconnected fields is likely to lead to progress in others.

CICART also promised wider impact in establishing a new program in Integrated Applied Mathematics (IAM) in the College of Engineering and Applied Sciences (CEPS) at UNH. This is a College-wide program at UNH, involving the Departments of Chemical Engineering, Chemistry, Civil Engineering, Computer Science, Earth Sciences, Electrical and Computer Engineering, Mathematics and Statistics, and Physics.

1.1 Overview of the Research Program

CICART has a dual mission in research: it seeks fundamental advances in physical understanding and proposes to achieve these advances by means of innovations in computer simulation methods and theoretical models. While our primary focus is fusion physics, the topics we address are fundamental, have broad impact, and cut across disciplinary boundaries.

CICART research foci:

1. Impulsive Reconnection During Sawtooth Crashes and their Nonlinear Stabilization
2. Long-time Gyrokinetic and Particle-In-Cell Studies of Island Dynamics
3. Anisotropic Two-Fluid (or Hall MHD) Turbulence in Low-Beta Plasmas:

High-Performance Computing Tools:

1. The Magnetic Reconnection Code (MRC), based on extended two-fluid (or Hall-MHD) equations, in an adaptive mesh refinement (AMR) framework and using implicit time integration.
2. The Explicit Particle-In-Cell (ExPIC) Code, a fully electromagnetic 3D Particle-in-Cell (PIC) code.
3. GS2, an Eulerian, electromagnetic, kinetic code that simulates the nonlinear gyrokinetic equations, together with a self-consistent set of Maxwell's equations.

2 Recent Progress

2.1 Programmatic News

CICART was officially inaugurated during a visit by Dr. Kristin Bennettt (Office of Basic Energy Sciences) and Dr. John Mandrekas (Office of Fusion Energy Sciences) at the University of New Hampshire on October 5, 2007.

The College of Engineering and Physical Sciences at UNH, in partnership with CICART created a tenure-track faculty position in the Department of

Physics and the newly established program in Integrated Applied Mathematics (IAM), with emphasis on computational physics and high-performance computing. The search lead to the recruitment of Dr. Kai Germaschewski. He is the architect of the Magnetic Reconnection Code (MRC), one of the principal computer simulation codes of CICART.

CICART has established the following Advisory Committee: Prof. William Dorland, University of Maryland and Co-Director, DoE Center for Multiscale Plasma Dynamics, Prof. Stewart Prager, University of Wisconsin-Madison and Director, NSF/DoE Physics Frontier Center on Magnetic Self-Organization, and Prof. Robert Rosner, University of Chicago and Director, Argonne National Laboratory. The Advisory Committee visited CICART on July 7, 2008.

2.2 Research Accomplishments

While considerable progress has been made in all of our research topics, in this presentation we will focus on accomplishments in the area of impulsive reconnection and new computational developments.

2.2.1 Impulsive Reconnection

Plasma is a state of matter often described as a "fourth aggregate state", where gases are ionized and thus electromagnetic interactions become important. Most of the matter in the universe is in plasma state, and even on earth, plasmas are important for many applications, not the least being fusion devices.

Plasmas can be modeled as fluids, leading to equations known as magnetohydrodynamics (MHD) which are similar to regular hydrodynamics but also take into account the effects of magnetic fields and Lorentz force. In an ideal plasma, that is one of infinite conductivity, magnetic field lines are frozen to the plasma flow and change of magnetic topology is thus not possible. In real plasmas however, nonideal effects described by a (extended) Ohm's law allow for reconnection of magnetic field lines and conversion of magnetic energy into kinetic energy and heat.

Reconnection phenomena observed in experiments (e.g. fusion) and nature (e.g. solar flares, magnetospheric substorms) often show an impulsive dynamics, ie. a sudden change in the time

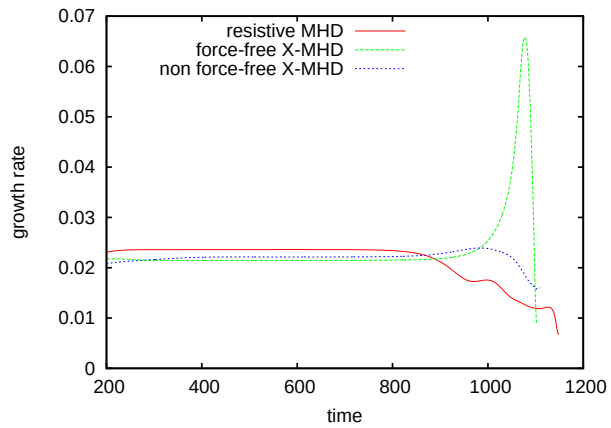

Figure 1: Comparison of the growth rate of the kinetic energy for resistive MHD, and XMHD with a force-free and non force-free equilibrium

derivative of the reconnection rate that cannot be explained in the context of resistive MHD. At scales smaller than the ion skin depth, electrons and ions do not move together as one fluid anymore, and an extended description (XMHD) including two-fluid effects like Hall term and electron pressure gradient becomes necessary.

The Magnetic Reconnection Code (MRC) has been used to simulate the nonlinear evolution of the $m = 1$ tokamak tearing mode in the XMHD model. Fig. 1 gives an overview of the examined cases. It shows the growth rate of the kinetic energy in the system as magnetic energy is converted by magnetic reconnection. The resistive MHD curve confirms the well-known "slow reconnection" that is expected from this model and explained by the Sweet-Parker theory, showing an extended current sheet (see Fig. 2(a)). Obviously, this model fails to explain the sudden increase in growth rate observed in tokamaks as so-called "sawtooth oscillations".

The force-free XMHD simulation confirms the predictions that Aydemir[1] made using a simplified four-field model. Instead of an extended Sweet-Parker current sheet, an X-point configuration is observed, which creates a nonlinear phase of fast reconnection, Fig. 2(b).

Finally, an initial equilibrium with a non-vanishing pressure gradient will cause diamagnetic rotation of the plasma column. Fig. 2(c) shows how the current sheet has been rotated and torn. We observe a Rayleigh-Taylor instability of the flow and destruction of the proper reconnection geometry of

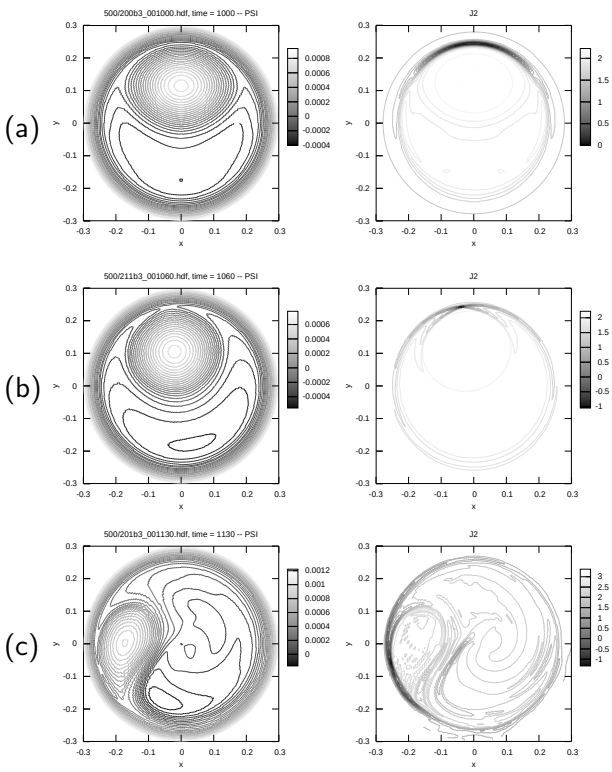

Figure 2: reconnection leading to the formation of a new magnetic island (helical flux function, left), current density J (right) in the nonlinear stage for (a) resistive MHD, (b) force-free XMHD, (c) non force-free XMHD

coinciding flow and magnetic field and thus diamagnetically stabilizing the nonlinear growth phase observed previously.

2.2.2 Magnetic Reconnection Code

The Magnetic Reconnection Code (MRC) [2] is a suite of advanced numerical codes used to study reconnection in extended MHD (XMHD) systems.

These models pose two major challenges to numerical integration: In particular in collisionless systems, the nonideal regions where reconnection occurs are very thin current sheets. Therefore, a large range of spatial scales need to be resolved. Some versions of the MRC support block-structured adaptive mesh refinement, but the XMHD simulations of the $m = 1$ tearing mode are performed with a static non-uniform grid, which is sufficient as the location of the current sheet (the $q = 1$ surface) is known in advance.

The spatial discretization used is a non-staggered, conservative, $\nabla \cdot \vec{B} = 0$, finite-volume scheme introduced by Chacon[3]. It supports arbitrary curvilinear coordinate systems, currently we are using cylindrical and helical coordinates.

XMHD supports dispersive waves ($\omega \propto k^2$). This introduces very fast wave time scales due to the fine spatial scales necessary to resolve the reconnection layer, while the time scale of the reconnection process at interest is many orders of magnitude slower. In explicit schemes, those fast time scales have to be resolved due to the CFL stability constraint. The MRC incorporates the option for implicit time integration using Newton iteration to solve the nonlinear implicit equations. The inner linear solve can be chosen to be a matrix-free Krylov-Schwarz iterative solver, or a direct solver (SuperLU). Due to lack of efficient preconditioners (a topic of ongoing research), we found the latter to perform much better for up to medium sized simulations.

We developed a code generator that takes the PDE system in symbolic form (with discretization hints) and generates C code to evaluate the r.h.s. and sparse Jacobian matrix needed for the direct solver. We obtain numerous advantages from being able to generate an optimal code for a given problem (grid, coordinate transform, set of physical parameters) while preserving easy maintainability.

2.2.3 OpenGGCM

The Open Global Geospace Circulation Model (OpenGGCM) [4] has been used within CICART for study of 3D reconnection processes in the Earth's magnetosphere.

We ported OpenGGCM to run efficiently on a new processor architecture, the Cell BE. These processors can achieve very high performance ($>$ 200 GFlops per processor) but require special programming. We again used a code generator approach, which from one source will generate optimal code for either a given conventional architecture like x86_64 or the Cell BE. A development version is finished and has been shown to achieve a speedup of a factor of 25, and is now running on a cluster of 40 Playstation 3's. Even on an x86_64 architecture, a three times speedup has been achieved by exploiting the SSE2 SIMD instruction set.

3 Future Work

3.1 Impulsive Reconnection

We plan to extend our simulations and analysis of the $m = 1$ tearing mode in fusion devices. Using different initial conditions, we should be able to see multiple sawtooth oscillations instead of the single one we are currently focusing on, and we would like to investigate the experimentally observed feature of incomplete reconnection.

3.2 Magnetic Reconnection Code

The MRC already has built-in support for arbitrary curvilinear geometries, however currently a cylindrical tokamak model has been used. We will implement and simulate more realistic geometries.

Current simulations are mostly run in 2D mode using helical symmetry. We will work on new preconditioning schemes and iterative solvers to make high resolution 3D simulations more tractable. We are also planning on exploiting the computational power of new processor architectures like the Cell BE, extending our existing code generation infrastructure and using knowledge gained from porting OpenGGCM. Profiling results show that there is room for even more performance improvements.

References

[1] A. Y. Aydemir, Nonlinear studies of m=1 modes in high-temperature plasmas, Physics of Fluids B: Plasma Physics 4 (11) (1992) 3469–3472.

[2] K. Germaschewski, A. Bhattacharjee, C. Ng, The Magnetic Reconnection Code: an AMR-based fully implicit simulation suite, Vol. 359, ASP Conference Series, 2006, p. 151.

[3] L. Chacón, A non-staggered, conservative, $\nabla \cdot \vec{b} = 0$, finite-volume scheme for 3d implicit extended magnetohydrodynamics in curvilinear geometries, Computer Physics Communications 163 (2004) 143–171.

[4] J. Raeder, J. Berchem, M. Ashour-Abdalla, The Geospace Environment Modeling grand challenge: Results from a Global Geospace Circulation Model, J. Geophys. Res. 103 (1998) 14787.

DOE Sponsored Publications

1. Current sheet formation and non-ideal behavior at three-dimensional magnetic null points, D. I. Pontin, A. Bhattacharjee, and K. Galsgaard, Physics of Plasmas 14, 052106 (2007).
2. Current sheets at three-dimensional magnetic nulls: effect of compressibility, D. I. Pontin, A. Bhattacharjee, and K. Galsgaard, Physics of Plasmas 14, 052109 (2007).
3. Observation of energetic electrons within magnetic islands, L.-J. Chen, A. Bhattacharjee, P. Puhl-Quinn, H. Yang, N. Bessho, S. Imada, S. Muhlbachler, P. W. Daly, Y. Khotyaintsev, A. Vaivads, B. Lefebvre, and A. Fazakerley, Nature Physics doi:10.1038/nphys2007 (2007).
4. Gyrokinetic simulations of collisionless magnetic reconnection, B. N. Rogers, S. Kobayashi, W. Dorland, T. Tatsuno, and J. Drake, Physics of Plasmas 14, 092110, doi: 10.1063/1.2774003 (2007).
5. Reduced magnetohydrodynamic equations with coupled Alfven and sound wave dynamics, R. Denton, B. N. Rogers, W. Lotko, Physics of Plasmas 14, 102906, doi: 10.1063/1.2786060 (2007).
6. Preferential perpendicular heating of coronal hole minor ions by the Fermi mechanism, P. A. Isenberg and B. J. Vasquez, The Astrophysical Journal 668, 546 (2007).
7. Alfven wave dynamics in reduced magnetohydrodynamics and symmetry boundary conditions, R. Denton, B. N. Rogers, W. Lotko, A. Streltsov, Physics of Plasmas 14, doi: 10.1063/1.2786060 (2007).
8. Anisotropic MHD turbulence, C. S. Ng and A. Bhattacharjee, in Turbulence and Nonlinear Processes in Astrophysical Plasmas, edited by D. Shaikh and G. Zank, AIP Conference Proceedings 932 (American Institute of Physics, New York, 2007), pp. 137- 143.
9. A constrained tectonics model for coronal heating, C.-S. Ng and A. Bhattacharjee, The Astrophysical Journal 675, 899 (2008).
10. A Comparison of Spectral Element and Finite Difference Methods Using Statically Refined Nonconforming Grids for the MHD Island Coalescence Instability Problem, C. S. Ng, D. Rosenberg, K. Germaschewski, A. Pouquet, and A. Bhattacharjee, to appear in The Astrophysical Journal Supplement, 2008.
11. Strong anisotropic MHD turbulence with cross-helicity, B. Chandran, to appear in The Astrophysical Journal, 2008.
12. Defining and identifying three-dimensional magnetic reconnection in resistive MHD simulations of Earths magnetosphere, J. Dorelli and A. Bhattacharjee, to appear in the Physics of Plasmas, 2008.
13. The scaling of forced magnetic reconnection in three dimensions, B. Sullivan and B. N. Rogers, submitted to the Physics of Plasmas, 2008.
14. Nonlinear finite-Larmor-radius effects in reduced fluid models, A. Brizard, R. Denton, B. Rogers, and W. Lotko, submitted to the Physics of Plasmas, 2008.
15. High and low confinement modes in simple magnetized toroidal plasmas, P. Ricci, B. Rogers, and S. Brunner, submitted to the Physical Review Letters, 2008.

North Dakota's DOE EPSCoR Infrastructure Improvement Program, "Advances in the Fundamental Understanding of Coal Combustion Emission Mechanisms"

Principal Investigator: Professor Wayne S. Seames
Co-Investigator(s): Professor Mark Hoffmann and Professor John Hershberger
Organization: Office of Basic Energy Sciences

Institutions: University of North Dakota (UND) and North Dakota State University (NDSU)
Departments: UND Chemical Engineering, UND Chemistry, NDSU Chemistry
Address of PI Department: 241 Centennial Drive, Stop 7101
Grand Forks, ND 58202-7101

Fiscal Year: 2007-2009
Funding: $1,500,000 / 36 Months
Related Project URL: http://www.und.nodak.edu/dept/sunrise

Date Last Updated: 4/10/2008

This research initiative formulates an interrelated set of projects focused on improving our understanding of the fundamental chemistry that determines the emissions profile of particulate matter and trace inorganic elements during coal combustion. A balance of experimental and computational studies focus on how trace elements and fine fragmentation particulate matter are formed during the coal combustion process and how the reaction products transform to their ultimate fates as emitted flue gas or collected fly ash. An integrated team of nine researchers from both North Dakota research universities has been assembled. This program will serve as a foundation project to develop the team's capabilities into a nationally recognized, highly funded center for research in sustainable energy. Competitiveness in sustainable energy research is one of two priority focus areas of the ND EPSCoR program. Extensive collaboration with DOE laboratories is planned as well as outreach activities and junior faculty development programs.

Optoelectronic Properties of Carbon Nanostructures

John W. Mintmire, Thushari Jayasekera, Junwen Li, Pavan Pillalamarri and Vasantha Jogireddy

Department of Physics, Oklahoma State University, Stillwater, OK, 74075

Program Scope

Solar energy is our major long-term renewable energy source, and photovoltaic devices are the most direct way of converting solar energy to electricity. Demand for solar energy has grown steadily over the past two decades with growth rates of 20-25% per year. Photovoltaic devices based on organic, carbon-based nanostructures, or similar inorganic nanostructures, offer the possibility of developing low cost, easily processed thin films which function as photovoltaic materials. Such devices can be competitive with other sources of energy if power efficiencies of the order of 10% can be obtained.

One major approach for efficient polymeric photovoltaic cells lies in the use of bulk heterojunctions, which mix two different organic polymeric materials acting as donor and acceptor semiconductors. In these bulk heterojunctions the donor polymer typically acts as the light absorber, creating an electron-hole pair and then donating the excited electron to the acceptor polymer. A good theoretical understanding of the physical processes at work in these materials requires a knowledge of the electron states near the Fermi level for both the donor and acceptor. Our DOE EPSCoR research program is using first-principles electronic structure methods to study the electronic properties of nanostructured materials with potential application to photovoltaic devices.

This project is part of our research group's long-range research program in the electronic and structural properties of low-dimensional materials. The aim of our current DOE EPSCoR program is to use forefront computational tools to study the electronic structures of potential photovoltaic polymers and carbon nanotube structures, with the goal of providing characteristic data for these materials that will be of use to experimentalists and other theorists in developing better bulk heterojunction photovoltaic devices. Our specific goals for this project include carrying out first-principles simulations for a range of quasi-one-dimensional polymer, nanotube, and nanowire systems, investigating possible low band-gap donor systems, and using results from our first-principles band structure simulations as input to calculations of the electron and hole transport properties in nanostructured materials. This work will be carried out in collaboration with the Computational Chemical Sciences (CCS) Group at Oak Ridge National Laboratory, which has active programs in computational studies of nanoscale materials.

Recent Progress

Over the past year we have made substantial progress in developing an approach for first-principles transport calculations on quasi-one-dimensional nanostructures with helical symmetry. We are currently working on electronic structure and transport calculations for a range of promising materials for photovoltaic applications, with a goal of increasing our understanding of electron transport processes in bulk heterojunction materials. Pure carbon single-wall nanotubes (SWNTs) have been shown to be ballistic conductors having a phase coherence length on the order of microns. However, in the presence of defects or other foreign systems, the phase coherence length of these systems decreases and ballistic electron transport models may not be adequate to analyze the electron transport in these systems. While the Landauer-Büttiker formalism has been successful

in explaining electron transport in ballistic systems, it is worthwhile to compare electron transport properties in SWNT functionalized and composite systems using a "quasi-ballistic" model. We have applied the Büttiker phase-breaking technique to electron transport in these "quasi-ballistic" systems. [1–4] We first applied this technique to study long-range electron transfer through graphene nanoribbon systems. We investigated the difference between the pure phase randomization and phase/momentum randomization boundary conditions. [5] While momentum randomization adds an extra resistance caused by backward scattering, pure phase randomization boundary conditions smooth the conductance oscillations caused by interference effects.

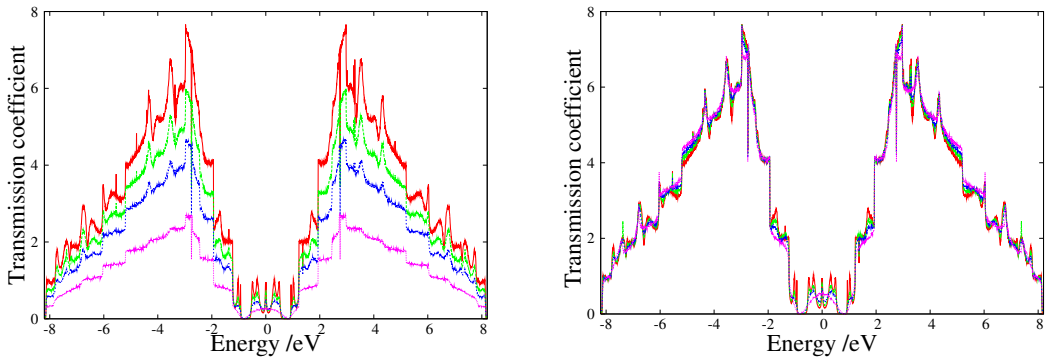

FIG. 1: The transmission coefficient for three nanoribbon segments. The left figure depicts the results for backscattering free phase randomization boundary conditions and the right figure for pure phase randomization boundary conditions. Different lines in each figure depicts the transmission coefficient at different dephasing strengths.

When the conductor region is longer than the phase coherence length of electrons in the system, we cannot use methods that assume simple ballistic transport. However, we can treat the system as a connected series of coherent scattering systems. Each coherent segment is treated as a quantum mechanical scattering problem with ballistic transport, and we then combine these segments using Büttiker phase-breaking techniques. Figure 1 shows the calculated transmission coefficients, at different dephasing strengths, for three graphene nanoribbon segments with a single lattice vacancy. The results in the left panel use the backscattering free boundary conditions whereas the results in the right panel use the pure phase randomization boundary conditions. These results show that the interference effects diminish as we limit coherence by increasing the dephasing strength ϵ, thus only true quantum oscillations survive. The pure-phase randomization boundary conditions only restrict the interference so that there is no significant change in the magnitude of the transmission (right panel) while back-scattering free boundary conditions add an extra impedance to the system (left panel).

We have also carried out studies of transport in SWNTs with defects and in carbon double-wall nanotubes (DWNTs), with the goal of combining our first-principles electronic structures results with the Büttiker phase-breaking techniques for calculating transport. We have used the chemisorption of fluorine atoms to SWNTs as our initial model for SWNT defects, as fluorination is a technologically important method of functionalizing SWNTs. [6] Although several groups have reported results for fluorinated achiral zigzag and armchair SWNTs, [7–12], to our knowledge no results have been reported for chiral SWNTs. During the past year, we have carried out geometry optimization, band structure, and electronic transport calculations for (10,13) and (10,11) SWNTs with fluorine substituents. While most theoretical calculations have been carried out for higher fluorine concentrations, we are focusing on the effects of low concentrations of chemisorbed

substituents on transport. Our results appear to be the first first-principles electronic transport calculations for chiral SWNTs using helical symmetry. To carry out these simulations, we combine the use of band structure codes developed at Oklahoma State University with an electron transport code developed at ORNL. DWNTs have also been used for photovoltaic materials, [13] and we are carrying out band structure and transport calculations for a range of chiral DWNT systems.

Future Plans

Recently, Meunier and Sumpter at ORNL found that tetracyanoethylene (TCNE) molecules encapsulated in SWNTs can potentially be used as nonvolatile memory elements. [14] In collaboration with the ORNL group, we are planning to study the properties of a series of TCNE molecules encapsulated in SWNTs in different orientations. We are also planning calculations of electron transport in conjugated polymer materials, with a goal of studying the effect of the length and the dihedral angle on the transport properties in these materials.

We are also beginning studies of silicon nanowires, which have attracted much attention because of their potential applications in recent years. They can be used as building blocks of nanoscale electrical and optoelectronic devices such as field-effect transistors, [15–17] as high-performance anodes in lithium batteries, [18] and as thermoelectric materials because of their low thermal but high electrical conductivity. [19, 20] Silicon nanowires have also been used to convert light into electricity in photovoltaic devices. [21–29] It was shown that single-nanowire solar cells could be made with minority carrier diffusion lengths of roughly 2 μm. [25] Because of the one-dimensional periodicity of Si nanowires, they can form cylindrical configurations with a p- or n-type core and an n- or p-type shell with short radial lengths for improved carrier collection while maintaining long axial lengths for good light absorption, with potential conversion efficiencies up to 18%. [26, 27]

The small diameter of these nanowires leads to a large surface-to-volume ratio, which enhances the effect of surface properties on the electronic and transport properties of these materials. Differences in surface passivation could be used to tune the band gap and conductance of Si nanowires. [17, 30–32] We plan to carry out first-principles calculations on the electronic structure of Si nanowires with different surface passivations of H, CH_3 and OH. In preliminary calculations, surface hydrogen atoms passivate the radical sites at the surface and eliminate dangling-bond bands from the vicinity of the Fermi level. OH-substituents are found to reduce the band gap both in our calculations and as reported by others [30] as a result of the hybridization between Si $3p$ and O $2p$ orbitals. In addition to decreasing the band gaps compared to H-passivated wires, CH_3 passivation changes the band gap from direct to indirect. We plan to continue our preliminary work, and use our band structure results as input to electron transport simulations.

---

[1] Büttiker M, 1986 Phys Rev B **33** 3020.
[2] Li XQ, Yan YJ, 2002 Phys Rev B **65** 155326.
[3] Li XQ Yan YJ, 2001 J Chem Phys **115** 4169.
[4] Golizadeh-Mojarad R, Datta S, 2007 Phys Rev B **75** 81301.
[5] Jayasekera T, Pillalamarri P, Mintmire JW, Meunier V, Int J Quantum Chem, in press.
[6] Mickelson ET. Huffman CB, Rinzler AG, Smalley RE, Hauge RH, Margrave JL, 1998 Chem Phys Lett **296** 188; Kelly KF, Chiang IW, Mickelson ET, Hauge RH, Margrave JL, Wang X, Scuseria GE, Radloff C, Halas NJ, 2000 Chem Phys Lett **313** 445.
[7] Bauschlicher CW, 2000 Chem Phys Lett **322** 237.
[8] Kudin KN, Bettinger HF, Scuseria GE, 2001 Phys Rev B **63** 45413.
[9] Park KA, Choi YS, Lee YH, Kim CW 2003 Phys Rev B **68** 45429.

[10] Bettinger HF, Kudin KN, Scuseria GE, 2001 J Am Chem Soc **123** 12849.
[11] Park H, Zhao J, Lu JP, 2005 Nanotechnology **16**, 635; Park H, Zhao J, Lu JP, 2006 Nano Lett **6**, 916.
[12] Pan H, Feng YP, Lin JY, 2006 J Phys Condens Matter **18**, 5175.
[13] Wei JQ, Jia Y, Shu Q, Gu Z, Wang K, Zhang D, Zhang G, Wang Z, Luo J, Cao A, Wu D, 2007 Nano Lett **7**, 2371.
[14] Meunier V, Sumpter BG, 2007 Nanotechnology **18**, 424032.
[15] Cui Y, Duan X, Hu J, Lieber CM, 2000 J Phys Chem **104** 5213.
[16] Cui Y, Lieber CM, 2001 Science **291** 851.
[17] Cui Y, Zhong Z, Wang D, Wang WU, Lieber CM, 2003 Nano Lett **3** 149.
[18] Chan CK, Peng HL, Liu G, McIlwrath K, Zhang XF, Huggins RA, Cui Y, 2008 Nature Nanotechnology **3** 31.
[19] Hochbaum AI, Chen RK, Delgado RD, Liang WJ, Garnett EC, Najarian M, Majumdar A, Yang PD, 2008 Nature **451** 163.
[20] Boukai AI, Bunimovich Y, Tahir-Kheli J, Yu JK, Goddard WA, Heath JR, 2008 Nature **451** 168.
[21] Hu L, Chen G, 2007 Nano Lett **7** 3249.
[22] Peng K, Xu Y, Wu Y, Yan Y, Lee S, Zhu J, 2005 Small **1**, 1062.
[23] Fang H, Li X, Song S, Xu Y, Zhu J, 2008 Nanotechnology **19** 255703.
[24] Tsakalakos L, Balch J, Fronheiser J, Korevaar BA, Sulima O, Rand J, 2007 Appl Phys Lett **97** 233117.
[25] Kelzenberg MD, Turner-Evans DB, Kayes BM, Filler KA, Putnam MC, Lewis NS, Atwater HA, 2008 Nano Lett **8** 710.
[26] Kayes BM, Atwater HA, Lewis NS, 2005 J Appl Phys **97** 114302.
[27] Zhang Y, Wang LW, Mascarenhas A, 2007 Nano Lett **7** 1264.
[28] Stelzner T, Pietsch M, Andrä G, Falk F, Ose E, Christiansen S, 2008 Nanotechnology **19** 295203.
[29] Tian B, Zheng X, Kempa TJ, Fang Y, Yu N, Yu G, Huang J, Lieber CM, 2007 Nature **449** 885.
[30] Nolan M, O'Callaghan S, Fagas G, Greer JC, Frauenheim T, 2007 Nano Lett **7** 34.
[31] Leu PW, Shan B, Cho K, 2006 Phys Rev B **73** 195320.
[32] Blase X, Fernández-Serra MV, 2008 Phys Rev Lett **100** 046802.

DOE sponsored publications: 2007-2008

- "First-Principles Properties of Organic Photovoltaic Materials", T. Jayasekera, M. S. Monigold, S. L. Elizondo, and J. W. Mintmire, Int. J. Quantum Chem. **107**, 3120 (2007).
- "Lattice Vacancy Effects on Electron Transport in Multiterminal Graphene Nanodevices", T. Jayasekera and J. W. Mintmire, Int. J. Quantum Chem. **207**, 3071 (2007).
- "Hidden One-Electron Interactions in Carbon Nanotubes Revealed in Graphene Nanostrips", C. T. White, J. W. Li, D. Gunlycke, and J. W. Mintmire, Nano Lett. **7**, 825 (2007).
- "Transport in Multiterminal Graphene Nanodevices", T. Jayasekera and J. W. Mintmire, Nanotechnology **18**, 424033 (2007).
- "Altering Low-Bias Transport in Zigzag-Edge Graphene Nanostrips with Edge Chemistry", D. Gunlycke, J. W. Li, J. W. Mintmire, and C. T. White, Appl. Phys. Lett. **91**, 112108 (2007).
- "Graphene Nanostrip Digital Memory Device", D. Gunlycke, D. A. Areshkin, J. W. Li, J. W. Mintmire, and C. T. White, Nano Lett. **7**, 3608 (2007).
- "Effect of Phase Breaking Events on Electron Transport in Mesoscopic and Nanodevices", T. Jayasekera, P. Pillalamarri, J. W. Mintmire, and V. Meunier, Int. J. Quantum Chem., accepted for publication.
- "First-Principles Simulations of Chiral Double-Wall Carbon Nanotubes", T. Jayasekera, B. A. Landis, and J. W. Mintmire, Int. J. Quantum Chem., accepted for publication.

Ro-vibrational Relaxation Dynamics of PbF Molecules

Neil Shafer-Ray*, Gregory Hall**, and Trevor Sears**
*University of Oklahoma Homer L. Dodge Department of Physics and Astronomy (shaferry@physics.ou.edu)
**Brookhaven National Laboratory

1) Program Scope

In 1950 Purcell and Ramsey[1] suggested that the electron might have a CP-violating electric dipole moment (e-EDM) proportional to its spin angular momentum. This possibility initiated an ongoing hunt for the e-EDM that has been spurred on by the recognition of the importance of CP-violation to the formation of a matter-dominated universe[2] as well as a difference in magnitude of the Supersymmetric[3] and Standard Model[4] prediction for its value. The current limit on the e-EDM is 1.6×10^{-27}e·cm as determined in a Ramsey beam resonance study of the Tl atom[5].

The PbF molecule provides a unique opportunity to measure the e-EDM. The molecule's odd electron, heavy mass, and large internal field combine to give it an intrinsic sensitivity to an e-EDM that is over three orders of magnitude bigger than that of the Tl atom[6]. In addition to this increased intrinsic sensitivity, the ground state of the PbF molecule allows for a "magic" electric field at which the magnetic moment vanishes[7]. All of these advantages create an opportunity to significantly lower the current limit on the e-EDM. These advantages can only be realized if an intense source of ground-state PbF molecules can be created and detected with high efficiency. The scope of this project is to (1) create a rotationally cold molecular beam source of PbF, (2) achieve a continuous ionization scheme for sensitive state selective detection of the PbF molecule.

2) Recent Progress

2.1) Direct measurement of the lifetime of the D state of PbF

The publication listed in section 5 details an extensive investigation of schemes to ionize the PbF molecule carried out over a three year period. This work includes the DOE-sponsored measurement of the lifetime of the D state of PbF described here.

The A state is the only electronically excited state of PbF known to have a lifetime that is sufficiently long to allow for state-selective detection. Unfortunately, direct ionization of this state proves to be impractical: The uv laser radiation required to ionize the A state also directly ionizes the ground state via an efficient $1+1$ ionization process. This non-state-selective one-color process completely swamps any state-selective two-color $1+1$ ionization process that might occur. This fact led us to the $1+1+1$ doubly resonance enhanced ionization scheme

$$X \underset{436\,\mathrm{nm}}{\rightarrow} A \underset{477\,\mathrm{nm}}{\rightarrow} D \underset{532\,\mathrm{nm}}{\rightarrow} PbF^{+}. \tag{1}$$

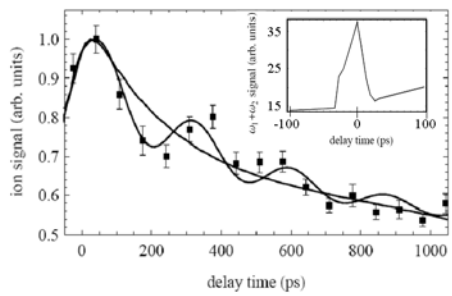

Figure 1: Decay of the D state of PbF

Knowledge of the $D-$state lifetime is critical to the design of an optimal laser system to implement this ionization scheme. Unfortunately the bandwidth of the Nd:YAG pumped dye laser system used to discover the $A \rightarrow D \rightarrow PbF^+$ ionization pathway is not sufficiently narrow to make a conclusive statement about the $D-$state lifetime. For this reason we coaxed our 7-ns Nd:YAG laser system to perform a time domain measurement with picosecond resolution. To accomplish this we took advantage of the temporal mode structure of our unseeded Nd:YAG laser. Specifically, we used the 532-nm output of this laser to pump a dye laser at 863.3 nm. The 1064-nm laser radiation of the Nd:YAG laser was then mixed with the dye laser radiation to create 476.6-nm laser radiation. By creating 476.6-nm laser radiation in this way, the radiation is modulated with the temporal structure of the Nd:YAG laser. This coherence is observed in an auto-correlation measurement that monitors the 251-nm radiation resulting from sum-frequency generation of 532-nm and 476.6-nm laser radiation in a BBO crystal as a function of an optical delay between the two input wavelengths (Figure 1, inset.) The lifetime of the D state of PbF is made by observing the PbF^+ ionization signal as a function of the delay between the 476.6-nm and 532-nm laser radiation. The resulting time-dependent ionization signal is shown in Figure 2 and indicates a lifetime of 250 ± 150 ps.

The $D-$state lifetime is short enough to dramatically reduce the efficiency of an ionization scheme utilizing continuous wave radiation. For this reason, we will employ a pseudo-continuous source of laser radiation producing 6 ps pulses of laser radiation at a repetition rate of 76 MHz.

2.2) Characterization of the $A \rightarrow D$ transition of PbF

We have begun a detailed interpretation of the two-dimensional $X_1\ ^2\Pi_{1/2} \rightarrow A^2\Sigma_{1/2} \rightarrow D$ spectrum shown in Figure 2 and published in the reference listed in section 5. The energy levels of the X_1, A, and D states are well described by the spin rotational Hamiltonian for $\Omega = 1/2$ molecules described by Kopp and Hougen and others[8, 6]. These energy levels are given by Eq 2.

	X_1	A	D
p/β	-0.605	2.996	-1.04

$$\beta J(J+1) \pm p(J+\tfrac{1}{2}) \qquad (2)$$

Here β is the rotational constant, J the total angular momentum (excluding nuclear spin) and p the Ω doubling constant. The rotational constant and spin-doubling constant for the X_1 and A states have been measured previously[9][10]. We have found that, for the D state of PbF, $\beta_D = 0.24$ and $p = -0.25$. The fact that $p_D/\beta_D \approx -1.0$ is significant and may help lead to a better understanding of the electronic structure of the ground X_1 state.

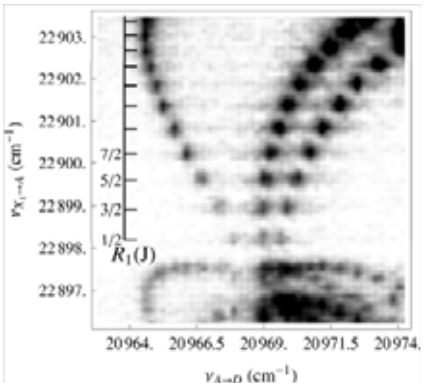

Figure 2: 2-D spectrum of the $X_1 \rightarrow A \rightarrow D$ transition.

For a $^2\Pi_{1/2}$ molecule, the $J-$labeled energy states are nearly degenerate and $p/\beta << 1$. For the case of a $^2\Sigma_{1/2}$ molecule, $p/\beta \approx -2$ and $N-$labeled energy states are nearly degenerate with energies $\beta N(N+1)$. From the table above, one can see that neither of these conditions are met for any of the states considered. Kopp and Hougen have considered the physics of a mixed $^2\Pi_{3/2}$, $^2\Sigma_{1/2}$, $^2\Pi_{1/2}$ system[8]. Here the value of p is free to take on a range of values, but with the constraint that the sum $(p_1/\beta_1 + p_2/\beta_2) = \pm 2$. It has long been assumed[10] that the $X_1(^2\Pi_{1/2})$, $X_2(^2\Pi_{3/2})$ and $A(^2\Sigma_{1/2})$ state form such a mixed system. However, the $p_1/\beta_1 + p_2/\beta_2$ sum rule is very closely followed by the $A - D$ system. In addition, the $A - D$ energy split is smaller than the $X_1 - A$ energy split. Thus it is likely that the A and D states are strongly mixed along with a yet-to-be-discovered $^2\Pi_{3/2}$ state.

In a separate work we have found that the hyperfine constants of the X_1 state of ^{207}PbF does not agree with that in the literature. Specifically, we find $A_\perp = 7200 \pm 100$ MHz differs in sign from its predicted[6] value. Perhaps this disagreement may be explained by the complex interaction between the X_1, A, and D states.

We have observed that R_2 and P_1 branches of the $A \rightarrow D$ transition are suppressed in our spectra. This propensity may be understood in terms of a transition dipole moment that violates parity considerations in the simple Born-Oppenheimer picture, but obeys parity selection rules when the complete spin-rotational system is considered. Specifically, overall parity of the spin-rotational wave functions allow for two possible transition dipole moments:

$$\vec{\mu}_{ZY} = \mu_{||}\hat{z}' + i\mu_\perp \hat{y}' \text{ or } \vec{\mu}_X = \mu_\perp \hat{x}'.$$

Here $\hat{z}'$ refers to the internuclear axis, $\hat{y}'$ the molecular fixed coordinate in the plane containing $\hat{z}'$ and the rotational axis. One finds that the R_2 and P_1

transitions may vanish in the $\vec{\mu}_{ZY}$ case. Our data both allows us to conclude that the transition is one of the form $\vec{\mu}_{ZY}$ and to determine the relative value of $\mu_{||}$ and $\mu_{\perp}$. This ratio is sensitive to the details of the electronic nature of the A and D state[8].

3) Future Plans

Rotational cooling of our molecular beam source of PbF has the potential to increase our sensitivity to an e-EDM by as much as a factor of 100 and is a central goal of this research grant. At the onset of this project, our pumping speed was limited by a small foreline pump (originally purchased for a much less demanding pulsed molecular beam experiments.) During this reporting period we have replaced vacuum plumbing and a mechanical pump in order to increase the pumping speed of our forline by a factor of 40. We have almost completed the construction of a larger source chamber pumped by a 10-inch (rather than 6-inch) diffusion pump. This source chamber is scheduled to be installed in September and will allow us to investigate possibility of rotational cooling.

Much of this year has been spent thoroughly characterizing the $A \rightarrow D$ transition. Our current understanding of the line intensities, energy levels, and lifetime of the A and D states has allowed us to optimize the specifications for a laser system to perform state-selective ionization of the molecule. This laser system has been constructed by HighQLaser Inc. At the time of writing this report, this laser system had just arrived to the Physics Department for installation during the second week of July 2008. We look forward to testing this new system in the upcoming months.

4) References

[1] E. Purcell, N. Ramsey, *Phys Rev*, 78 807 (1950).
[2] Sakharov, *JETP Lett*, 5 24 (1967).
[3] R. Arnowitt, B. Dutta, Y. Santoso, *Phys Rev D* 64 113010 (2001).
[4] F. Hoogeveen, *Nuc Phys*, B341 322 (1990).
[5] Regan, Commins, Schmidt, DeMille, *Phys Rev Let* 88 71805 (2002).
[6] Kozlov, Fomichev, Dmitriev, Labzovsky, Titov, *J Phys B* 20 4039 (1987).
[7] N. E. Shafer-Ray, *Phys Rev A* 73 34102 (2006).
[8] I. Kopp, J. Hougen, *Can J Phys* 45 2581 (1967).
[9] Rochester, *Proc R Soc Lon A* 153 407 (1936).
[10] D. Lumley, R. Barrow, *J Phys B* 10 1537 (1977).

5) DOE Sponsored Publication

State-selective detection of the PbF molecule by double resonant multiphoton ionization, P. Sivakumar, C.P. McRaven, Dustin Combs, N.E. Shafer-Ray, and Victor Ezhov, *Phys. Rev. A* 77, 062508 (2008.)

EPSCoR program at OCHEP

Mike Strauss
The University of Oklahoma
Homer L. Dodge Department of Physics and Astronomy
Norman, OK 73019
strauss@nhn.ou.edu

The Oklahoma Center for High Energy Physics (OCHEP), an inter-university center for research and education in High Energy Physics (HEP), was established in 2004 with the support from a DOE EPSCoR implementation grant. A renewal of the grant has extended the DOE funding until 2010. The center is a consortium of three universities, Oklahoma State University (OSU), the University of Oklahoma (OU), and Langston University (LU), with all active high energy physicists in the state of Oklahoma participating as members in the center. The two major objectives of the DOE EPSCoR grant were initially (1) to initiate an experimental HEP program at OSU and (2) to establish a grid computing facility at OU. These two objectives were accomplished during the first three years of the implementation grant. Experimental groups at all three universities are part of the D0 (Dee-Zero) collaboration at Fermilab and the ATLAS collaboration at CERN. In addition, OU and LU are part of the Southwest Tier 2 Center for ATLAS and are contributing actively to Large Hadron Collider (LHC) and Tevatron data processing and Monte Carlo simulation. The focus of the three year EPSCoR renewal is to solidify, expand, and permanently establish the two programs that were initiated. The renewal will allow the OSU experimental program to hire one more faculty member and to set up permanent IT positions and resources to run an ATLAS Tier 2 grid computing facility.

1 Experimental Projects

In the past four years, the OCHEP experimental group has performed research using the D0 experiment at the Fermilab Tevatron and using the ATLAS experiment at the CERN LHC.

Members of OCHEP have made significant contributions to the D0 experiment through their research and leadership roles in crucial areas of the experiment. These include:

- **Discovery of the single top quark production.** The D0 experiment was the first to observe evidence of single top quark production [1]. The primary OCHEP contributor was S. Jain, a postdoctoral fellow working together with OU professor Dr. P. Gutierrez. She has also investigated the production of single top quarks through flavor-changing neutral current interactions. Dr. Rizatdinova finalized her analysis on ratio of the branching fraction $t \to Wb$ to the total branching fraction $t \to Wq$. This measurement published in [3] sets an new limit on the mixing of the top quark with possible undiscovered fermions.

- **Higgs boson searches.** OCHEP member Dr. Khanov from OSU leads the D0 Collaboration efforts in searches for both Standard Model (SM) and non-SM Higgs bosons as a co-convenor of the D0 Higgs group. Several papers have been submitted to the publication under his leadership. He also conducted a search for the associated SM Higgs production ($p\bar{p} \to WH$) where Higgs decays to a pair of W bosons. The result [4] represents the world's best upper limit on Higgs boson production in this mode. OU group (Dr. Guttierrez, Drs. S. Jain, and S. Hossain) are looking for a charged Higgs boson production in the top quark decays.

- B **Physics Analysis.** Drs. B. Abbott, P. Gutierrez and M. Strauss from OU are active participants of the B-physics group at D0. Abbott served as a co-convener of this group, and later served as a convener of B mixing and lifetime subgroup. D0 has published the first evidence for B_s oscillations [5] with the frequency consistent with the SM expectations. In addition, Dr. B. Abbott led a group of researchers who discovered the first baryon containing quarks from three different generations, the Ξ_B baryon. [6].

- **Tracking and trigger at D0.** One of the most important areas of the D0 experiment is identifying charged particles and measuring their position and momentum. Dr. Strauss has served as a co-convener of the tracking group. Under his leadership, Dr. Khanov and Dr. Rizatdinova adapted the newly installed silicon tracker layer into tracking software, and studied the tracking performance of the upgraded tracker. Postdoctoral fellow Dr. A. Pompos from OU was in charge of the trigger operations and the maintenance of the trigger lists.

Research interests of the OCHEP group at the LHC are focused on understanding the mechanism for electroweak symmetry breaking (EWSB). One of our primary focus has been on the search for a heavy charged Higgs boson predicted by extensions of the SM. Presence of heavy flavor jets is a characteristic feature for many physics channels involving charged Higgs boson production and decay. In addition, we are investigating methods of measuring the cross section of top pair production using di-lepton decays. This can be done early in the ATLAS data-taking period and can be used to study the top quark properties and to calibrate the detector. At ATLAS, OCHEP members mainly contribute to:

- b**-tagging algorithms.** Drs. Rizatdinova and Khanov have implemented and tuned a simple b-tagging algorithm that has been initially developed by them for the D0 experiment. The tagging performance of the algorithm has been studied. Currently, the algorithm became a one of the default ATLAS b-tagging algorithms.

- **Upgrade of the pixel detector.** Drs. Rizatdinova's and Skubic's interest in hardware development is focused on vertex detectors. They are committed to pixel detector research and development to improve the characteristics of the existing pixel detector. OCHEP members together with colleagues from Ohio State University have irradiated four optoboards with PIN and VCSEL arrays from various vendors using 24 GeV protons at CERN. It was found that responsivity of PiN diodes went down by factor of 2. All VCSEL arrays except the one died after irradiation to the level of SLHC doses. The next step is the creation of the test stand for further measurements of the PIN diodes lifetimes.

2 Theoretical Projects

The OCHEP theoretical group is involved in cutting edge research in a wide range of theoretical HEP topics. The focus is on phenomenology of Higgs boson physics, physics of extra dimensions, neutrino masses and oscillations, grand unified theories, dark matter, PT-symmetric quantum field theory, and the Casimir effect. A brief summary of these projects completed in the last four years is given below.

- **A new Higgs doublet model** has been proposed by Dr. Nandi and his graduate student Gabriel. It provides an alternative mechanism for tiny mass of neutrinos and predicts new signals for Higgs boson at LHC. One of the features of this model is that it predicts that the SM Higgs boson will decay to two practically massless Higgs bosons [7].

- **Unification of all the SM particles in extra dimensions** has been considered by Dr. Nandi and his collaborators. Dr. Nandi together with his colleagues constructed a model based on the $SU(8)$ gauge symmetry in six dimensions with $N = 2$ supersymmetry. The model predicts unification of the Yukawa couplings for the third family fermions with the gauge couplings at the unification scale of 2×10^{16}. They also constructed a model which unifies the Higgs couplings of the NMSSM with the gauge couplings, which predicts an interesting implications for the Higgs mass and top quark mass [8].

- **Family symmetry based on $SO(10)$.** Dr. Babu and collaborators have suggested unification based on the group $SO(10)^3 \times S_3$. Each family has its own $SO(10)$ group, and the S_3 permutes the three families and $SO(10)$ factors. This is the maximal local symmetry for the known fermions. Family unification is achieved in the sense that all known fermions are in a single irreducible multiplet of the symmetry. The symmetry suppresses SUSY flavor changing effects by making all squarks and sleptons degenerate in the symmetry limit. Non-trivial and realistic structure of the quark and lepton masses emerges from the gauge symmetry.

- **Models of neutrino masses and mixings.** New modeld of inverted neutrino mass hierarchy has been suggested by Dr. Babu and collaborators based on permutation symmetry. The reactor neutrino mixing angle θ_{13} is predicted to be large in this class of models, $\theta_{13} \geq 0.13$. This scenario also explains naturally the observed baryon asymmetry of the universe via resonant leptogenesis. The masses of the decaying right–handed neutrinos can be in the range $(10^3 - 10^7)$ GeV, which would avoid the generic gravitino problem of supersymmetric models.

- **Post-sphaleron baryogenesis.** Dr. Babu has proposed a new mechanism for generating the baryon asymmetry of the universe [9]. In this scheme, a SM singlet scalar field S which has a mass of order of 100 GeV decays directly into baryons and antibaryons and produces asymmetry. S couples to $\Delta B = 2$ operator via exchange of colored scalars, which arise naturally in Pati-Salam SM extension. Babu's model predicts the LHC should see colored scalars carrying baryon number with masses of order of TeV. It also predicts existence of neutron-antineutron oscillations that are within the reach of the next generation experiments.

- **Nonperturbative quantum field theory** is the focus area of Dr. Milton. Specifically, he has helped to set new limits on monopole masses, studied the temperature and local divergence structure of quantum vacuum energy, and developed new alternative non-Hermitian quantum field theories which may have an important implications in describing new physics. His research group has now shown how to compute exact interactions between macroscopic bodies due to quantum electrodynamic fluctuations. [10]

- **Electroweak symmetry breaking** Dr. Kao is investigating a mechanism by which particles acquire their masses, the reasons why top quark is so heavy and neutrino is so light, supersymmetry between bosons and fermions.

3 Distributed Computing

OCHEP institutions have been chosen by ATLAS management to be part of the Southwest Tier 2 facility. OCHEP has purchased and deployed a large computing cluster with 260 compute cores and 16 terabytes of disk space as part of facility encompassing diverse computing resources. This facility serves as a regional analysis center with a significant effort devoted to Tevatron and LHC

experiments. In addition, a Condor pool of student lab computers provided an additional 460 CPU's for Monte Carlo generation and simulation. These facilities have produced over 35 million events and almost 3 terabytes of simulation data for D0 in the last twelve months. OCHEP personnel have contributed to grid computing in many ways. Dr. H. Severini has been one of the leaders in the effort to develop and test distributed computing models, software, and applications for the ATLAS and D0 collaboration. Information technology specialist Karthik Arunachalam has helped to develop submission and monitoring software for grid applications. Dr. Joel Snow serves as the Monte Carlo production coordinator for D0 and is the designer, developer, operator, and maintainer of automatic Monte Carlo production software at Fermilab. Dr. Abbott served as computing coordinator for the D0 experiment.

4 Education and Outreach

OCHEP supports education and science outreach throughout the state. Every other summer we have conducted a two week workshop for high school teachers. The workshop has enhanced teachers' understanding and appreciation of particle physics and scientific methods, and developed curriculum for teachers to use in their classroom. In alternate summers, OCHEP supports an eight week reserach experience for high school teachers. During the last four years, about 25 Oklahoma high school teachers have participated in the program.

5 Conclusions

OCHEP is a fully operational center consiting of all High Energy physics faculty in the state of Oklahoma, performing collaborative research and promoting science education throughout the state. Faculty members, postdocs and graduate students have published over 150 research articles and have presented over 100 talks at national and international conferences during four years of EPSCoR support.

References

[1] V.M. Abazov et al. [D0 Collaboration], Phys. Rev. Lett. 98, 181802 (2007)

[2] V.M. Abazov et al. [D0 Collaboration], submitted to Phys. Rev. Lett. (hep-ex/0702005)

[3] V.M. Abazov et al. [D0 Collaboration], Phys. Lett. B 639, 616 (2006)

[4] V.M. Abazov et al. [D0 Collaboration], Phys. Rev.Lett. 97, 151804 (2006)

[5] V.M. Abazov et al. [D0 Collaboration], Phys. Rev.Lett. 97, 021802 (2006)

[6] V.M. Abazov et al. [D0 Collaboration], Phys. Rev.Lett. 99, 052001 (2007)

[7] S. Gabriel and S. Nandi, hep-ph/0610253

[8] I. Gogoladze, T. Lu, Y. Mimura and S. Nandi, Phys. Rev. D72, 055006 (2005)

[9] K.S. Babu, R.N. Mohapatra and S. Nasri, Phys. Rev. Lett. 97, 131301 (2006)

[10] K.A. Milton and J. Wagner, Phys. Rev. D 77, 04005 (2008)

Surface Anchoring of Nematic Phase on Carbon Nanotubes: Nanostructure of Ultra-High Temperature Materials

PI: Dr. Amod A. Ogale
Professor, Chemical Engineering, and
Dy. Director, Center for Advanced Engineering Fibers and Films
ogale@clemson.edu
Associated Students: Rebecca Alway-Cooper, Marlon Morales
Post-Doctoral Research Associate: Dr. Sungho Lee

Program Scope

Nuclear energy is a dependable source of electricity for the US because of the large size of the plants and their continuous periods of operation [1]. Nuclear power also has the second-lowest production cost of the major sources of electricity (1.7 cents/kWh) in comparison to that of hydroelectric (0.5 cents/kWh), coal (1.9 cents/kWh), natural gas (5.9 cents/kWh), and petroleum (5.4 cents/kWh) [1]. Because fuel supply sources are available domestically, nuclear energy can be a strong domestic industry that can reduce dependence on foreign energy sources. It is noted that only 20% of electricity produced in the US is from nuclear source, whereas some industrialized nations, such as France and Japan, produce over half of their electricity from nuclear sources.

Commercial nuclear power plants have extensive security measures to protect the facility from intruders [1]. However, additional research efforts are needed to increase the process safety of nuclear energy plants to protect the public in the event of a reactor malfunction. The next generation nuclear plant (NGNP) is envisioned to potentially operate on a helium-cooled nuclear reactor in the range 650-1000°C [2]. One of the most important safety design requirements for this reactor is that it must be *inherently safe*, i.e., the reactor must shut down safely in the event that the coolant flow is interrupted [2]. This next-generation, *Gen IV* reactor must operate in an inherently safe mode where the off-normal temperatures may reach 1500°C due to coolant-flow interruption. Metallic alloys used currently in reactor internals (e.g., control-rods) will melt at such temperatures.

Structural materials that will not melt at such ultra-high temperatures are carbon fibers and carbon-matrix composites that contain a high level of graphitic crystallinity. Graphite does not have a measurable melting point; it is known to sublime at about 3600°C [3]. However, neutron radiation-damage effects on carbon fibers are poorly understood. Therefore, the goal of this project is to obtain a fundamental understanding of the mechanisms of surface anchoring of the liquid crystalline precursors and the resulting "pinning" of the graphene layers by carbon nanotubes that could lead to neutron-damage resistance of the resulting carbon fibers. The goal of the proposed research is to generate novel carbonaceous nanostructures for radiation-stability in ultra-high temperature materials. The nanostructures are expected to generate high crystallinity, but not anisotropy, so that dimensional changes do not result in distortion.

Although graphite has been used in nuclear environment for almost 50 years by DOE, DoD, and NASA, unfortunately, polygranular graphites are not suitable for structural applications because they do not possess adequate strength, stiffness, or toughness that is required of structural components such as reaction control-rods, upper plenum shroud, and lower core-support plate [2,4]. For structural purposes, composites consisting of strong carbon fibers embedded in a carbon matrix are needed. Such carbon/carbon (C/C) composites have been used in aerospace industry to produce missile nose cones, space shuttle leading edge, and aircraft brake-pads [5]. However, radiation-tolerance of such materials is not adequately known because only limited radiation studies have been performed on C/C composites, which suggest that pitch-based carbon fibers have better dimensional stability than that of polyacrylonitrile (PAN) based fibers [6]. The thermodynamically-stable state of graphitic crystalline packing of carbon atoms derived from mesophase pitch (rather than PAN) leads to a greater stability during neutron irradiation.

Recent Progress

The severe axial orientation of graphene layers obtained from mesophase pitch precursors results in highly directional properties such as unusually high axial tensile modulus and axial thermal conductivity. However, the compressive strength of such fibers is an order of magnitude lower than its tensile strength, due to the severe anisotropy. In ongoing studies, cosponsored by NSF and AFRL, we incorporated carbon multiwall nanotubes (MWNT) into mesophase pitch in a very dilute concentration of up to 0.3 wt% [7]. Carbon fibers derived from pure mesophase pitch displayed a highly anisotropic structure. In contrast, the presence of 0.3 wt% nanotubes in the mesophase pitch led to a texture that was significantly less anisotropic in the plane. We emphasize that in our carbon fibers, nanotubes are added in ultra-dilute concentration, only about 0.3 wt%. Therefore, the materials are not cost-prohibitive.

Our recent data of MWNT-modified carbon fibers indicates that the compressive strength of the nanotube-reinforced fibers is at least equivalent or slightly improved, as compared with pure mesophase-based carbon fibers [8]. Moreover, it is noteworthy that the ratios of recoil compressive strengths to tensile strength of nanostructured fibers are much higher (the difference is at least 10% or higher) than those for the commercial counterparts and even than those for PAN-based commercial carbon fibers.
In a recent study, co-funded by AFRL, thermal conductivity of various carbon fibers was measured by a laser flash technique. Pure pitch-based carbon fibers possessed a thermal conductivity of 195 W/m.K whereas the nanomodified fibers, with the more uniform in-plane texture still retained a value of 190 W/m.K. Thus, nanotubes are helping to reduce anisotropy in carbon fibers, which has typically resulted in very high tensile strength but very poor compressive strength, while retaining the graphitic crystallinity that is important for ultrahigh thermal conductivity.

To probe the nanotexture of the fibers, transmission electron microscopy (TEM) was conducted (Hitachi H 7600 and H 9500). TEM micrographs from stabilized sample showed fairly dispersed CNTs in pitch matrix. Further, for oxidized samples, the selected

area electron diffraction (SAED) technique was used during TEM to analyze the microstructure. SAED pattern of CNT in stabilized sample is shown in Figure 1c. A set of arcs, associated with (002), was observed. It should be noted that due to the limit of beam size (0.2 μm), and masking effect of matrix, a strong pattern was not obtained. Ongoing studies are investigating advanced TEM techniques for probing the graphitic development within 10-100 nm of the nanotube because we have evidence from recent results that the nematic phase consists of disk-like molecules approximately 1.2 nm in their lateral size as measured by WAXD and MALDI-TOF techniques [9].

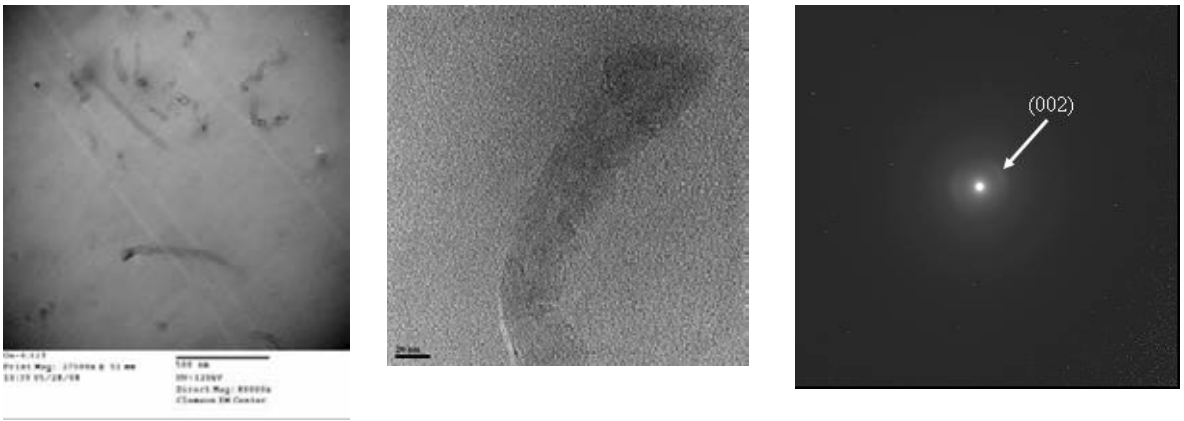

(a) (b) (c)

Fig. 1: TEM microsgraphs of (a) stabilized mesophase pitch- 0.3 wt% MWNT fibers; (b) high resolution micrograph in the vicinity of a nanotube, and (c) a selected area electron diffraction (SAED) pattern in the vicinity of the nanotube.

Future Plans

Mechanisms of neutron-damage for such ultra-high temperature materials will be investigated next in collaboration with Dr. Tim Burchell, Group Leader for Carbon Materials Group at ORNL. Dr. Burchell visited Clemson University (April 2008) as a part of the collaborative effort to discuss Clemson results, and to present a research seminar for graduate students of Chemical Engineering and Center for Advanced Engineering Fibers and Films. An experimental protocol for the irradiation studies is being developed using the High Flux Isotope Reactor (HFIR). All of the irradiation studies will be conducted by ORNL collaborators using standard procedures developed from their extensive research expertise in radiation-damage in nuclear graphites. Rabbit irradiation capsules and an irradiation temperature of 600°C is being targeted, allowing comparison with prior data for carbon-carbon composites. The target irradiation dose will be 2-4 displacements per atom (dpa), which corresponds to 2-4 cycles in the HFIR. Post irradiation examination (PIE) of the samples will indicate the extent to which structural manipulation has influenced the neutron irradiation stability.

References

[1] www.nei.org website for Nuclear Energy Institute, Washington, D.C. 20006-3708

[2] W. R. Corwin, *Advanced Reactor, Fuel Cycle, and Energy Products Workshop for Universities*, Workshop for Universities, Gaithersburg, MD, June 16-17, 2005

[3] J. P. Scahffer, A. Saxena, S. Antolovich, T. H. Sanders, and S. B. Warner, *The Science and Design of Engineering Materials*, 2nd Ed., WCB-McGraw Hill, Boston, 1999

[4] T. D. Burchell, , MRS Bulletin, 22(4), 29-35 (1997)

[5] J. D. Buckley and D. D. Edie, *Carbon-Carbon Materials and Composites*, NASA Reference Publication 1254, 1992.

[6] T. D. Burchell, W. P. Eatherly, J. M. Robbins and J. P. Strizak, J. Nuclear Materials, 191-194, 295-299 (1992)

[7] A. A. Ogale*, D. D. Edie, and A. Rao, US Patent 7,153,452, issued Dec 2006

[8] Y.S. Lee, A. A. Ogale, Young Rack Ahn, Chang Hun Yun, Chong Rae Park, *Fibers and Polymers, 7(10), 85-87, 2006*.

[9] S. Kundu, A. K. Naskar, A. A. Ogale*, D. P. Anderson and J. R. Arnold**,** ”Observations on a low-angle x-ray diffraction peak for AR-HP mesophase pitch”, Carbon (2008), doi:10.1016/j.carbon.2008.03.014

DOE-Sponsored Publication

“Thermal conductivity measurements for carbon fibers”, *Rebecca Alway-Cooper, Merlin Theodore, David P. Anderson, Amod A. Ogale*, P0466, paper accepted for presentation at CARBON 2008, Nagano, Japan (co-funded by AFRL)

"Phase II: The Next Generation Thermoelectric Materials for Solid State Cooling & Power Generation Applications"

Terry M. Tritt (PI), Joe Kolis*, Jian He**, Fivos Drymiotis**, Murray Daw, Catalina Marinescu and Apparao Rao
Clemson University, Dept. of Physics & Astronomy, Clemson, SC 29634
* Department of Chemistry, Clemson University
** New Hire Supported by DOE Phase I and II programs
ttritt@clemson.edu, 864-656-5319

I.) Program Scope:

The demand for alternative energy technology to reduce our reliance on fossil fuels, along with the environmental impacts, leads to important regimes of research, including that of direct thermal-to-electrical energy conversion using thermoelectric (TE) devices. Being all solid assembly, responsive, and moving part free, the modular aspects of TE device make it easy to couple to other energy conversion techniques. As an example, a solar collector/concentrator-TE hybrid device can be fabricated, with the solar cell covering and the TE device covering the ultraviolet and infrared part of the energy spectrum, respectively. It is important to recognize that no single technology can solve all the nation's energy needs of the 21st century, more likely, it will be a combination of many technologies, one of which we believe will be TE energy conversion. An excellent overview of the state of the art TE materials, as well as an overview of recent developments is given in the following references. [1, 2]

Over the past decade there has been a heightened interest in the field of thermoelectrics driven by the need for more efficient TE materials for both electronic refrigeration and power generation. [3, 4] Refrigeration aspects include applications such as cooling electronics (e.g. CPU chips) and optoelectronics (IR detectors and laser diodes) for enhanced performance. [5] One of the largest current markets is to incorporate TE cooling devices into automotive seat coolers. Power generation applications are especially important in deep space missions (NASA) where the need for a reliable long-term power source is an absolute necessity. Given the soaring price of fossil fuels lately experienced in the United States and the ever decreasing fossil fuel supply worldwide, there is even a more pressing need to investigate alternative energy conversion technologies, including thermoelectrics. As an example, utilizing TE power generation to recover the large amount of waste heat (≈ 2/3 of generated power) from an automobile's exhaust or engine and harvesting this into usable "on-board" electrical energy can provide a reduced demand for fossil fuels and reduce their detrimental impact on the environment. [6]

II.) Recent Progress:

The major programmatic impacts of Phase I and II funding are three-fold, (1) the hiring of 4 new faculty members, (2) the acquisition of several major pieces of experimental equipment, and (3) some significant scientific findings. Each of these aspects will be discussed in the following.

(1) Prof. Fivos Drymiotis was hired under the Phase I part of the program. He was able to establish a state-of-the-art bulk materials synthesis laboratory. Dr Jian He, Dr. Hye-jung Kang and Dr. Sumatan Tewari are hired under the Phase II part of the program. Dr. He will focus on the synthesis and characterization of the oxides TE materials and nanocomposite materials; Dr. Kang

is a neutron scattering expert, she will inspect the TE materials with complex structures from the phonon point of view; and, Dr. Tewari is a theorist who will work on band structure calculation and transport property modeling.

(2) The influx of money from this DOE/EPSCoR Implementation Program has allowed us to accomplish some excellent facilities and infrastructure within the Phase I and beginning of Phase II of this program. These include: (a) a Netzsch 457 laser flash diffusivity system, (b) a Netzsch 404 high temperature DSC (c) a Thermal Technology hot isostatic press (HIP) used to provide high quality densified polycrystalline materials, (d) a Rigaku X-Ray Diffractometer, (e) an Ulvac ZEM-2 high temperature resistivity and Seebeck measurement system and (f) a UV-visible spectrometer that was used to determine the position of the surface plasmon absorption peak Bi nanowires (10 nm), (g) a Spark plasma sintering system (SPS) used to prepare nanocomposite TE materials and highly densified oxide materials, (h) a resonance ultrasound spectroscopy system. The specific pieces of equipment, the HIP and SPS, makes Clemson University one of the very few places in the world having such capabilities. We are planning to buy an infrared image floating zone system to strengthen the capability of growing large high quality single crystals.

(3) One of our major scientific successes in Phase II of this DOE Implementation program has been the ability to synthesize TE nanocomposite materials. This research direction has been motivated by several theoretical and experimental investigations. It was early proposed by Hicks *et al.* that an increase in ZT can be expected due to an increase in the electronic DOS per unit volume in quantum-well structures. [7] The results from an experimental measurement of a 2-D PbTe/$Pb_{1-x}Eu_xTe$ quantum well system found such a large increase in the figure of merit confirming this prediction. [8] Thus, by reducing the dimension of conventional TE materials to the nanoscale the materials may have higher efficiency (ZT). [9, 10] Certainly low dimensional structures of TE materials have shown to possess higher ZT values than their bulk counterparts such as the PbTe quantum dot structures [11] and the Bi_2Te_3/Sb_2Te_3 superlattice materials have already been shown to be quite feasible. [12] However, the superlattice/quantum well approach is costly and hard to scale up, which prompted the cost effective nanocomposite approach.

The basic idea behind the TE nanocomposite approach is to introduce numerous interfaces (grain boundary interfaces) that are specially chosen to: 1) scatter phonon more than electron, and 2) to increase the Seebeck coefficient (for example, by carrier-energy filtering or by quantum confinement) more than increasing the electrical resistivity. A nanocomposite is in bulk form, which is comprised of a bulk matrix of one TE material that has a fraction of nanostructures incorporated, *in situ* or *ex situ*, into the bulk phase. This inclusion can be of same or different composition. One challenge is to uniformly disperse the nanostructures in the host, as it is hard to control in the traditional mechanical mixing of the bulk and nano phases. In the $CoSb_3$-based nanocomposite material, we have developed a novel method to grow nanoparticles of $CoSb_3$ directly on the $La_{0.9}Co_3Sb_{12}$ bulk grain, achieving an improved uniformity. [13]

A prerequisite for making nanocomposites is that one must be able to synthesize large quantities of the nanomaterials with controlled micro-morphology. We have been successful in using both CVD (chemical vapor deposition) and hyrdrothermal/solvothermal synthesis of large amounts of TE nanomaterials, such as PbTe, Bi_2Te_3, Bi_2S_3 and $CoSb_3$, LAST-m compounds. [14,15,16,17,18] The nanomaterials vary in size from several nanometers to submicron, with the composition well controlled.

One of our current focuses is on the grain boundary of the coarse-grain system. We have established the correlation between the micro-morphology of the grain boundary and the thermal

transport and the figure of merit in PbSnTe, [15] following our early work of fabricating 2-D nanostructures directly onto seed particles. [16]

III.) Future Plans:

We plan to:

- Utilize the current method of hydrothermal/solvothermal synthesis of nanostructures in order to incorporate these nanostructures into a matrix of a high-ZT TE materials by hotpressing or SPS, thus forming a TE nanocomposite. The as-grown nanostructures must be not only physically nanosized but also chemically active. The previous growths using oxygen-containing solution often led to passivated surface. The density and size dependences of the TE properties are topics we plan to investigate.
- Develop the TE phenomenology of nanocomposites through investigation of effects of micro-morphology on the Seebeck coefficient and transport properties in order to provide the basis for identifying and evaluating the relevant transport mechanisms that can contribute to the enhancement of the figure of merit. As an exploratory study, we have inspected the micro-morphology-transport property correlation in the Pb/PbTe composite materials, and tried to extract the contribution from the grain boundary using the Hashin-Shtriktman approximation.
- Neutron scattering study of the rattler effect in the single- and double-filled Skutterudites (the phonon density of state, phonon dispersion curve etc.).

IV.) References:

1. *Harvesting Energy through Thermoelectrics: Power Generation & Cooling*, special edition MRS Bulletin, Vol. **31**, 2006 guest editors: Terry M. Tritt and M. A. Subramanian.
2. G. S. Nolas, J. Sharp and H. J. Goldsmid, *Thermoelectrics: Basic Principles and New Materials Developments*, Springer New York (2000)
3. The reader is referred to many of the recent MRS Proceedings on the topic of thermoelectric materials and energy conversion technologies. MRS Proceedings, **478** (1997), **545** (1998), **626** (2000), **691**(2001), **793** (2003) and **886** (2005)
4. Terry M. Tritt, (volumes editor): *"Recent Trends in Thermoelectric Materials Research"*, Semiconductors and Semimetals, Volumes **69**, **70** and **71**, Treatise editors, R. K. Willardson and E. Weber, Academic Press, New York, (2000)
5. Andrew W. Allen, Detector Handbook, *Thermoelectrically Cooled IR Detectors Beat the Heat*, Laser Focus World, Volume **33**, pS15, March issue 1997.
6. *Thermoelectric Materials for Space and Automotive Power Applications*, J.Yang and T. Caillat, special edition MRS Bulletin, Vol. **31**, 2006
7. Hicks et al., Phys Rev B, **47**, 12727 (1993).
8. Hicks et al., Phys Rev B, **53**, R10493 (1996).
9. M.S. Dresselhaus, G. Chen, M.Y. Tang, R.G. Yang, H. Lee, D.Z. Wang, Z.F. Ren, J.P. Fleurial, and P. Gogna, Mater. Res. Soc. Symp. Proc. 886, 170056 (2005)
10. Terry M. Tritt, *et.al.*, MRS Fall 2005, MRS Proceedings Volume **886,** p53 (2005)
11. T.C. Harman, P.J. Taylor, M.P. Walsh, and B.E. LaForge, Science **297,** 2229 (2002).
12. R. Venkatasubramanian, E. Siivola, T, Colpitts, and B. O'Quinn, Nature **413**, 597 (2001).
13. P. Alboni, X. Ji, J. He, N. Gothard and Terry M. Trrit, J. Appl. Phys. **103**, 113707 (2008).
14. B. Zhang, J. He and Terry M. Tritt, Appl. Phys. Lett., **88**, 043119 (2006)
15. X. Ji, B. Zhang, Z,.Su, T. Holgate, J. He, and Terry M. Tritt, submitted to Adv. Func. Materials.
16. B. Zhang, J. He and Terry M. Tritt, Appl. Phys. Lett., **88**, 043119 (2006).

V.) DOE Sponsored Publications (Selected Highlights): 2006-2008

Laser-assisted Synthesis and Optical Properties of Bismuth Nanorods
Jason Reppert, Rahul Rao, Malcolm Skove, Jian He, Matthew Craps, Terry Tritt, Apparao M Rao, Chem. Phys. Lett., 442, 334 (2007).

Size-Selective High-yield Growth of Lead Telluride (PbTe) Nanocrystals Using a CVD Technique, Bo Zhang, J. He and Terry M. Tritt, Appl. Phys. Lett., **88**, 043119 (2006)

Controlled Two-Dimensional Coated Nanostructures for Bulk Thermoelectric Composites
B. Zhang, J. He, X. Ji and Terry M. Tritt, Amar Kumbhar, Appl. Phys. Lett., **89**, 163114 (2006)
Selected for The Virtual Journal of Nanoscale Science & Technology *(Oct. 30, 2006 issue)*

Sample Probe to Measure Resistivity and Thermopower in theTemperature Range: 300 – 1000 K
V. Ponnambalam, S. Lindsey, N. S. Hickman and Terry M. Tritt, Rev. of Sci. Instrum, **77**, 073904 (2006)

Thermoelectric properties of the new polytelluride $Ba_3Cu_{14-\delta}Te_{12}$,
Abdeljalil Assoud, Stephanie Thomas, Brodie Sutherland, Huqin Zhang, Terry M. Tritt, Holger Kleinke, Chem. Mater. **18**, pp 3866-06 (2006)

New Directions in Bulk Thermoelectric Materials Research.
Terry M. Tritt MRS Fall 2005, MRS Proceedings Volume **886,** p53 (2006)**.**

First principles study of the electronic, optical and lattice vibrational properties of $AgSbTe_2$,
L. Ye, K. Hoang, A.J. Freeman, S. D. Mahanti, J. He, Terry M. Tritt and M.G. Kanatzidis, Phys. Rev. B 77, 245203 (2008).

Thermoelectric properties of $La_{0.9}CoFe_3Sb_{12}$*–*$CoSb_3$ *skutterudite nanocomposites,*
P. Alboni, X. Ji, J. He, N. Gothard and Terry M. Trrit, J. Appl. Phys. **103**, 113707 (2008).

Thermoelectric properties of p-type half-Heusler alloys $Zr_{1-x}TixCoSn_ySb_{1-y}$ *(0.0<x<0.5;y=0.15 and 0.3),*
V. Ponnambalam, Paola N. Alboni,J. Edwards, Terry M. Tritt, Slade R. Culp, and S. Joseph Poon, J. Appl. Phys. 103, 063716 (2008).

Analysis and Development of A Robust Fuel for Gas-Cooled Fast Reactors

Travis W. Knight
*University of South Carolina, Department of Mechanical Engineering
Columbia, SC 29208; twknight@sc.edu

I.) Program Scope

Ceramic-ceramic (cercer) composites are a candidate fuel form for gas-cooled fast reactor (GFR) applications [1, 2]. Because of its fast neutron spectrum, GFR have the potential to utilize a wide range of fuels including recycled, spent nuclear fuel to reduce high-level waste. Because of its high temperature operation, it can also be used for the future production of hydrogen to replace fossil fuels for transportation. Key to the realization of the GFR is the development of a robust fuel. This fuel form must accommodate a wide variety of elements including transuranics found in recycled fuels and perform safely at very high temperatures by trapping fission products in the fuel form itself.

A promising cercer design under investigation consists of mixed carbide fuel kernels coated with a low density carbon buffer layer to allow for expansion of the kernels under irradiation and a uniform, high density ZrC layer for fission product retention at high temperature. These kernels are dispersed in a ZrC matrix to form the composite fuel. The choice of ZrC was selected for its high temperature properties including good thermal conductivity and improved retention of fission products to temperatures beyond that of traditional SiC based coated particle fuels used in current high temperature reactors. The recycled nuclear fuels will contain higher concentrations of transuranics including different minor actinides such as americium and curium in order to incinerate them in the fast neutron spectrum of the GFR. Certain of these minor actinides such as americium have high vapor pressures when processed by traditional powder metallurgical operations and experience high losses potentially. Therefore, this effort also seeks to reduce anticipated minor actinide losses during fabrication by developing techniques that minimize the time that these fuels are exposed to high temperatures during fabrication.

II.) Recent Progress

Production of fuel kernels

Techniques of spark erosion similar to electro-discharge machining were previously reported on for the production of fuel kernels and more recently a similar method was tested involving rotating electrode. The process involves an electric arc used to melt a small portion of a spinning electrode. The centrifugal force acting on the melt flings it into a surrounding inert gas medium where it forms a sphere to due to surface tension, minimizing surface energy and is quenched in water, kerosene, or other medium. Here the aim was to minimize the time required for fabrication at high temperature where traditional methods of production from sol-gel technique require a long time at high temperature for carbothermic reduction and sintering. Both the spark erosion technique and the rotating electrode method require fabrication of an electrode from the starting material in this case uranium carbide or mixed carbide of the homogenously recycled fuels. For this work, uranium carbide electrodes were produced from the reaction of natural uranium with graphite via a combustion synthesis process. The exothermic reaction converts the reactants and also provides some heat for sintering of the compacts (intended electrodes). This work demonstrated the need for additional sintering of the compacts at 1929°C for up to two hours in order to achieve sufficient density and consolidation of the electrodes to withstand the thermal and mechanical stresses of the rotating electrode method. The spark erosion method similar to electric discharge machining provides for better size distribution control over the

kernels produced and was suitable for several surrogate test materials. However, its low current capability of less than 50 A was insufficient to yield a large enough fraction of larger sized kernels as needed for this work in the range of 300 to 1000 microns. The rotating electrode method with higher current greater than 80 A successfully produced kernels up to 1000 microns (Figure 1). The microstructure of the as fabricated kernels is shown in Figure 2 showing a highly dendritic structure indicative of rapid cooling. Further work at characterizing the fuel kernels is ongoing.

Matrix fabrication

Traditional techniques for compact manufacture require long sintering times at temperatures of at least two-thirds the melting temperature of the material. In order to control the purity of samples and limit the time that kernels are exposed to high temperatures, a combustion synthesis process has been tested to form the ceramic matrix by using a direct exothermic reaction of zirconium and graphite powders. A relationship has been developed between the initial powder size, applied pressure, and compact heat rate to achieve high density compacts with good mechanical strength. Cylindrical compacts (12 mm diameter) of pure, stoichiometric ZrC have been produced with up to 92% theoretical density (TD). This high density was accomplished by employing a method of uniaxial pressing at a minimum of 5.2 MPa similar to hot pressing to provide an additional driving force for sintering. These high density samples were produced with smaller size zirconium and graphite powders of approximately 3 and 44 microns respectively.

Integrated fabrication with fuel kernels

The fuel kernels produced were integrated into the ZrC matrix via the combustion synthesis method described above (Figure 3). The integrity of the fuel kernels were confirmed by scanning electron microscopy. Only limited and isolated instances of uranium diffusion into the ZrC matrix was noted via electron microprobe (Figures 4-6). Studies are underway to fully characterize these composite fuels and understand under what conditions the diffusion of uranium into the matrix can be prevented. Work on the coating of the fuel kernels with a carbon buffer coating and a high density ZrC layer is now underway and should better promote protection of the kernels during the fabrication process.

Figure 1. UC particles produced by the rotating electrode method.

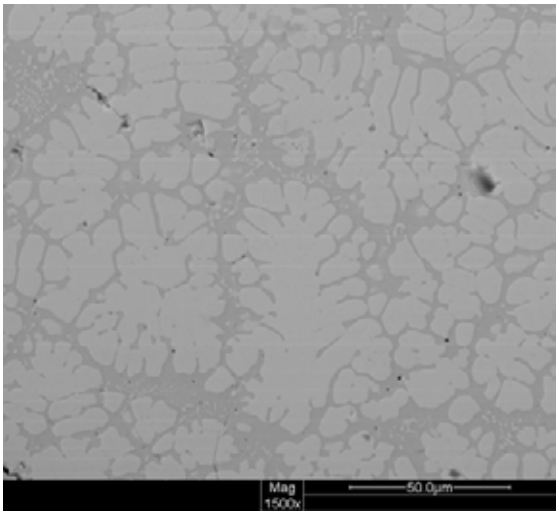

Figure 2. Microstructure of UC particles produced by rotating electrode mechanism showing a highly dendritic structure.

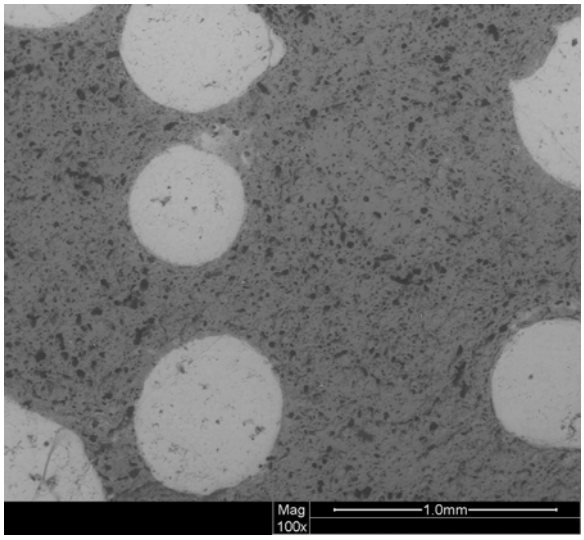

Figure 3. Composite compacts of UC particles dispersed in a ZrC matrix.

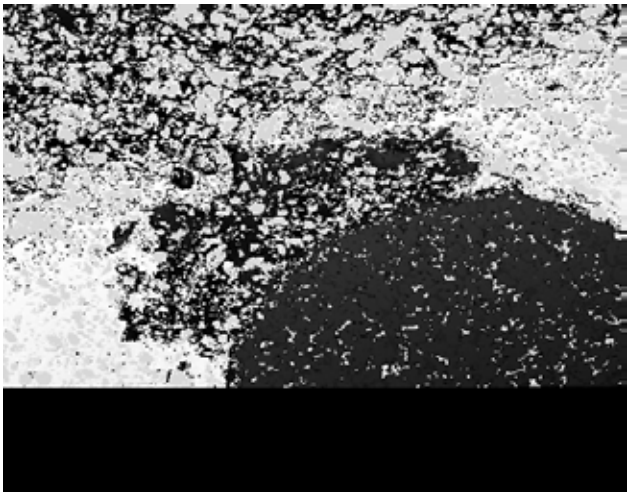

Figure 4. Compositional contrast image showing diffusion of uranium into the ZrC matrix following the high temperature combustion synthesis of the composite.

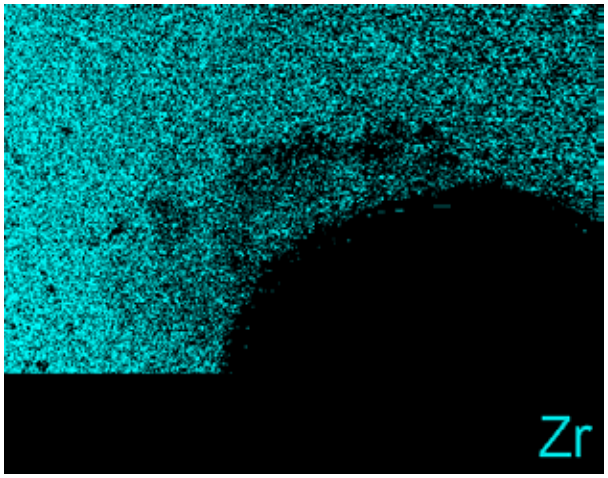

Figure 5. Elemental mapping of the same image in Figure 4 showing location of zirconium.

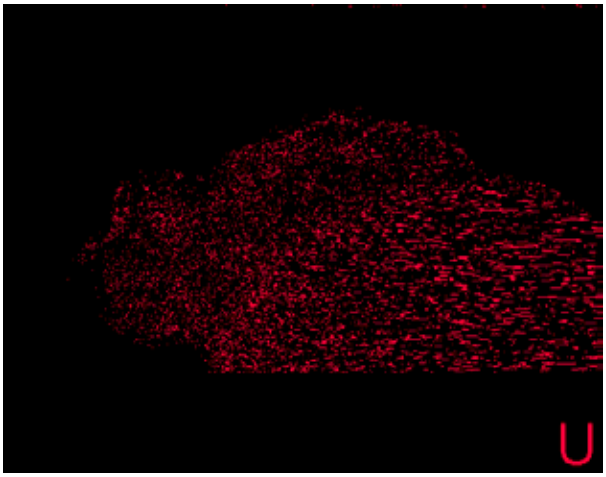

Figure 6. Elemental mapping of the same image in Figure 4 showing location of uranium.

III.) <u>Future Plans</u>

Additional characterization of the as fabricated UC electrodes and kernels is underway to understand the changes in composition and specifically carbon to metal ratio and explain the microstructure of the produced fuel kernels. Work continues to determine if there is significant uranium diffusion during the composite manufacture. Efforts are also ongoing for the coating of the fuel kernels with a buffer layer and a high density ZrC layer to allow for kernel swelling during irradiation and fission product retention, respectively.

These will then be integrated into the final ZrC matrix similar to those already demonstrated.

IV.) References

1. M. K. Meyer, A Report on the feasibility of GFR fuel for Minor Actinide Management, Argonne National Laboratory, (2004).
2. M. K. Meyer, et al., Fuel development for gas-cooled fast reactors, Journal of Nuclear Materials, 371, 1-3, 2007, pp 281-287.

V.) DOE Sponsored Publications (2005-2008)

Vasudevamurthy, G., **T. W. Knight**, E. Roberts, and T. Adams, "Laboratory Production of Zirconium Carbide Compacts for Use in Composite Nuclear Fuels", *Journal of Nuclear Materials*, **347**, 1-2, 2008, pp. 241-247

Vasudevamurthy, G. and **T. W. Knight**, "Effect of system parameters on size distribution of 304 Stainless Steel particles produced by Electrical Discharge Mechanism", *Materials Letters*, **61**, 27, November 2007

Vasudevamurthy, G., **T. W. Knight**, "Production of High Density Uranium Carbide compacts for use in Composite Nuclear Fuels", *Nuclear Technology*, In Press

"Lattice-Mismatched III-V Epilayers for High-Efficiency Photovoltaics"

S. P. Ahrenkiel (PI), R. J. Nesheim, M. W. Wanlass*, J. J. Carapella*
South Dakota School of Mines & Technology, Rapid City, SD 57701
*National Renewable Energy Laboratory, Golden, CO 80401

I.) Program Scope:

Lattice-mismatched (LMM) III-V heterostructures have shown great potential for use in high-efficiency multijunction photovoltaic devices [1]. Multijunction devices allow the reduction of losses that result from differences between the photon energy and the semiconductor optical bandgap. The bandgaps of the III-V alloys span the energy range needed for efficient conversion of the solar spectrum, but mismatch between arbitrary alloy compositions remains a challenge, often considered insurmountable**.** Mismatch produces strain and dislocations in thin films, which degrade the electronic properties. However, several engineering concepts have been identified that make LMM heterostructures for device applications a realistic possibility. We will apply these concepts to materials that offer potential improvements in PV conversion efficiencies.

We will explore various grading schemes based on III-V alloys, with general formula $(Al,Ga)_xIn_{1-x}As_yP_{1-y}$, that connect arbitrary endpoint compounds. The quaternaries permit simultaneous tuning of both bandgap and lattice constant, and can be used for transparent grades between selected absorbers, without the thermal-expansion mismatch that results from abrupt changes between alloy systems. However, rapid characterization feedback and careful refinement of growth conditions is needed to navigate the III-V quaternary system, and this has prevented much previous exploration of LMM compositions. We propose several LMM heterostructures, which include quaternary grades and absorbers, specifically designed for high-efficiency generation of electricity from solar radiation.

An underlying concept in our approach to controlling defects and strain associated in LMM systems is the use of overshoot in the misfit of the buffer layer terminating the compositional grade [2]. Separate calibration of the buffer strain allows prediction of the amount of overshoot needed to precisely lattice match the in-plane lattice constant of the buffer to the bulk (unstrained) lattice constant of a particular active layer. A further refinement is the incorporation of an intermediate region between the buffer and active layer. This spatially isolates the active region from the grade and reduces dislocation motion into the active region. A suitable test structure is produced by omission of the relevant active layer and simplification of the intermediate region to a single epilayer. This can reduce complications associated with interface formation in heteroepitaxy.

II.) Recent Progress:

Deposition: Initial materials synthesis by metal-organic vapor phase epitaxy (MOVPE) will be performed at NREL, typically on 2"-diameter substrates. This system uses a custom, atmospheric-pressure reactor design, and can produce high-quality materials that are ready for electrical characterization and device fabrication at NREL. The emphasis of growth at NREL will be on developing a high-gap top cell, particularly $Ga_xIn_{1-x}P$ using $GaAs \rightarrow GaAs_yP_{1-y}$. This could be incorporated into inverted tandem structures, which can

be processed by transferring the films to an appropriate “handle”, then removing the substrate for possible recovery [3].

Figure 1. OMVPE system at SDSM&T: (left) Rear view showing gas inlet and purification components and manifold; (right) control panel.

MOVPE synthesis of LMM films is simultaneously in development at SDSM&T with a custom system formerly used by the Electrical Engineering Department for device fabrication [Figure 1]. The focus here will be on grade design for LMM structures. In particular, following system calibration, we will seek to demonstrate quaternary grades, particularly GaAs→$Ga_xIn_{1-x}P$, and $Ga_xIn_{1-x}P$ →$(Al,Ga)_xIn_{1-x}P$.

Characterization: The emphasis of this work is on structural characterization of materials for optimization of LMM heterostructures. The primary tool will be the H-7000 FA transmission electron microscope (TEM) at SDSM&T. Our analysis will rely on cross-sectional specimen preparation for examination of dislocation character and morphology. Standard sample polishing and ion-milling techniques will be employed. Following a planned upgrade of the existing energy-dispersive x-ray spectrometer (EDX) accessory on our TEM, standards-based measurement procedures and algorithms for compositional calibration of quaternary III-V alloys will be developed [4].

X-ray diffraction (XRD) will be used for strain determination of the LMM films. High-resolution XRD at NREL will be used to examine select samples. Reciprocal-space mapping is a powerful approach to this analysis, but can require considerable beam time. Therefore, methods devised for previous work on $Ga_xIn_{1-x}As/InAs_yP_{1-y}$ LMM structures, based on specific alignment criteria and radial XRD scans, will be adapted to allow a more streamlined approach to data acquisition.

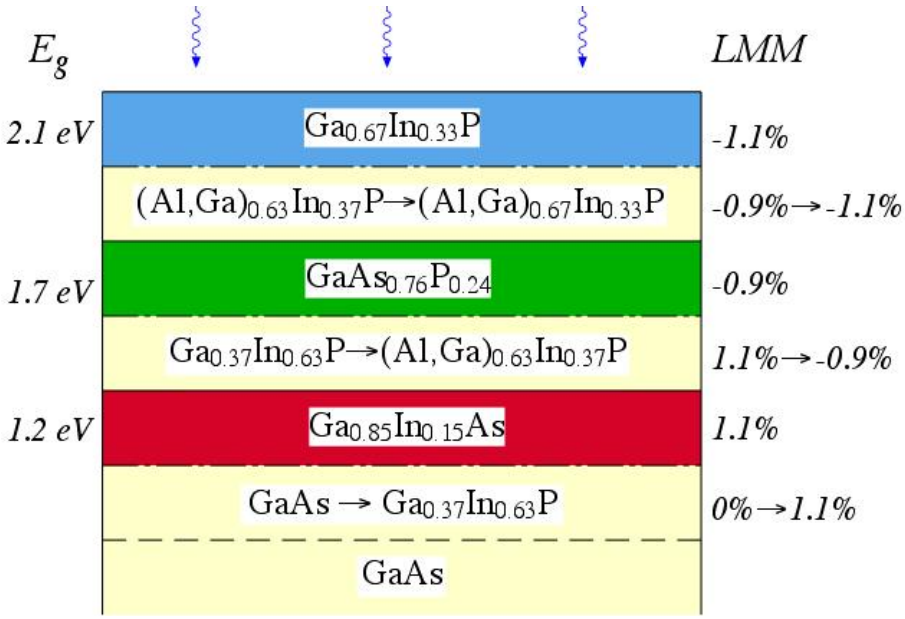

Figure 2. Three-junction, non-inverted test structure to be developed.

III.) <u>Future Plans</u>

This work will commence with the characterization and optimization of structures already under investigation at NREL. The initial system of study will be graded $GaAs \rightarrow GaAs_yP_{1-y}$. Deposition at SDSM&T will begin with lattice-matched $Ga_xIn_{1-x}P$ on GaAs. Using XRD for accurate determine of ternary compositions, we will identify appropriate standards for EDX calibration. We will then explore graded quaternaries, with the aim to develop structures for non-inverted tandem devices [Figure 2].

IV.) <u>References:</u>

1. R. R. King,_ D. C. Law, K. M. Edmondson, C. M. Fetzer, G. S. Kinsey, H. Yoon, R. A. Sherif, N. H. Karam, "40% efficient metamorphic GaInP/GaInAs/Ge multijunction solar cells", *Appl. Phys. Lett.* **90**, 183516 (2007).

2. S. P. Ahrenkiel, M. W. Wanlass, J. J. Carapella, R. K. Ahrenkiel, S. W. Johnston, L. M. Gedvilas, "Optimization of Buffer Layers for Lattice-Mismatched Epitaxy of $Ga_xIn_{1-x}As/InAs_yP_{1-y}$ Double-Heterostructures on InP", *Solar Energy Mat. & Solar Cells* **91**, 908-918 (2007).

3. J. F. Geisz, Sarah Kurtz, M. W. Wanlass, J. S. Ward, A. Duda, D. J. Friedman, J. M. Olson, W. E. McMahon, T. E. Moriarty, J. T. Kiehl" High-efficiency GaInP/GaAs/InGaAs triple-junction solar cells grown inverted with a metamorphic bottom junction", *Appl. Phys. Lett.* **91**, 023502 (2007).

4. J. Goldstein, D. Newbury, D. Joy, C. Lyman, P. Echlin, E. Lifshin, L. Sawyer, J. Michael, <u>Scanning Electron Microscopy and X-Ray Microanalysis</u>, Springer, New York, (2003).

Liquid Argon-Based Direct Dark Matter Searches at Homestake

Collaboration: DARE for **D**EPLETED **AR**GON **E**XPERIMENT
Principal Investigator: Dongming Mei, Department of Physics, The University of South Dakota, Vermillion, SD 57069

Collaborators: Yongchen Sun[1], Christina Keller[1], Asai Asaithambi[1], Kai Wang[1], Robert McTaggart[2], Barbara Szczerbinska[3], William M. Roggenthen[4], Andrew Hime[5], Kevin Lesko[6], Yuen-Dat Chan[6], Elliot Bernstein[7]
1: The University of South Dakota, 2: South Dakota State University, 3: Dakota State University, 4: South Dakota School of Mines & Technology, 5: Los Alamos National Laboratory, 6: Lawrence Berkeley National Laboratory, 7: Colorado State University.

Program Scope

The objectives of this proposal, submitted on behalf of the DARE collaboration, are to: 1) evaluate two different depletion techniques (thermal diffusion column and ion source laser isotope separation) to deplete ^{39}Ar in natural argon by a factor of 10^3 to 10^6 compared to atmospheric levels; 2) construct a facility to produce ^{39}Ar-depleted argon for the next generation of argon-based dark matter detectors at the Sanford Lab within five years and at DUSEL within 10 years; and 3) verify the depletion factor with Accelerated Mass Spectroscopy (AMS) or MiniCLEAN detector. Fig. 1 schematically represents the components of the research project.

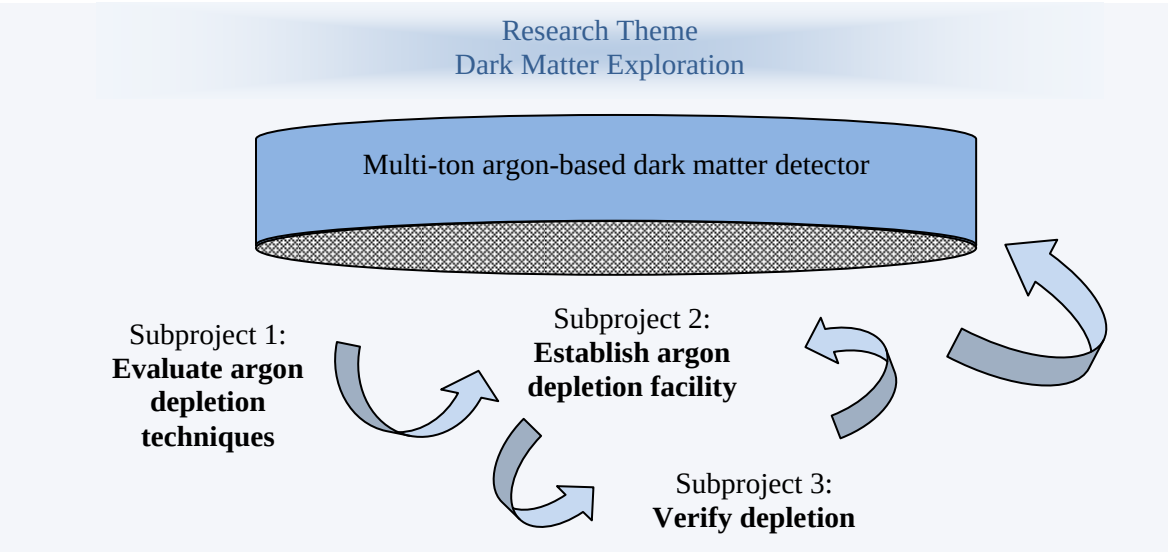

Fig.1 Integration of subprojects within the research theme.

As the collaboration pursues the research objectives described above, the long-range outcome to the state is significant. First, the proposal will allow South Dakota researchers to hire supporting personnel such as post-doctoral researchers and technicians to complement the existing faculty expertise, and provide the support that will make the South Dakota collaboration nationally competitive in seeking additional funding. Second, it will contribute to the state's efforts to begin its first doctoral program in physics and will build on our institutions' strong traditions of including undergraduate students in research activities.

Third, it will assist in maintaining the existing collaboration among the SD institutions and the two national labs, thus supporting several young faculty numbers who are just beginning their professional careers. Finally, the proposal will contribute significantly to the technical resources in the state through the purchase of equipment necessary to build the physical infrastructure so that South Dakota institutions will be able to play a key role in the worldwide dark matter program at DUSEL for decades to come.

Recent Progress

Observation of the rotation curves of spiral galaxies shows that a large fraction (~96%) of the mass-energy density of the universe cannot be accounted for with ordinary matter. Such a significant percentage of the missing ``dark matter'' suggests that the universe may consist of new types of elementary particles. A compelling explanation for the new particles is the existence of Weakly Interacting Massive Particles (WIMPs), non-baryonic particles characterized by particle physics theories beyond the Standard Model, thus the terrestrial discovery of WIMPs would have enormous intellectual merit [1-3]. WIMPs are believed to have a typical mass of about 100 GeV and to be moving at speeds relative to the Earth of about 220 km/s. Such cold particles can only deposit several tens of keV when they interact with nuclei. Moreover, they only interact through the weak force and gravity; hence the interaction cross-section with ordinary matter is extremely small. Therefore, experimental techniques that combine low radioactivity, low energy thresholds, efficient discrimination against electronic recoil backgrounds, and scalability to large detector masses can only be performed in a deep underground environment.

The Homestake Mine in Lead, South Dakota, has been selected by the National Science Foundation (NSF) as the site for the Deep Underground Science and Engineering Laboratory (DUSEL). Conversion of this facility will enable it to host a variety of physics, geoscience, geomicrobiology, and engineering projects. The state of South Dakota and a private donor, Mr. T. Denny Sanford, have committed a total of $115M for refurbishment and construction of the Sanford Laboratory at the 4850-ft level at Homestake. The Sanford Lab will be up and running within the next couple of years to pave the way for the creation of DUSEL in five years. Based upon Letters of Intent submitted to a Homestake organizational meeting held in February 2006, it is clear that much of the science being performed at DUSEL, including the project described herein, will be of particular interest to the Department of Energy. Centered on the theme of dark matter exploration, the subprojects proposed here will establish the infrastructure for dark matter and double-beta decay research. The outcomes of the individual subprojects are the production of depleted argon and its use in the subsequent creation of detectors to search for dark matter.

A prototype facility (thermal diffusion columns) is under construction at USD with a state competitive research grant award ($80,000). Six undergraduate students and a postdoctoral researcher are working on this project under supervision of Dr. Mei (PI), Dr. Sun (Co-PI), and Dr. Keller (senior personnel). A paper has been accepted by *Astroparticle Physics* for publication.

3. Future Plans

The research plan is to develop a method to separate isotopes of argon gas so that the quantity of radioactive ^{39}Ar will be reduced by several orders of magnitude, a reduction factor significantly greater than that currently achievable. The same techniques may also be used to remove other radioactive impurities, namely ^{85}Kr, from the argon gas. The reduction of ^{85}Kr is expected to be about eight orders of magnitude, which again represents a significant improvement over current technologies. Moreover, the techniques must be able to produce a large amount of the depleted argon with 1) a desired depletion factor of 10^3 for a next generation dark matter detector at Sanford Lab in five years and 2) a desired depletion factor of 10^6 for a more sensitive detector at DUSEL in a decade. The techniques described below will satisfy these requirements for a phased-approach dark matter program at Sanford Lab and DUSEL. These

techniques will be the most effective ways in the world to deplete the argon gas used in experiments for dark matter detection. The technology, as applied to solids, could then be adopted in the broader business community in the production of various radioactive isotopes for medical research and medical applications. For example, the use of radioactive isotopes as tracers for the study of metabolic phenomena, as diagnostic aids in clinical medicine, and finally their role in therapy are three principal categories in medical research. Laser-based analysis of the tracer isotopes provides yet another avenue with sufficient sensitivity and selectivity for these types of applications [4]. Because ^{39}Ar isotope can be produced by spallation reactions, electromagnetic interactions with cosmic muons [5], or by neutron interactions with stable argon isotopes, the storage of large amounts of depleted argon must be conducted in a quiet underground environment in order to avoid the possibility for recontamination once the argon has been depleted.

Hot-wire thermal diffusion columns have proven to be of great value in the isotopic enrichment of certain gaseous compounds [6, 7]. A simple, long vertical tube, closed at both ends, and containing argon gas comprises the column. A wire to be heated by an electric current is passed along the axis of the tube. On the one hand, the induced effect of thermal diffusion is to drive the lighter molecules toward the hot wire, so that they enter the rising convection current that exists near the wire. The lighter molecules are thus carried upward, and the heavier ones downward, so that a convection gradient is set up along the tube. On the other hand, the two convection currents, one rising near the wire and the other descending near the cooled wall of the tube, are essentially mixing processes that tend to neutralize any concentration gradient along the tube. The final equilibrium concentration gradient along the tube will therefore result from a compromise among the two convection currents and the remixing effect of ordinary diffusion along the tube.

Our goal is to design a thermal separation column that is effective for reducing the concentration of ^{39}Ar. We present here the design of an apparatus (Fig. 2) that has a separation factor of three orders of magnitude; that is to say, it will reduce the concentration of ^{39}Ar from an atmospheric level of 8.1×10^{-16}g/g to 8.1×10^{-19}g/g.

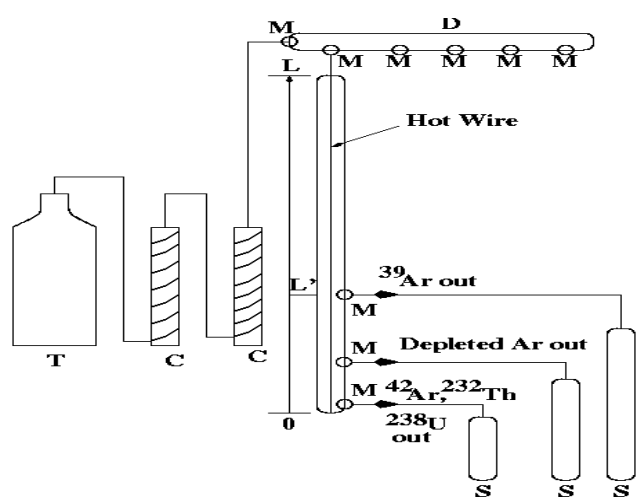

Fig. 2 Schematic diagram of a single thermal diffusion column apparatus for depleting argon. T: Argon cylinder, C: hot calcium traps, M: McKay valves, L: the length of the column; L': the length of the column where the depleted argon is extracted out; D: argon gas distributors; S: gas storage cylinders.

The effective length is 1400 cm that consists of three stages. The first two stages are 490 cm long. The third stage is 420 cm in length. The tube and the hotwire are made of copper and tungsten, respectively. The electric current passing through the wire required to generate the temperature of 1192 Kelvin (K) is about 0.5 A. To keep this wire centered, crosswires will be spotwelded on to it at 75 cm intervals. These crosswires may carry quartz sleeves of 1-mm o.d., which are longer than the wires so that the latter cannot touch the cold metal wall. The thermal expansion of the wire at 1200 K is computed to be about 0.3%. Rubber O-rings may be used as gaskets to make tight pressure seals between those fittings and the pipe ends.

The design described above gives a depletion factor, Q = 1125. The facility is composed of 3000 columns. The production rate is targeted at a level of 2 kg per day, 0.73 ton per year.

The ^{39}Ar depleted argon gas will be collected and stored using standard gas containers at the 300-ft level at Homestake. The concentrated radioactive gas including ^{39}Ar, ^{42}Ar, ^{232}Th, and ^{232}U will be collected and stored at the surface building provided by Sanford Lab (see the support letter from Sanford). The gas cylinders are standard containers. The safety measures will be provided as needed by the safety officers on the site at the laboratory.

References:

[1] G. Jungman *et al*., Physics Reports **267**, 195 (1996).
[2] M. W. Goodman and E. Witten, Phys. Rev. D **31**, 3059 (1985).
[3] B. W. Lee and S. Weinberg, Phys. Rev. Lett. **39**, 165 (1977).
[4] J.S. O'Connell and F.J. Shima, Phys. Rev. D **38** (1988) 2277.
[5] F. Arneodo et al. (ICARUS-Milano Collaboration) – Phys. Rev. D **74**, (2006) 11.
[6] R. Clark Jones and W. H. Furry, Reviews of Modern Physics, V **18**, 151 (1946).
[7] W. W. Watson, L. Onsager, and A. Zucker, Rev. of Sci. Instr. V **20**, 924 (1949).

DOE Sponsored Publications in 2005 – 2008

1. D.-M. Mei, Z.-B. Yin, L. C. Stonehill, and A. Hime, A Model of Nuclear Recoil Scintillation Efficiency in Noble Liquids, arXiv:0712.2470, accepted by Astroparticle Physics for Publication.
2. D.-M. Mei, S. R. Elliott, V. M. Gehman, A. Hime and K. Kazkaz, Neutron Inelastic Scattering Processes as Background for Double-Beta Decay Experiments
PRC, V77, 054614, 2008. Nucl-ex/0704.0306 (2007).
3. D.-M. Mei and A. Hime, Muon-induced Background Study for Unerground Laboratories
PRD 73, 053004 (2006)
4. S. R. Elliott, V. M. Gehman, K. Kazkaz, A. R. Young, Pulse shape analysis in segmented detectors as a technique for background reduction in Ge double-beta decay experiments
NIM A 558 (2006) 504
5. D.S. Akerib (Co-chair), E. Aprile (Co-chair), E.A. Baltz, M.R. Dragowsky, P. Gondolo, R.J. Gaitskell, A. Hime, C.J. Martoff, D.-M. Mei, H. Nelson, B. Sadoulet, R.W. Schnee, A.H. Sonnenschein and L.E. Strigari, Deep Underground Science and Engineering Lab S1 Dark Matter Working Group Report , astro-ph/0605719
6. D.-M. Mei, A. Hime, S.R. Elliott, V.M. Gehman and K.Kazkaz, Depth-Sensitivity Relation (DSR) for Underground Laboratories, Particles and Nuclei, Proceedings of the seventeenth International Conference on Particles and Nuclei, Santa Fe, New Mexico, 23-30 October 2005.

Resonant Ultrasound Studies of Spin Glasses and Geometrically Frustrated Magnets

P.I.: **Veerle Keppens**, The University of Tennessee
Student supported by DOE EPSCoR grant: **Yanbing Luan**, The University of Tennessee
External collaborators: **Ovidiu Garlea, Rongying Jin,** and **David Mandrus**, ORNL

Program Scope

In this program, the powerful technique of Resonant Ultrasound Spectroscopy (RUS) is brought to bear on spin glasses and geometrically frustrated magnets. As only the canonical spin glasses (dilute magnetic alloys of a noble metal host (Cu, Au, Ag) and a magnetic impurity (Cr, Mn, Fe)) have been subjected to ultrasonic studies, and no elastic measurements have been reported for geometrically frustrated magnets, we have the unique opportunity to start a systematic study of the elastic response of new and less conventional spin glasses. The elastic properties of a material provide information about how a material responds to strain. Near a phase transition, the temperature dependence of the elastic moduli will provide information about the coupling of the order parameter to the strain. Since RUS is extremely sensitive to transitions and ordering phenomena, we also expect effects like orbital ordering (that are easily missed with other experimental techniques) to show up in our measurements.

Recent Progress

i) Orbital-Spin Coupling in MnV_2O_4

Under the current DOE-EPSCoR research grant, we have started a study of the elastic response of MnV_2O_4 as a function of temperature. Although spin-orbit coupling is one way to couple spin and orbital degrees of freedom, there are other ways involving the fact that exchange interactions between moments depend on the direction and occupancy of orbitals. In MnV_2O_4, however, a magnetic field was recently observed to induce orbital ordering [1], and thus the direct coupling between orbital and spin degrees of freedom was demonstrated in this material.

Crystals of MnV_2O_4 were recently grown at ORNL in an optical floating zone furnace. An unoriented crystalline shard was studied with RUS as a function of temperature and magnetic field. Figure 1 shows a representative resonant frequency[1] as measured using Resonant Ultrasound Spectroscopy (RUS) [2]. Whereas the temperature-dependence of the elastic response of "conventional" materials shows a gradual increase or "stiffening" with decreasing temperatures [3], the result shown in figure 1 clearly illustrate how unusual the behavior of MnV_2O_4 is. A softening over a large temperature range is typically associated with an orbital ordering transition, but in Fig. 1 the minimum occurs at the *magnetic* transition; the orbital transition occurs several degrees lower. In fact,

[1] The resonant frequencies of a given sample are directly proportional to the square-root of its elastic moduli, and give therefore clear information about the elastic response of the material.

measurements in magnetic field reveal a feature near 50 K. This could represent a striking manifestation of direct spin-orbital coupling, and it will be interesting to carefully sort out what is going on. Our planned research on this material involves crystal growth in collaboration with the Mandrus group at ORNL, followed by in-depth RUS measurements as a function of temperature and magnetic field on oriented single crystals, in order to determine the full elastic tensor. Some sort of "magnetic control of elasticity" may be possible via orbital occupation

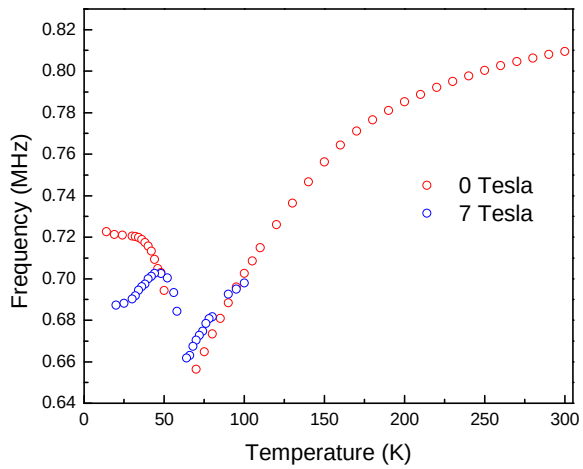

Fig. 1: Resonant frequency versus temperature for MnV_2O_4.

ii) RUS studies of polycrystalline $Na_{0.75}CoO_2$.

This correlated electron system has a layered triangular lattice and initially attracted attention as an oxide thermoelectric material (totally confounding the conventional wisdom that oxides are not a good place to look for new thermoelectrics) [4-6]. Although initial attention was focused almost exclusively on the CoO_2 layers, it is becoming increasingly clear that the role of the Na ions is crucial for understanding the physical properties of this system.

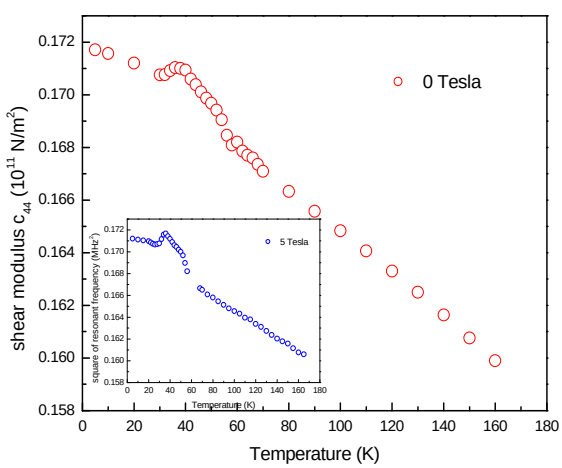

Fig. 2: Shear modulus versus temperature for polycrystalline $Na_{0.75}CoO_2$. Inset: Representative resonant frequency for the polycrystalline sample in 5 Tesla magnetic field.

Resonant Ultrasound Spectroscopy was used to determine the elastic tensor of polycrystalline $Na_{0.75}CoO_2$. As polycrystals are elastically isotropic, only 2 elastic moduli need to be determined, the shear modulus c_{44} and longitudinal modulus c_{11}. Fig. 2 shows the temperature-dependence of the shear modulus, measured in zero field. The elastic response of $Na_{0.75}CoO_2$ shows a broad "hump" around 40 K. As is shown in the inset of Fig. 2., the elastic response in magnetic field is similar to the zero field data. Specific heat, resistivity and magnetization measurements have revealed a spin-density-wave (SDW) transition in $Na_{0.75}CoO_2$, but it occurs at 22 K, which is substantially lower

than the temperature of the "hump" in our RUS data. We therefore believe that the anomaly revealed by RUS is not linked to the SDW, but is most likely due to an order-disorder transition that takes place via the rearrangement of Na atoms between the CoO_2 layers.

iii)RUS studies of single crystalline $Na_{0.77}CoO_2$.

Single crystals are grown in an optical furnace, as shown in figure 3. Fig. 4 shows the

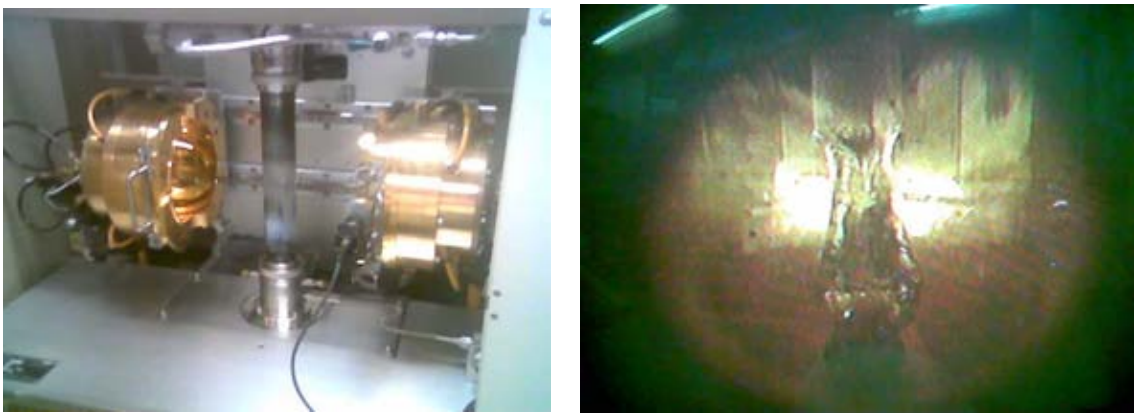

Fig.3: Floating zone growth of single crystalline Na_xCoO_2, using the optical image furnace.

temperature-dependence of several representative resonant frequencies of a single crystalline sample of $Na_{0.77}CoO_2$, measured in 5 Tesla. The data clearly show a "hump" similar to the polycrystalline data discussed above, but it appears to be less broad and more pronounced. As mentioned above, the physics behind this feature is currently not clear, but a detailed analysis of the data, yielding the full elastic tensor is expected to shed light on this issue. Since $Na_{0.77}CoO_2$ is hexagonal, the tensor will include 5 independent moduli, and we can obtain information about the directional dependence of the elastic response.

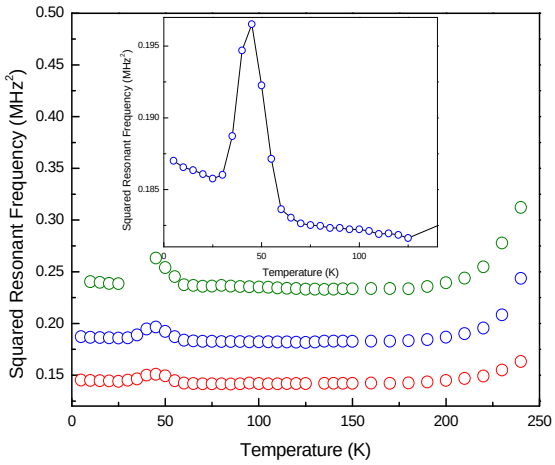

Fig. 4: Shear modulus versus temperature for polycrystalline $Na_{0.75}CoO_2$ in 5 Tesla magnetic field. Inset: detail of the "hump" observed at 40 K.

Future Plans

The results above clearly show that the elastic response of MnV_2O_4 and $NaCoO_2$ is very unusual. In order to elucidate this intriguing behavior, a full analysis with determination of the elastic tensor will be essential. This will be our main focus in the next few months. We are currently working on orienting the MnV_2O_4 shard, which will allow us to obtain the elastic tensor of this material. In addition, analysis of the RUS data on an oriented $NaCoO_2$ single crystal is under way.

References

[1] K. Adachi, T. Suzuki, K. Kato, K. Osaka, M. Takata, T. Katsufuji, , Physical Review Letters **95**, 197202 (2005).

[2] A. Migliori and J. L. Sarrao, Resonant ultrasound spectroscopy (Wiley and Sons, Inc., 1997); J. Maynard, Resonant Ultrasound Spectroscopy, Physics Today, 26 (1996).

[3 Y.P. Varschni, phys. Rev. B 2, 3592 (1970).

[4] R. Jin, P. Khalifah, and D. Mandrus, Phys. Rev. Lett. **91**, 217001 (2003); B.C. Sales *et al.*, Phys. Rev. B **70**, 174419 (2004).

[5] I. Terasaki *et al*., Phys. Rev. B **56**, 12685 (1997), K. Takahata *et al*., Phys. Rev. B **61**, 12551 (2000).

[6] B. C. Sales, D. Mandrus, and B. C. Chakoumakos, in Semiconductors and Semimetals Vol **70**, Edited by T. M. Tritt (Academic Press, New York, 2001) pp. 1-36.

High Throughput Analysis of the Low Dose Radiation Transcriptome*

Michael A. Langston[1†], Elissa J. Chesler[2] and Brynn H. Voy[2]

[1] Department of Electrical Engineering and Computer Science, University of Tennessee, Knoxville, TN 37996
[2] Biological Sciences Division, Oak Ridge National Laboratory, Oak Ridge, TN 37831-6445

Program Scope

The tools of molecular biology and the evolving tools of genomics can now be exploited to study the genetic regulatory mechanisms that control cellular responses to a wide variety of stimuli. These responses are highly complex, and involve many genes and gene products.

Our primary target is the elucidation of genetic regulatory mechanisms that control cellular responses to low dose ionizing radiation (IR). A low-dose exposure, as defined here, is an exposure of at most ten centigrays (rads). While the net health risk of low dose exposures continues to be debated, recent findings support the concept of risk even at very low doses. We aim to use genome scale gene expression data after IR exposure in vivo to identify the pathways that are activated or repressed as a tissue responds to the radiation insult. The driving motivation is that knowledge of these pathways will help clarify and interpret physiological responses to IR, which will advance our understanding of how low dose radiation exposures pose an increased risk to human health.

This research is of long-term significance to DOE and the nation at large. Understanding the health risks of exposure to low levels of radiation is critical if we are to protect the nation's workforce while making the most effective use of our national resources. The National Academy of Sciences recently issued a report [1] summarizing the most current evidence of the health effects of low levels of IR. This report supports the concept of a "linear-no-threshold" risk model, which holds that even the smallest doses of IR have the potential to increase the risk of cancer. Over the next several decades, it is expected that the majority of radiation exposures associated with human activity will be low dose in nature. These may arise from medical diagnostics, hazardous waste abatement, handling materials for nuclear weapons and power systems, and even terrorist acts such as dirty bombs. The major type of exposures will be low dose IR (primarily X-radiation and gamma-radiation) from fission products.

DOE's Office of Biological and Environmental Research has a long-standing interest in low dose radiation research, with particular recent concentration on molecular mechanisms and pathways [2]. Microarrays and other advances in technology provide a means to begin to extract such mechanisms and pathways without *a priori* knowledge of genes that might be involved. By focusing on gene co-regulation and putative network mechanisms, we seek to characterize radiation-induced perturbations of normal physiological processes. This should greatly enhance our understanding of low dose radiation's effects at all levels of biological organization, from genes to cells to tissues and finally to organisms.

Recent Progress

Thresholding. Our methods are based on combinatorial optimization, graph theory and high performance computation. From microarray data, we are able to build correlation matrices so that individual gene-gene interactions may be inferred. To form a graph from such a matrix, a cutoff value, or threshold, must be chosen above which an edge connecting two genes is

* This work is supported by the EPSCoR and Low Dose Radiation Research Programs, with UT-Battelle LLC the managing organization of ORNL for the U.S. DOE.
† Electronic queries should be addressed to: langston@eecs.utk.edu.

created, and below which the two genes are left unconnected. This decision is of critical importance, because graph metrics are highly dependent on the starting graph. We have recently studied a variety of approaches to thresholding [3]. These approaches include the analysis of control spot verification, false discovery rates, maximal cliques, power analysis, spectral clustering and top percentages of correlation. Maximal clique has proven to be the top performer, as measured by ontological similarity. Spectral clustering has also shown promise.

Noise Reduction. There are many sources and varieties of noise inherent in data generated with microarray technology. To account for this, we have refined and generalized our use of the paraclique algorithm first proposed in [4]. Informally, a paraclique is an extremely densely-connected subgraph, but one that may be missing a small number of edges and thus is not, strictly speaking, a clique. In our application, this corresponds to a very highly intercorrelated group of putatively co-regulated genes whose transcript expression levels, as reflected in real and surely somewhat dirty microarray data, show highly significant but not necessarily perfect pair-wise correlations. To illustrate, suppose we begin with a clique C of size k. For example, it may be that k is the size of the largest clique in the graph. And suppose the correlation matrix was transformed into a correlation graph using threshold t. We set a connectivity factor, f, at some value strictly less than k. We also set an edge weight bound, b, at some value strictly less than t. We now consider each non-clique vertex, v, in turn. We mark v if and only if it is adjacent to at least f vertices in C and if and only if the weight of the correlation coefficient on any "missing" edge is at least b. After each vertex has been considered, we set the paraclique, P, to be the union of C and the set of all marked vertices. We now remove P from the graph and iterate.

Biclique Extraction. The challenge, once the correlation graph is created, is not to study the graph in its entirety, but rather to extract its embedded subgraphs, or small, tightly connected regions of the graph that represent subsets of genes with strong correlations between every pair of its members and thus likely to represent biologically significant interactions. In the most extreme case, in which a subgraph contains all possible edges between its vertices, this structure is called a *clique*. The importance of clique lies in the fact that each and every pair of vertices is joined by an edge, from which we can infer some form of co-regulation among the corresponding genes. Clique is particularly useful in microarray analysis, because it addresses the shortcomings of traditional clustering algorithms: clusters need not be disjoint, negative correlations are easily handled, and edge density is maximized. In this setting, bipartite graphs have proven useful in representing relationships across heterogeneous data types, with the interpretation of these relationships accomplished through an enumeration of maximal bicliques. Unfortunately, most previously-known algorithms are highly inefficient and do not scale for this important task. In a recent paper [5], we present a fast and novel algorithm that finds all maximal bicliques in a bipartite graph. Unlike other techniques that have been proposed for this problem, our new method neither places undue restrictions on the input nor inflates the problem size. Efficiency is achieved by exploiting structure inherent in bipartite graphs, and by ensuring that biclique enumeration avoids duplication while pruning nonmaximal candidates. Without a fast implementation of biclique on bipartite graphs, a systematic examination of bipartite graphs would not have been possible. Experiments using gene expression data indicate that our new approach can be as much as two orders of magnitude faster than the best previous alternatives.

Genetic Analysis. We have applied our methods to microarray data collected from the spleens of six strains of mice exposed *in vivo* to low dose IR (10 cGy of X-rays). We have also devised powerful new forms of differential analysis, with which we identify sets of genes whose interactions (correlations) appear to be differentially impacted by radiation exposure [6]. We have compiled several examples of multiple gene interactions that are altered by radiation exposure and thus represent potential molecular pathways that mediate the radiation response. We are now expanding our work to incorporate both genotypic and physiological data,

permitting us to extract coexpression networks that are linked to the overlying radiation adaptation and to identify network nodes that are potential points of genetic variation.

Future Plans

Low Dose Studies. We aim to continue the development of our tools using data sets that focus on the *in vivo* biological response to exposure to low doses of IR. Accumulating evidence suggests that the genes and pathways altered by lower doses are not merely a subset of those altered by higher doses [7]. Therefore low dose IR may exert its own unique set of cellular responses. Initially we will focus on microarray data from tissues of mice exposed to an acute low dose of IR. These exposures are part of an ongoing DOE-funded project designed to determine the extent to which varying genetic backgrounds alter the response to IR as defined by gene expression profiles. We are harvesting tissues from over 50 strains of BXD mice, and have already begun the initial analysis of spleen and skin tissues to identify differentially expressed genes, that is, genes with expression levels that increase or decrease in response to IR exposure. These data indicate that multiple pathways respond to IR. In spleen, for example, differentially expressed gene sets are enriched in genes involved in apoptosis, regulation of transcription, and many novel, uncharacterized genes. A significant percentage of the genes that are differentially expressed in at least one strain upon IR exposure encode products that mediate immunity, suggesting that low doses of IR may initiate an immune response.

MicroRNA Data Analysis. As a matter of course, we prioritize and confirm the results we attain with orthogonal metrics. For example, we typically sort any cliques our methods produce by the extent to which their elements share common ontological categorizations, *cis* regulatory elements (CREs), quantitative trait loci, literature citations and so forth. We plan to build out our toolchain to include data on microRNAs. These are short, single strands of RNA whose main function seems to be the down-regulation of gene expression. They appear to be more accurate to map than, say, CREs, but currently have far fewer useful extraction and matching tools. We plan to automate the process for their use in our work on the biological impact of low dose IR.

References

1. Committee to Assess Health Risks from Exposure to Low Levels of Ionizing Radiation, N.R.C., *Health Risks from Exposure to Low Levels of Ionizing Radiation: BEIR VII Phase 2*. 2005, National Academies Press: Washington, DC.
2. DOE. *Low Dose Radiation Research Program - Molecular Mechanisms and Pathways*. Office of Science Notice DE-FG01-04ER04-21 2004 [cited; Available from: http://www.science.doe.gov/grants/FAPN04-21.html.
3. Borate, B.R., *A Comparative Analysis of Microarray Thesholding Methods*, in *M.S. Thesis, Genomics Science and Technology Program*. 2008, University of Tennessee.
4. Chesler, E.J. and M.A. Langston. *Combinatorial genetic regulatory network analysis tools for high throughput transcriptomic data*. in *Proceedings, RECOMB Satellite Workshop on Systems Biology and Regulatory Genomics*. 2005. San Diego.
5. Zhang, Y., E.J. Chesler, and M.A. Langston. *On Finding Bicliques in Bipartite Graphs: a Novel Algorithm with Application to the Integration of Diverse Biological Data Types*. in *Proceedings, Hawai'i International Conference on System Sciences*. 2008. Big Island, HI.
6. Voy, B.H., et al., *Extracting gene networks for low dose radiation using graph theoretical algorithms.* PLoS Computational Biology, 2006. **2**(7): p. e89.
7. Yin, E., et al., *Gene expression changes in mouse brain after exposure to low-dose ionizing radiation.* Int J Radiat Biol 2003. **70**(10): p. 759-775.

Recent DOE Sponsored Publications

- Abu-Khzam, F.N. and M.A. Langston, *Linear-Time Algorithms for Planar Graphs of Fixed Disk Dimension.* Information Processing Letters, 2007. **101**: p. 36-40.
- Abu-Khzam, F.N., et al., *Crown Structures for Vertex Cover Kernelization.* Theory of Computing Systems, 2007. **41**: p. 411-430.
- Bodlaender, H.L., et al. *Quadratic Kernelization for Convex Recoloring of Trees*. in *Proceedings, International Conference on Computing and Combinatorics*. 2007. Banff, Alberta, Canada.
- Borate, B.R., *A Comparative Analysis of Microarray Thesholding Methods*, in *M.S. Thesis, Genomics Science and Technology Program*. 2008, University of Tennessee.
- Chesler, E.J. and M.A. Langston. *Combinatorial genetic regulatory network analysis tools for high throughput transcriptomic data*. in *Proceedings, RECOMB Satellite Workshop on Systems Biology and Regulatory Genomics*. 2005. San Diego.
- Cotta, C., M.A. Langston, and P. Moscato, *Combinatorial and Algorithmic Issues for Microarray Analysis*, in *Approximation Algorithms and Metaheuristics*, T.F. Gonzales, Editor. 2007, Taylor & Francis, 74.1--74.14.
- Dehne, F., et al., *An O*(2O(k)) FPT Algorithm for the Undirected Feedback Vertex Set Problem.* Theory of Computing Systems, 2007. **41**: p. 479-492.
- Downey, R.G., M.R. Fellows, and M.A. Langston, *Parameterized Complexity, An Introduction to the Special Issue.* The Computer Journal, 2008. **51**: p. 1-6.
- Eblen, J.D., et al., *Graph Algorithms for Integrated Biological Analysis, with Applications to Type 1 Diabetes Data*, in *Clustering Challenges in Biological Networks*, W.A. Chaovalitwongse, Editor. 2008, World Scientific.
- Fellows, M.R., et al. *Efficient Parameterized Preprocessing for Cluster Editing*. in *Proceedings, International Symposium on Fundamentals of Computation Theory*. 2007. Budapest, Hungary.
- Gatti, D., et al., *Genome-level analysis of genetic regulation of liver gene expression networks.* Hepatology, 2007. **46**: p. 548-557.
- Langston, M.A. *Algorithmic Challenges for Systems-Level Correlational Analysis: A Tale of Two Datasets (A Plenary Lecture).* in *Proceedings, International Workshop on Algorithms and Data Structures*. 2007. Halifax, Nova Scotia, Canada.
- Langston, M.A., et al., *Innovative Computational Methods for Transcriptomic Data Analysis: A Case Study in the Use of FPT for Practical Algorithm Design and Implementation.* The Computer Journal, 2008. **51**: p. 26-38.
- Saxton, A.M., M.A. Langston, and B.H. Voy, *Tools are Needed for Microarray Expression and Co-Expression*, in *Prediction with Regression: A Comparison of Methods*, R.J. Freund, Editor. 2007, American Statistical Association. p. 4381-4386.
- Song, M., et al. *Inferring transcriptional regulation through logical networks from temporal mouse brain gene expression data*. in *Proceedings, Foundations of Systems Biology in Engineering (FOSBE)*. 2007. Stuttgart, Germany.
- Voy, B.H., et al., *Extracting gene networks for low dose radiation using graph theoretical algorithms.* PLoS Computational Biology, 2006. **2**(7): p. e89.
- Zhang, Y., E.J. Chesler, and M.A. Langston. *On Finding Bicliques in Bipartite Graphs: a Novel Algorithm with Application to the Integration of Diverse Biological Data Types*. in *Proceedings, Hawai'i International Conference on System Sciences*. 2008. Big Island, HI.

Direct Utilization of Coal Syngas in High Temperature Fuel Cells

Prof. Ismail Celik
Mechanical and Aerospace Engineering Department
West Virginia University, PO Box 6106, Morgantown, WV, 26505
Phone: (304) 293-3111 x 2325; Fax: (304) 293-6689 E-mail: ismail.celik@mail.wvu.edu

DOE Project Manager: Tim Fitzsimmons
Phone: (301) 903-9830 E-mail: tim.fitzsimmons@science.doe.gov

Objectives

- Characterize the effects of major trace contaminants in coal syngas on solid oxide fuel cell performance.
- Identify the fundamental mechanisms through which these impurities affect performance.
- Develop novel materials to minimize impact of contaminants.
- Propose remedies for adverse effects of contaminants on fuel cell performance.

Accomplishments

- Built or extended research infrastructure: 5 labs and the CFD lab
- Developed in-house capability for SOFC fabrication
- Developed computational and experimental techniques for analysis of SOFCs
- Performed experiments and simulations with H_2S and PH_3 containing coal syngas
- Disseminated results via presentations and publications
- Organized a mini symposium on coal based fuel cell technology
- Trained Post Doctoral fellows, graduate and undergraduate students

Introduction

This project is supported under the DOE EPSCoR, a program designed to enhance the capabilities of EPSCoR states in energy research and economic development through the support of advanced research at academic institutions. Our vision is to establish an internationally recognized, sustainable fuel cell research center for coal-based clean power generation which serves as a technology resource for the emerging fuel cell industry in West Virginia. Our strengths are in applying nano-technology to develop and fabricate materials for advanced coal-based fuel cells; establishing a state-of-the-art material characterization and fuel cell testing laboratory; and modeling fuel cells from atomistic to continuum scales using high performance computing. We have formed a multidisciplinary team of research professionals who have worked together for several years and have strong credentials in their respective areas of expertise. Under the present project, we will develop a laboratory infrastructure, solidify interactive working relationships, and attain national recognition for the work conducted by the center in the area of coal-based clean power generation via fuel cells. Our project will be conducted in collaboration with the National Energy Technology Laboratory (NETL). This project is to be funded for a 3-year effort. The project effectively started in December 2006.

Approach

The research cluster is based on a multi-scale, multi-disciplinary approach conducted by nine faculty members in four departments at West Virginia University (WVU). The work is organized under four integrated projects: (1) anode material development and experimental characterization of fuel cell anodes, (2) sub-micro-scale modeling, (3) multi-scale continuum modeling, and (4) laboratory testing of individual fuel cells and fuel cell systems. The strength of the research cluster is in the integration of knowledge obtained from experiments (Projects 1 and 4) with multi-scale computational models (Projects 2 and 3). At all stages, information, predictions, and data will be exchanged between researchers in the projects.

At the end of three years, we anticipate four outcomes. First, we will have identified the fundamental processes characterizing the operation of SOFC anodes in the presence of coal syngas from the atomic level to the level of the operating fuel cell. Second, strategies will be developed to enable SOFCs exhibit stable operation with coal syngas. Third, the research infrastructure (equipment for analysis and for cell fabrication, computers for modeling) and collaborations across disciplines and departments at WVU will be well developed for future research on fuel cells. Fourth, a program of educating and training future energy researchers will be established.

Results

Anode Materials Development and Characterization

This research task seeks to characterize the behavior of SOFC anodes exposed to simulated coal syngas using a combination of in-situ and ex-situ experimental methods including EIS (Electrochemical Impedance Spectroscopy) and ASR (Area Specific Resistance) measurements under operating conditions, to fabricate fuel cells with custom anodes; and to systematically explore several anode compositions and double-layered structure.

An optical setup, based on phase-shift Sagnac Interferometry method, is applied to obtain out of plane deformation of a button cell exposed to coal syngas with and without impurities whereby EIS, ASR and IR (Infra Red) measurements can be performed simultaneously. Measured interferometric fringe patterns at room temperature (Fig. 1) are in good agreement with the FEA results, with an error of less than 5%. Similar results are obtained for high temperature measurement at 800 ^{o}C. The results from these simulations will be used to validate the models developed under Project 3.

Electrochemical and microstructural analyses are performed on the half cell made of Ni-YSZ cermet operated in the simulated coal-derived syngas containing 30.6% H_2, 30% CO, 11.8% CO_2, 27.6% H_2O and 20 ppm PH_3. Both the charge transfer resistance and the diffusion resistance increase with time (see Fig 2a) which suggests that the incorporation of phosphorus impurity into the electrode not only impedes the charge transfer but also blocks the channels of gas diffusion. Figure 2b shows a linear tail at low frequencies, implying that the impedance is dominated by the diffusion control of the reactant gases.

X-ray diffraction (XRD) and X-ray photoelectron spectroscopy (XPS) (Fig.3) measurements have demonstrated that the incorporation of P into the electrode results in the formation of the secondary phases which causes the electrode to lose the electrocatalytic activity toward oxidation of the fuel gas and inhibits the ability of electrode to transport oxygen ions in the electrode.

Therefore, the charge transfer resistance increases with time during exposure to the PH_3-containing syngas.

Advanced anode-supported planar SOFC with >1W/cm^2 power density for direct utilization of coal syngas have been developed with industrially-robust and cost-effective fabrication methods. These cells perform as good as if not better than the cells that are available commercially, and are being tested in Project 4.

Novel sulfur-tolerant anode has been developed by impregnating doped ceria into the MSRI (Utah, U.S) NiO-YSZ anode supported cell. Sulfur-poisoning test in simulated syngas (30% H_2, 23%CO, 21%CO_2, 26%H_2O) with 20 ppm H_2S indicated the impregnated doped ceria component is able to enhance sulfur tolerance of anode supported cell by reacting chemically with H_2S to protect anode from sulfur poisoning at the incipient period.

Sub-Micro-Scale Modeling

Using an *ab-initio* tight-binding method, we modeled a number of contaminant species including H_2S, PH_3 and AsH_3, and simulated their adsorption process on Ni's (1,0,0) surface. In all cases, the contaminant species are found to be chemically bonded to the Ni surface after molecular decomposition. In contrast, when the same species are placed near the Cu's (1,0,0) surface, only physical adsorption occurs. We also analyzed and compared the electronic structures and chemical bonding properties of Ni and Cu surfaces to search for electronic states that are responsible for the different contaminant effects.

A molecular dynamics code, ReMoDy, was developed for computing reactive gas mixtures, including catalytic reactions at active surfaces based on the Collision Theory. This is a probabilistic approach and needs input from ab-initio simulations. To be able to trace the motion and interactions of millions of molecules efficiently, a domain segmentation algorithm was implemented, which enabled to reduce the time of processing interactions from N^2 to a near-linear dependence. The code was implemented in C++ programming language. Simulation inside one micron pore under atmospheric conditions performed on a 2.66 GHz CPU, 4GB RAM workstation took about one week. The program enables simulations involving up to 10^6 molecules per each Gigabyte of RAM.

Multi-Scale Continuum Modeling

Several sub models are developed including multi-component mass transfer, electrochemistry with simultaneous oxidation of hydrogen and carbon monoxide, bulk reaction chemistry and surface reaction chemistry. Two gas phase mechanisms were investigated for Water Gas Shift (WGS) and Methane Steam Reforming (MSR): (i) A two reaction model developed for catalytic methane reforming and (ii) an Augmented Reduced Mechanism (ARM 9) originally developed for combustion. In addition, a detailed surface mechanism with 42 reactions and 18 species was implemented using an open source chemical kinetics code CANTERA. Calculated surface coverage of Ni agrees well with similar results in the literature.

The button cell was simulated in parallel to the experiments (Project 4) with simulated coal syngas. The comparison between the VI curves obtained from the simulations and the experiments (Fig. 4) shows a good agreement between the two. The diffusion limitation of the cell could be predicted upon modifying the diffusion coefficients using a newly proposed correction on the effective diffusivity as a function of local current (Fig. 4).

We have identified several degradation mechanisms such as thermal stresses, thermal aging, redox cycle, and coal syngas impurities that may damage SOFC anode structural properties during long-term operation and reduce its strength and useful life. To predict long-term anode structural behavior, we are developing a continuum damage model and implementing it in the Finite Element Analysis (FEA) package ABAQUS™ .

Cell and System Laboratory Testing

The Solartron potentiostat was used to acquire open circuit voltages, polarization curves, cyclic voltammograms with and without current interrupt, and impedance spectra. Long term tests have been conducted for the MSRI and the WVU cells manufactured under Project 1.

Very stable operation is observed over 450 hours with a MSRI cell running on hydrogen fuel. MSRI cell is also operated with a syngas mixture with and without phosphine impurities. Stable operation in the clean syngas mixture is evident for 230 hours however, irreversible cell voltage degradation with time was observed after addition of 10ppm PH_3 (Fig.5a). From impedance characterization it was observed that series and polarization resistances increase after addition of the phosphine impurity (Fig.5b). Prototype SOFCs made at WVU have also been tested and maximum power density of 1.15 W/cm^2 was obtained at 800^oC which is higher than that of the commercial MSRI cell at the same temperature.

A variety of observations based on in-situ electrochemical experiments point to a lack of understanding of basic SOFC performance, a need for improving the experimental protocol, and a need for developing non-electrochemical in-situ probes. In tests run in Project 4, ex-situ analyses (SEM with EDX, Raman spectroscopy) have not clearly identified phosphorus-containing species after prolonged exposure to phosphine gas.

Future Work

- The test SOFC button cell will be subjected to simulated coal syngas with and without impurities (As and P). Out of plane surface deformations will be measured at specified time intervals each with a series of increasing applied pressure. The Infrared temperature measurement technique will be further refined in order to get a precise measurement on the small spot location of the button cell surface during SOFC testing at 800^oC.
- The effect of Phosphorous (P) on the performance of SOFC anode will be investigated further with different P concentrations and operating temperatures. Similar analysis will be extended to Arsenic.
- Atomistic and molecular dynamics simulations will be continued to investigate adsorption and charge transfer mechanisms for impurities other than H_2S, PH_3 and AsH_3 and nobel metals and recommendations will be made with regards to potential materials to reduce degradation rates.
- Equilibrium calculations will also be performed using CANTERA to estimate the most significant forms (or species) of impurities found under stable conditions. Both kinetic and equilibrium calculations will be performed in tandem with the cell testing under project 4 to obtain maximum benefit from computations and experiments.
- Long term tests of commercial SOFCs and SOFCs manufactured in-house with exposure to selected impurities (phosphine, arsine) will continue. More sensitive post-mortem surface analyses and non-electrochemical in-situ probes for SOFCs will be developed. Ni migration behavior will be investigated in the Ni-YSZ anode resulting from direct exposure to syngas and syngas with impurities.

FY 2008 Publications/Presentations

1. M. Zhi, X. Chen, H. Finklea, I. Celik, N.Q. Wu, Electrochemical and microstructural analysis of Ni-yttria stabilized zirconia electrode operated in phosphorus-containing syngas, J. Power Sources, DOI information: 10.1016/j.jpowsour.2008.05.055, published online (http://dx.doi.org/10.1016/j.jpowsour.2008.05.055)
2. M. Gong, X. Liu, J. Trembly, C. Johnson: Sulfur-Tolerant Anode Materials for Solid Oxide Fuel Cell Application, Accepted by Journal of Power Sources (2007), 168: 289-298
3. Cayan F.N., Zhi M., Pakalapati S.R., Celik I., Wu N., Gemmen R., Effects of Coal Syngas Impurities on Anodes of Solid Oxide Fuel Cells: A Review, Accepted by Journal of Power Sources, 2008 (POWER-D-08-00834)
4. Cayan F.N., Pakalapati S.R., Celik I., Modeling of Diffusion Inside the Porous Electrodes, Proceedings of the Second European Fuel Cell Technology and Applications Conference EFC2007, Rome, December 11-14, 2007
5. Cayan F.N., Pakalapati S.R., Elizalde-Blancas F., Celik I., On Modeling Multi-Component Diffusion Inside the Porous Anode of Solid Oxide Fuel Cells Using Fick's Model, Submitted to FuelCell2008 6th International Fuel Cell Science, Engineering and Technology Conference, Denver, CO June 16-18, 2008
6. Cayan F.N., Zhi M., Pakalapati S.R., Celik I., Wu N., Gemmen R., Effects of Coal Syngas Contaminants on SOFC Anodes: A Review, Submitted to 2008 Pittsburgh Coal Conference, Sept. 28-Oct. 2, 2008
7. Elizalde-Blancas F., Pakalapati S. R., Escobar-Vargas J., Celik I. B., Numerical Evaluation and Comparison of Different Reduced Mechanisms for Predicting the Performance of a SOFC Operating on Coal Syngas, Submitted to the ASME Fluids Engineering Division Summer Conference, Jacksonville, Florida, August 10-14, 2008
8. Gong M., Liu X., Gemmen R., Improving sulfur-tolerance of Ni-YSZ anode in SOFC by impregnation of doped ceria. 213th Electrochemical Society Meeting (2008)(abstract accepted)
9. Gong M., Liu X., Jiang Y., Xu C., Zondlo J., Johnson C., Gemmen R., Anode supported SOFC fabricated by tape casting and co-sintering of anode and electrolyte. Materials Science & Technology 2008 Conference (abstract accepted)
10. Zhi M., Madhiri N., Finklea H., Celik I., Kang B., Liu X., Bajura R., Wu N. Q., Impedance Analysis of Phosphorous Impurity Effect on Performance of Ni-YSZ Anode of SOFC, Accepted by Electrochemistry Society Transactions, 2007
11. Zhi M., Wu N. Q., Degradation of Ni-YSZ anode in phosphorous-containing coal syngas, Army Research Office Workshop on soldier-portable power sources, College Park, MD, Feb.20-21, 2008 (poster)
12. Demircan O., Finklea H. O., Zondlo J., Xu C., The effect of PH3 impurity in coal syngas on SOFC Performance, Submitted to 2008 International Pittsburgh Coal Conference, Sept. 28-Oct. 2, 2008

Figure Captions

Figure 1. Fringe patterns on Ni mesh measured using Sagnac Interferometer Integrated with PROBOSTAT™ SOFC Test System at r = 3 mm with different applied pressures(a) 0 psi, (b) 5 psi, (c) 7 psi, (d) 9 psi, (e) 11 psi and (f) 13 psi

Figure 2. Nyquist plot of impedance obtained from the half cell at 900°C. (a) unloaded cell (b) loaded cell

Figure 3. Survey scan of the XPS spectra obtained from the Ni-YSZ working electrode under different conditions; (i) the electrode after exposure to the clean syngas (clean cell), (ii) the electrode after exposure to the PH_3-containing syngas at the open circuit (open circuit cell), and (iii) the electrode after exposure to the PH_3-containing syngas at the applied DC bias of 0.7 V (loaded cell)

Figure 4. a) Comparison of the VI curves obtained from numerical simulations with that obtained from experiments. (b) Maximum error in concentration over the whole domain in Fick's model predictions plotted as a function of cell current density for cases with and without the proposed correction.

Figure 5. Results from Long Term tests on MSRI cell at T=800°C (a) exposed to syngas before/after adding 10ppm PH_3, J =0.5A/cm^2 (b) normalized impedance data before/after adding 10ppm PH_3

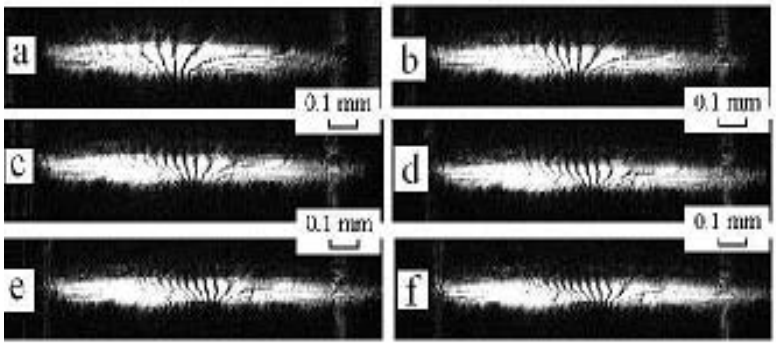

Figure 1

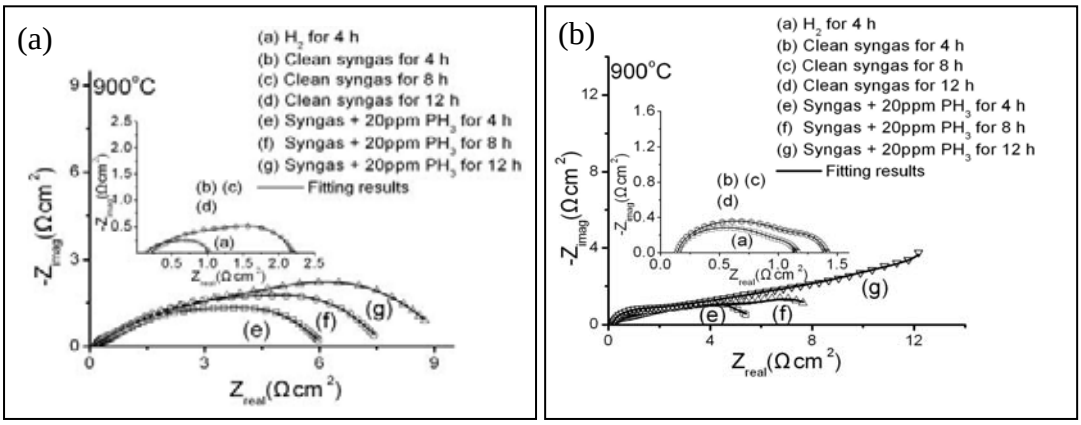

Figure 2

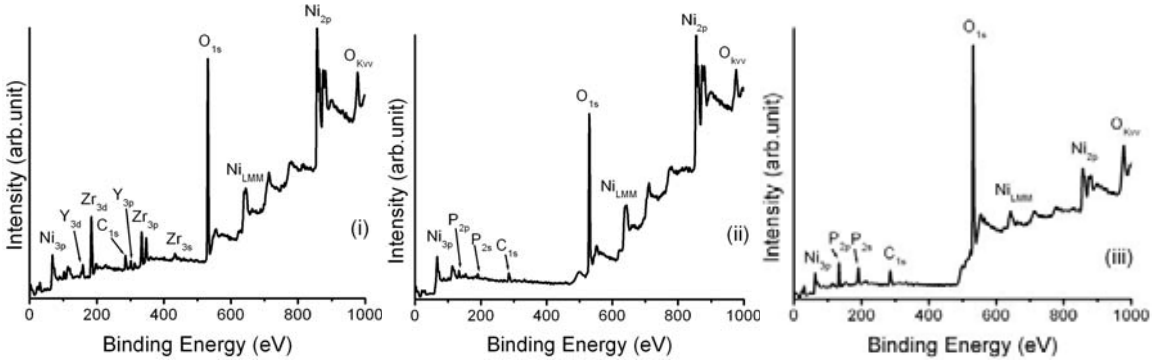

Figure 3

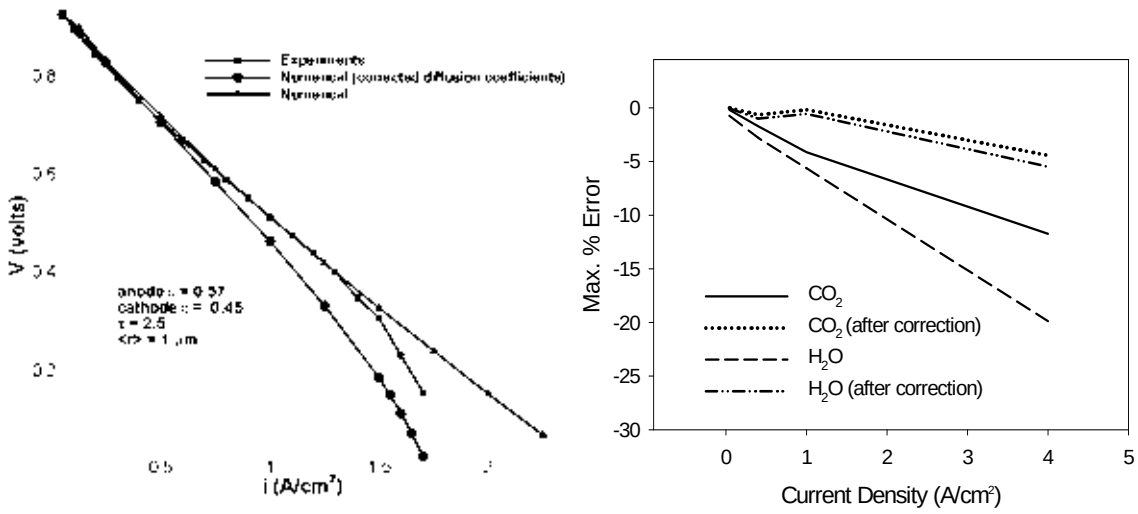

(a) **(b)**

Figure 4

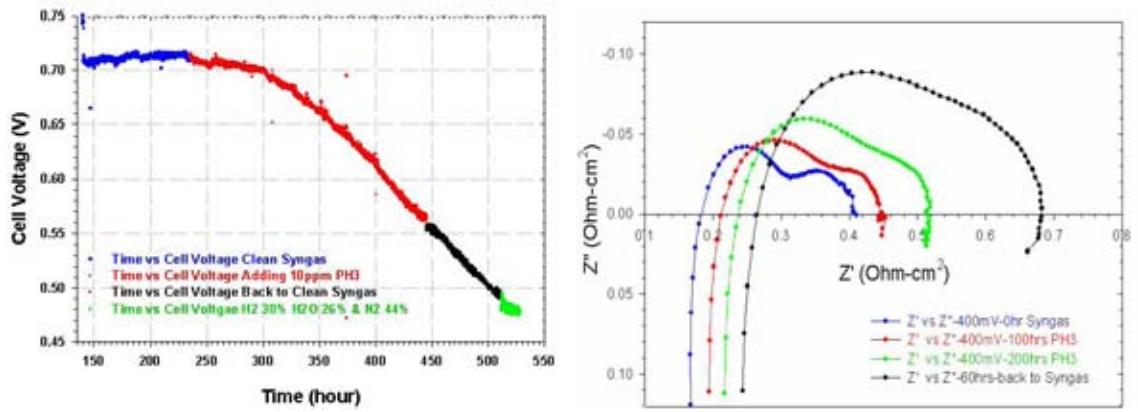

(a) **(b)**

Figure 5

Land Reclamation for Bioenergy: Genomics of Adaptation of *Populus* to Marginal Sites

Stephen P. DiFazio (PI)[1], Danielle Ellis[1], Jonathan R. Cumming[1], Brahma Reddy Induri[1], Dhiraj Naik[1], Gancho T. Slavov[1], and Timothy J. Tschaplinski[2]

[1] Department of Biology, West Virginia University, Morgantown, WV 26506

[2] Environmental Sciences Division, Oak Ridge National Laboratory, Oak Ridge, TN 97331

I.) Program Scope

Biofuels production and carbon sequestration in the U.S. can be substantially increased by enhancing plant stress tolerance, thus enabling cultivation of currently marginal lands. A major factor limiting plant growth is high soil conductivity, primarily driven by salinity, which affects more than 387 million hectares worldwide. Post-reclamation surface mines provide one striking example, occupying an estimated 1 million ha in the eastern United States. Conversion of these sites to forest would greatly enhance their productivity and C sequestration potential. For example, in West Virginia alone, reforestation of surface mines established since 1992 would result in at least 1 Tg of C sequestration per year, the highest total of any state by far. However, it has been estimated that 85-90% of previously forested surface mine sites in West Virginia have been converted to grassland or sparsely vegetated scrubland. We propose to substantially enhance salinity tolerance of *Populus* trees in order to enhance establishment, survival, and growth of these trees on such marginal sites.

Our overall research goals are (1) elucidate the molecular bases of salinity tolerance in *Populus* trees and (2) develop *Populus* genotypes that can be used for economically feasible production of biofuels on marginal lands like surface mine sites in the southeastern U.S. and arid lands of the western U.S. Our specific objectives are to:

Objective 1: Identify genomic loci associated with *Populus* salinity tolerance.

Objective 2: Determine metabolite and whole genome gene expression profiles for trees with contrasting salinity tolerance.

Objective 3: Develop a comprehensive list of candidate genes for salinity tolerance in *Populus*.

Objective 4: Functionally characterize the most promising candidate genes using transgenic *Arabidopsis*.

To accomplish these goals we will use a combination of hypothesis-driven candidate gene testing and *de novo* gene discovery using genomics, metabolomics, and quantitative genetics tools. Our research will leverage the recently-completed *Populus* genome sequence and interface with a newly-created Bioenergy Science Center at Oak Ridge National Laboratory. Our project will directly contribute toward the expansion of *Populus* cultivation to currently barren lands, thereby substantially increasing the biofuels production and carbon sequestration potential of the United States.

Hydrogen Absorption in Pd-based Nanostructures

David Lederman
Department of Physics, West Virginia University, Morgantown, WV 26506-6315
David.Lederman@mail.wvu.edu

Program Scope

Hydrogen-metal systems have motivated numerous studies over the years due to their direct technological applications which include fuel cell technology and hydrogen gas purification and their need for highly sensitive and compact hydrogen gas sensors. In particular Pd based compounds have received a lot of interest due to Pd's capability of absorbing 900 times its volume of hydrogen under specific conditions of pressure and temperature, inducing dramatic and in most cases reversible changes in its physical and structural properties. When Pd is exposed to a hydrogen gas atmosphere, molecular hydrogen (H_2) is chemisorbed on the Pd surface where it dissociates into two H atoms (dissociative chemisorption).[1] After donating its electron to Pd, the atomic H diffuses into the Pd lattice as a proton.[2,3] At low hydrogen pressures the α phase of PdH_x is formed where the H atoms occupy interstitial sites in the *fcc* Pd lattice. The H atoms are widely believed to reside in octahedral sites, although calculations[4] have shown that tetrahedral sites may also be a favourable location. Further H absorption in Pd causes an expansion of the lattice, characteristic of the hydride phase (β) with the resulting change in the lattice constant being around 3.3%.[5,6]

Magnetic properties are also influenced by the insertion of hydrogen. In bulk FePd alloys the magnetic moment weakens upon hydrogen absorption[7] whereas an increase has been reported in the case of Fe/V multilayers.[8] These changes could be due to purely electronic effects (i.e., addition of electrons to the electronic energy bands due to the absorption) or due to structural changes that in turn cause electronic changes. F. Klose and co-workers have shown, via magnetization and neutron reflectivity measurements, that hydrogen absorption in Fe/Nb multilayers causes the coupling between Fe layers to switch between ferromagnetic and antiferromagnetic configurations.[9] The authors of the study attributed this effect to a change in the effective Fermi wavevector of the Nb layers, which in turn causes a change in the sign of the electronic RKKY interaction responsible for coupling between Nb layers. Nevertheless, a close examination of the data indicates that an expansion of the lattice along the growth direction occurs upon hydrogen absorption (the neutron scattering peaks move to smaller angles), indicating that perhaps the effect is due to structural changes, rather than a purely electronic effect. Indeed, significant structural changes induced by hydrogen absorption have been observed via neutron and x-ray scattering in Fe/Nb and W/Nb multilayers,[10] as well as in Nb/Pd multilayers via x-ray diffraction.[11]

Regarding the magnetic properties of Pd-based films, there is evidence that the magnetic properties of nominally magnetic transition metals (i.e., Ni , Co, Fe) are influenced by hydrogen absorption. For example, the local magnetic properties of Ni atoms in amorphous NiMg alloy films are strongly influenced by hydrogen absorption, as determined by x-ray magnetic circular dichroism (XMCD), which measures the density of states of unoccupied *d*-electron states at the Fermi level.[12] In bilayer films (ferromagnetic materials with Pd overlayers), however, the evidence for enhanced magnetization remains elusive. The PI and collaborators, for example, have demonstrated that in 4.0 nm thick Co films with 5.3 nm thick Pd overlayers there are significant changes in the optical index of refraction, but mostly due to the hydrogen absorption

in the Pd overlayer. In particular, no evidence was found for changes in the magnetization characteristics (absolute magnetization or coercivity) upon hydrogen loading.[13] In thinner structures, however, magnetization changes have been detected.

Some research has also been performed on complex oxides, particularly due to their possible applications in fuel cell technology where the oxide serves as the electrolyte.[14] Nevertheless, relatively little work has been performed on ferroelectric or magnetic oxide thin films that exploits the magnetic or ferroelectric properties of these materials. An example of research in this area includes the study of $Pd/Ba_xSr_{1-x}TiO_3/Pt$ heterostructures for hydrogen gas detection, where the conductivity characteristics change significantly upon hydrogen absorption.[15] In this case, the BST films were amorphous. Another example is the piezoelectric langasite family of crystals, where surface and bulk acoustic wave characteristics can be modified by the hydrogen absorption in a Pd overlayer.[16] Ceramic-metal composites, composed of oxide ceramics and palladium metals, have also been studied for hydrogen separation applications.[17]

Recent Progress

N/A (started 07/01/2008)

Future Plans

This project will investigate the effects of hydrogen absorption on the magnetoelectronic properties of Pd-based nanostructures, including magnetic nanodots and ferroelectric and multiferroic complex oxide thin films. Electronic changes will be monitored by performing magnetization, magnetoresistance, and magnetoelectric measurements as a function of hydrogen absorption and temperature by the PI at West Virginia University. Neutron scattering measurements, performed in collaboration with Dr. Michael Fitzsimmons at the Los Alamos Neutron Science Center (LANSCE), will reveal the extent of the hydrogen and deuterium penetration via neutron reflectivity measurements. Changes in the depth profile of the magnetic properties as a result of hydrogen absorption, complementary to the magnetic measurements performed at WVU, will be measured at LANSCE using polarized neutron scattering. The samples' structure (crystallinity, interface disorder, and defect density) will be thoroughly assessed in order to separate the intrinsic (i.e., those resulting from the properties of the materials and their interfaces) from the extrinsic (i.e., those resulting from defects) effects.

References

[1] W. Auer and H. J. Grabke, "The kinetics of hydrogen adsorption in palladium (α- and β-phase) and palladium-silver-alloys", *Ber. Bunsenges.* **78**, 58 (1974).

[2] C. Gabrielli, P. P. Grand, A. Lasia, and H. Perrot, "Investigation of hydrogen adsorption-absorption into thin palladium films I. theory", *J. Electrochem. Soc.* **151**, A1925 (2004).

[3] A.L. Cabrera, E. Morales, and J. N. Armor, "Kinetics of hydrogen desorption from palladium and ruthenium-palladium foils", *J. Mater. Res.* **10**, 779 (1995).

[4] R. Caputo and A. Alavi, "Where do the H atoms reside in PdH_x systems?", *Mol. Phys.* **101**, 1781 (2003).

[5] R.J. Wolf, M. W. Lee, R. C. Davis, P. J. Fay, and J. R. Ray, "Pressure-composition isotherms for palladium hydride", *Phys. Rev. B* **48**, 12415 (1993).

[6] R. Feenstra, R. Griessen, and D. G. de Groot, "Hydrogen induced lattice expansion and effective H-H interaction in single phase PdH_c", *J.Phys. F: (Met. Phys.)* **16**, 1933 (1986).

[7] J. A. Mydosh, "From giant moment to Kondo and spin glass behaviour: the electrical resistivity of PdFe and (PdFe)H", *Phys. Rev. Lett.* **33**, 1562 (1974).
[8] D. Labergerie, K. Westerholt, H. Zabel, and B. Hjörvarsson, "Hydrogen induced change of the atomic magnetic moments in Fe/V-superlattices", *J. Magn. Magn. Mat.* **225**, 373 (2001).
[9] F. Klose, Ch. Rehm, D. Nagengast, H. Maletta, and A. Weidinger, "Continuous and reversible change of the magnetic coupling in an Fe/Nb multilayer induced by hydrogen charging", *Phys. Rev. Lett.* **78**, 1150 (1997).
[10] Ch. Rehm, H. Maletta, M. Fieber-Erdmann, E. Holub-Krappe, and F. Klose, "Anomalous layer expansion in thin niobium films during hydrogen absorption", *Phys. Rev. B* **65**, 113404 (2002).
[11] Q. M. Yang, G. Schmitz, S. Fähler, H. U. Krebs, and R. Kirchheim, "Hydrogen in Pd/Nb multilayers", *Phys. Rev. B* **54**, 9131 (1996).
[12] B. Farangis, P. Nachimuthu, T. J. Richardson, J. L. Slack, R. C. C. Perera, E. M. Gullikson, D. W. Lindle, and M. Rubin, "In situ x-ray-absorption spectroscopy study of hydrogen absorption by nickel-magnesium thin films", *Phys. Rev. B* **67**, 085106 (2003).
[13] D. Lederman, Y. Wang, E. H. Morales, R. J. Matelon, G. B. Cabrera, U. G. Volkmann, and A. L. Cabrera, "Magnetooptic properties of Fe/Pd and Co/Pd bilayers under hydrogen absorption", *Appl. Phys. Lett.* **85**, 615 (2004).
[14] N. Sakai, T. Horita, K. Yamaji, M. E. Brito, H. Yokokawa, A. Kawakami, S. Matsuoka, N. Watanabe, and A. Ueno, "Interface Stability Among Solid Oxide Fuel Cell Materials and Perovskite Structures", *J. Electrochem. Soc.* **153**, A621 (2006).
[15] J. Deng, O. Kiang Tan, W. Zhu, X. Chen, and Xi Yao, "Investigation of Influence of Hydrogen Gas on Pd/BST/Pt Device by Impedance Spectroscopy", *IEEE Transactions of Ultrasonics, Ferroelectrics, and Frequency Control* **51**, 923 (2004).
[16] J. A. Thiele and M. Pereira da Cunha, "Dual Configuration High Temperature Hydrogen Sensor on LGS SAW Devices", *2004 IEEE International Ultrasonics, Ferroelectrics, and Frequency Control Joint 50th Anniversary Conference Proceedings*, p. 809 (2004).
[17] R. V. Siriwardane, J. A. Poston Jr., E. P. fisher, T. H. Lee, S. E. Dorris, and U. Balachandran, "Characterization of ceramic-metal composite hydrogen separation membranes consisting of barium oxide, cerium, oxide, yttrium oxide, and palladium", *Appl. Surf. Science* **217**, 43 (2003).

New Catalysts for Ionic Hydrogenations

Dean M. Roddick[a], R. Morris Bullock[b]
a) University of Wyoming, Chemistry Dept. Laramie, WY
b) Pacific Northwest National Lab, Chemical and Material Sciences Div. Richland, WA

Program scope

Ionic hydrogenation catalysis offers a promising route to efficient and selective organic transformations which are difficult to achieve by conventional methods. Mechanistic studies[1,2] have shown that these metal dihydride catalysts operate through sequential transfer of H^+ and H^- to substrate, followed by regeneration with H_2 (Scheme 1). This project utilizes perfluoroalkyl phosphine ligands[3] to support a variety of metal dihydride complexes. The steric bulk of these ligands is expected to promote catalysis by encouraging dissociation of adducts at the metal center. The electron-withdrawing capacity of these ligands should increase the acidity of the dihydride complexes, promoting the initial proton transfer step, which is thermodynamically unfavorable for previously studied alkyl phosphine complexes.[1] The specific goals of this project include synthesizing and characterizing a variety of isolable dihydride cation complexes with perfluoroalkylphosphine ligands, determining solvent systems compatible with these complexes, determining the scope of substrates which can be hydrogenated, and studying the kinetics and thermodynamics of key reaction steps. Potential substrates which could be hydrogenated in such systems include aromatics, heteroaromatics, and fluoroalkenes. Understanding these systems will aid in the development of improved catalysts for reactions of significant interest to the Department of Energy, including hydrodesulfurization, hydrodenitrogenation, and hydrofluorocarbon synthesis.

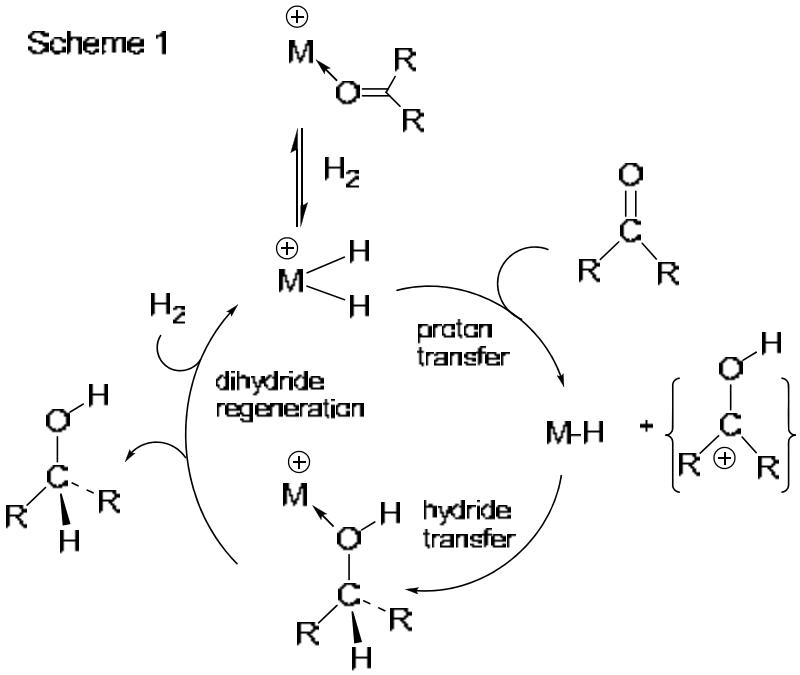

Recent Progress

Earlier studies have clearly shown that perfluoroaklylphosphine ligands greatly enhance the acidity of metal centers compared to their alkylphosphine congeners. $[CpRu(dfepe)(\eta^2\text{-}H_2)]^+OTf$ (dfepe = $(C_2F_5)_2PCH_2CH_2P(C_2F_5)_2)^4$ has proven difficult to study due to a propensity for H_2 loss and coordination of the counterion. Efforts to develop more tractable metal complexes have focused on using weakly coordinating counterions, such as $B(C_6F_5)_4^-$ and $[CB_{11}H_6Br_6]^-$. These complexes have now been synthesized in small quantities, along with the less acidic analog $[(MeC_5H_4)Ru(dfepe)(\eta^2\text{-}H_2)]^+$ which is less reactive and easier to isolate. These cationic dihydride complexes are capable of proton transfer o substrates such as acetone (as in Scheme 1) but do not appear to be active toward the hydride transfer reaction.

Previous work under this grant explored the synthesis and reactivity of Mo complexes including $[CpMo(dfppe)H_2]^+$ and $[CpMo(dfmppe)H_2]^+$ (dfppe = $(C_6F_5)_2PCH_2CH_2P(C_6F_5)_2$), dmppe = $(3,5\text{-}(CF_3)_2C_6H_3)_2PCH_2CH_2P(3,5\text{-}(CF_3)_2C_6H_3)_2$). These species were not efficient ionic hydrogenation catalysts for ketone substrates. More strongly electron withdrawing phosphine ligands such as dfepe have proven difficult to access in high yield.

Future Plans

In addition to continuing fundamental studies and exploring the ionic hydrogenation capabilities of the systems described above, we have recently synthesized perfluoroalkyl versions of the well known PCP pincher ligand. Pincher complexes are well known dehydrogenation catalysts.[5] Ir and Pt complexes of CF_3-PCP have been prepared, and these strongly electrophilic metal centers may prove useful in ionic hydrogenation. Preliminary attempts to synthesize a Pt- dihyride cation have so far resulted in formation of a hydride-bridged cationic dimer (shown below). This compound may prove a useful catalyst precursor, and future work will explore it's reactivity in the presence of substrate under an H_2 atmosphere.

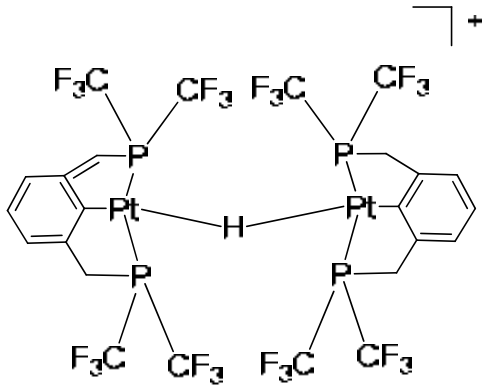

References

[1] Bullock, R. M.; Voges, M. H. *J. Am. Chem. Soc.* **2000**, *122*, 12594.

[2] Voges, M. H.; Bullock, R. M. *J. Chem. Soc. Dalton Trans.* **2002**, 759.

[3] Ernst, M. E.; Roddick, D. M. *Inorg. Chem.* **1989**, *28*, 1624-1627.

[4] Ontko, A. C.; Houlis, J. F.; Schnabel, R. C.; Roddick, D. M.; Fong, T. P.; Lough, A. J.; Morris, R. H. *Organomet.* **1998**, *17*, 5467-5476.

[5] A. Ray, K. Zhu, Y. V. Kissin, A. E. Cherian, G. W. Coates and A. S. Goldman *Chem. Commun.* **2005,** 3388-3390. – Get better ref from Jeramie

DOE Sponsored Publications in last 2 years

Jeffrey L. Butikofer, Thomas G. Parson, and Dean M. Roddick **Adduct Studies and Reactivity of *trans*-[$(C_2F_5)_2MeP]_2Pt(Me)X$ (X = O_2CCF_3, OTF, OSO_2F)** *Organometallics* **2006,** *25*, 6108-6114.

Jeong-Sup Song, Jennifer Look, Dean M Roddick, Morris Bullock **Perfluoroalkyl Phoshine Molybdenum Complexes: Relevance to Ionic Hydrogenation.** Manuscript in preparation .

Author Index

S. P. Ahrenkiel 100
A. Bhattacharjee 71
Jason Cassibry 17
Ismail Celik 115
Boris Chernomordik 34
Clara Deal 18
Stephen DiFazio 123
Stephen Ducharme 56
S. Dumpala 35
Sherry Faye 68
Jeffrey Fergus 9
Ryszard Jankowiak 30
Veerel Keppens 107
Travis W. Knight 96
Michael A. Langston 111
Patrick LeClair 13
David Lederman 8, 124
Aaron Lindenberg 1
Zhiqiang Mao 44
Praveen Meduri 36
Dongming Mei 103
John Mintmire 76
John J. Neumeier 52
Teri Odom 6
Amod Ogale 88
Hemant Pendse 7, 48
Chandrashekhar Pendyala 37
Dean M. Roddick 127
Rene Rodriguez 2
Wayne Seames 75
Neil Shafer-Ray 80
Gregory Snow 60
Valeria Stoleru 22
Michael Strauss 84
M. K. Sunkara 38
Jyothish Thangala 39
Terry M. Tritt 92
Ilya Vekhter 41
John Xiao 26
Jianting Zhu 64

Participant List

Sherine Abdelhak
University of Louisiana at Lafayette

Scott Ahrenkiel
South Dakota School of Mines and Technology

Jose Aldana
University of Arkansas

Rebecca Alway-Cooper
Clemson University, Chemical and Biomolecular Engineering Department

Richard Bajura
West Virginia University, National Research Center for Coal and Energy

Stephen Borleske
Delaware EPSCoR Office

James Brainard
National Renewable Energy Laboratory

Alysia Bridgman
South Carolina EPSCoR/IDeA

Jerry J. Bromenshenk
University of Montana

Jennifer Carpenter
Technology Transfer

Kathleen Carrado
Center for Nanoscale Materials, Argonne National Laboratory

Ismail Celik
West Virginia University

Vidhya Chakrapani
University of Louisville

Boris Chernomordik
University of Louisville

Fred Choobineh
Nebraska Experimental Program to Stimulate Competitive Research

Gretchen Cisco
Brookhaven National Laboratory

Joseph M. Cleary
National Renewable Energy Laboratory

Tammy Click
Oak Ridge Institute for Science and Education

Barbara Cohen
Oak Ridge Institute for Science and Education

Pamela Crowell
Idaho State University

Dustin Cummins
University of Louisville

Nhan Dang
Kansas State University

Clara Deal
International Arctic Research Center, University of Alaska Fairbanks

Nilesh Dhote
UAHuntsville

Stephen DiFazio
West Virginia University

Stephen Ducharme
University of Nebraska

Rupa Dumpala
University of Louisville

Debra Easterly
Idaho State University

Takeshi Egami
University of Tennessee

Allen Ekkebus
Oak Ridge National Laboratory

Danielle Ellis
West Virginia University

Bilal El-Zahab
Louisiana State University

Sherry Faye
University of Nevada, Las Vegas

Jeffrey Fergus
Auburn University

Timothy Fitzsimmons
US Department of Energy

Jerald Fletcher
West Virginia University

Brian Frederick
Univ. of Maine

Yanfei Gao
Oak Ridge National Laboratory

Marie Garcia
Sandia National Laboratories

Deborah Garland
Oak Ridge Institute for Science and Education

Arlene Garrison
University of Tennessee

Kai Germaschewski
University of New Hampshire

William Gern
University of Wyoming, Office of Research and Economic Development

James Gershey
Louisiana Board of Regents

Soumik Ghosh
The Center for Advanced Computer Studies, University of Louisiana at Lafayette

James Gilboy
The University of Arkansas Microelectronics-Photonics Program

Derrick Gilmore
Alabama A&M University

Manuel Gomez
University of Puerto Rico

Eric Grulke
University of Kentucky

Suresh Gubbala
University of Louisville

Junpeng Guo
University of Alabama in Huntsville

Jian He
Clemson University

David Hercules
Vanderbilt University

David Hill
Idaho National Laboratory

James Hoehn
EPSCoR/IDeA Foundation

James Iatridis
Vermont EPSCoR

Denise Jackson
University of Tennessee

Jeremy Jay
University of Tennessee

Cynthia Jenks
Ames Laboratory

Ram Katiyar
University of Puerto Rico

Veerel Keppens
The University of Tennessee

Michael Khonsari
Louisiana Board of Regents

Barbara Kimbell
University of New Mexico

Sophia Kitts
Oak Ridge Institute for Science and Education

Sarah Koerber
University of Idaho

Silpa Kona
University of Louisville

Mathieu Kourouma
Southern University, Baton Rouge

Vivekanand Kumar
University of Louisville

Patrick Kung
University of Alabama

Allen L. Landers
Auburn University

Michael A. Langston
University of Tennessee

Patrick LeClair
University of Alabama

David Lederman
West Virginia University

Sungho Lee
Clemson University

Adam Lewis
University of Louisiana at Lafayette

Aaron Lindenberg
Stanford University

Yanbing Luan
The University of Tennessee

Lisa Majkowski
New Mexico EPSCoR

Omar Manasreh
University of Arkansas

Reinhold Mann
Oak Ridge National Laboratory

Zhiqiang Mao
Tulane University

Praveen Meduri
University of Louisville

Monica Mehanna
University of Kentucky

Dongming Mei
University of South Dakota

Jonathan Mielenz
Oak Ridge National Laboratory

John Mintmire
Oklahoma State University

David Mudd
University of Louisville

Dean Myles
Oak Ridge National Laboratory

Harold Myron
Argonne National Laboratory

Sudhir Naswa
Unversity of Tennessee

John J. Neumeier
Montana State University

Edmund Nowak
University of Delaware - Physics

Teri Odom
Northwestern University

Amod Ogale
Clemson University

William Painter
Oak Ridge National Laboratory

Jennifer Palmer
Partnerships Directorate

Anup Pancholi
University of Delaware

Minseo Park
Auburn University

Hemant Pendse
University of Maine

Chandrashekhar Pendyala
University of Louisville

Rachel Pollock
University of Maine

Sheri Powell
Alabama DOE EPSCoR

Roger Pynn
Indiana University

Xiao Qin
Auburn University

Stephen Rankin
University of Kentucky

James Rice
South Dakota EPSCoR

James Roberto
Oak Ridge National Laboratory

Rene Rodriguez
Idaho State University

Gary Rogers Jr.
University of Tennessee

Nancy Sauer
Los Alamos National Laboratory
Institutes Office

Doug Schulz
North Dakota State University

Andrew Schwartz
DOE Basic Energy Sciences

Wayne Seames
University of North Dakota Dept. of
Chemical Engineering

Gregory Sedrick
University of Tennessee Space Institute

Neil Shafer-Ray
University of Oklahoma

Michael Simpson
Oak Ridge National Laboratory
Dennis Smith
Clemson University

Gregory Snow
University of Nebraska

Jason Spaans
University of South Dakota

John Steadman
University of South Alabama

Michael Strauss
The University of Oklahoma

Kelly Sullivan
Pacific Northwest National Laboratory

Gamini Sumanasekera
University of Louisville

Mahendra Sunkara
University of Louisville

Jyothish Thangala
University of Louisville

Donna Thomas
Oak Ridge Institute for Science and Education

Kenneth Tobin
Oak Ridge National Laboratory

Peter Tortorelli
Oak Ridge National Laboratory

Judy Trimble
Oak Ridge National Laboratory

Roberto Triolo
University of Palermo (Italy)

Christoffer Turner
University of Alabama

Nian-Feng Tzeng
University of Louisiana at Lafayette

Walter Varhue
University of Vermont

Ilya Vekhter
Louisiana State University

James Vincent
University of Vermont

Isiah Warner
Louisiana State University

Marshall Wheeler
University of Maine Chemical and Biological Engineering

James Wicksted
Oklahoma EPSCoR

Herschel Workman
PartTec, Ltd.

Jiang Wu
University of Arkansas Fayetteville

John Xiao
University of Delaware

Juchao Yan
Eastern New Mexico University

Yun Zhang
University of Tennessee

Jianting Zhu
Desert Research Institute